AD NUMBER
AD378805
CLASSIFICATION CHANGES
TO: unclassified
FROM: confidential
LIMITATION CHANGES
TO: Approved for public release, distribution unlimited
FROM: Distribution authorized to U.S. Gov't. agencies and their contractors; Critical Technology; DEC 1966. Other requests shall be referred to US Air Force Rocket Propulsion Laboratory, Attn: RPPR-STINFO, Edwards AFB, CA 93523.
AUTHORITY
31 Dec 1972, per document marking; AFRPL ltr 7 May 1973

GENERAL DECLASSIFICATION SCHEDULE

IN ACCORDANCE WITH
DOD 5200.1-R & EXECUTIVE ORDER 11652

THIS DOCUMENT IS:

Subject to General Declassification Schedule of Executive Order 11652-Automatically Downgraded at 2 Years Intervals- DECLASSIFIED ON DECEMBER 31, 1972

BY

Defense Documentation Center
Defense Supply Agency
Cameron Station
Alexandria, Virginia 22314

SECURITY MARKING

The classified or limited status of this report applies to each page, unless otherwise marked.
Separate page printouts MUST be marked accordingly.

THIS DOCUMENT CONTAINS INFORMATION AFFECTING THE NATIONAL DEFENSE OF THE UNITED STATES WITHIN THE MEANING OF THE ESPIONAGE LAWS, TITLE 18, U.S.C., SECTIONS 793 AND 794. THE TRANSMISSION OR THE REVELATION OF ITS CONTENTS IN ANY MANNER TO AN UNAUTHORIZED PERSON IS PROHIBITED BY LAW.

NOTICE: When government or other drawings, specifications or other data are used for any purpose other than in connection with a definitely related government procurement operation, the U. S. Government thereby incurs no responsibility, nor any obligation whatsoever; and the fact that the Government may have formulated, furnished, or in any way supplied the said drawings, specifications, or other data is not to be regarded by implication or otherwise as in any manner licensing the holder or any other person or corporation, or conveying any rights or permission to manufacture, use or sell any patented invention that may in any way be related thereto.

(Unclassified Title)

DEVELOPMENT AND TEST OF HIGH ENERGY SOLID PROPELLANTS

FINAL TECHNICAL REPORT, AFRPL-TR-

DECEMBER 1966

HERCULES INCORPORATED
BACCHUS WORKS MAGNA, UTAH

AIR FORCE ROCKET PROPULSION LABORATORY
RESEARCH AND TECHNOLOGY DIVISION
AIR FORCE SYSTEMS COMMAND

(Unclassified Title)

DEVELOPMENT AND TEST OF HIGH ENERGY SOLID PROPELLANTS

FINAL TECHNICAL REPORT

December 1966

HERCULES INCORPORATED
BACCHUS WORKS, MAGNA, UTAH

In addition to security requirements which must be met, this document is subject to special export controls and each transmittal to foreign governments or foreign nationals may be made only with prior approval of AFRPL (RPPR-STINFO), Edwards, Calif 93523.

AIR FORCE ROCKET PROPULSION LABORATORY
RESEARCH AND TECHNOLOGY DIVISION
AIR FORCE SYSTEMS COMMAND
UNITED STATES AIR FORCE
EDWARDS, CALIFORNIA

NOTICES

When U. S. Government drawings, specifications, or other data are used for any purpose other than a definitely related Government procurement operation, the Government thereby incurs no responsibility nor any obligation whatsoever, and the fact that the Government may have formulated, furnished, or in any way supplied the said drawings, specifications, or other data is not to be regarded by implication or otherwise, or in any manner licensing the holder or any other person or corporation, or conveying any rights or permission to manufacture, use, or sell any patented invention that may in any way be related thereto.

Do not return this copy. When not needed, destroy in accordance with pertinent security regulations.

FOREWORD

This is the final report under Contract AF 04(611)-10754. This report was prepared by the Propellant Development Group, Bacchus Works, Chemical Propulsion Division, Hercules Incorporated. The report was written by R. F. Keller with contributions by J. L. Judkins (Ballistic Testing), G. R. Gibson (Laboratory Formulation), and J. M. Trowell (Laboratory Analytical Support). Major contributions were also made by Dr. B. Brown, Dr. K. P. McCarty, and J. W. Schowengerdt in analyzing the impulse efficiency losses associated with beryllium and LMH-2 propellants and by J. W. Schowengerdt in formulation design. The AP and wax LMH-2 posttreatments were initially developed by Dr. H. C. Dehm and D. F. Mellow under an IR&D program. This report was approved by Dr. K. P. McCarty and Dr. R. L. Schaefer.

Preparation of this report is authorized under Contract AF 04(611)-10754, in accordance with line item 6 of "Contractor Data Requirement List," Form DD 1423. The report is classified confidential to protect a compilation of information, or a complete analysis of the subject, from individually unclassified items of information.

The cognizant Air Force Officers are F. W. Joffs and R. Miller, First Lieutenants, RPMCP, Edwards Air Force Base, California.

Published by

The Publications Group
General Services Department
HERCULES INCORPORATED
Bacchus Works
Magna, Utah

CONFIDENTIAL ABSTRACT

The objective of this contract was to conduct theoretical and experimental investigations resulting in the demonstration of beryllium hydride (LMH-2) solid propellants delivering in excess of 280 lbf-sec/lbm at standard conditions. The program consisted of three tasks: Task I, Analysis and Data Correlation; Task II, Formulation and Ballistic Evaluation; and Task III, Advanced Concepts.

LMH-2 fueled, double-base propellants having theoretical specific impulse values up to 314 lbf-sec/lbm were developed. LMH-2 loadings as high as 19 percent were achieved at 60 percent total volume solids loadings. These propellants gave delivered specific impulse values in 15-pound-charge (15PC) motors in the range of 280 to 282 lbf-sec/lbm; the first demonstration of the original ARPA Project PRINCIPIA goal. The developed propellants were characterized for sensitivity, thermal stability, processibility, mechanical properties, and explosive classification. Satisfactory processing characteristics were obtained by using surface treatments and grinding to improve bulk density of LMH-2.

Seventy beryllium (Be) and thirty-five LMH-2 15PC motors were fired to develop efficiency correlations based on motor and propellant parameters. The efficiency of Be propellants was found strongly dependent on flame temperature and, to a lesser extent, oxidation ratio. For LMH-2 propellants, flame temperature, oxidation ratio, and motor residence time were controlling factors. Efficiency losses for LMH-2 propellants were related to surface agglomeration of unburned Be. A limited amount of testing indicated a fluorine-rich environment is beneficial for LMH-2 combustion.

TABLE OF CONTENTS

LIST OF FIGURES

LIST OF FIGURES (Cont)

LIST OF FIGURES (Cont)

LIST OF FIGURES (Cont)

LIST OF FIGURES (Cont)

LIST OF TABLES

LIST OF TABLES (Cont)

LIST OF TABLES (Cont)

LIST OF TABLES (Cont)

LIST OF ABBREVIATIONS

Abbreviation	Meaning
2-NDPA	2-Nitrodiphenylamine
5PC	5-pound charge
15PC	15-pound charge
AL	Aluminum
AN	Ammonium nitrate
AP	Ammonium perchlorate
Be	Beryllium
BeO	Beryllium oxide
C5A	Pentyl fluoroalkyl acrylate
C7A	Fluorinated acrylate adhesive
C7M	Fluorinated acrylate adhesive
C9M	Nonylfluoroalkyl methacrylate
CMDB	Composite modified double-base
DTA	Differential thermal analysis
ESD	Electrostatic discharge
FAAV	20 C7A, 60 C7M, 20 viton
FAV	23 C5A, 67 C9M, 10 viton
FPC	40-pound charge
HC	Polybutadiene type rubber (Thiokol)
HDP	Hydrazine diperchlorate
Hg	Mercury
HMX	Cyclotetramethylene tetranitramine
JANAF	Joint Army, Navy, Air Force
K	Kelvin

LIST OF ABBREVIATIONS (Cont)

Abbreviation	Meaning
LI	Lithium
LIP	Lithium perchlorate
LMH-2	Beryllium hydride
MG	Magnesium
MFPA	1, 2-bis (Difluoramino) propyl acetate
NG	Nitroglycerin
NP	Nitronium perchlorate
PNC	Plastisol nitrocellulose
P-K-r	Pressure-K-burning rate
RES	Resorcinol
SI	Silicon
TA	Triacetin
TAGN, $TAGNO_3$	Triaminoguanidine nitrate
TAZ	Triaminoguanidine azide
TDI	Toluene diisocyanate
TFLN	Teflon
TVOPA	Hexakis (Difluoramino) vinoxy propane
VCP	Ba/CMX propellant formulation
VITON	Viton rubber
ZR	Zirconium

SECTION I

INTRODUCTION

A. OBJECTIVE

Solid propellants containing beryllium hydride (BeH_2) have a theoretical specific impulse (Isp) up to 30 sec greater than that of Be-fueled propellants. In the past, firings of test motors containing BeH_2 propellants had not yielded the expected gain in delivered specific impulse. Motor and propellant parameters of chamber temperature, chamber pressure, mass-flow rate, expansion ratio, oxidation ratio, oxidizer particle size, hydride content, metal/hydride ratio, and total metal content were investigated under various government contracts. Although much was learned about BeH_2 propellants during this period, the high Isp promised by the hydride was still not realized.

The objective of this program was to conduct theoretical and experimental investigations resulting in the demonstration of BeH_2 solid propellant delivering an Isp in excess of 280 lb-sec/lb at standard conditions, and thus significantly advance the performance levels obtained from BeH_2 propellants.

B. SCOPE

The program is a three task effort. In Task I, the results of previous Be and BeH_2 firings were correlated to define the parameters important for higher delivered impulses. The results of this effort were applied in Task II to formulate and test candidate high-performance propellant systems. In Task III advanced formulation techniques were studied to improve BeH_2 combustion.

SECTION II

TASK I - ANALYSIS AND DATA CORRELATION

A. SCOPE

The objective of this task was to evaluate and correlate available Be and LMH-2 motor firing data. Particular emphasis was placed on the correlation of motor efficiency with motor and formulation variables. Theoretical Isp calculations were conducted on a wide variety of formulations to establish the relationship between propellant parameters and theoretical performance of Be and LMH-2 propellants. Based on the correlations and theoretical performance calculations, formulations were designed which were predicted to deliver Isp values capable of meeting the program objectives. Six candidate LMH-2 formulations were selected for motor evaluation. In addition to the advanced formulation effort, Be formulations were investigated to confirm the validity of the developed correlations and, where necessary, to extend their useful range. In particular, the performance of Be systems containing high metal levels equivalent to those of LMH-2 propellants having high theoretical performance potential were investigated. These results were combined with earlier correlations and those obtained on concurrent related programs to allow accurate predictions to be made for Be and LMH-2 propellants and to gain some insight into the possible causes of performance losses.

B. INITIAL DATA CORRELATIONS

The following discussion describes the data analysis and correlations developed from a review of the available Be and LMH-2 motor data at the start of this program.

The basic assumption was made that LMH-2 decomposes to the parent metal at temperatures of approximately 300° C.[1] With this assumption, the factors affecting impulse efficiency of Be propellants become important for LMH-2 propellants for determining expected LMH-2 performance levels. As a consequence, a large amount of effort was expended establishing correlations for Be propellants. However, it has been suggested by various workers[2] that as LMH-2 decomposes, a cloud of hydrogen surrounds the metal particle, suppressing final conversion to the oxide. Thus, some basic differences in the correlations between Be and LMH-2 can be expected. To gain possible insight into the performance of metallized propellants in general, a limited comparison was made between Be and Al efficiencies.

The following parameters were considered of prime importance in defining the performance efficiency of Be and LMH-2 propellants:

(1) Motor parameters

(a) Chamber pressure

[1,2]Refer to List of References

(b) Characteristic length (L*)

(c) Mass flow rate

(d) Expansion ratio

(e) Nozzle geometry

(2) Propellant parameters

(a) Chamber temperature

(b) LMH-2 content and particle size

(c) Total Be metal content

(d) Oxidation ratio $\frac{\text{Moles O}}{\text{Moles C + moles metal}}$

(e) Oxidizer particle size

(f) Binder type

(g) Oxygen source

A literature survey was conducted to accumulate data from recent major propellant contracts on all of the above listed parameters. Since performance data was obtained by the various contractors over a wide range of test conditions and motor configurations, initial emphasis was placed on developing scaling curves for each propellant. This allowed comparison on a common motor basis for evaluation of propellant parameters and determination of the effect of propellant parameters on motor scaling. In addition, theoretical performance calculations were performed on the Bacchus Free Energy Program for all propellants used in the final correlations. This eliminated differences in theoretical calculations among contractors and allowed for updating of JANAF thermochemical data.

All Isp efficiencies, unless otherwise stated, were calculated by dividing the delivered impulse by the theoretical equilibrium flow impulse, calculated at the actual chamber pressure and expansion half angle. All reported Isp_{1000} values were calculated by multiplying the theoretical impulse at standard conditions by the efficiency determined at the actual firing conditions.

1. Motor Parameters

The majority of data on the motor efficiency of Be propellants has been obtained under Air Force contracts. The Air Force programs performed by Atlantic Research Corporation, Aerojet-General Corporation, Thiokol Chemical Corporation, and Hercules Incorporated were reviewed. Priority for selection of propellants for correlations was given to those

propellants which had been tested at a wide variety of motor conditions and, preferably, in motors of propellant weight greater than 30 lb. Only those propellants for which the final performance could be reasonably predicted at large motor conditions were used in the final correlations. Table I contains a summary of the propellants selected for the final correlations.

Figure 1 shows the effect of mass-flow rate for 5-, 15-, 40-, and 400-lb motors containing Be-fueled VCP propellant and is typical of the motor scaling curve found for efficient Al and Be propellants. Figure 1 also shows effeciency as a function of chamber pressure for 15-, 40-, and 400-lb motors and indicates no loss in efficiency down to 400 psia. Atlantic Research has also shown scaling curves for various Be propellants as presented in Figure 2. A strong dependence of mass-flow rate on efficiency for each motor size is also indicated in this figure. This phenomenon may be explained by considering scaling equations such as those developed by Rohm and Haas, where for constant heat flux, thermal efficiency, and mass-flow rate, heat losses are proportional to the internal area exposed. Decreased particle lag with the larger nozzles used at high-mass flow is probably also important.

For the Hercules 40-lb charge (FTC) motor, the Rohm and Haas scaling equation predicts an insignificant loss in efficiency for mass-flow rates in the 5- to 10-lb/sec region. Data obtained from four Hercules propellants are plotted in Figure 3. These data show a significant loss in efficiency when the mass-flow rate is decreased from 10 lb/sec to 5 lb/sec for two of the propellants, whereas no loss in efficiency is shown for the other two. The primary difference between the two pair of propellants is a significantly higher oxidation ratio for the group showing no efficiency loss with decreasing chamber pressure for the lower-oxidation-ratio propellants. The decrease in efficiency for the lower-oxidation-ratio curve is characteristic of that reported by other contractors for losses in efficiency with decreasing pressure. One possible explanation for this efficiency loss is insufficient residence time for combustion with propellants containing little excess oxygen. This possibility is illustrated in Figure 4, where efficiency is plotted as a function of residence time in terms of the characteristic chamber length (L*). This figure shows that L* correlates as well with efficiency as chamber pressure. Unfortunately, the two effects cannot be separated.

Figures 5 through 7 illustrate pressure and scaling effects on efficiency for several Atlantic Research propellants. Of particular interest are Figures 5 and 6, which show the effect of pressure on efficiency for Arcocel propellants 319 and 191 where mass-flow rate was kept essentially constant (keyed points). Little pressure effect on efficiency was observed; however, the constant mass-flow rate was maintained at low pressure by a considerable increase in L*. The increased L* values may explain the lack of efficiency loss with decreasing pressure. Figure 7 shows pressure and mass-flow effects on efficiency for Arcocel 333E. A sharp decrease in efficiency for both decreasing mass-flow rate and pressure was observed in 50-lb motors.

TABLE I

SUMMARY OF PROPELLANTS SELECTED FOR FINAL EFFICIENCY CORRELATIONS

Designation	Company*	Type Formulation**	Binder Level (Wt %)	AP (Wt %)	HMX (Wt %)	Be (Wt %)	Al (Wt %)	Other (Wt %)	T_{p} (1000/M.?) A	T_{p} (1000/M.?) B	T_{c} (°K) A	T_{c} (°K) B	Oxidation Ratio A	Oxidation Ratio B
WTP	HPC	DB	32	9	29	10	--	--	--	283.0	--	3838	--	1.218
WOR	HPC	DB	63.6	5.9	17.5	13	--	--	--	283.9	--	3895	--	1.060
WHE	HPC	DB	62.6	7.4	17.0	12	--	--	--	283.0	--	3870	--	1.10
WHK	HPC	DB	63.6	5.9	20.5	10	--	--	--	281.8	--	3773	--	1.189
WHT	HPC	DB	32.0	--	54.0	8	--	--	--	285.4	--	3785	--	1.170
WOG	HPC	DB	48.0	20.5	--	12	--	19.5 (TAZ)	--	291.2	--	3674	--	1.01
EJC	HPC	DB	51.0	5.0	26.0	--	18.0	--	--	270.4	--	[illegible]	--	[illegible]
317	ARC	DB	60.0	--	27.0	13.0	--	--	281.2	283.1	3537	3767	1.067	1.067
3198	ARC	DB	50.0	12.3	26.2	11.5	--	--	284.4	286.4	3589	3649	1.02	1.02
191	ARC	DB	50.0	36.0	--	14.0	--	--	280.1	281.2	3788	3852	1.08	1.086
3338	ARC	DB	65.0	22.0	--	13.0	--	--	281.9	283.8	3599	3638	1.089	1.086
365	ARC	DB	42.29	26.26	--	11.55	--	19.90 (TAZ)	289.1	290.2	3481	3531	1.08	0.998
AMP-2991-ModIA	AGC	NFU	26.0	60.0	--	14.0	--	--	280.5	283.2	3459	3646	1.038	1.037
AMB-3212	AGC	CTPB	13.0	72.5	--	14.5	--	--	284.3	283.2	--	3842	--	0.988
XP-93	AGC	CTPB	15.0	72.0	--	13.0	--	--	285.6	284.1	--	3682	--	0.992
XP-96	AGC	CTPB	13.0	74.0	--	13.0	--	--	284.0	283.1	--	3829	--	1.08
XP-112	AGC	CTPB	14.0	72.0	--	15.0	--	--	284.9	283.8	--	3869	--	1.036
TP-H-3108	TOC	CTPB	14.0	74.0	--	12.0	--	--	282.1	282.8	3566	3561	1.10	1.088
538	ARC	PU	--	--	--	--	--	--	282.5	--	3457	--	1.09	--
248	AGC	PU	--	--	--	--	--	--	279.1	--	3383	--	1.26	--

*Company:
HPC - Hercules Powder Company
ARC - Atlantic Research Corporation
TOC - Thiokol Chemical Corporation
AGC - Aerojet-General Corporation

**Type Formulation:
DB = Double Base
NFU = Nitroplasticized Polyurethane
CTPB = Carboxyterminated Polybutadiene
PU = Polyurethane

A - Reported by Contractor
B - Hercules Calculations

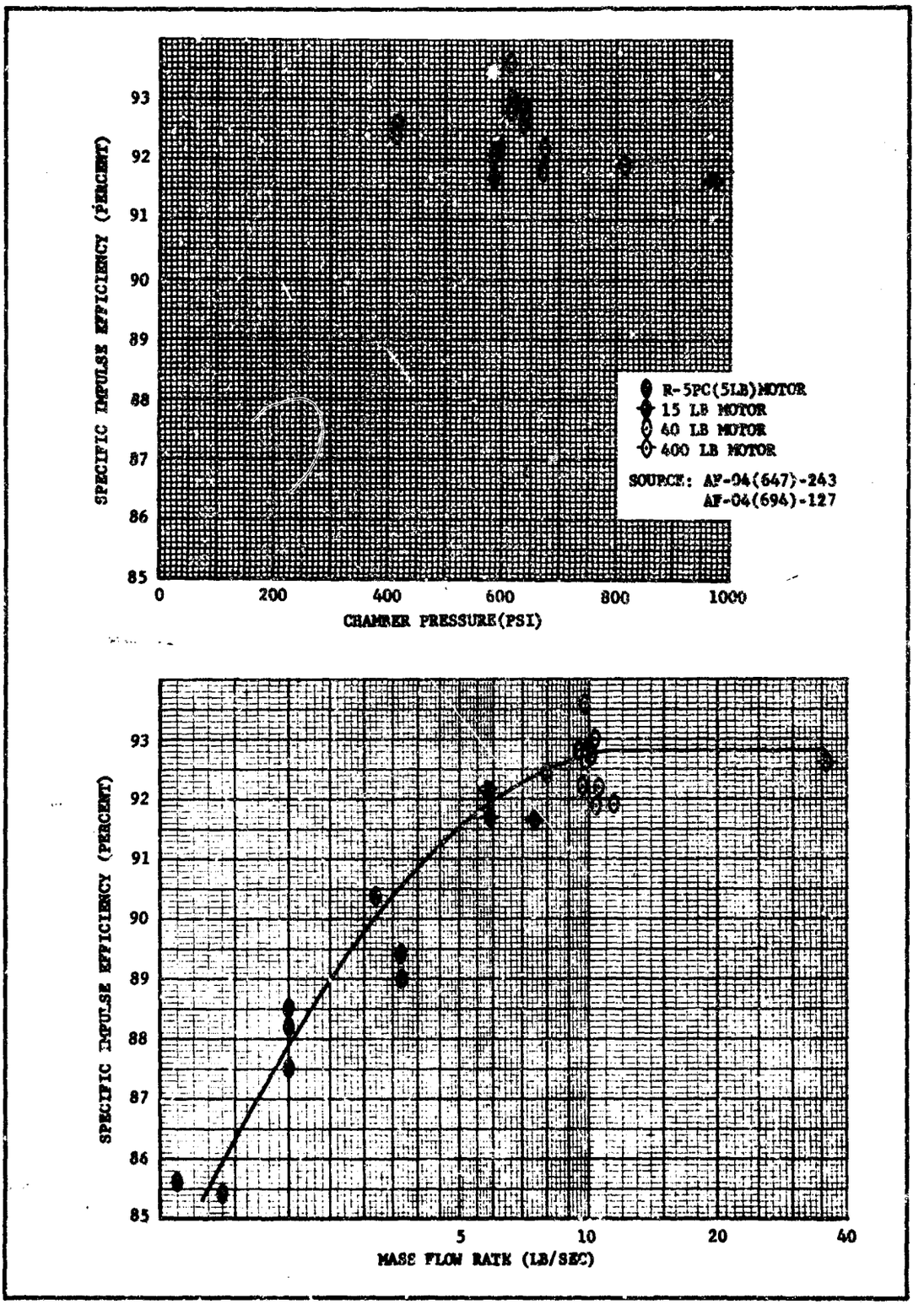

Figure 1. Effect of Chamber Pressure and Mass-Flow Rate on Specific Impulse Efficiency of VCP

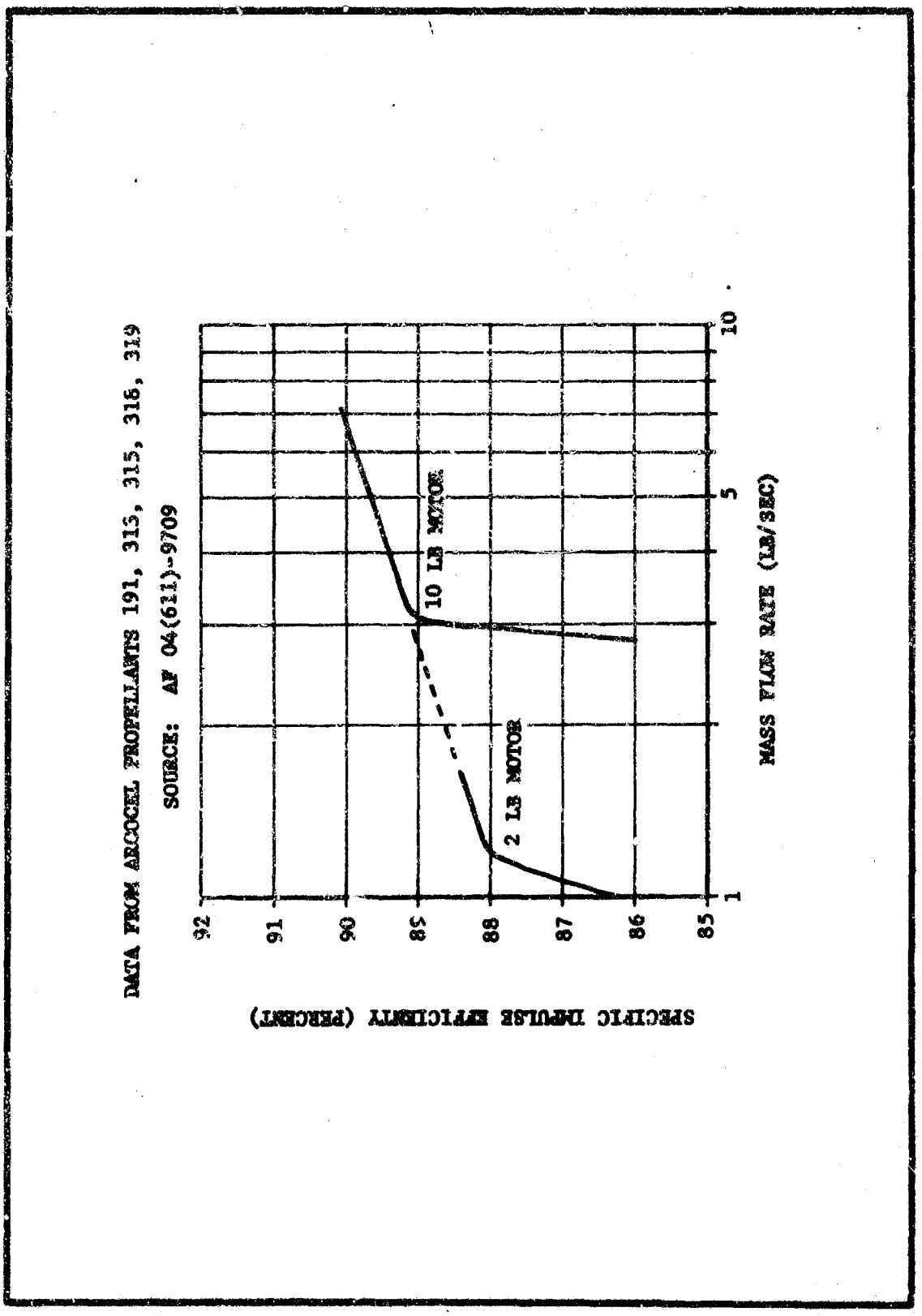

Figure 2. Effect of Mass-Flow Rate on Specific Impulse Efficiency for Four Atlantic Research Corporation Propellants

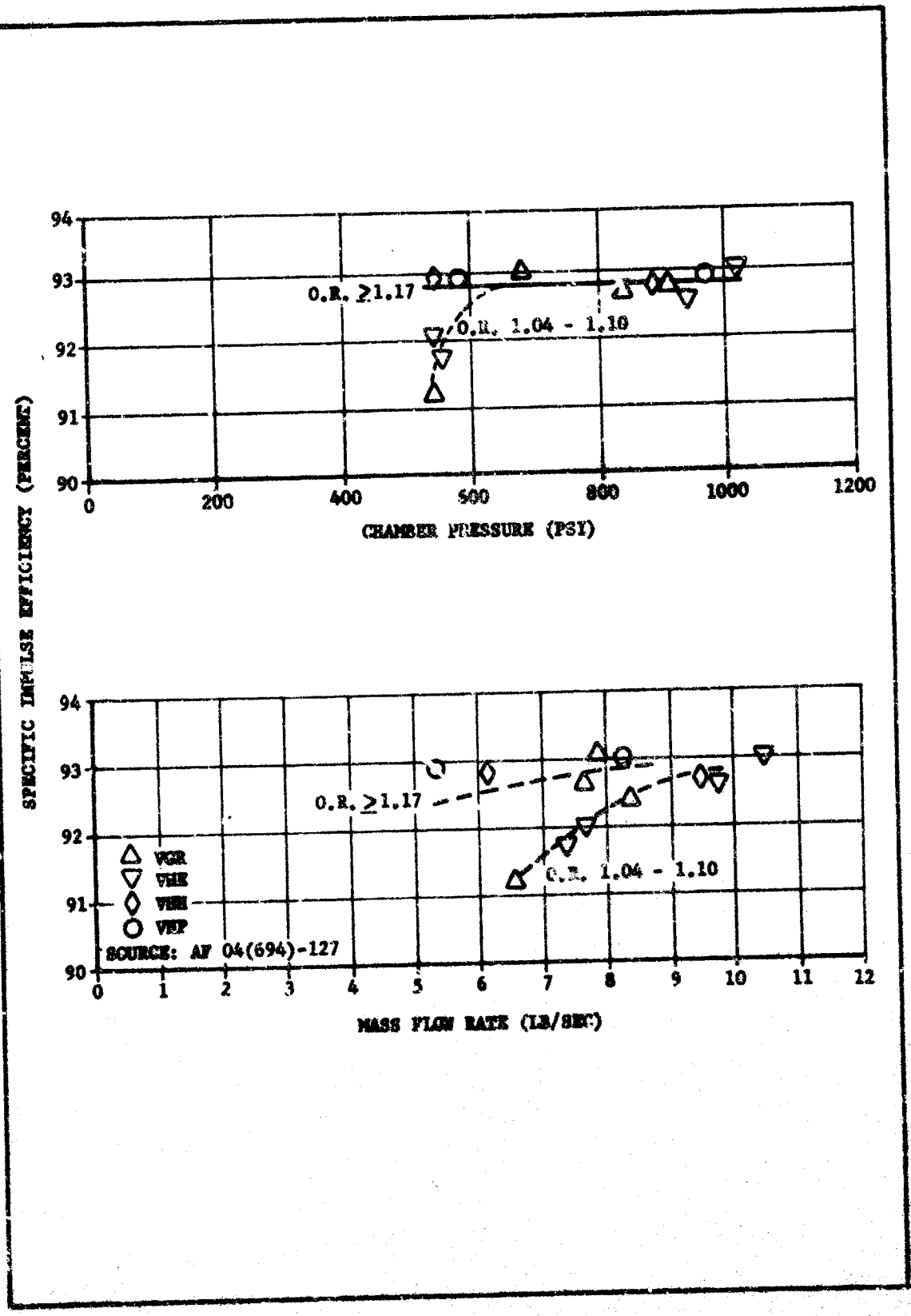

Figure 3. Effect of Chamber Pressure and Mass-Flow Rate on Specific Impulse Efficiency for Four Hercules Ba Propellants

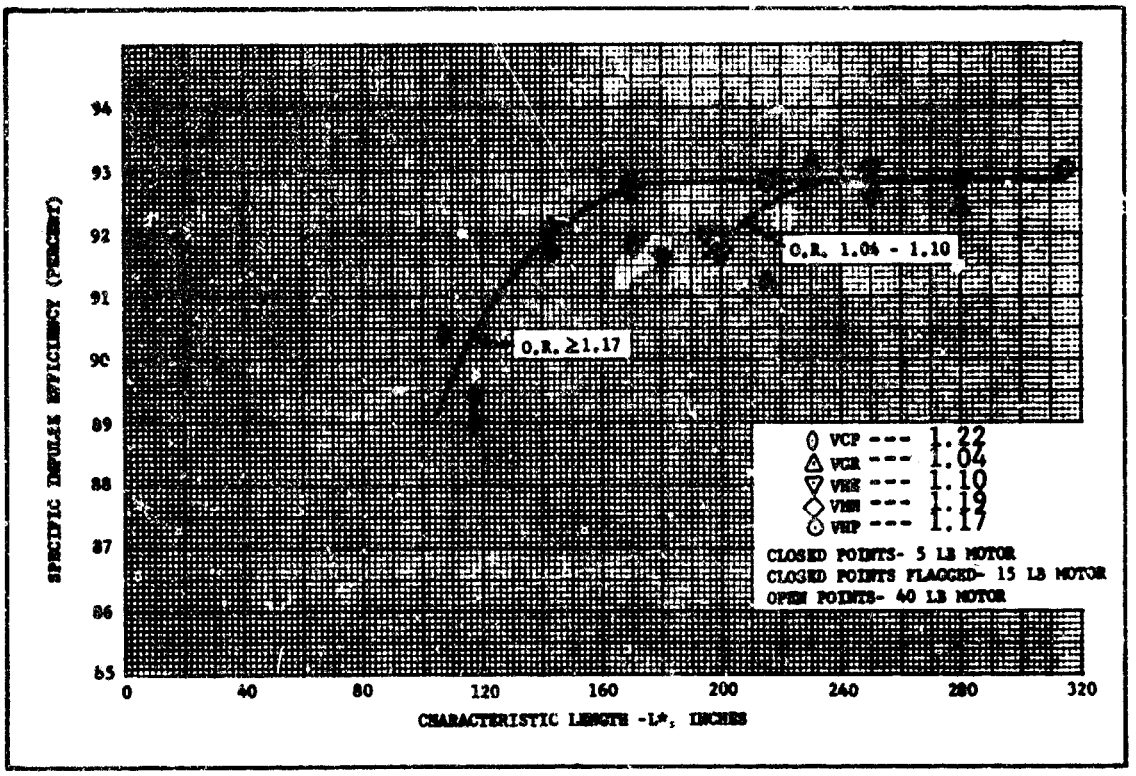

Figure 4. Effect of L* on Specific Impulse Efficiency for Five Hercules Be Propellants

Figures 8 and 9 show a comparison of Be propellants on the basis of mass-flow rate and L*. The following trends appear:

(a) Beryllium propellants with high flame temperatures (>3700° K) and high oxidation ratios show the highest impulse efficiencies.

(b) Beryllium propellants showing no L* effect above 200 for a given motor also show no pressure effect on impulse efficiency.

(c) Beryllium propellants with low flame temperatures and low oxidation ratios require large L* values and high mass-flow rates to approach good impulse efficiencies.

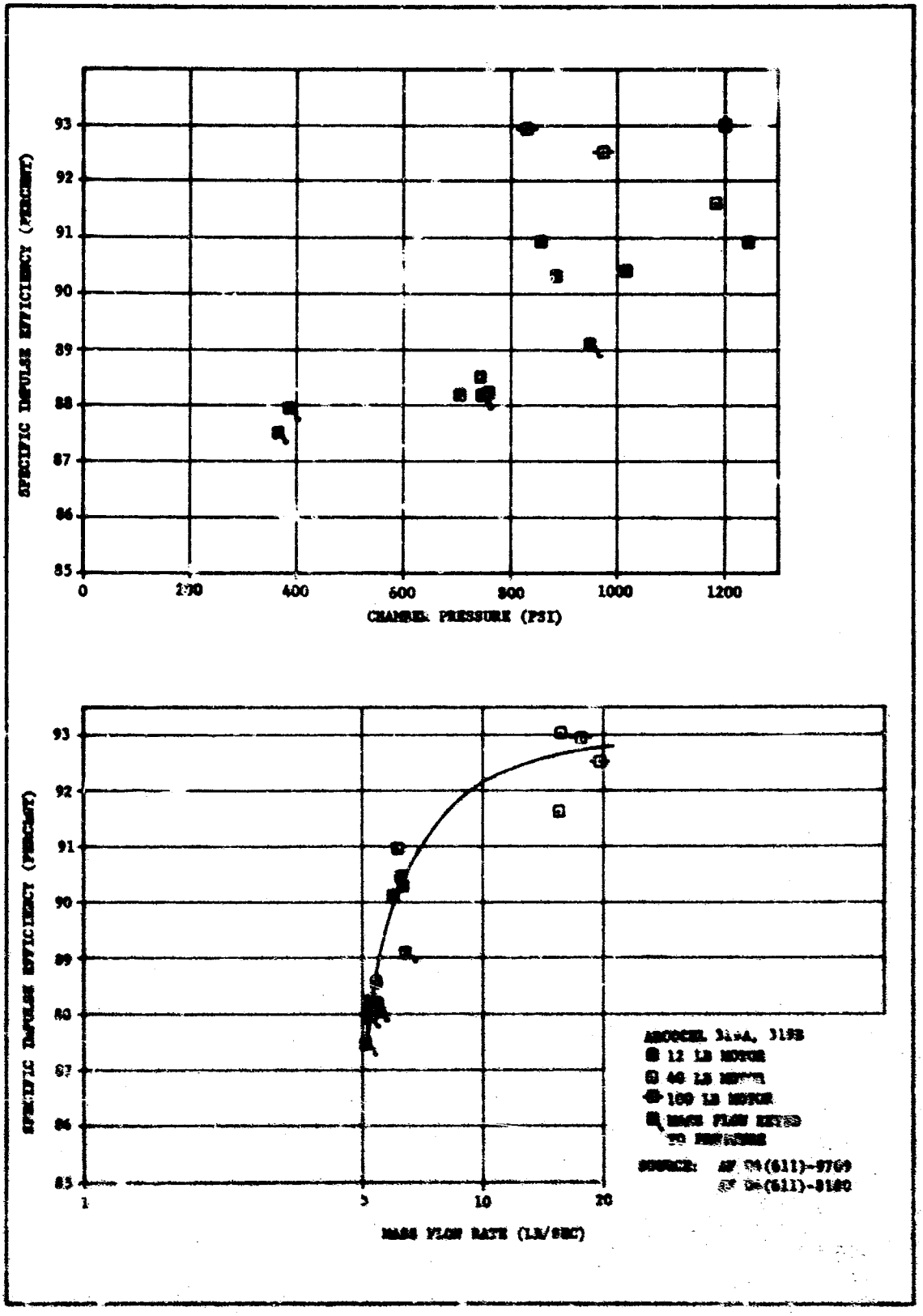

Figure 5. Effect of Chamber Pressure and Mass-Flow Rate on Specific Impulse Efficiency of Arcocel 319

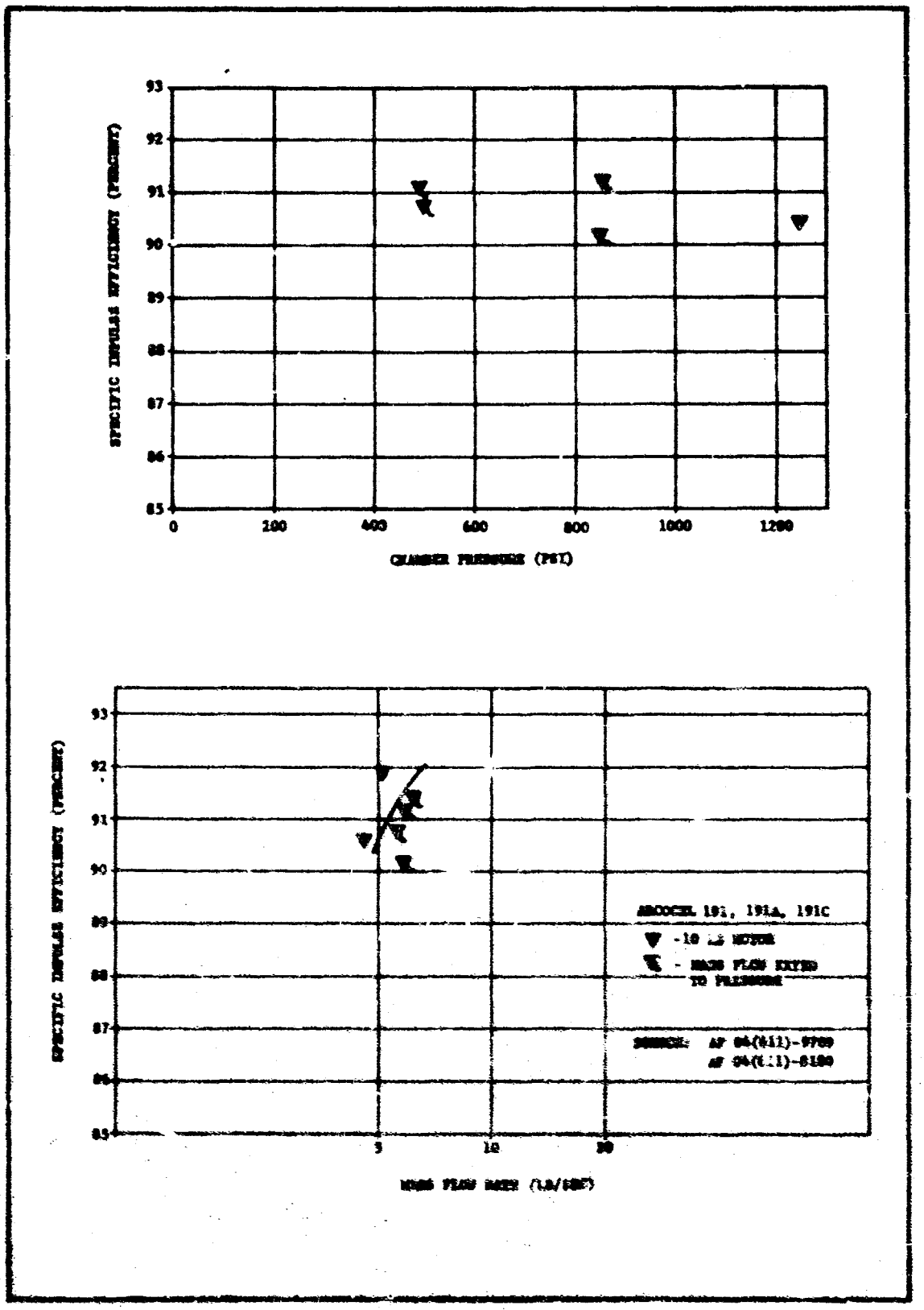

Figure 6. Effect of Chamber Pressure and Mass-Flow Rate on Specific Impulse Efficiency of Aerocel 191

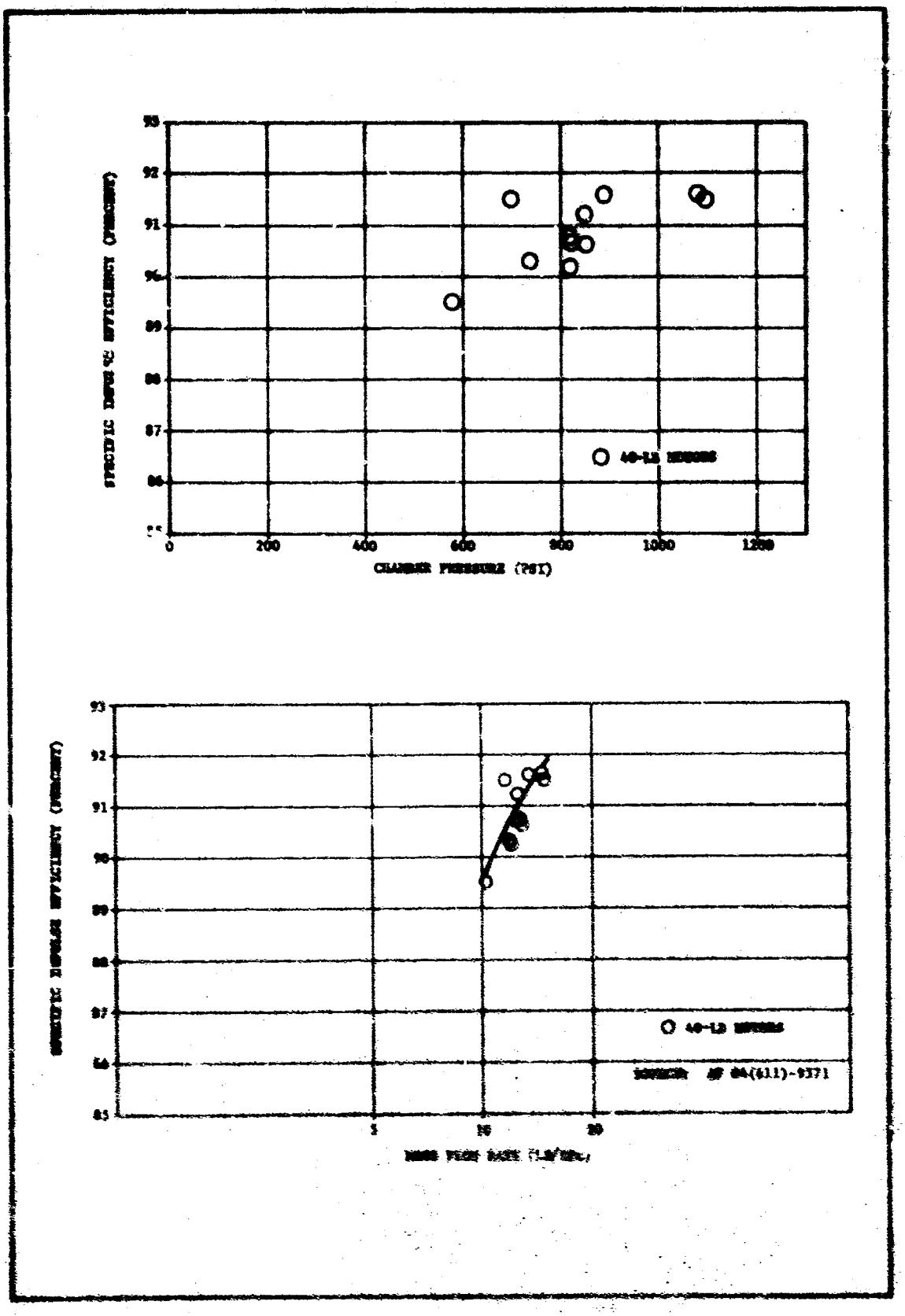

Figure 7. Effect of Chamber Pressure and Mass-Flow Rate on Specific Impulse Efficiency of Aerocel 333

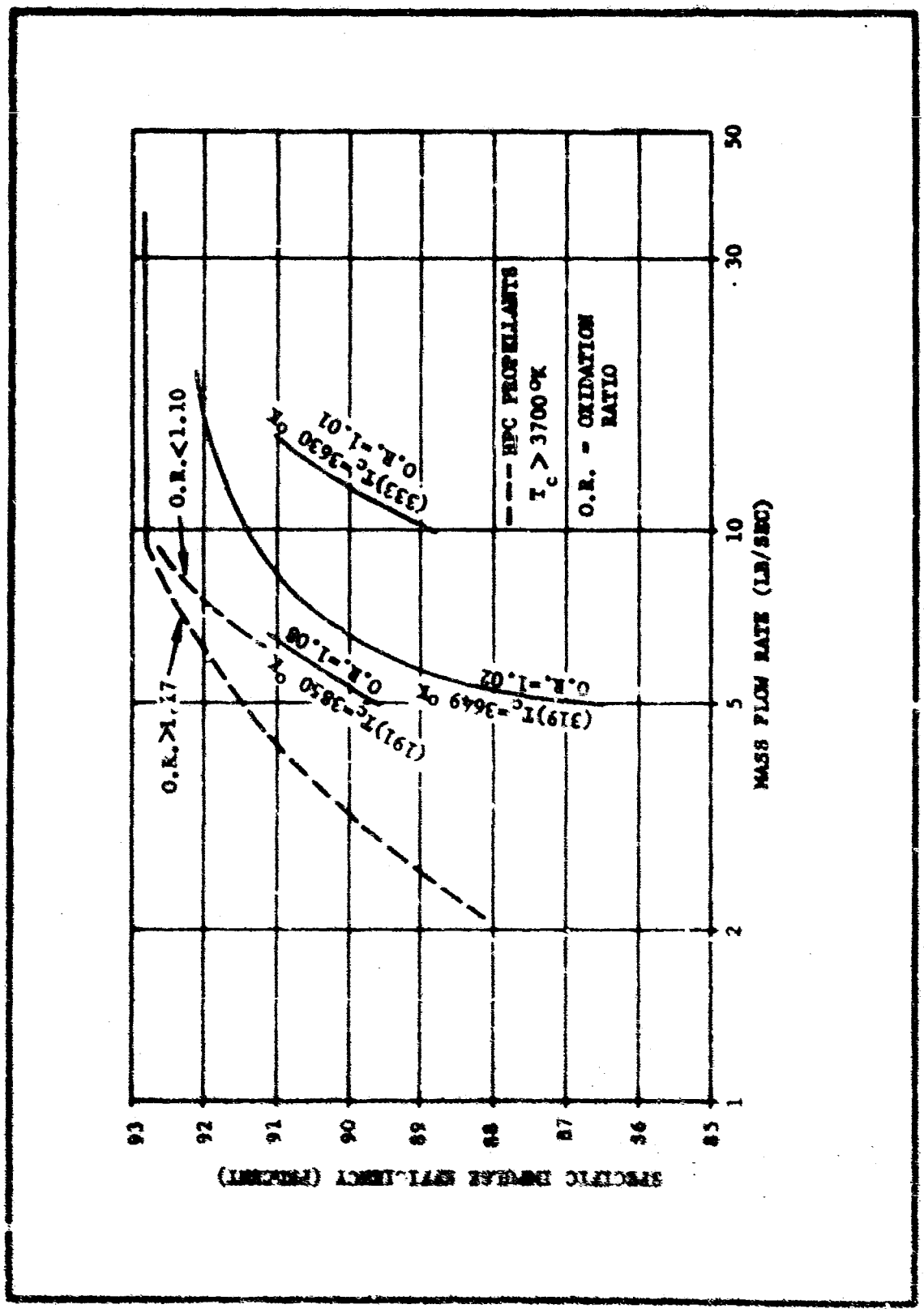

Figure 8. Effect of Motor Scaling on Specific Impulse Efficiency of Selected Propellants

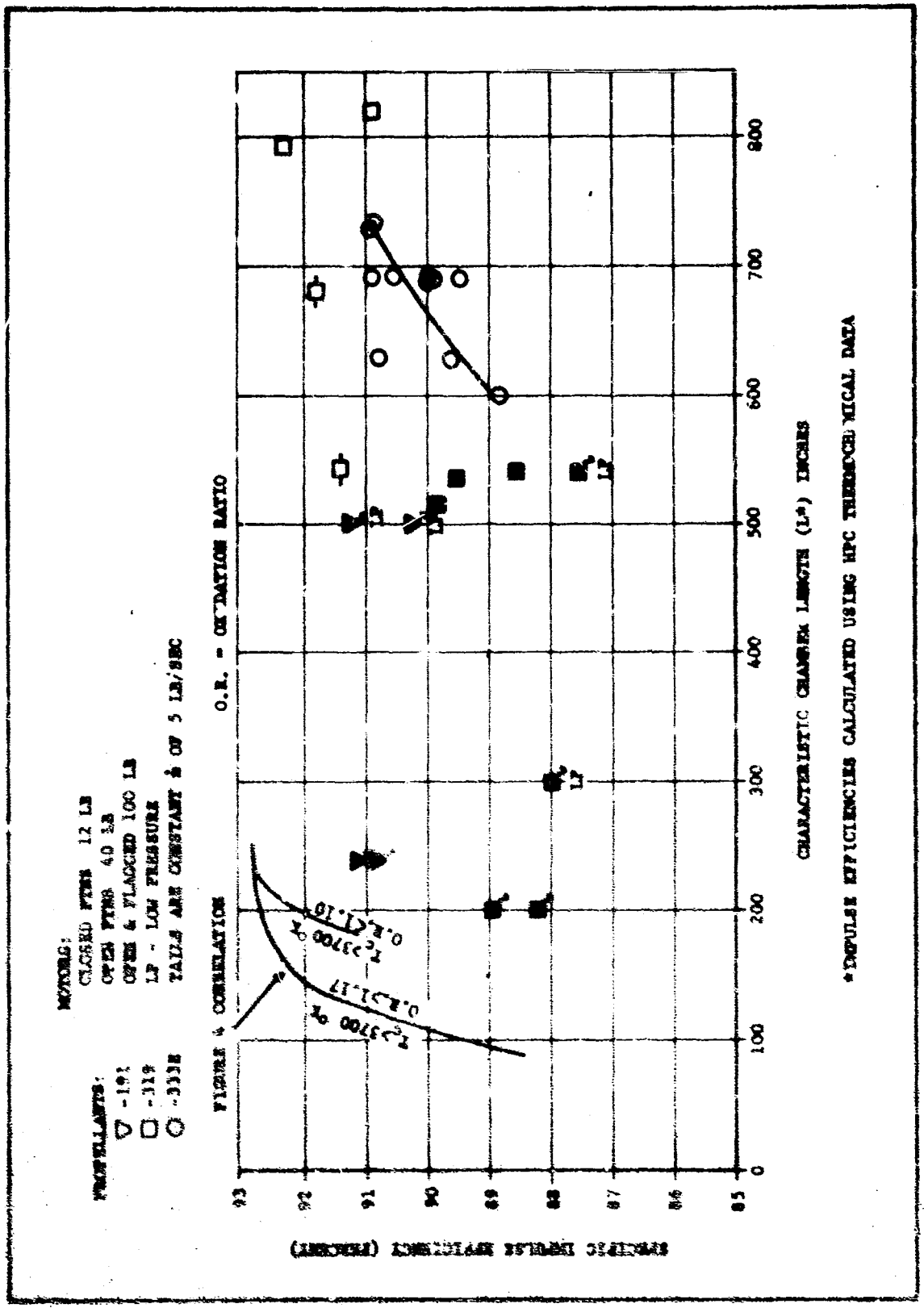

Figure 9. Effect of L* on Specific Impulse Efficiency of Selected Propellants

These trends are not absolute and additional testing is required for confirmation.

A comparison of the Be mass-flow rate curves at high and low temperatures to those of several LMH-2 propellants is shown in Figure 10. The majority of the LMH-2 mass-flow-rate curves follow those of a low-temperature Be propellant. It is also significant that Arcocel 340A (oxidation ratio of 1.0) is less efficient than the higher oxidation ratio propellants. Figure 10 also shows the effect of chamber pressure on efficiency for Arcocels 332 and 332A. No loss in efficiency occurred down to 450 psia. The results of Atlantic Research firings of a variety of propellants show a trend toward increased efficiency with increased L*, although other factors tend to obscure the correlation. Increased efficiency with increased flame temperature and higher oxidation ratio is also apparent in Figure 11.

The nozzle expansion ratio can influence efficiency by:

(a) Particle lags (velocity and thermal)

(b) Failure of gas phase reactions to reach completion

(c) Increased boundary layer friction losses occasioned by increased nozzle surface area

(d) Metal oxide fusion lag

(e) Errors in thermochemical data

(f) Heat exchange between gas and nozzle wall

Data showing the effect of increased expansion ratio on efficiency of Al propellants have been collected and are plotted on a common basis in Figure 12. All data appear to exhibit a consistent downward trend with increasing expansion ratio, although a leveling off at high expansion ratios is indicated for some propellants.

The effects of enthalpy loss from the gas stream to the nozzle wall and corresponding entropy decrease of the gas have been discussed in an Atlantic Research report.[3] Results of this calculation for Arcane 24, based on a 10-lb motor, predict a 1-percent Isp loss at an expansion ratio of 10, and 2-percent loss at an expansion ratio of 100. The data indicate a loss of over 3 percent between expansion ratios of 1 and 100; thus heat loss explains only part of the total loss.

Data for the effect of expansion ratio on efficiency of Be and LMH-2 propellants as determined by Hercules and Atlantic Research are summarized in Figure 13. The line through the Al data of Figure 12 is replotted for comparison. A distinct drop in efficiency with increasing expansion ratio is noted for all propellants. The efficiency loss is largest at the lower pressure. When data are recalculated assuming frozen flow, the low-temperature propellants, Arcane 24 and Arcane 53, show essentially

[3] Refer to List of References

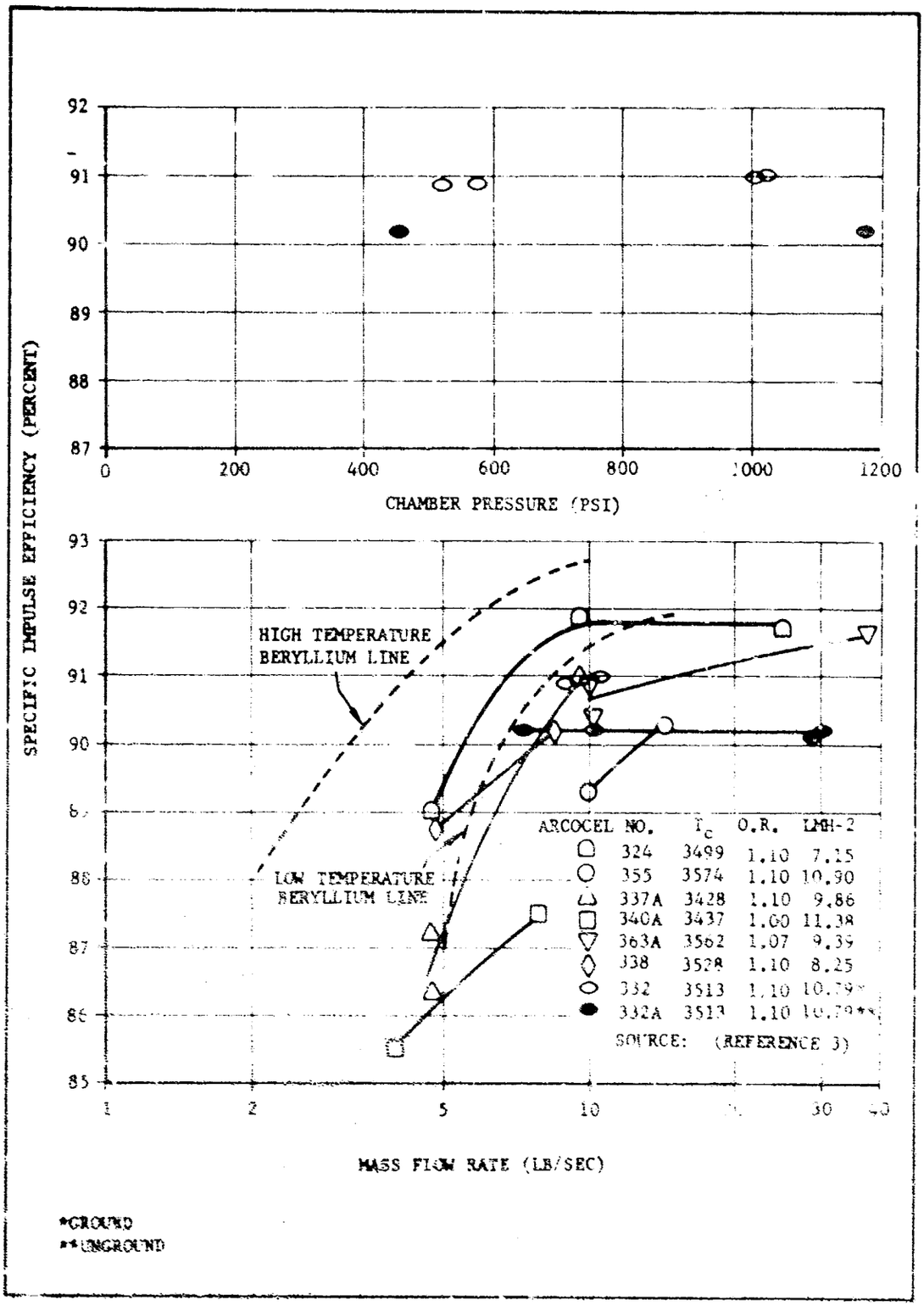

Figure 10. Effect of Chamber Pressure and Mass-Flow Rate on Specific Impulse Efficiency of LMH-2 Propellants

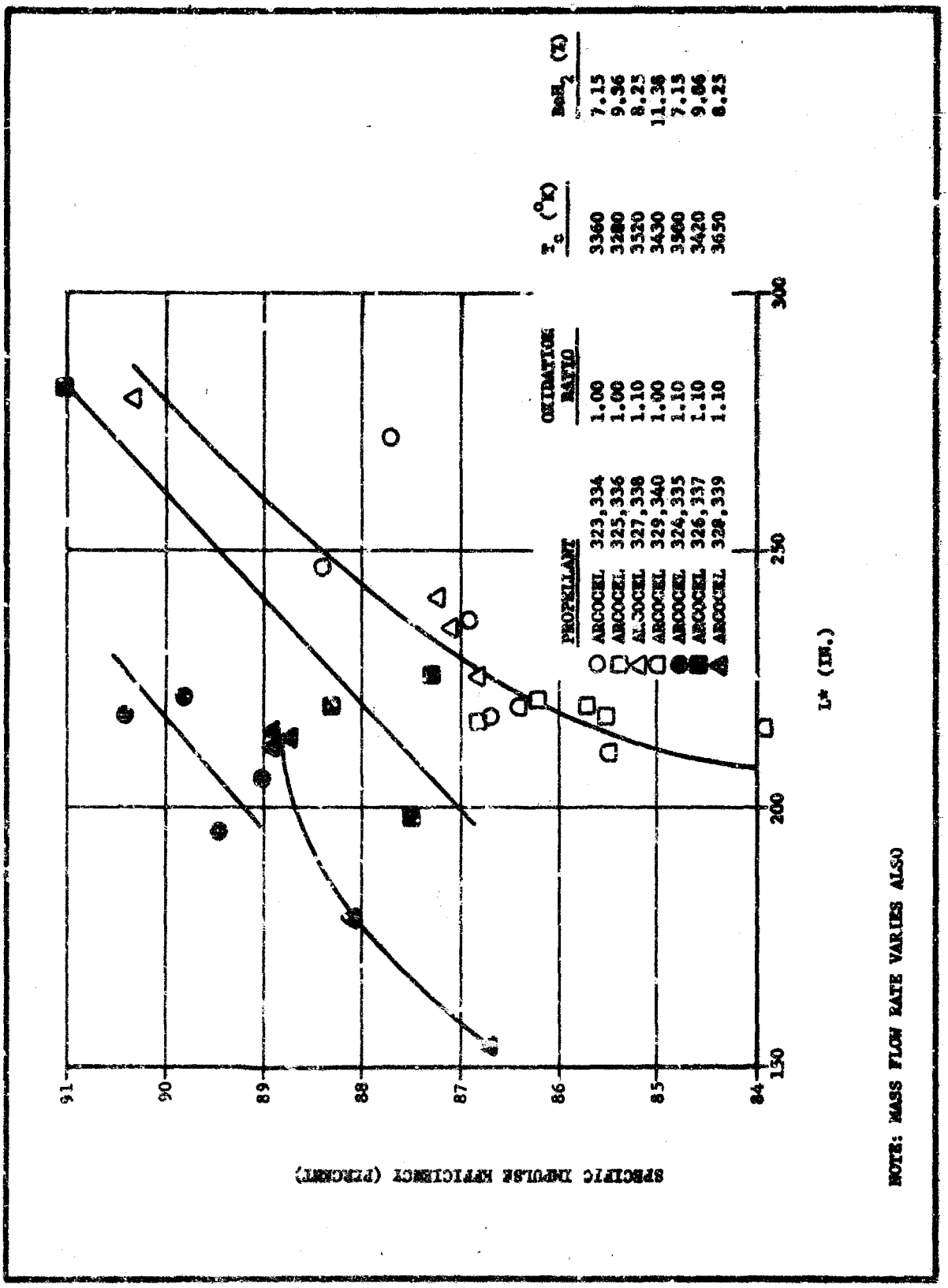

Figure 11. Effect of Residence Time (L*) on Specific Impulse Efficiency

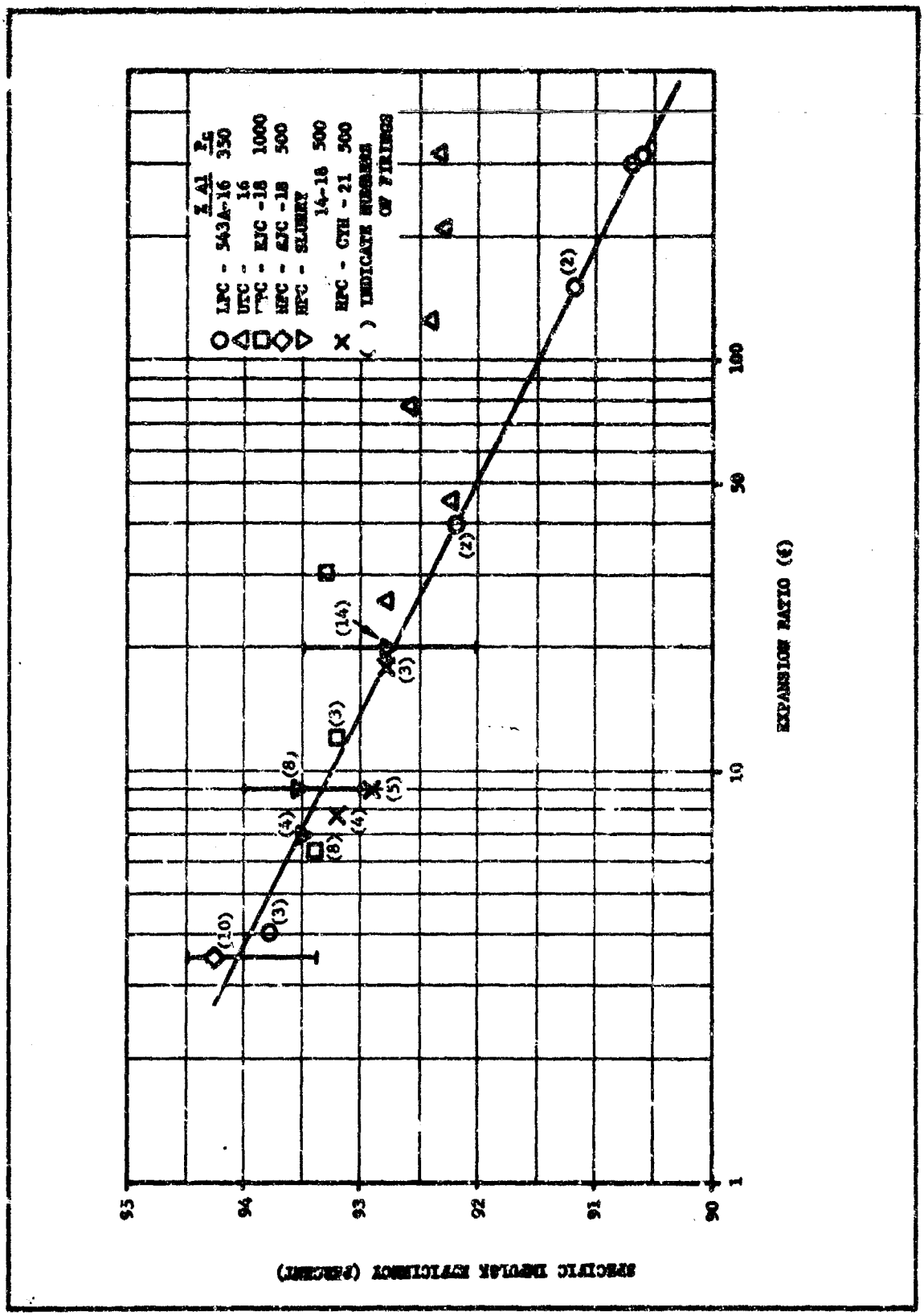

Figure 12. Effect of Expansion Ratio on Specific Impulse Efficiency of Al Propellants

constant efficiency, indicating possible frozen-flow behavior for these formulations. Arcocel 191 shows an apparent increase in efficiency with expansion ratio, followed by constant efficiency at higher expansion ratios, indicating equilibrium flow for exit temperatures above approximately 2000° K and frozen flow thereafter. These correlations do not prove frozen flow, since other effects (items (a) and (b) above) could give similar results.

All three LMH-2 propellants for which data are available exhibit the same type efficiency behavior with expansion ratio as do the Be formulations. All three are intermediate in flame temperature, and all three contain considerable Be in addition to the LMH-2. The data are insufficient for definite conclusions at this time. Arcane 24 shows 1.5-percent efficiency loss between expansion ratios of 10 and 100, not greatly different from the loss predicted from considering heat transfer to the nozzle wall. All the other Be and LMH-2 propellants show at least 2-percent loss, indicating that another loss is also operative.

One important facet of obtaining good impulse efficiencies with metalized propellants is the minimization of velocity lag. This becomes increasingly important at high-metal levels, since the efficiency losses due to velocity lag can be expected to be proportioned to the percentage of condensables present. Thus, particularly at high-metal loadings, nozzle geometry must be optimum in order to achieve good efficiencies. Of particular importance is a good approach contour. Figures 14 and 15 show the effect of nozzle contouring on impulse efficiency as given by B. Brown.[4] Minimizing the approach angle and use of a large approach contour radius are shown to be necessary for good efficiency. In small motors, however, these factors must be balanced against increased heat losses for the longer nozzle. As a consequence, the present Hercules 15-lb-charge (15PC) motor has an approach angle of 30 degrees with a contour radius equal to the throat diameter; whereas the FPC motor has a 15 degree approach with the same contour radius ratio.

Design of these contours was based on experience with aluminized propellants and may not be optimum for LMH-2 propellants or the high Be analog formulations. There is some evidence to indicate that the 15 degree approach for FPC motors may not be optimum for even the low-metal VCP formulation. For example, FPC-motor, sea-level firings of VCP at Bacchus with the 15 degree approach consistently give efficiencies of 92.4 percent. But, several FPC altitude firings of VCP at Arnold Center with a 5 degree approach have given efficiencies of 93 percent. These data are also plotted in Figure 15. This reversal of the expected decrease in efficiency with increasing expansion ratio may have been due to the shallow approach angle. Nozzle approach contouring as a means of improving impulse efficiency at high metal loadings was therefore included in the program.

[4]Refer to List of References

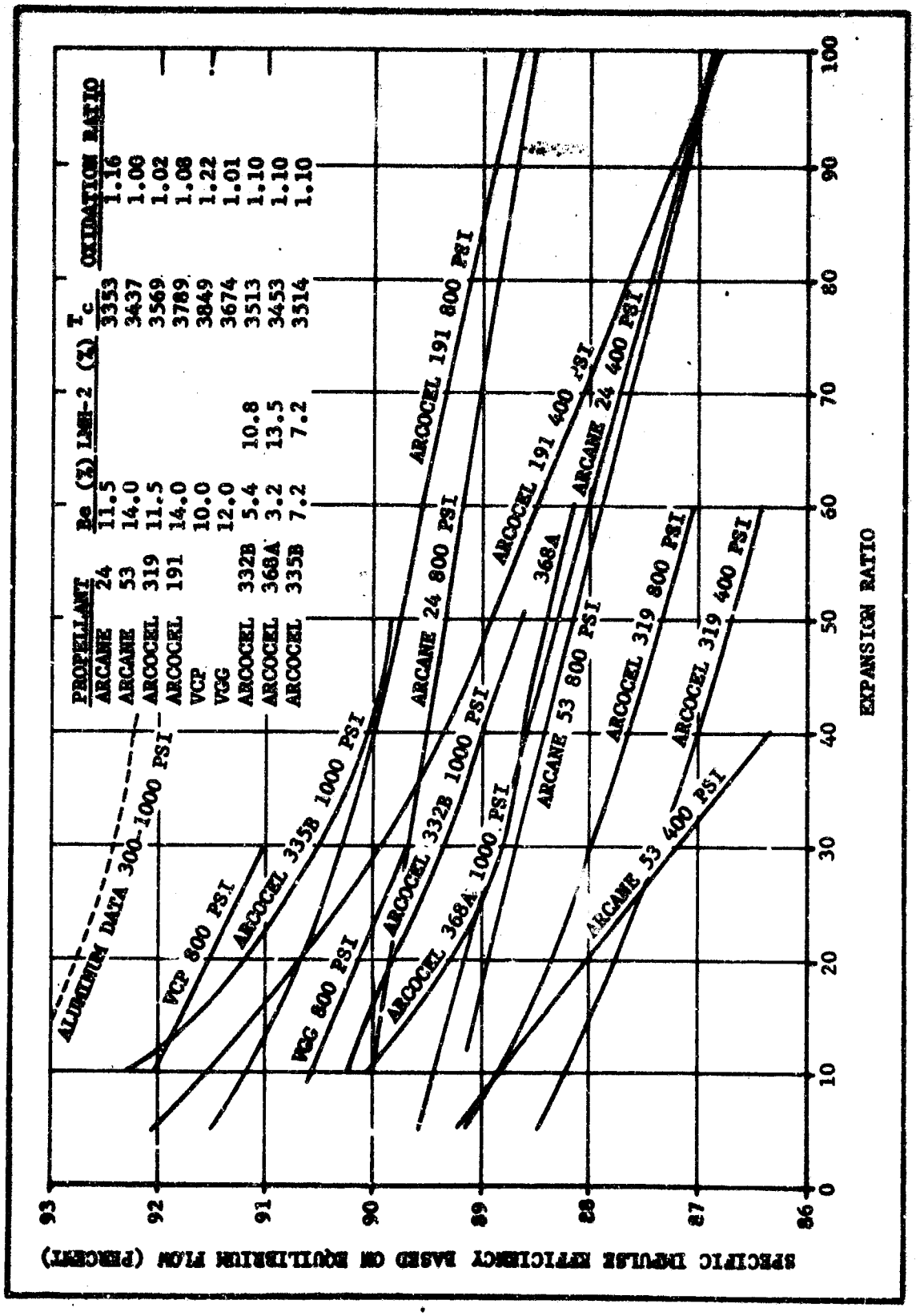

Figure 13. Effect of Expansion Ratio on Efficiency of Be and LMH-2 Propellants

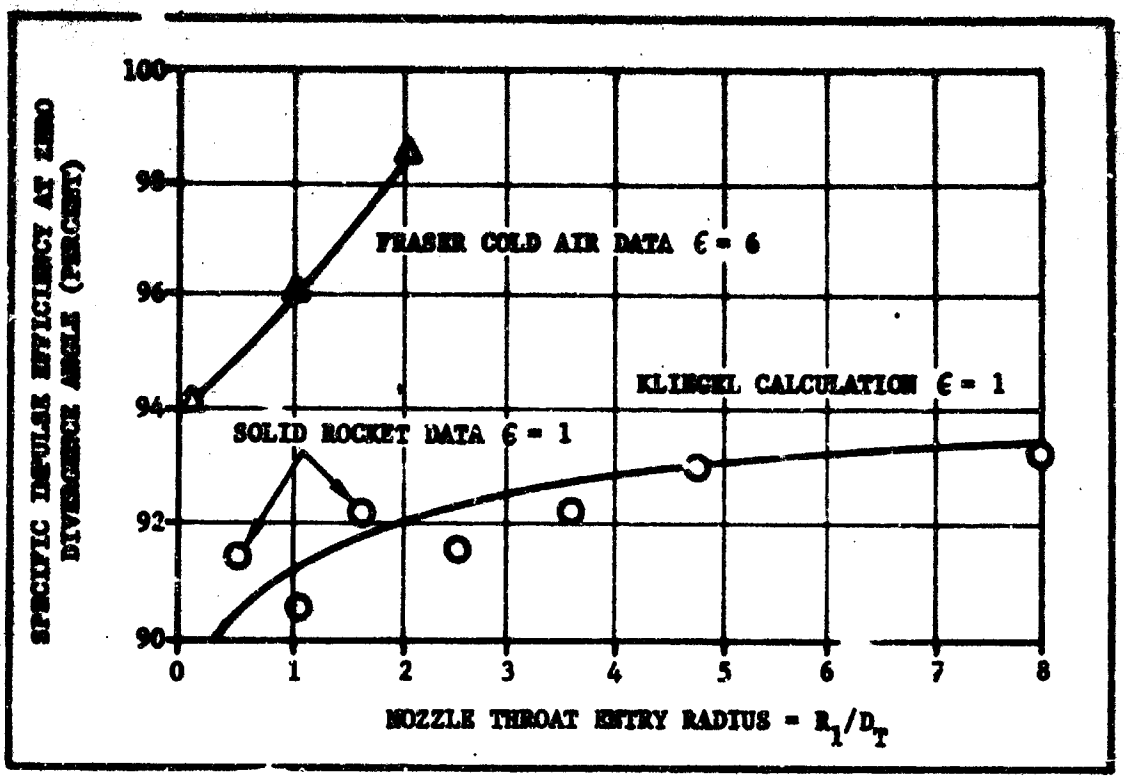

Figure 14. Effect of Nozzle Throat Contour on Efficiency

2. Propellant Parameters

The available data has demonstrated that motor efficiency is decreased at low combustion temperatures. This effect has already been noted in the discussion of L* and mass-flow rate. The following discussion shows that a chamber temperature of about 3700° K is required for efficient combustion of Be or LMH-2 propellants.

Figure 16 shows efficiency as a function of flame temperature for Be propellants. As shown, two distinct lines can apparently be drawn: one for hydrocarbon propellants (AP sole oxygen source) and one for nitrasol propellants. The hydrocarbon line shows a higher efficiency at a given flame temperature. However, this line is based on data from Aerojet, obtained in progressive 100-lb motor firings. A round-robin series of firings conducted between Hercules and Aerojet[5] has shown a 1-percent bias between the Aerojet motor and the Hercules FPC motor. As a consequence, 1 percent was subtracted from the Aerojet data. The same data is corrected for this bias in Figure 17 and shows little effect of oxygen source (AP versus nitrasol binders) on impulse efficiency. Attempts to remove the scatter from this data by combining flame temperature with total metal were unsuccessful. However, when Figure 17 is replotted with parameters of constant oxidation ratio (Figure 18), a trend toward higher efficiencies with higher

[5]Refer to List of References

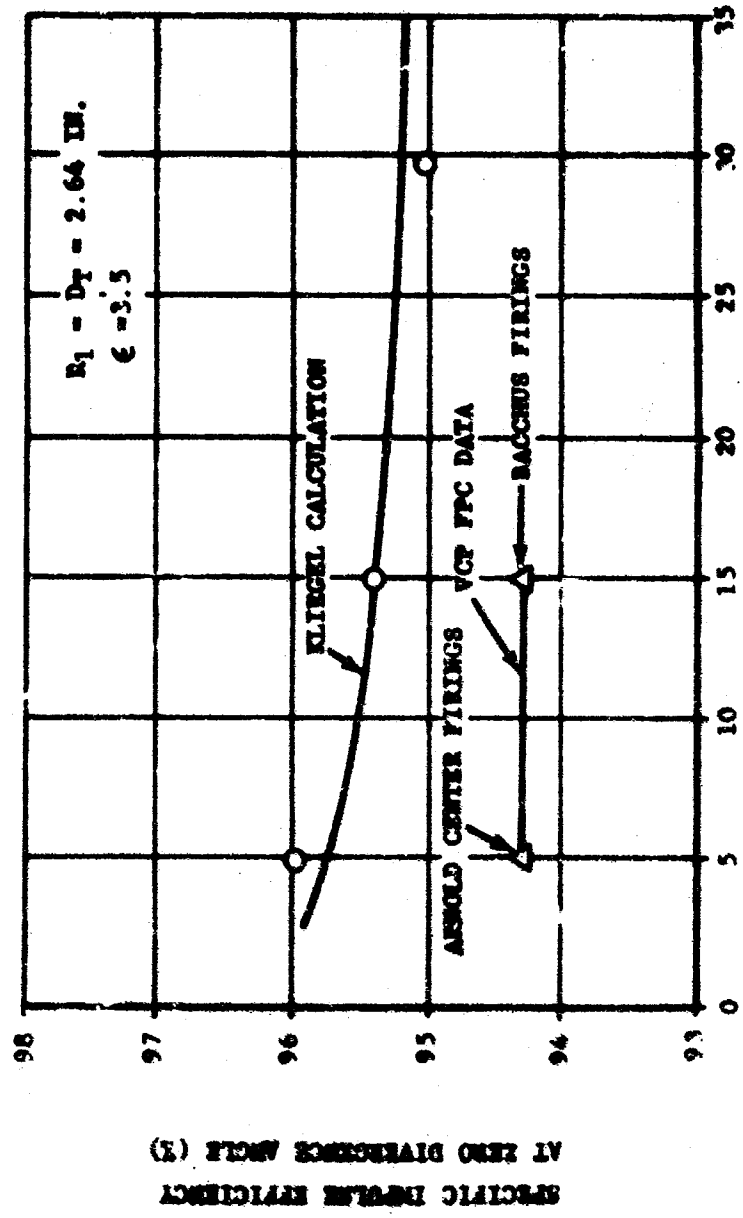

Figure 15. Effect of Convergence Angle on Nozzle Efficiency

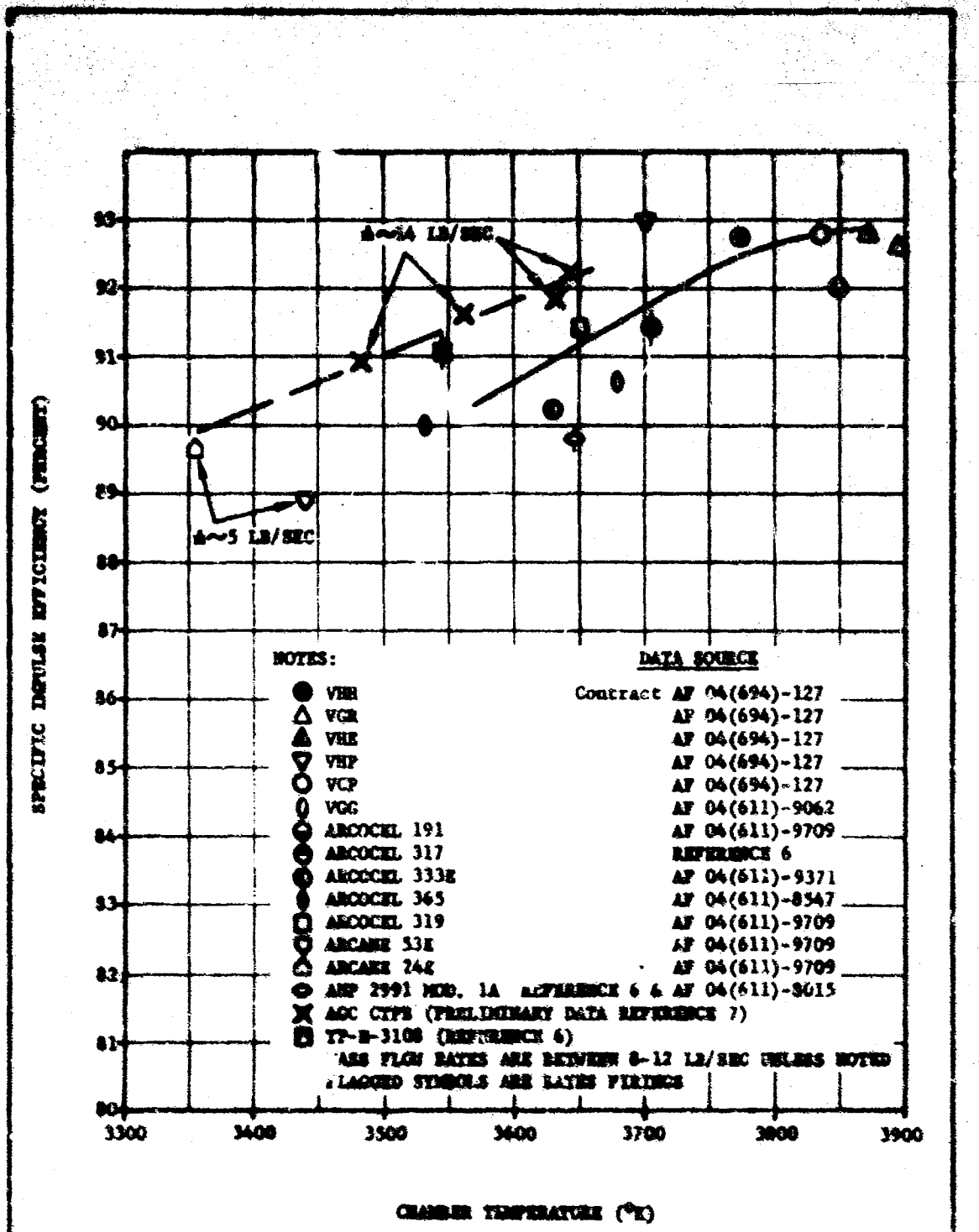

[6,7] Refer to List of References

Figure 16. Effect of Chamber Temperature on Specific Impulse Efficiency of Selected Be Propellants

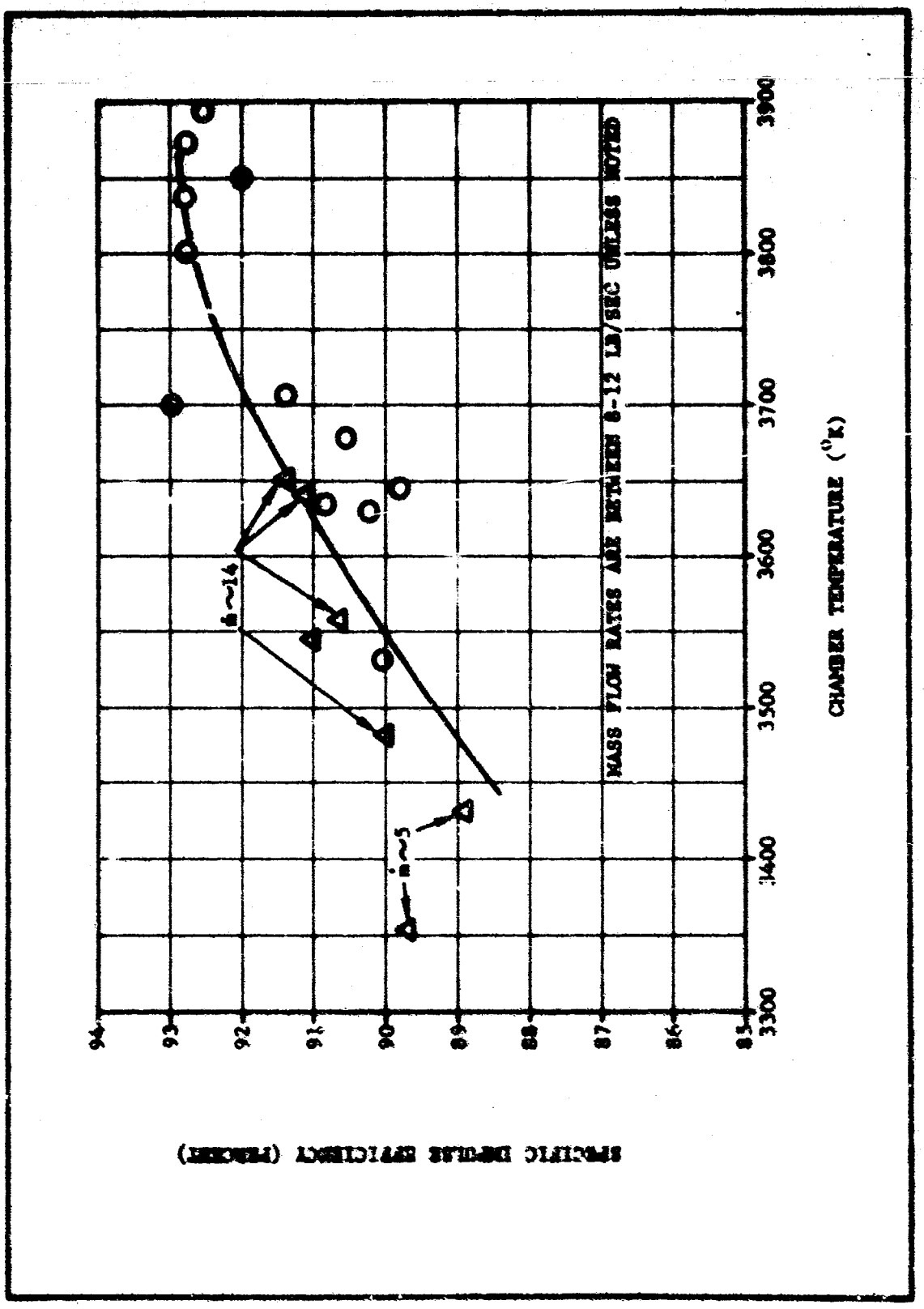

Figure 17. Effect of Chamber Temperature on Specific Impulse Efficiency (Corrected) of Selected Be Propellants

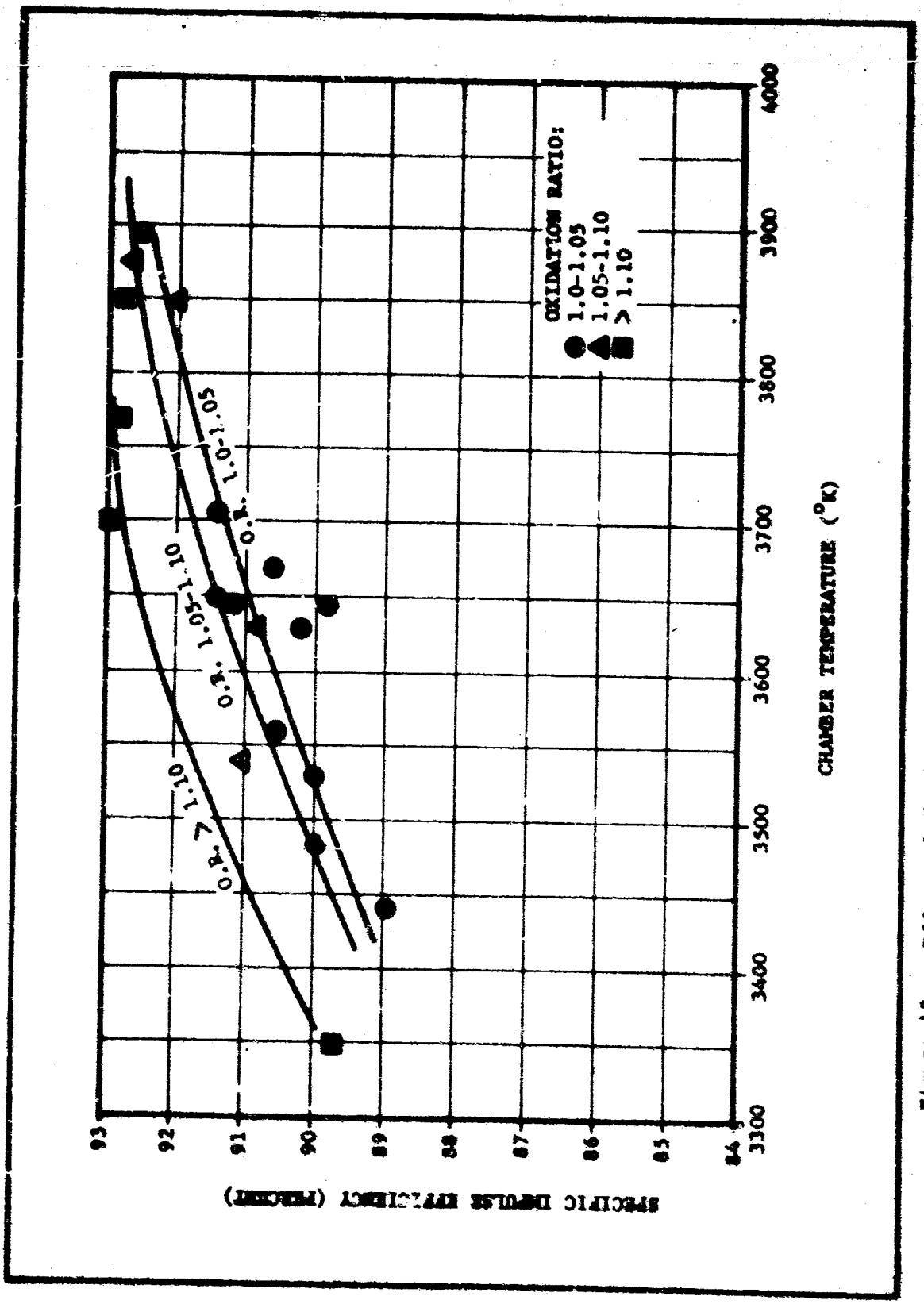

Figure 18. Effect of Chamber Temperature and Oxidation Ratio on Specific Impulse Efficiency of Be Propellants

oxidation ratios at constant temperature appears. Unfortunately, data at high oxidation ratios for low-flame-temperature propellants is limited, and the correlation requires further investigation.

The substitution of HMX for AP affords the possibility of extending the range of the ratio AP/Be to zero. The effect on efficiency of varying this parameter is shown in Figure 19. A decrease in efficiency is evident. This decrease may be: (a) Due to decreased chamber temperatures at the higher AP/Be ratios; (b) an indication that the heat of formation of one or more of the Be-Cl species may be in error; and (c) an indication of an effect of oxygen source on combustion efficiency.

Extension of the Be temperature correlation to LMH-2 propellants is shown in Figure 20. A much larger scatter is noted with the Be line correlating only approximately 75 percent of the data within ± 1 compared to 95 percent of the Be data. Based on the success of the Be-vs-temperature plot at constant oxidation ratio, the LMH-2 data was next correlated on this basis, as shown in Figure 21. However, no real trend as shown with Be propellants was observed. In order to compare the results of the success of this correlation with other correlations, an envelope of data points was constructed, as shown in Figure 21. This envelope accounted for approximately 85 percent of all the data points.

Attempts at correlating the data based on total metal and oxidation ratio met with less success. Figure 22 shows efficiency as a function of LMH-2 loading. Again the data is widely scattered, but shows a definite loss in efficiency at high LMH-2 loadings and is best shown by an envelope of data points. The effect of the ratio of the excess oxygen to weight percent LMH-2 on efficiency is shown in Figure 23. A trend toward higher efficiencies with excess oxygen is shown, but again only an envelope can be drawn. Based on these correlations it is observed that flame temperature influences LMH-2 efficiency more than any other parameter. Consequently, the extremes of the temperature envelope shown in Figure 21 were used to design formulations capable of meeting the program objective.

Three other factors have also been investigated, which show an effect on LMH-2 efficiency, two of which are related to the oxygen source. Atlantic Research has reported that both the ratio of AP/LMH-2 and the AP particle size affect LMH-2 efficiency. Figure 24 shows the effect of AP particle size on impulse efficiency for both Al and Be propellants. The LMH-2 data show a decrease in efficiency with increased AP particles size consistent with the Al propellant data. The third factor is LMH-2 particle size. Figure 10 compared pressure effects on efficiency for Arcocel 332A containing unground LMH-2 with Arcocel 332 containing ground LMH-2. The efficiency is 0.7 percent better with the ground LMH-2. All three of these factors point toward more intimate contact between LMH-2 and the primary oxidizer as a means of improving combustion efficiency of LMH-2.

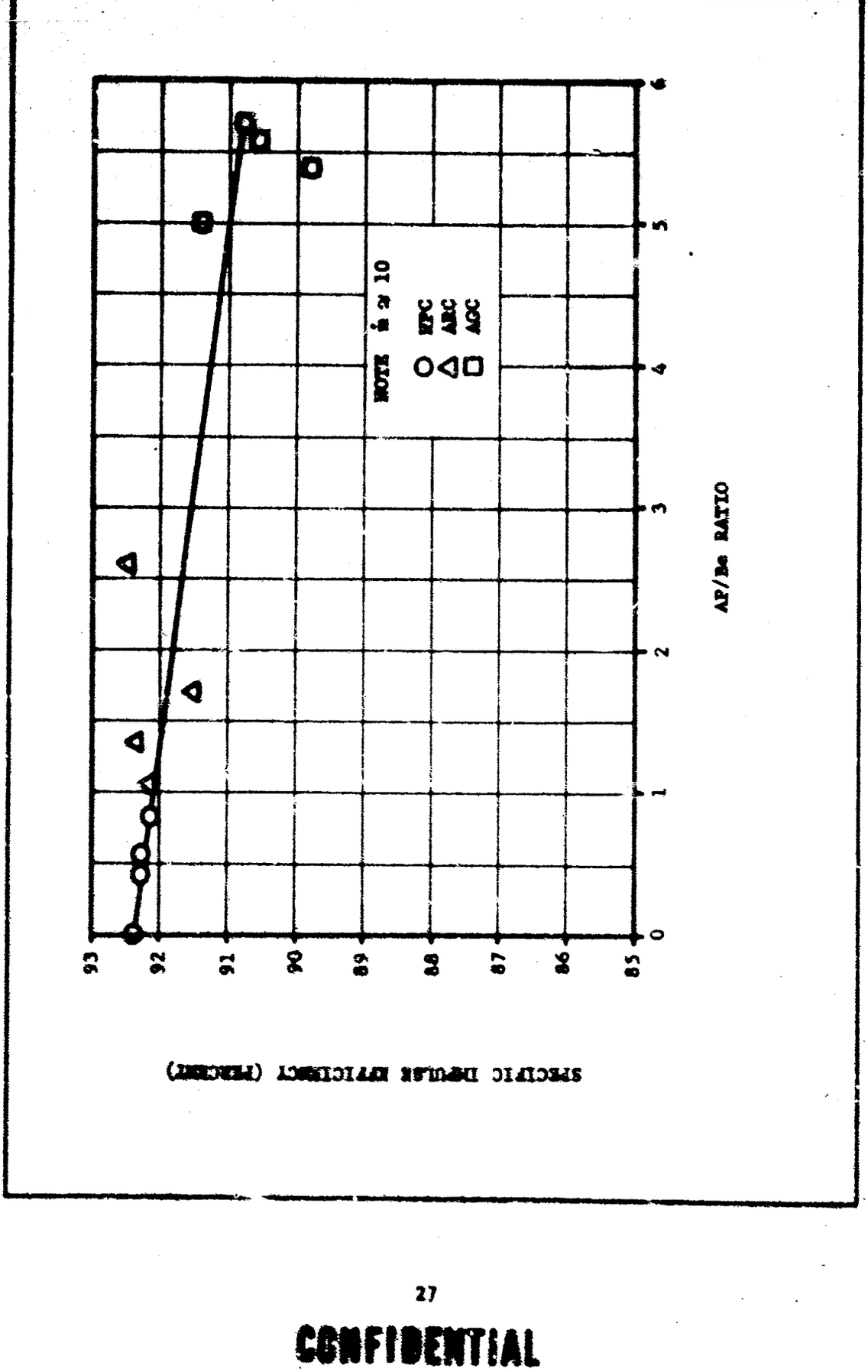

Figure 19. Effect of Oxygen/Oxidizer Source on Specific Impulse Efficiency

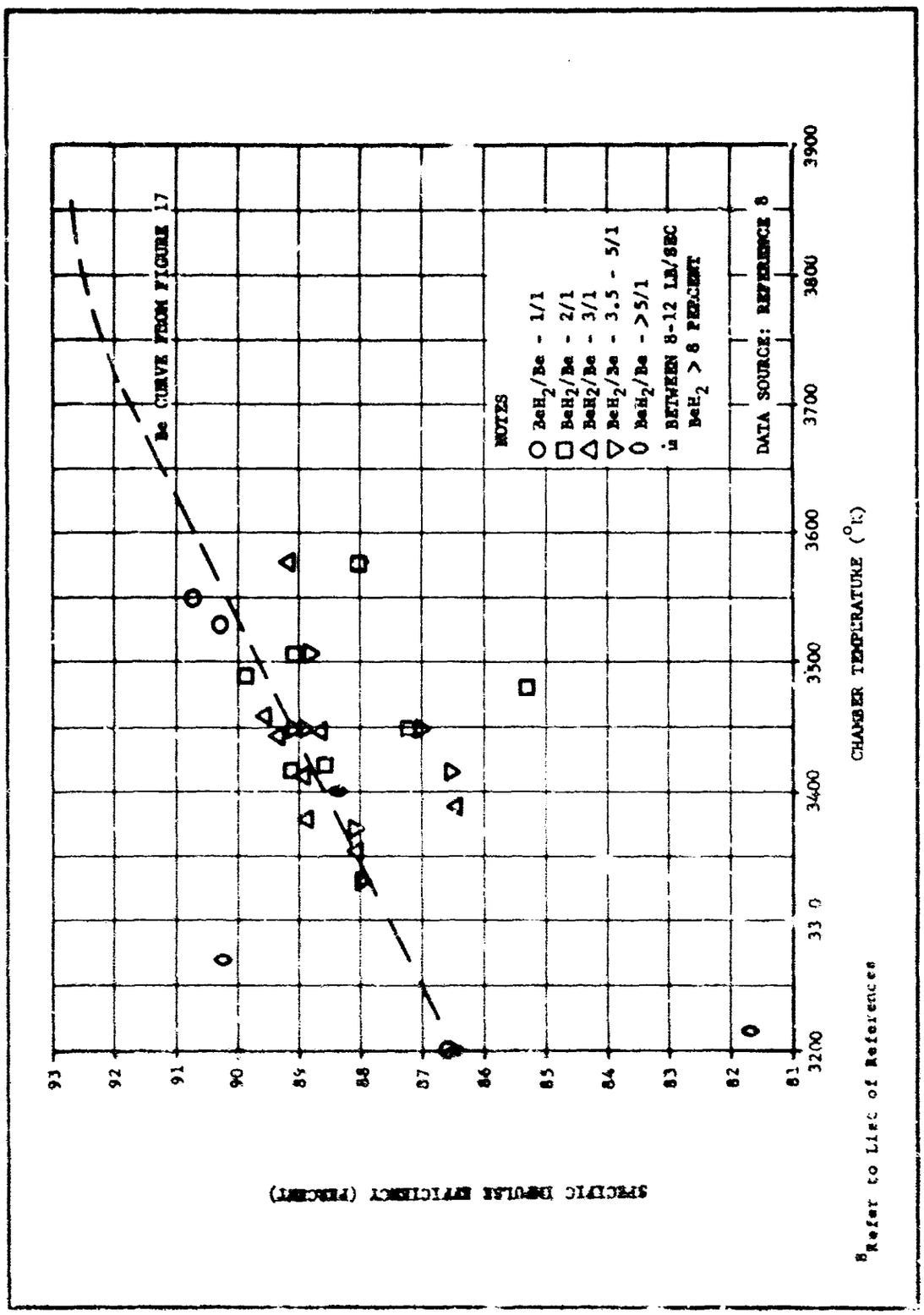

[a] Refer to List of References

Figure 20. Effect of Chamber Temperature on Specific Impulse Efficiency for LMH-2 Propellants

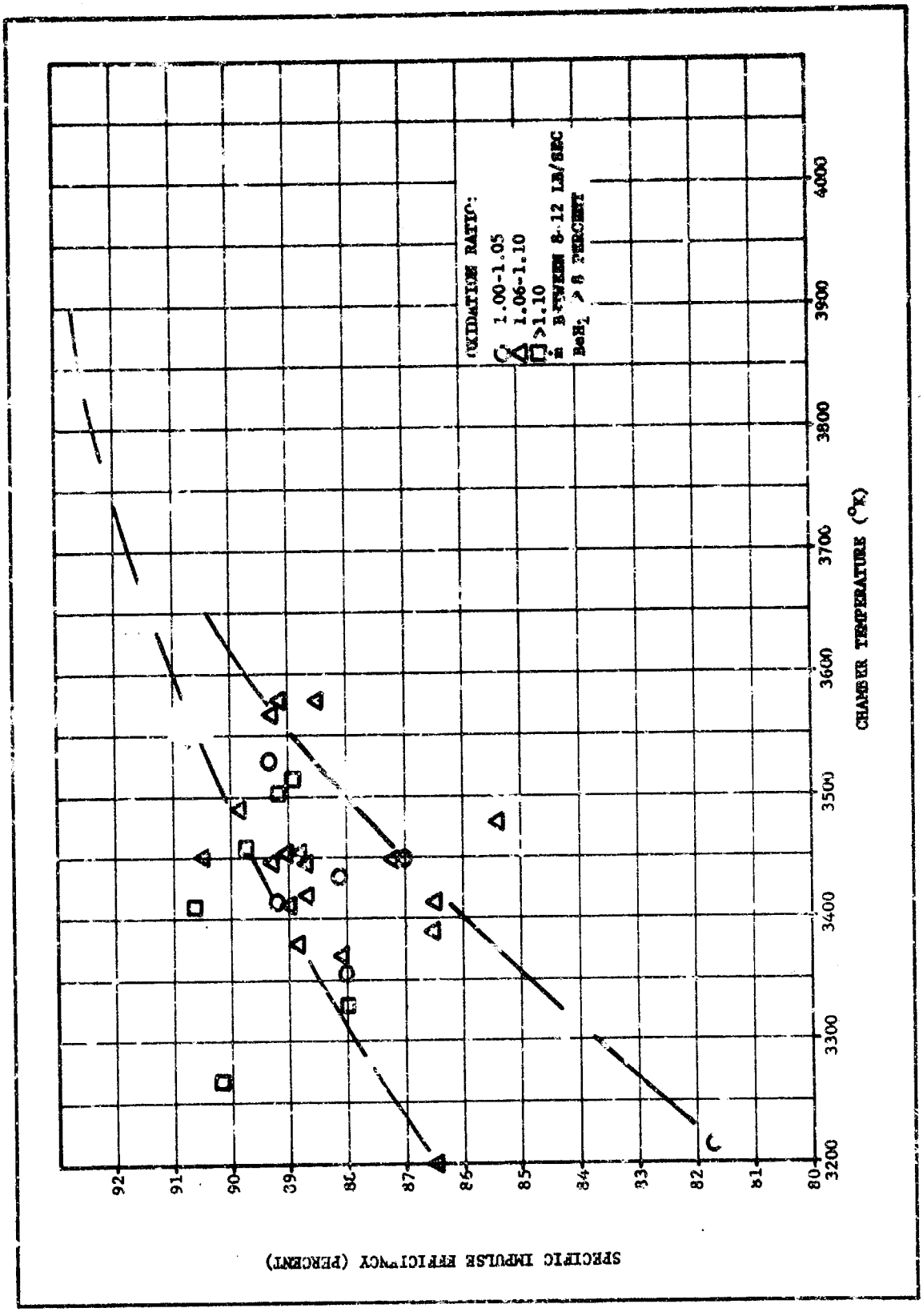

Figure 21. Effect of Chamber Temperature and Oxidation Ratio on Specific Impulse Efficiency of LMH-2 Propellants

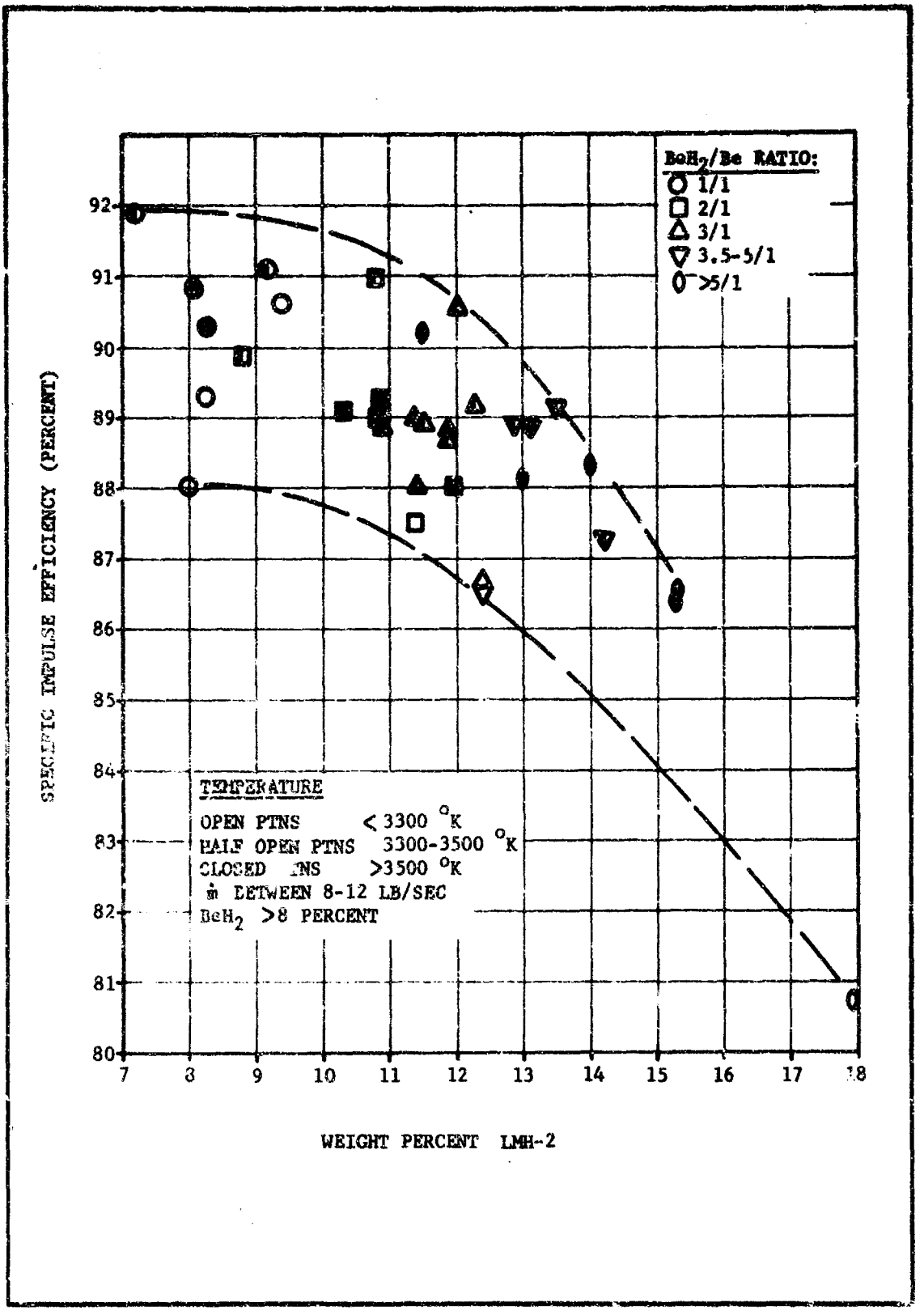

Figure 22. Effect of LMH-2 Content on Specific Impulse Efficiency

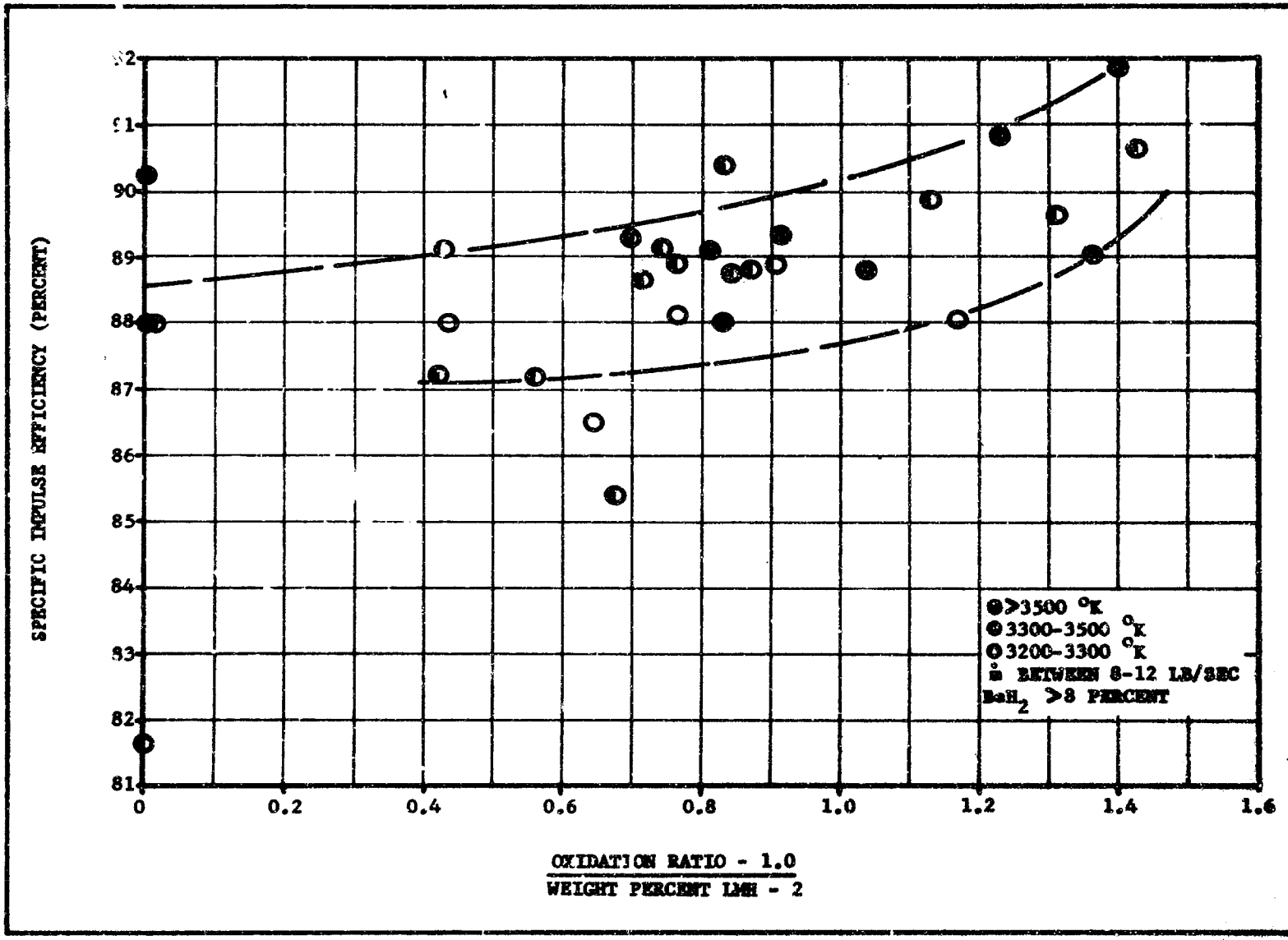

Figure 23. Effect of Excess Oxygen/LMH-2 Ratio on Specific Impulse Efficiency

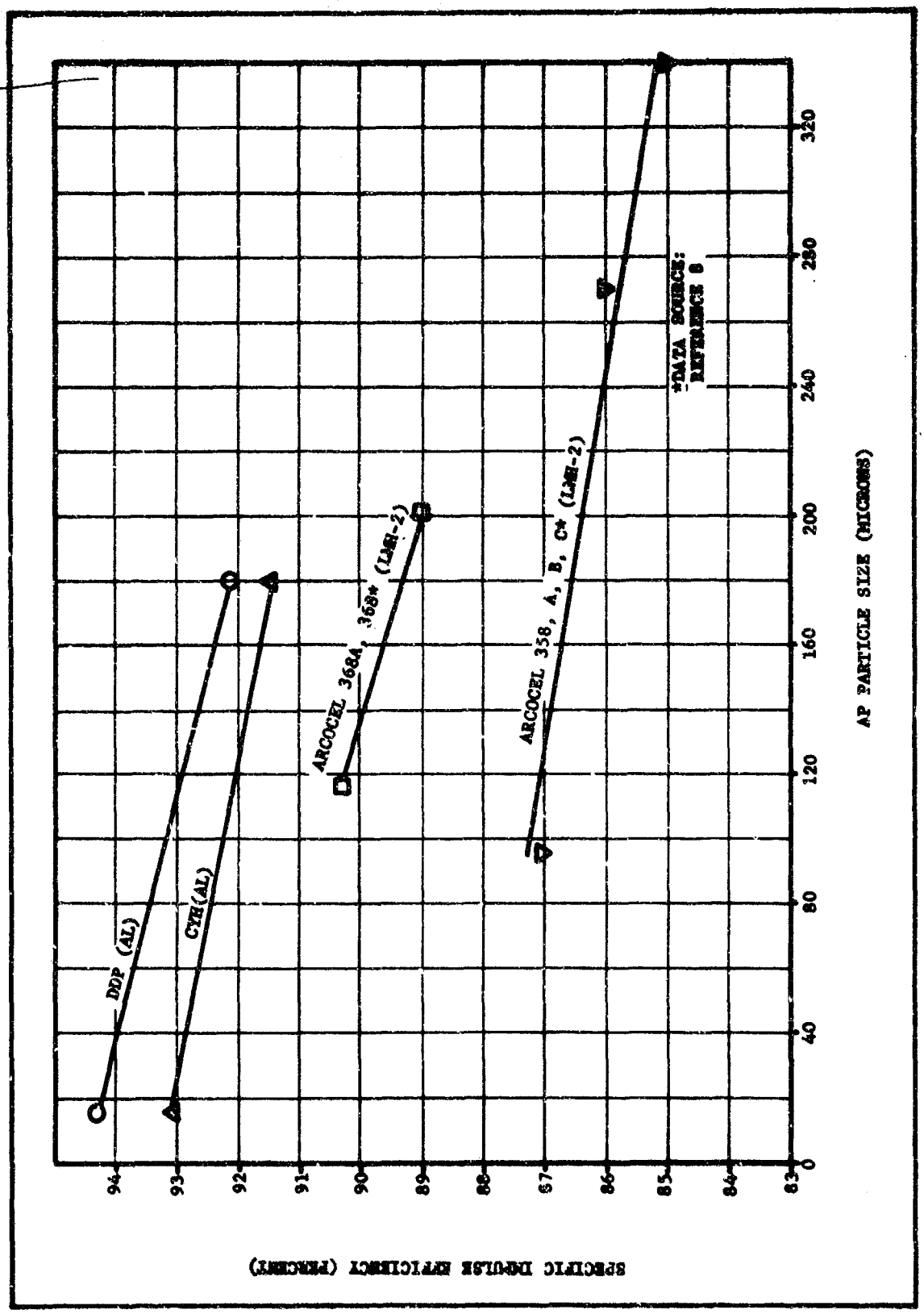

Figure 24. Effect of AP Particle Size on Specific Impulse Efficiency

CONFIDENTIAL

Based on this preliminary analysis, the following factors influencing the motor efficiency of LMH-2 and beryllium propellants appeared to be important:

(a) High-flame-temperature and high-oxidation-ratio propellants show no loss in efficiency with decreasing pressure down to 500 psia.

(b) Low-flame-temperature and low-oxidation-ratio propellants show losses in efficiency with decreasing pressure. This effect could not be completely separated from mass flow or residence time effects on efficiency.

(c) Both Be and LMH-2 propellants show a strong dependence on high flame temperatures for good efficiency.

(d) Oxidation ratio has a strong effect on the efficiency of low temperature Be propellants. There is an indication that oxidation ratio is important for LMH-2 efficiency, but only a general trend could be obtained.

(e) Correlations based on total LMH-2 content show a loss in efficiency at high-hydride loadings (greater than 15 percent).

(f) More intimate contact of oxidizer and fuel in LMH-2 systems should improve efficiency based on efficiency effects of AP particle size, AP/LMH-2 ratios, and ground LMH-2.

C. THEORETICAL SPECIFIC IMPULSE CALCULATIONS

Theoretical Isp calculations were made for a wide variety of systems containing Be and LMH-2 to support the formulation design effort. Details of these calculations are given in Appendix A. In summary, based on preliminary correlations it was found necessary to use as high an energy binder as practical with conventional oxidizers to ensure with reasonable confidence that specific impulse goals would be attained.

D. FORMULATION AND TEST DESIGN

The correlations showed several areas in which further investigation was needed before reliable predictions could be made for the performance of both Be and LMH-2 propellants. In general, the Be correlations were significantly better than for LMH-2 systems. Additional Be testing was warranted in the following areas for further clarification of propellant parameters on impulse efficiency:

(1) High metal levels (15.5 percent) at high flame temperatures and oxidation ratios

(2) High metal levels and high flame temperatures at low oxidation ratios

(3) Evaluation of oxidizers different from AP and HMX, such as AN and $TAGNO_3$

(4) Additional testing at high oxidation ratios and high flame temperatures for determining the effect of AP particle size

Further testing was also needed in the following areas for clarification of motor parameters:

(1) Optimization of nozzle geometry at high metal levels

(2) Increased L* studies for both efficient and inefficient Be propellants and LMH-2 propellants

For LMH-2 systems, the following testing was needed to clarify propellant parameters:

(1) High LMH-2 loadings at flame temperatures in excess of 3600° K and at high oxidation ratios

(2) Comparative evaluation of AP, AN, and HMX oxidizers

(3) More intimate contact between oxidizer and LMH-2

(4) Addition of fluorine to LMH-2 to aid combustion and to reduce two-phase flow losses.

The Task II and Task III effort was designed to clarify these areas for Be and LMH-2 propellants.

Table II contains a list of the Be formulations chosen for testing to better define the effect of propellant parameters on performance. VIH propellant was designed to have the same metal level and oxidation ratio as the proposed 19-percent LMH-2/AP formulation. VII was formulated to show the effect of efficiency of the AP:Be ratio at a constant metal level, flame temperature, and oxidation ratio. VIJ was also formulated with 45 and 180μAP to demonstrate the effect of AP particle size on impulse efficiency thus providing the performance trade off between AP particle size and LMH-2 loading necessary to optimize delivered impulse. The VIK, VIL, VIM, and VIN propellants represent the Be analogs of the 17-percent LMH-2, AP; 15-percent LMH-2, AP HMX; 19-percent LMH-2, AN; and 17-percent LMH-2, AN formulations, respectively, in both metal level and oxidation ratio. VIO was designed to determine the effect of oxidation ratio on efficiency at low metal levels, and VIG was formulated to evaluate $TAGNO_3$ as an oxidizer.

TABLE II

BERYLLIUM PROPELLANTS FOR FORMULATION SCREENING

Formulation	Be (wt %)	Oxidizer Type	I_{sp} (sec)	T_c (°K)	O.R.*	Number of Firings** 1000 psi	Number of Firings** 500 psi	Purpose
VCP	10	HMX/AP	283	3840	1.22	3	3	Control
VIH	15.5	AP	278	4173	1.17	3	3	LMH-2 19% Analog with respect to TM*** and O.R.
VII	15.5	AP	279	3971	1.05	3	3	LMH-2 19% Analog with respect to TM; lower O.R.
VIJ	15.5	AP	277	4145	1.17	3	--	Total AP effect
VIK	14.0	AP	277	4109	1.27	3	3	Analog with respect to TM and O.R.
VIL	12.0	HMX/AP	281	4008	1.24	3	3	LMH-2 15% Analog AP/HMX with respect to TM and O.R.
VIM	15.5	AN	281	3820	1.17	3	3	LMH-2 19% Analog with respect to TM and O.R.

*, **, ***, See end of table

TABLE II (Cont)

BERYLLIUM PROPELLANTS FOR FORMULATION SCREENING

Formulation	Be (wt %)	Oxidizer Type	I_{sp} (sec)	T_c (°K)	O.R.*	Number of Firings** 1000 psi	Number of Firings** 500 psi	Purpose
VIN	14.0	AM	279	3744	1.28	3	3	LMH-2 17% Analog with respect to TM and O.R.
VIO	8.0	HMX/AP	281	3745	1.38	3	--	O.R. effect at low TM
VIG	12.5	$TAGNO_3$/AP	291	3633	1.02	3	--	Evaluate $TAGNO_3$
						30	21	

*O.R. = Oxidation Ratio

**Optimum expansion ratio at Bacchus ambient, number of firings originally scheduled

***TM = Total metal level

Based on the theoretical calculations and using the temperature correlation derived in Figure 21, six candidate LMH-2 formulations were chosen which were designed to confirm the expected efficiency envelope and to attain the program objective of a demonstrated Isp≥280 sec. Table III contains the LMH-2 propellants together with the theoretical and predicted performance values.

Additional testing to determine the effect of motor parameters on the performance of Be and LMH-2 propellants was also accomplished in Task II as follows:

Motor Parameter	Formulation	Number of Firings
Nozzle Approach Angle		
15-degree Approach	VCP	2
15-degree Approach	VIJ	4
5-degree Approach	VCP	2
5-degree Approach	VIJ	3
High L*	VCP	2
High L*	VII	2
High L*	VIY	9

E. PROGRAM DATA ANALYSIS

1. Beryllium Firings

Data was available from the 70 Be firings on this program as outlined under Formulation and Test Design. Additional data was also available on three high-performance Be propellants (VIB, VID, and VIF) developed by Hercules under Contract AF 04(694)-127. Pertinent data on these formulations is given in Table IV.

A complete summary of the individual firings made on this program is given in Appendix B and additional details in Section III. Table V contains a summary of these data. A least squares analysis was performed on the Be efficiency firings for chamber pressure effects. (The data from this analysis are summarized in Table V.) This analysis allowed accurate comparison of all propellants tested at 1000 psia chamber pressure. In addition, efficiencies for the selected propellants specifically tested for pressure effects are summarized at 500 psia. Conclusions based on these data are contained in the following subparagraphs.

TABLE III

LMH-2 PROPELLANTS FOR FORMULATION SCREENING

Propellant Type	Binder Level (wt %)	Oxidizer (wt %)	LMH-2 (wt %)	I^{o}_{1000} (sec)	T_c (^{o}K)	O.R.*	Impulse Efficiency Range	Predicted I_{sp} Del (H)**	Predicted I_{sp} Del (L)***
VIX	62	AP	15	304	3678	1.34	90.7-91.6	279	276
VIY	62	AP	17	309	3679	1.22	90.7-91.6	283	280
VIZ	62	AP	19	314	3671	1.11	90.6-91.5	287	285
--(1)	62	AP/HMX	15	307	3636	1.23	90.2-91.2	280	277
VJA	61	HMX	15	309	3621	1.15	90.0-91.1	282	278
--(1)	62	AN	17	309	3529	1.25	88.6-90.4	279	274
VJI	61	HMX	17	314	3623	1.06	90.0-91.1	286	283
VJL	62	AP/HMX	17	313	3614	1.08	89.9-91.0	285	281

*Oxidation Ratio
**(H) High value expected from Figure 21
***(L) Low value expected from Figure 21

(1) The VJI and VJL formulations were substituted for these initial formulations

TABLE IV

ADVANCED Be PROPELLANTS

Propellant Type	VIB		VID		VIF	
Formulation (wt %)						
DB Binder	44.0		44.0		45.0	
AP	--		--		6.0	
HMX	47.0		44.0		37.0	
Be	9.0		12.0		12.0	
Theoretical Performance						
Isp (1000/14.7)	286.4		289.1		286.4	
Tc (^{o}K)	3780		3885		3897	
Oxidation Ratio	1.17		1.02		1.05	
Delivered Performance[1]						
Chamber Pressure (psia)	486	846	518	911	381	754
Mass Flow (lb/sec)	5.5	7.8	5.7	7.8	6.3	8.8
L* - VF/A_t	247	314	243	318	171	228
I_{sp1000}^{15} (lb_f-sec/lbm)	264.8	267.7	268.9	267.9	267.0	267.6
Efficiency	92.5	91.9	93.0	92.7	93.2	93.5
No. of Firings	3	3	3	3	2	2

(1) Determined in FPC motor firings

Note: Data obtained from Contract AF 04(694)-127

TABLE V

BALLISTIC PERFORMANCE SUMMARY

Formulation	Percent Be	Oxidizer	T_c[1] (°K)	OR[2]	P_c[3] (psia)	$\dot{w}$[4]	No. of Firings	Efficiency (%)	Isp_{1000}^{15} (lbf-sec/lbm)	Efficiency vs P_c
Efficiency Studies										
VCP	10.0	AP/HMX	3850	1.22	500	7.9	3	92.01	260.4	92.34 - 0.00065 P_c
					1000	8.2	3	91.69	259.5	
VIJ	15.5	AP	4145	1.17	500	8.2	3	92.27	236.0	91.67 + 0.00121 P_c
					1000	8.6	2	92.88	257.7	
VIH	15.5	AP	4173	1.17	1000	11.3	3	93.36	259.5	92.36 + 0.00100 P_c
VII	15.5	AP	3971	1.05	500	6.9	3	90.71	252.8	89.87 + 0.00169 P_c
					1000	6.4	3	91.56	255.2	
VIK	14.0	AP	4109	1.27	500	11.3	3	92.84	256.7	92.08 + 0.00151 P_c
					1000	11.2	3	93.60	258.8	
VIL	12.0	AP/HMX	4008	1.24	500	12.0	3	92.99	261.4	93.43 - 0.00089 P_c
					1000	12.2	3	92.54	260.1	
VIO	8.0	AP/HMX	3758	1.38	1000	8.4	3	92.59	260.3	91.94 + 0.00065 P_c
VIG	12.5	AP/TAGNO_3	3633	1.02	1000	6.8	3	88.50	257.3	88.79 - 0.00029 P_c
VIM[6]	14.0	AN	3744	1.28	1000	6.2	4	90.50	253.5	
AP Particle Size										
VLJ-5021[a]	15.5	AP	4145	1.17	810	6.8	3	92.19	255.7	
VLJ-5031[b]	15.5	AP	4145	1.17	800	8.2	2	92.70	257.1	
VLJ-3061[c]	15.5	AP	4145	1.17	760	9.0	2	93.24	257.4	
Nozzle Contouring										
VCP[d]	10.0	AP/HMX	3850	1.17	970	7.7	2	92.28	261.2	
e					1050	8.2	2	92.36	261.4	
f					1000	8.2	3	91.69	259.5	
VLJ[d]	15.5	AP	4145	1.17	970	8.0	3	93.77	260.1	
e					1040	8.4	3	93.41	259.1	
f					1000	8.6	2	92.53	257.7	

Notes:

1. T_c = Chamber temperature
2. OR = Oxidation ratio $\left(\frac{\text{moles O}}{\text{moles C + moles metal}}\right)$
3. P_c = Chamber pressure
4. $\dot{w}$ = Mass flow rate
5. Least squares analysis for pressure dependance
6. These firings showed a sharp decrease in efficiency with pressure, only high pressure data is shown

a = 180 μ AP

b = 90 μ AP normalized to 800 psia

c = 45 μ AP

d = 5° approach angle

e = 15° approach angle

f = 30° approach angle

a. Be/AP/HMX Propellants - Temperature-Oxidation Ratio Effect

For Be/AP/HMX propellants, the highest efficiency at 1000 psia was 93.6 percent, which was obtained with the high-temperature (4109° K) and high-oxidation-ratio (1.27) propellant, VIK. Increasing the oxidation ratio to 1.38 with a decrease in metal level and flame temperature decreased efficiency to 92.6 percent (VIO firings). Decreasing the oxidation ratio to 1.05 at essentially constant flame temperature decreased the efficiency to 91.6 percent (VII firings). All of the Be/AP/HMX firings appeared to fit the same generalized temperature and oxidation ratio relationship with impulse efficiency shown in Figure 18. The effect of flame temperature and oxidation ratio on efficiency is shown in Figure 25. As noted from the VIO firings, high efficiencies can still be maintained at lower flame temperature by increasing the oxidation ratio. An extension of the data obtained from Task II firings along with the three propellants presented in Table IV to the previous temperature-oxidation-ratio correlation is shown in Figure 26. These firings are in good agreement with the earlier correlation and confirm that a strong temperature-oxidation effect does exist for Be propellants. However, the spread in data indicated other factors exert considerable influence on efficiency as well.

b. Metal Level Effect

Particle lag considerations dictate that significant losses in impulse efficiency can occur as metal loadings are increased. It is significant, therefore, that the highest efficiencies obtained at 1000 psia were with the VIK and VIL formulations having the highest metal levels (14-and 15.5-percent Be, respectively). Because of the interrelation between flame temperature, oxidation ratio, and metal level coupled with the strong efficiency-temperature effect it is impossible to separate metal level and oxidation ratio effects. For example, the data shown in Figure 25, correlated on the basis of temperature and oxidation ratio, can be correlated equally well on the basis of temperature and metal level. There is also a strong indication that metal level influences efficiency at high expansion ratios and is partially responsible for chamber pressure losses.

c. VCP, VII, VIJ, VIK, and VIL Propellants - Pressure Effects

The five propellants, VCP, VII, VIJ, VIK, and VIL, were specifically tested for pressure effects. The correlations shown previously indicated the high-flame-temperature, high-oxidation-ratio propellants showed little or no efficiency loss with decreasing pressure. It was not possible in this initial correlation to separate the added effects of mass-flow rate and L*. In this program, the mass-flow rate was held essentially constant for a given propellant at two pressure levels. The effect of chamber pressure on impulse efficiency for the five propellants is shown in Figure 27. The three propellants, VII, VIJ, and VIK, showed efficiency losses ranging from 0.6 to 0.9 percent as the pressure was decreased from 1000 to 500 psia. In contrast the VCP and VIL propellants actually showed

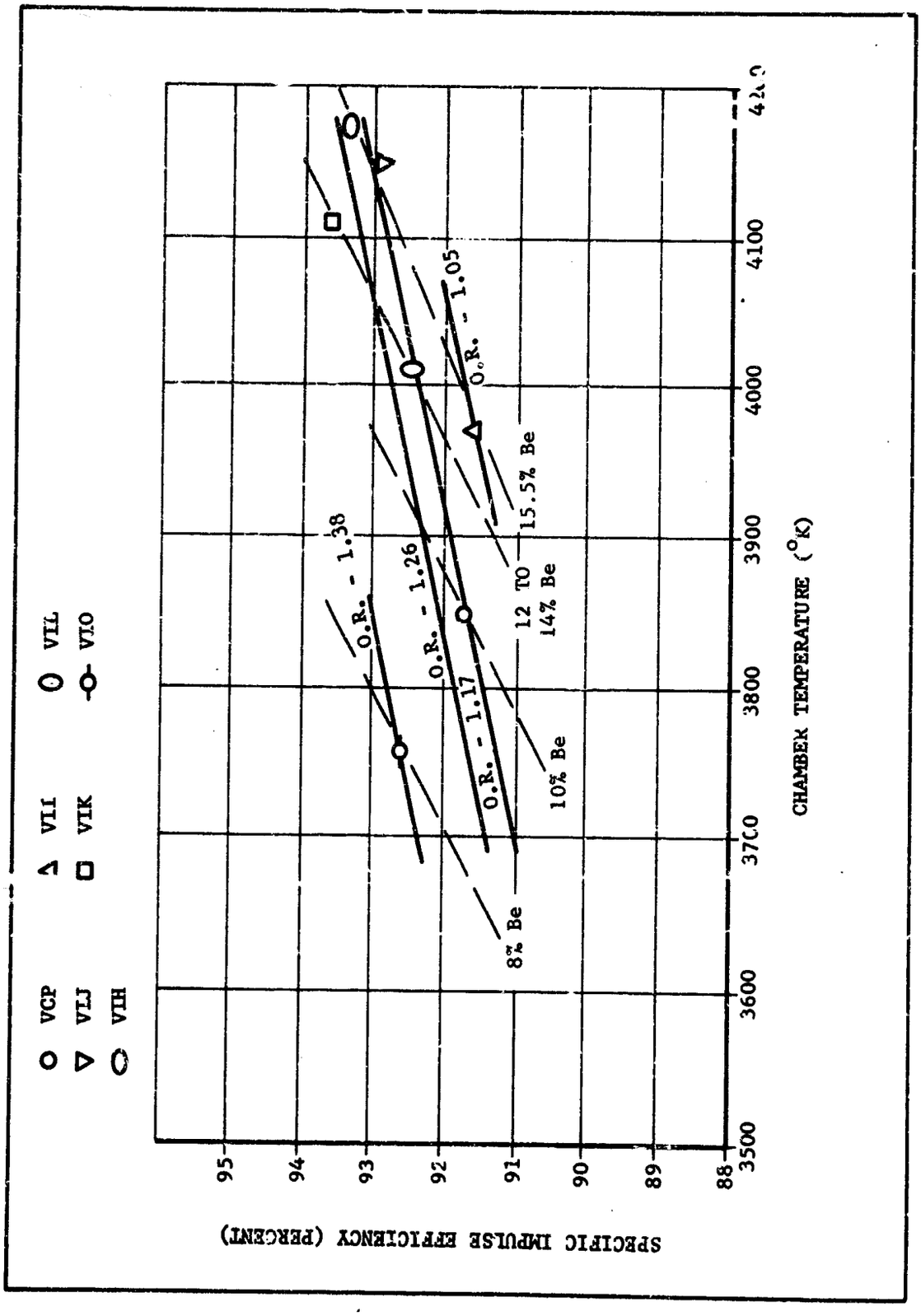

Figure 25. Effect of Chamber Temperature and Oxidation Ratio on Specific Impulse Efficiency of Task II Be Propellants

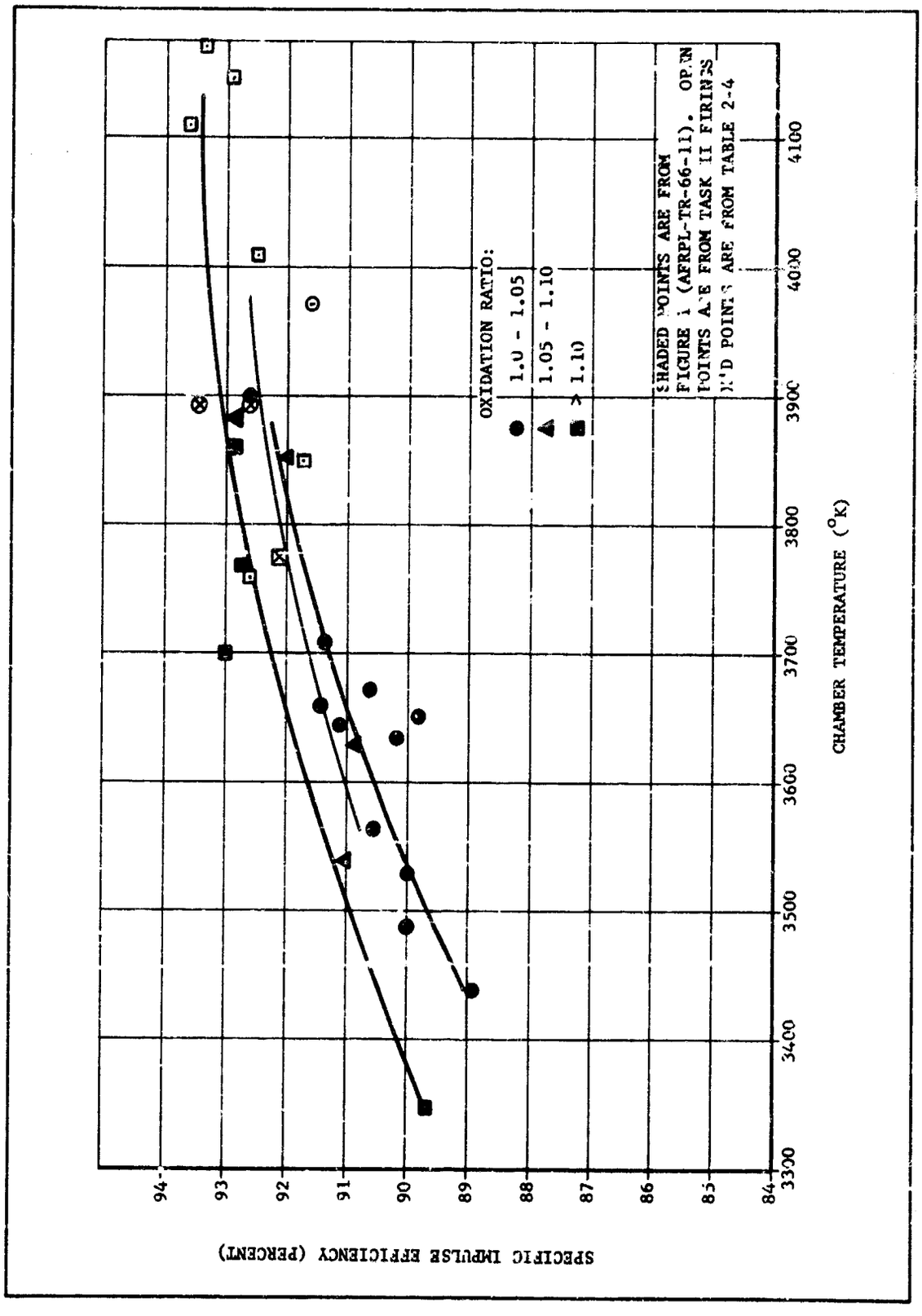

Figure 26. Effect of Chamber Temperature and Oxidation Ratio on Specific Impulse Efficiency of Fe Propellants (Revised)

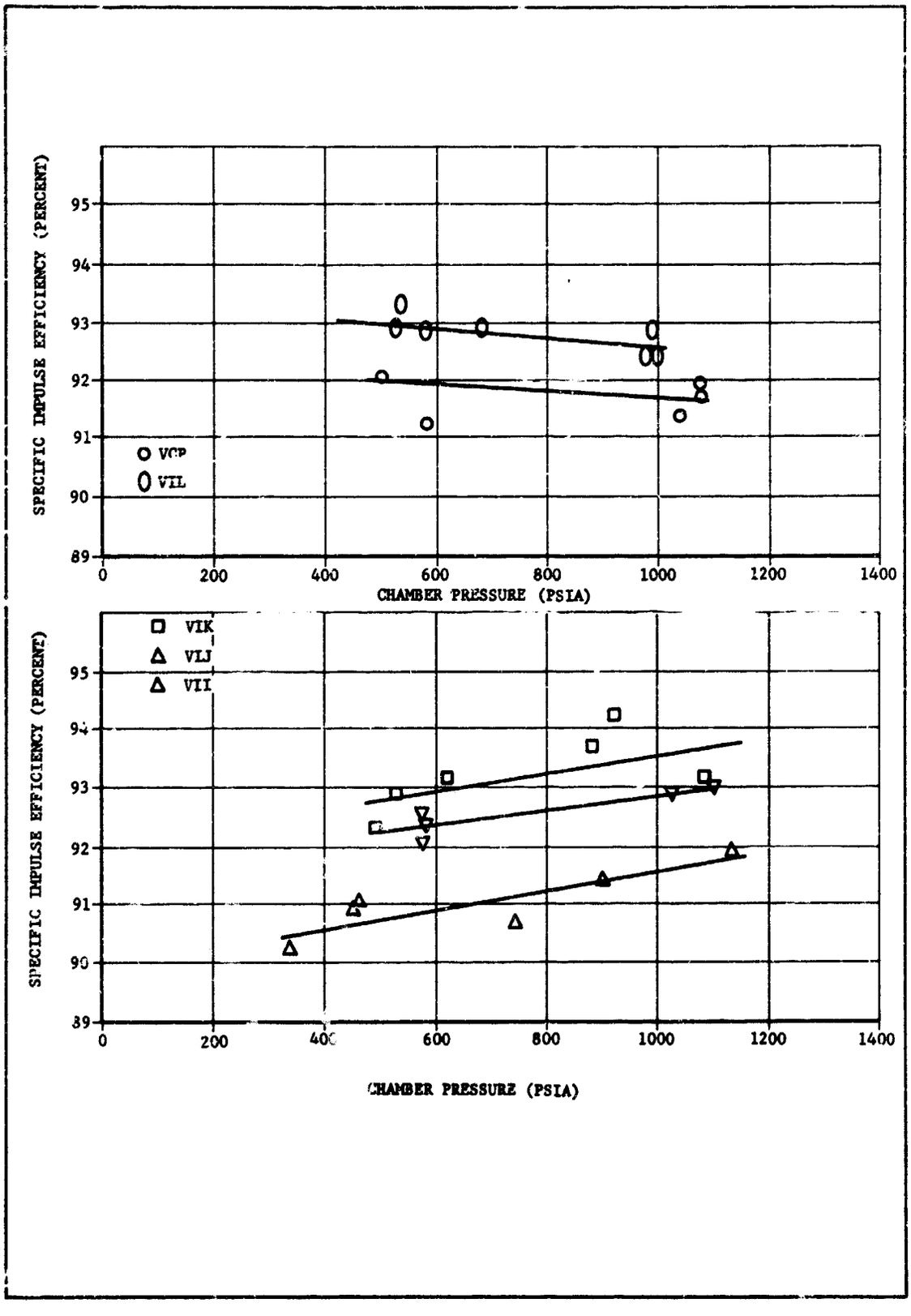

Figure 27. Effect of Chamber Pressure on Specific Impulse Efficiency of Be Propellants

a slight increase (0.3 to 0.5 percent) with decreasing pressure. A summary of the important propellant and motor parameters is contained in the following tabulation:

Propellant	Oxidation Ratio	Tc	Be	Oxidizer	$\dot{m}^{(1)}$	$L^{*(1)}$	$Eff^{(2)}$
VCP	1.22	3850	10.0	AP/HMX	6.7-8.4	130-180	+0.3
VIL	1.24	4008	12.0	AP/HMX	9.1-12.1	100-150	+0.5
VIJ	1.17	4145	15.5	AP	7.8-9.0	130-180	-0.6
VIK	1.27	4109	14.0	AP	10.1-12.1	86-142	-0.8
VII	1.05	3971	15.5	AP	6.0-8.0	170-260	-0.9

(1) Mass flow and L* range covered

(2) Efficiency at 500 psia minus efficiency at 1000 psia

As shown, chamber temperature and oxidation ratio had no apparent effect on the pressure effects obtained. Mass-flow rates were maintained over a narrow range for a given propellant, and in addition mass-flow rates overlapped for most propellants. Thus, mass-flow rate is not considered a factor in the pressure effects. This leaves differences in metal level, oxygen source, and L* as possible reasons for the observed pressure effects. Data from other sources were correlated in an attempt to relate the above variables to the efficiency losses with decreasing pressure.

Table VI contains a summary of pertinent data on 15 propellants for which the effect of chamber pressure on efficiency was available. However, the motor and propellant parameters are so widely scattered that only general observations can be made. These formulations fall into two basic groups. All of the formulations containing more than 12-percent Be, with the exception of VGR, utilize AP as the sole solid oxidizer. With the exception of Arcocel 191, all these formulations show decreased efficiency with decreasing pressure. The Arcocel 191 data are also unique in that low pressure firings were made at twice the L* of high pressure firings. Increased residence time may well explain the lack of pressure dependence exhibited by this formulation. The largest efficiency loss was observed for the Arcocel 333E formulation, which had the lowest temperature and oxidation ratio. The properties of this propellant are such that a large portion of efficiency losses can be attributed to combustion inefficiencies. For the remainder of the propellants, there was no apparent trend with flame temperature, oxidation ratio, or metal level on efficiency losses with decreasing pressure.

TABLE VI

PROPELLANTS AND PERTINENT DATA FOR EVALUATION OF EFFICIENCY LOSSES WITH CHAMBER PRESSURE

Propellant	O.R.(1)	T_c	Be	Oxidizer	$\dot{m}$	L*(2)	Eff(3)
VLJ	1.17	4145	15.5	AP	8-9	130-180	-0.6
VII	1.05	3971	15.5	AP	6-8	170-260	-0.9
VIK	1.27	4109	14.0	AP	10-12	86-142	-0.8
191	1.08	3852	14.0	AP	6-7	500-240	+0.4
VGR	1.04	3895	13.0	AP/HMX	7-9	230-280	-0.9
333E	1.01	3630	13.0	AP	10-15	600-720	-2.4
VIL	1.24	4008	12.0	AP/HMX	9-12	100-150	+0.5
VIF	1.05	3897	12.0	AP/HMX	6-9	170-230	-0.3
VID	1.02	3885	12.0	HMX	6-8	243-318	+0.3
VIE	1.10	3870	12.0	AP/HMX	8-10	200-250	-0.8
319B	1.02	3649	11.5	AP/HMX	5-7	540-200	-1.0
VCP	1.22	3850	10.0	AP/HMX	7-8	130-180	+0.3
VHH	1.19	3773	10.0	AP/HMX	6-9	215-250	-0.4
VIB	1.17	3780	9.0	HMX	[illegible]	250-315	+0.6
VHP	1.17	3703	8.0	HMX	[illegible]-8	280-320	0

(1) Oxidation ratio

(2) Mass flow and L* range covered

(3) Efficiency at 500 psia minus efficiency at 1000 psia

All the propellants presented in Table VI containing 12-percent Be or less utilized large percentages of HMX either as the sole solid oxidizer or in conjunction with AP. Efficiency losses in this group were in general much less than observed for the high metal group. Again, the formulation showing the greatest loss with decreasing chamber pressure had the lowest flame temperature and oxidation ratio (Arcocel 319F). However, no trends of efficiency with temperature and oxidation ratio were apparent for the remainder of the propellants. It is interesting to note that efficiency did not decrease with decreasing pressure for any of the all-HMX-oxidized propellants.

Based on the above observations, it appears that high flame temperatures and oxidation ratios are beneficial in reducing efficiency losses at low chamber pressures. Additional factors such as metal level and oxygen source appear to exert some influence. Increased residence time appeared to improve efficiency for at least one formulation.

d. Mass Flow and L* Effects

Figure 28 shows impulse efficiency as a function of mass-flow rate and L* for the propellants tested. All of the firings, with the exception of the low-burning-rate propellant (VIN containing AN), were conducted at mass-flow rates in excess of 6 lb/sec. The efficiency of the control propellant VCP, which shows no pressure effect, remained constant over a mass-flow range of 6 to 9 lb/sec. The efficiency data for the remainder of the propellants were widely scattered on the mass-flow plot with a general trend toward higher efficiencies at the higher mass-flow rates. However, if only high pressure firings are considered, no mass-flow effect is apparent.

The data shown on the L* plot in Figure 28 is also widely scattered. However, certain trends appear to exist. In particular, the three propellants, VIJ, VIK, and VII, which show pressure effects also show strong L* effects. A comparison of the data from this program with the L* relation previously developed (Figure 4) shows the higher temperature and oxidation ratio propellants, VIK and VIJ, maintain high efficiencies at relatively low L* values. In contrast, the high-temperature, low-oxidation-ratio propellant VII showed significant losses at relatively high L* values and approximated the low-temperature and low-oxidation curve, as shown. To further explore the effect of L* on efficiency, modifications were made to the standard 15PC to allow a large variation in L* to be made at constant pressure and mass-flow rate. Two Be propellants chosen for evaluation are presented in Table VII. VCP was chosen as the Be control propellant and previously showed no pressure effect or apparent L* effects. Propellant VII was chosen to determine if the efficiency of a high-temperature, low-oxidation-ratio propellant could be improved. Its demonstrated high pressure efficiency of 91.6 percent was considerably below that obtained with other propellants of equivalent temperatures but higher oxidation ratios. Combustion-bomb data also indicated its lower efficiency

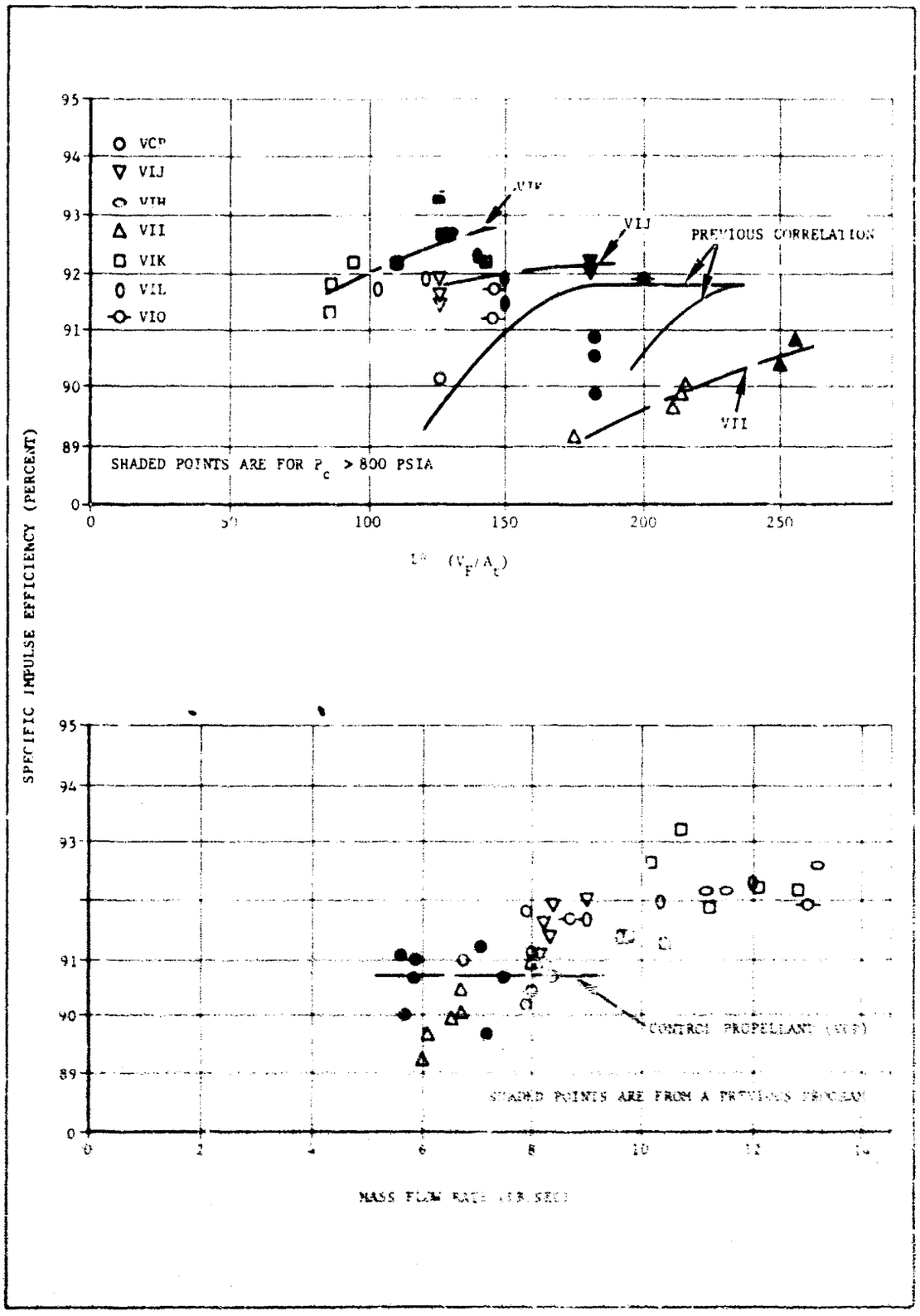

Figure 28. Effect of Mass-Flow Rate and L* on Specific Impulse Efficiency of Task II Be Propellants

might be due to combustion ineffifiency. (Refer to Table VII.) Propellant VII also showed a significant efficiency decrease with decreasing pressure and L*.

All high L* firings were made at approximately 1000 psia, although a greater effect would be predicted at lower pressures for VII and VIY.

Figure 29 shows the effect of L* on efficiency for the two Be propellants, VCP and VII. A comparison of the efficiency values obtained previously from the least squares analysis of pressure effects with the efficiencies obtained at high L*'s is listed in the following tabulation:

Propellant Type	VCP		VII	
L*	225	445	250	390
P_c	1033	1033	920	920
$\dot{m}$	8.2	8.0	6.4	6.7
Efficiency	91.67	91.67	91.43	91.81

As shown, only a marginal increase in efficiency was realized for either propellant. However, although the high L* motor provided more residence time, it also allowed more exposed surface for heat loss. The Minuteman Support Program[9] compared efficiency of various subscale motors and attempted to evaluate the losses due to increased exposed surface for heat loss. Based on their simplified assumptions, the heat loss is proportional to the internal area (other than propellant areas) exposed for thermal radiation and convection. The high L* motors should accordingly have about 60 percent more heat loss than the low L* motors. Assuming the low L* motors have a 1-percent efficiency loss due to heat loss, the high L* motors lose about 1.6-percent efficiency due to heat loss. Thus, some increase in efficiency was probably realized from the higher L* values, but was balanced by a corresponding decrease in efficiency due to heat loss.

e. Propellants with $TAGNO_3$ and AN

The propellants containing $TAGNO_3$ and AN were significantly less efficient than the Be/AP/HMX formulations. The average efficiency for firings of VIG propellant containing TAGNO was 88.5 percent at 1000 psia. For firings of VIN propellant containing AN, the average efficiency was 90.5 percent at 1000 psia. The VIN formulation also showed a 6.0 percent loss in efficiency with decreasing pressure from 1000 to 350 psia. Since the VIN formulation had both a reasonably high flame temperature and high oxidation ratio, the oxygen source is indicated as an important factor. Based on the poor performance of the VIN formulation, AN was eliminated from consideration for LMH-2 propellants. A comparison of oxygen sources is

[9]Refer to List of References

TABLE VII

PROPELLANTS FOR HIGH L* STUDY

Propellant Type	VCP	VII
Formulation (wt %)		
Binder	52	52
Be	10	15.5
LMH-2	--	--
AP	9	32.5
HMX	29	--
Theoretical		
T_c (^oK)	3850	3970
O.R.(1)	1.22	1.05
Ballistic performance		
Motor efficiency (%) (2)		
1000 psia	91.7	91.6
400 psia	92.0	90.6
Combustion-bomb efficiency (%)		
1000 psia	100	98.0
400 psia	100	91.0
Window-bomb agglomerate size (mils)		
1000 psia	<1	1.91
400 psia	<1	2.53

(1) Oxidation ratio
(2) Determined in standard 15PC motor firings

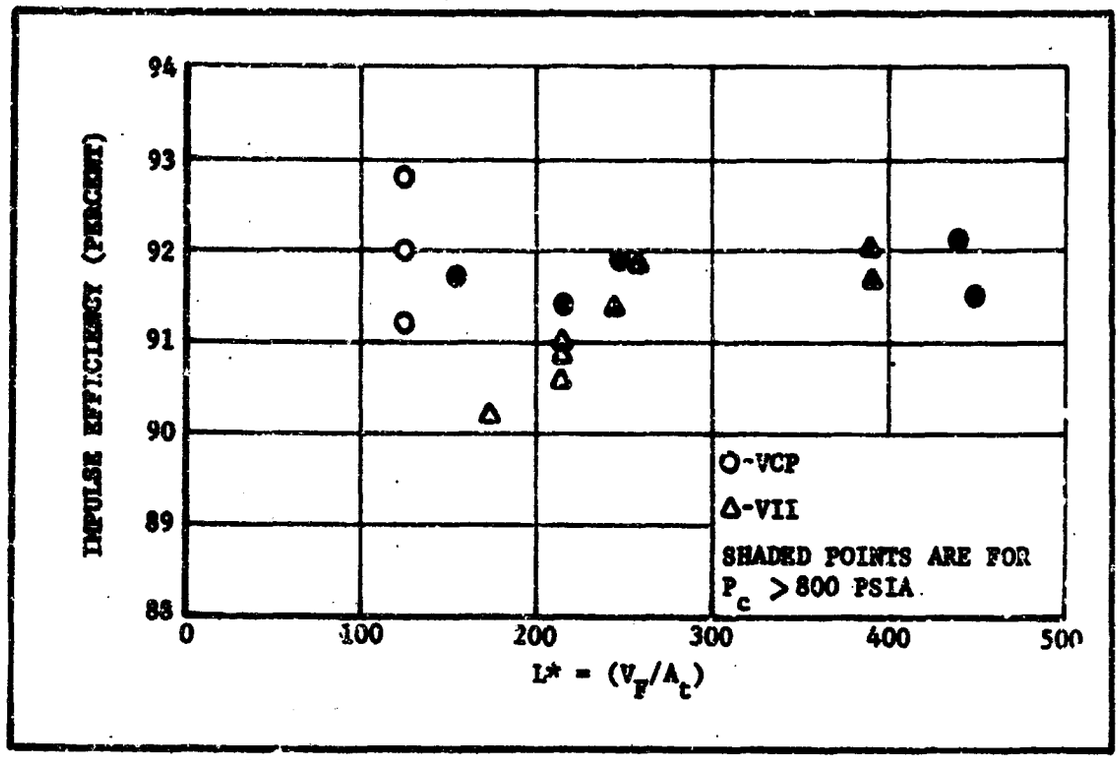

Figure 29. **Efficiency as a Function of L* For Be Propellants**

also available by comparing the VIJ formulation to VIH. Both formulations have the same oxidation ratio and equivalent flame temperatures. However VIH containing 5-percent NG in place of AP gave 0.5-percent higher efficiency. Bases on these results, a ranking of oxidizer effectiveness would be as follows: NG, AP, HMX, AN, and $TAGNO_3$.

f. Nozzle Approach Contour Effect

The effect of nozzle approach contour on efficiency for VCP and VIJ is shown in Figure 30. As shown, the efficiency increased 0.6 percent for VCP and 0.9 percent for VIJ when the approach angle was reduced from 30 to 5 degrees. Based on these data, the 15-degree approach appears near optimum and was used for the LMH-2 firings in the final characterization.

g. AP Particle Size Effect

The effect of AP particle size on efficiency for the VIJ formulation is shown in Figure 31. The efficiency increased 1.0 percent, from 180μ to 45μAP. All of the LMH-2/AP formulations contained 90μAP. These data indicate approximately 0.5-percent increase in efficiency could probably be realized with the LMH-2 formulations if 45μAP could be incorporated. Use of 45μAP in LMH-2 formulations was not possible due to processibility considerations.

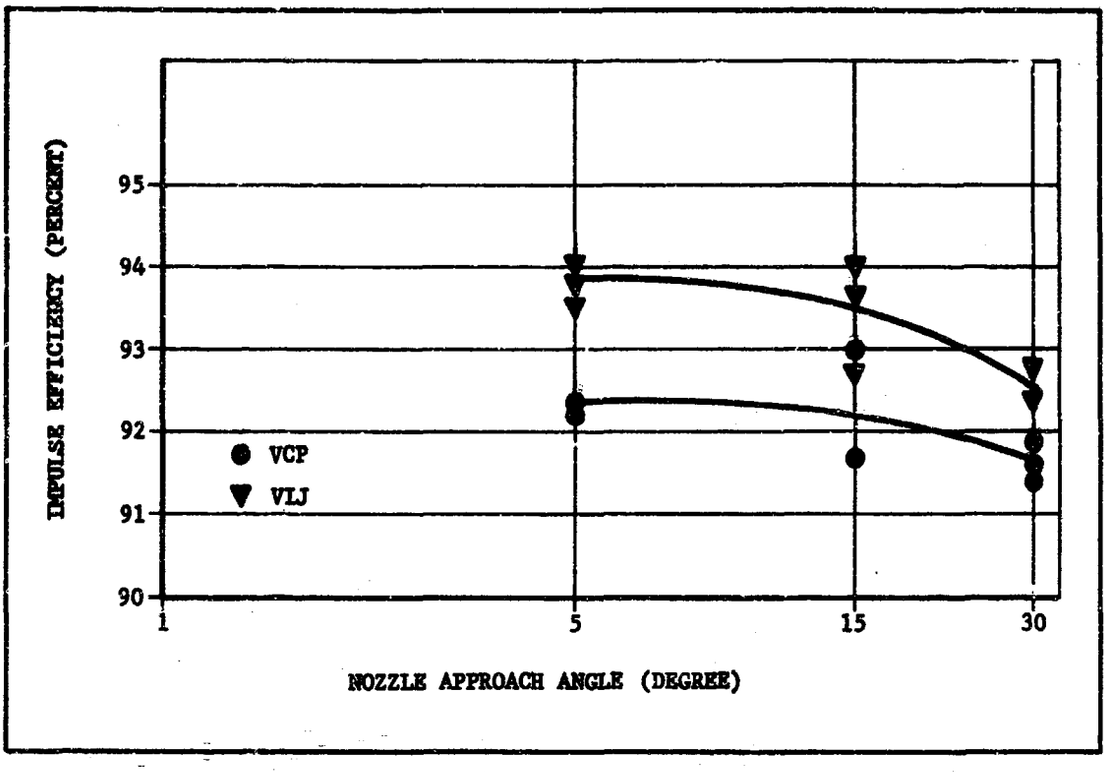

Figure 30. Impulse Efficiency as a Function of Nozzle Approach Angle

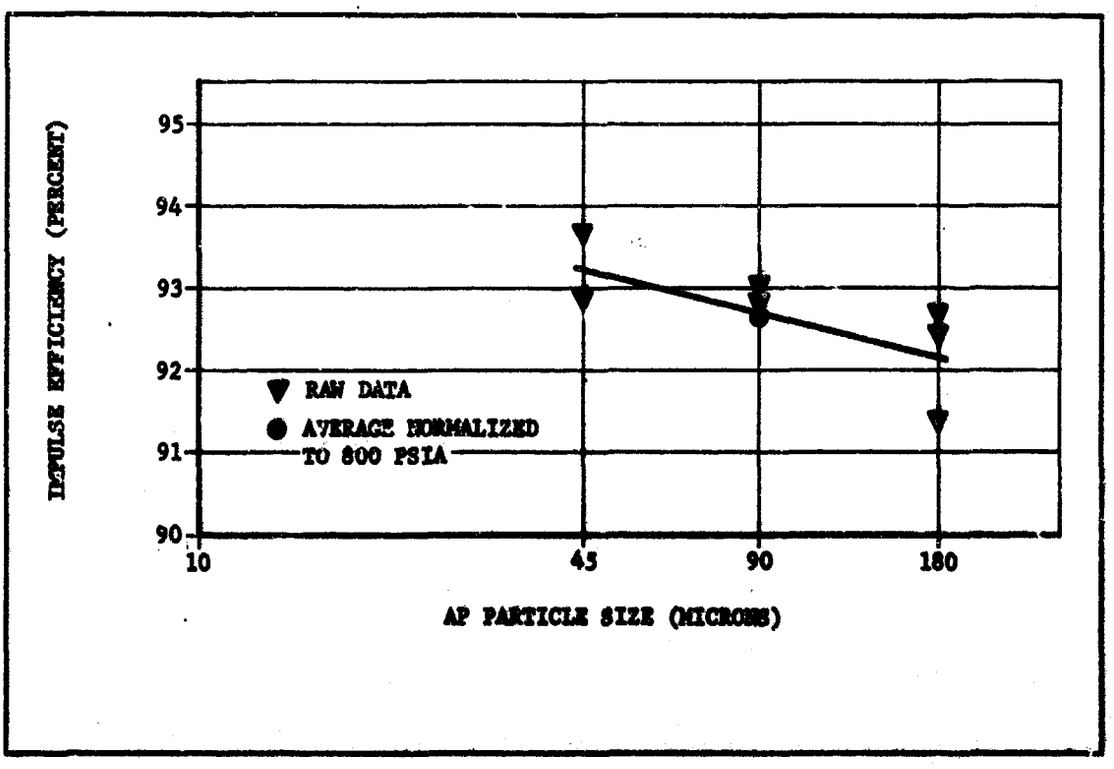

Figure 31. Impulse Efficiency as a Function of AP Particle Size in VIJ Formulations

2. LMH-2 Firings

Data from thirty-five 15PC firings of the six candidate formulations is presented in Table III. A complete summary of individual firings is contained in Appendix B, and formulation details are contained in Section IV.

Motor evaluation of the six candidate LMH-2 propellants began with an evaluation of the effect of L* on efficiency. The LMH-2 propellant selected for L* evaluation was VIY, containing wax-treated LMH-2, and VIY, containing AP-treated LMH-2. VIY was chosen because of its high impulse potential coupled with combustion-bomb data, indicating some combustion inefficiency could be expected, particularly with AP-treated material. A secondary purpose was to compare the effect of the two posttreatments on impulse efficiency.

In contrast to the Be results, the VIY firings (Figure 32) gave a significant increase in efficiency at the higher L* values. A summary of the impulse efficiency data is listed in the following tabulation:

Propellant Type	VIY (Wax treated)		VIY(AP treated)	
L*	145	234	119	311
Efficiency	90.25	91.01	89.51	90.98
Isp_{1000}^{15}	278.9	281.1	276.5	281.0

As shown, the efficiency of VIY containing wax-treated LMH-2 increased by 0.7 percent and for VIY containing AP-treated LMH-2 by 1.5 percent. The larger increase in efficiency with residence time for AP-treated LMH-2 is in agreement with the combustion-bomb results, which show the AP-treated material to be less efficient than the wax-treated material. Thus, residence time effects should be more significant for the AP-treated material.

Hardware limitations precluded additional exploration of the L* effect. All further LMH-2 firings were made with the high L* configuration.

A summary of ballistic data obtained from 15PC firings of candidate propellants is contained in Table VIII. As indicated, the first four propellants (VIX, VIY, VIZ, and VJA) met or exceeded the target impulse of 280 lbf-sec/lbm at standard conditions. The highest average delivered impulse of 281.8 lbf-sec/lbm for an efficiency of 89.8 percent was obtained with the AP-oxidized VIZ formulation containing 19-percent LMH-2. The highest efficiency of 92.2 percent was obtained with the AP-oxidized VIZ formulation containing 15-percent LMH-2. These firings gave the highest delivered Isp to date with LMH-2 solid propellants and demonstrated the excellent potential of this ingredient in high-energy systems.

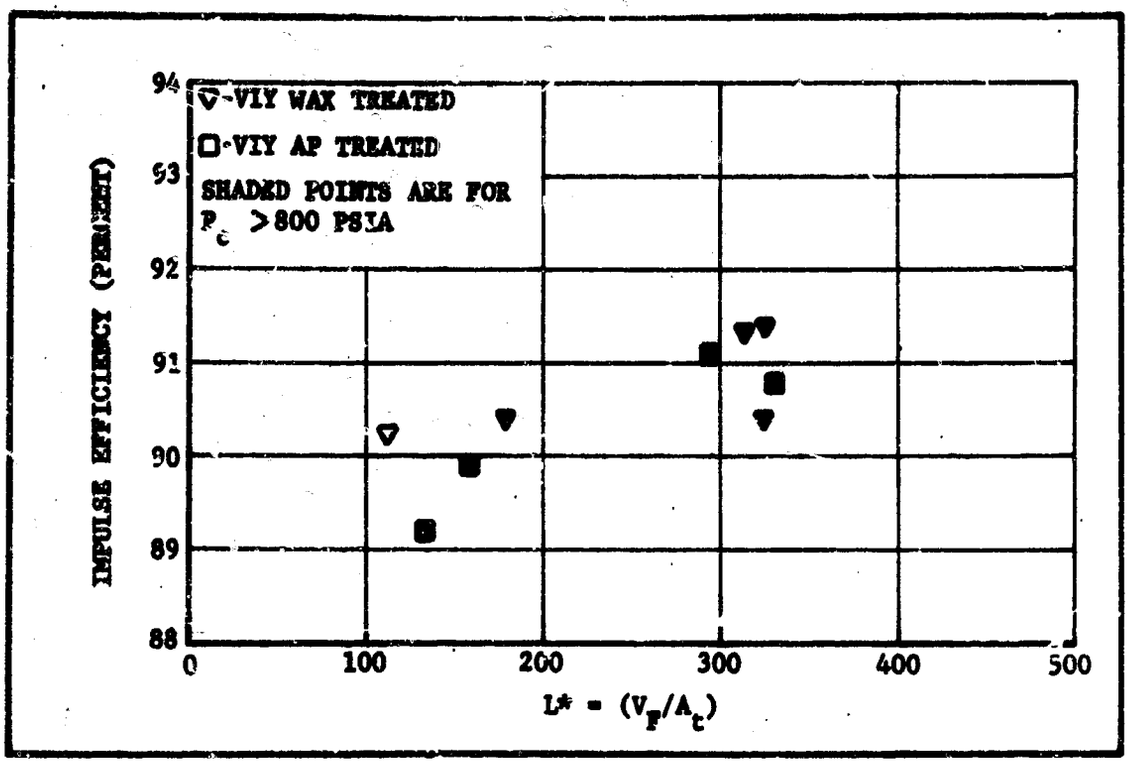

Figure 32. Efficiency as a Function of L* for LMH-2 Propellants

The remaining two LMH-2 candidate formulations (VJI and VJL) gave significantly lower performance than obtained with other formulations as presented in Table VIII. A comparison of the efficiency of candidate LMH-2 propellants tested with that of Be analog formulations on the basis of temperature and oxidation ratio is shown in Figure 33. The VIX, VJA, and Allegany Ballistic Laboratory FIQ formulations all appear to fit the same generalized curve as the Be propellants. However, some deviation of VIY and a major deviation of the remaining lower-oxidation-ratio LMH-2 propellants are apparent. This anomalous behavior is better illustrated in Figure 34, which shows a cross plot of Figure 33 of efficiency versus oxidation ratio at a temperature of approximately 3680° K for both Be and LMH-2 propellants. The efficiency of VIZ is approximately 1 percent below that predicted from the Be correlation. The data show that efficiencies of LMH-2 propellants are comparable to Be propellants for comparable temperature and oxidation ratios at LMH-2 loadings up to 15 to 17 percent and corresponding to oxidation ratios of greater than 1.15. At higher LMH-2 loadings and lower oxidation ratios, LMH-2 propellants appear to be unique.

3. Final LMH-2 Confirmation Firings

Based on the demonstrated high performance of VIY and VJA, these formulations were chosen for further ballistic characterization in 15PC firings. The test grid was designed to maintain as high a constant L* as possible while using the longer 15 degree approach and maintaining a mass-flow rate greater than 7 lb/sec. A summary of impulse and efficiency data

CONFIDENTIAL

TABLE VIII

LMH-2 FIRING SUMMARY

[illegible]	[illegible](1)		[illegible](2)					VII(3)				VIX(2)			VIX(2)			VIA(2)			VJI(2)			VJL(2)		
[illegible] Configuration	Standard		Standard		High			Standard		High		High			High			High			High			High		
Firing No.	1-8	1-9	2-60	2-65	2-62	2-69	2-78	2-61	2-64	2-63	2-70	2-71	2-72	2-75	2-79	2-80	2-81	2-74	2-76	2-77	2-82	2-83	2-84	2-86	2-87	2-8[illegible]
K [illegible]	131	120	100	122	122	122	117	127	111	122	111	118	120	122	145	140	136	127	142	136	149	150	156	109	130	132
Pa (psia)	[illegible]	[illegible]	671	[illegible]	673	881	897	1192	1042	1294	1033	1055	1006	1007	1016	1076	1110	752	898	[illegible]	842	857	922	683	889	948
Pb (psia)	[illegible]	[illegible]	[illegible]	[illegible]	[illegible]	904	946	1245	1100	1376	1100	1121	1046	1052	1060	1124	1156	759	920	915	879	886	962	724	931	993
r (in/sec)	[illegible]	[illegible]	[illegible]	0.906	0.912	0.905	0.949	1.166	1.254	1.389	1.183	1.112	0.995	1.011	0.941	0.976	1.021	0.647	0.745	0.738	0.719	0.760	0.738	0.794	0.844	0.867
ẇ (lb/sec)	7.11	7.16	6.71	8.00	7.41	7.20	7.53	9.83	9.04	10.91	9.27	8.82	8.36	8.34	7.41	7.75	8.16	7.49	8.08	8.05	7.63	7.71	7.99	6.18	6.76	7.6[illegible]
[illegible]	[illegible]	[illegible]	132	170	325	328	315	133	158	330	294	319	[illegible]	326	398	386	374	257	294	306	310	313	313	294	360	364
Isp del	283.3	270.4	270.6	270.8	283.0	279.6	282.7	282.3	281.9	288.7	285.3	284.0	283.0	284.9	285.7	286.2	287.3	276.6	282.2	282.1	271.9	269.4	270.6	269.1	276.9	281.6
Isp theoretical	[illegible]	[illegible]	300.0	300.5	300.6	300.5	30[illegible]	316.6	313.7	317.8	313.1	308.5	307.4	30[illegible].7	318.2	319.1	319.4	305.7	310.6	309.6	312.4	312.9	314.4	306.0	314.1	314.2
Efficiency	91.87	91.87	90.20	90.37	91.41	90.34	92.28	89.16	89.86	90.84	91.12	92.06	92.06	92.59	89.79	89.69	89.95	90.51	90.86	91.12	87.04	86.10	85.96	87.94	88.16	89.62
Isp [illegible]	278.7	282.4	278.6	279.2	284.4	279.1	282.0	275.4	277.6	280.6	281.5	279.6	279.6	281.2	281.8	281.5	282.3	280.0	281.0	280.9	273.3	270.4	269.9	275.0	275.7	280.2
Avg Eff	91.47		90.29		91.01			89.51		90.98		92.24			89.61			90.83			86.37			88.57		
Avg Isp	280.6		278.9		281.1			276.5		281.0		280.1			281.8			280.9			271.2			277.0		

Notes: (1) Contains 12 percent ungrouted [illegible] and was developed under contract AF 04(611)-107[illegible]2
Isp (1000/14.7) = 2[illegible].7
T_c = [illegible]
[illegible] = 1.40
(2) Contains [illegible]-coated [illegible]
(3) Contains AP-coated [illegible]

CONFIDENTIAL

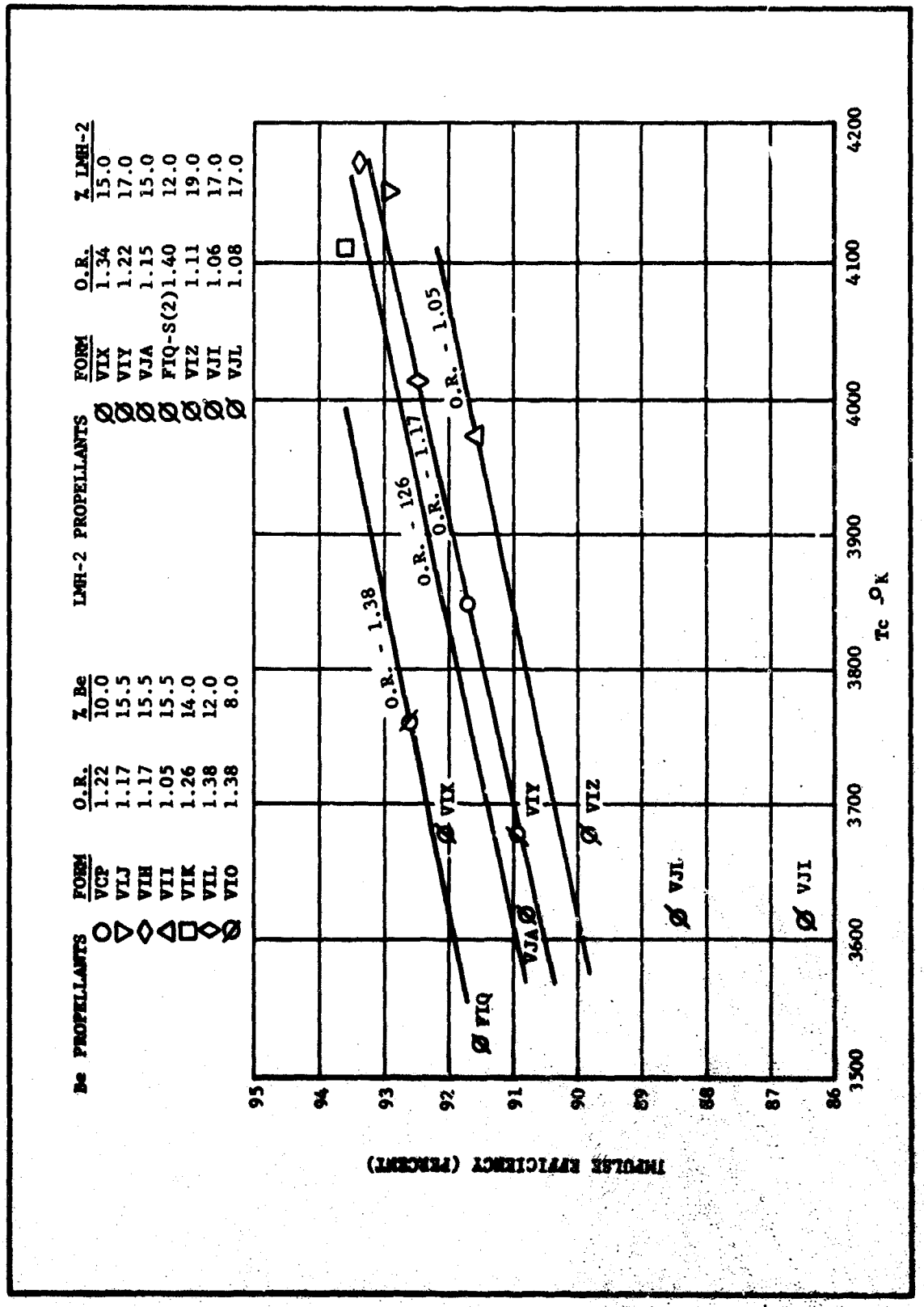

Figure 33. Effect of Chamber Temperature and Oxidation Ratio on Specific Impulse Efficiency of Be and LMH-2 Propellants

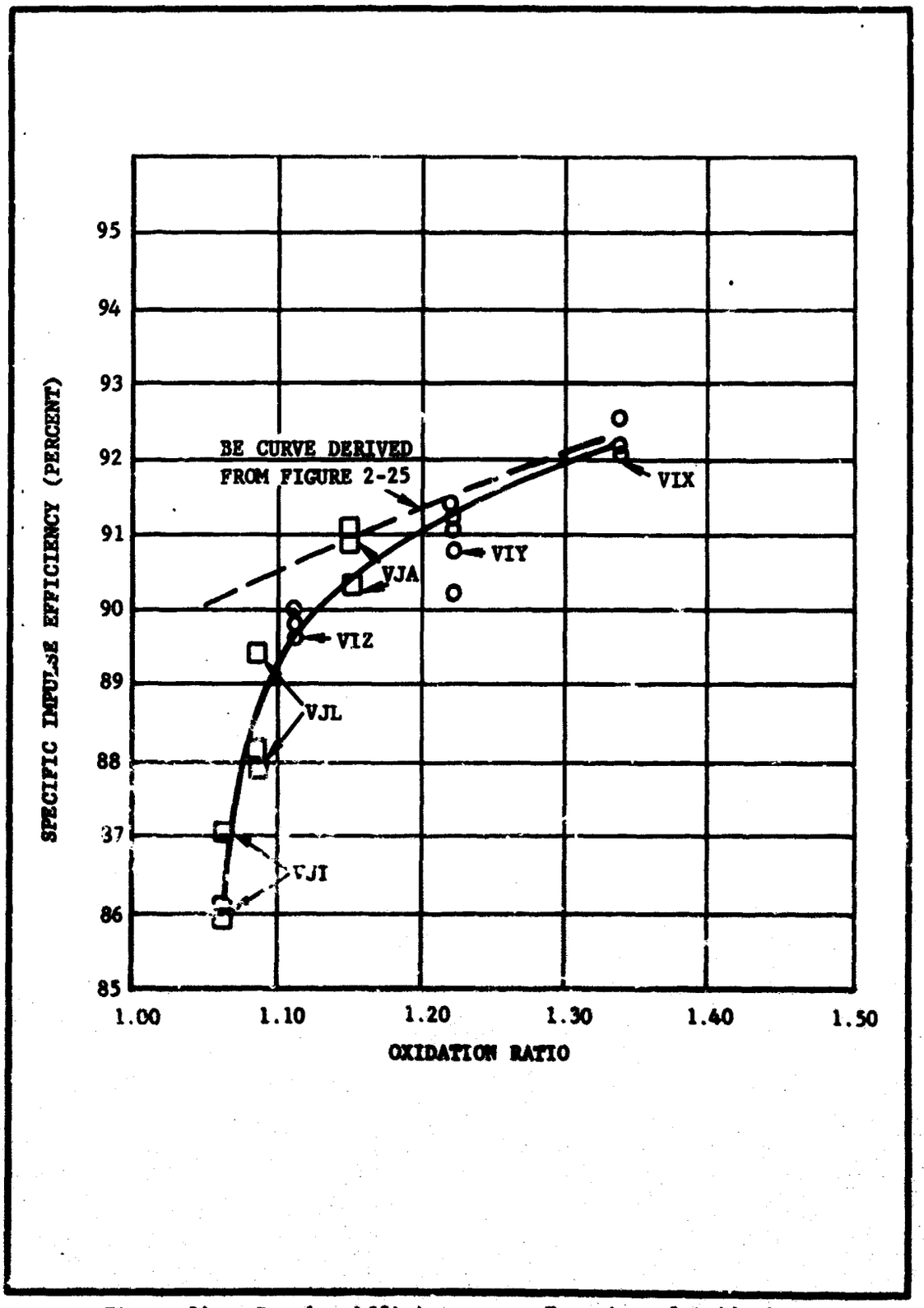

Figure 34. Impulse Efficiency as a Function of Oxidation Ratio for Be and IRM-2 Propellants

obtained from VIY and VJA firings, along with the data previously obtained, is presented in the following tabulation:

Formulation	VIY			VJA		
P_c	641	930*	1290	675	892*	1140
$\dot{m}$	7.1	7.3	8.9	7.2	8.1	7.1
L*	334	323	315	336	300	344
Efficiency	89.99	91.01	91.13	90.13	90.99	89.75
Isp^{15}_{1000}	278.0	281.1	281.5	278.8	281.4	277.6

*Data obtained from earlier firings

All of the confirmation firings, except the high-pressure, high-mass-flow-rate VIY firings, gave efficiencies 1 percent lower than previously obtained. These data show chamber pressure has little or no effect on the efficiency of VJA from 650 to 1250 psia. However, mass-flow rate appeared to significantly affect the efficiency of VJA with a 1-percent loss obtained by decreasing the mass-flow rate from 8 to 7 lb/sec. It should be pointed out that the longer 15 degree approach and corresponding greater heatsink may be a contributing factor to the apparent mass-flow effect. For VIY it was impossible to seperate the effects of mass-flow rate and chamber pressure on impulse efficiency. The lower mass-flow rate is suspected to be the major cause of the 1-percent lower efficiency obtained at the lower pressure level. Figure 35 shows the effect of mass-flow rate on efficiency for VJA and VIY appeared comparable at equivalent mass-flow rates with little performance penalty expected for chamber pressure down to 600 psia at high mass-flow rates.

Figure 36 shows efficiency as a function of mass flow for all of the LMH-2 propellants at high L* values compared to the VCP mass-flow curve. As shown, VIX follows the VCP scaling curve, whereas the VIY, VJA, and VJL formulations show a much more severe scaling curve. The VIZ and VJL formulations are less efficient than the VIY and VJA formulations and undoubtedly follow still more severe scaling curves. The apparent tendency of VJL to follow the VIY and VJA scaling curve leaves hope for good performance of this propellant at higher mass-flow rates. Since VJL has a 3-sec higher theoretical impulse than VIY and VJA, the delivered impulse of this propellant may well be higher than either VIY and VJA at high mass-flow rates.

These firings point out the limitations of optimizing performance of LMH-2 propellants in small motors by optimizing motor and propellant parameters. Of the three motor parameters considered--mass-flow rate, L*, and nozzle approach angle--optimization of one parameter can be made only at the expense of the other two parameters within the present hardware limitations. Based on these firings, mass-flow rate appears to be the controlling motor parameter below 8 lb/sec. At higher mass-flow rates, improvements in efficiency are obtained by increasing L*. From these tests it was impossible to detect if any improvement in efficiency was obtained by use of the 15 degree nozzle approach. In addition, some potential

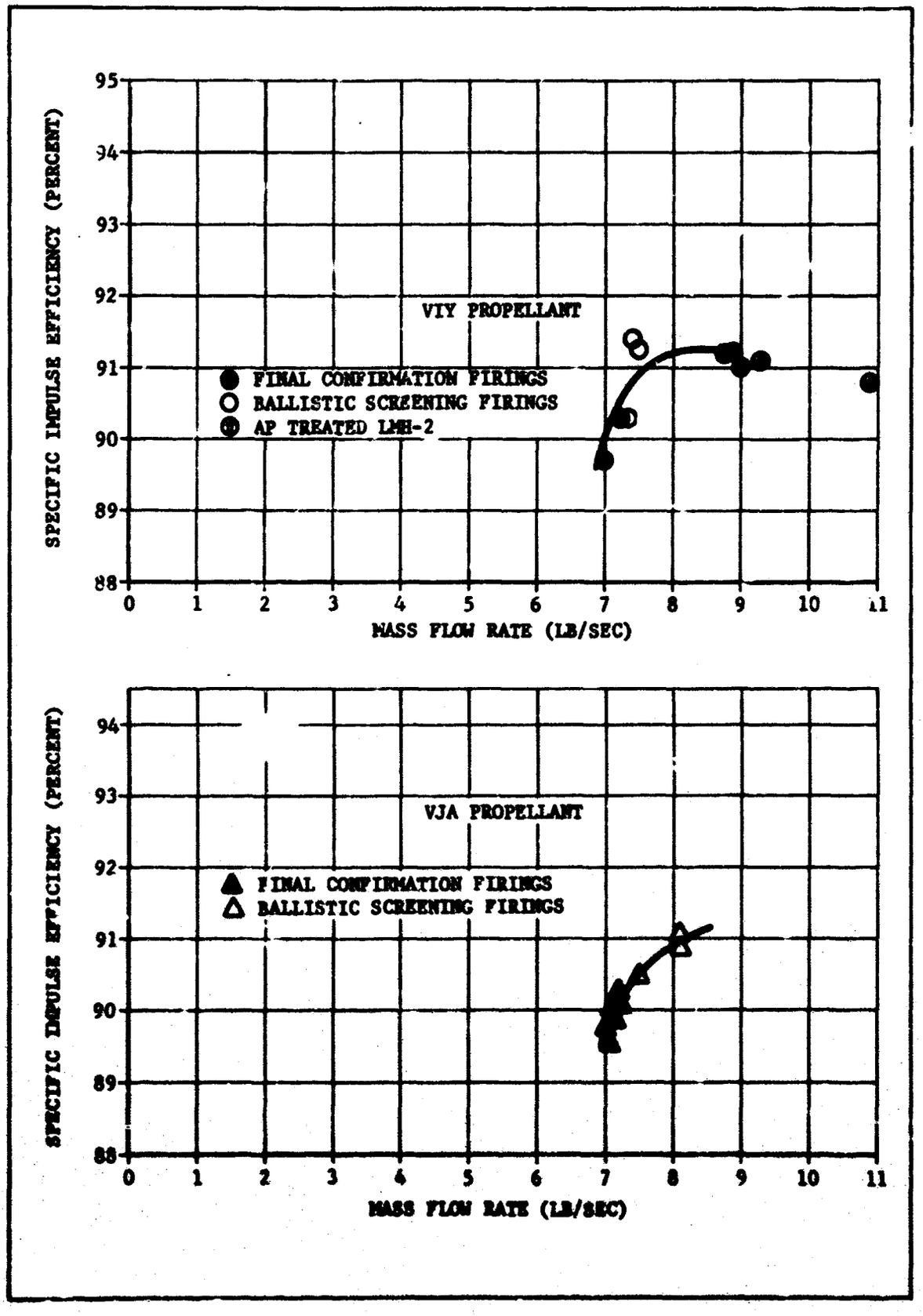

Figure 3 . Impulse Efficiency as a Function of Mass-Flow Rate for VIY and VJA Propellants

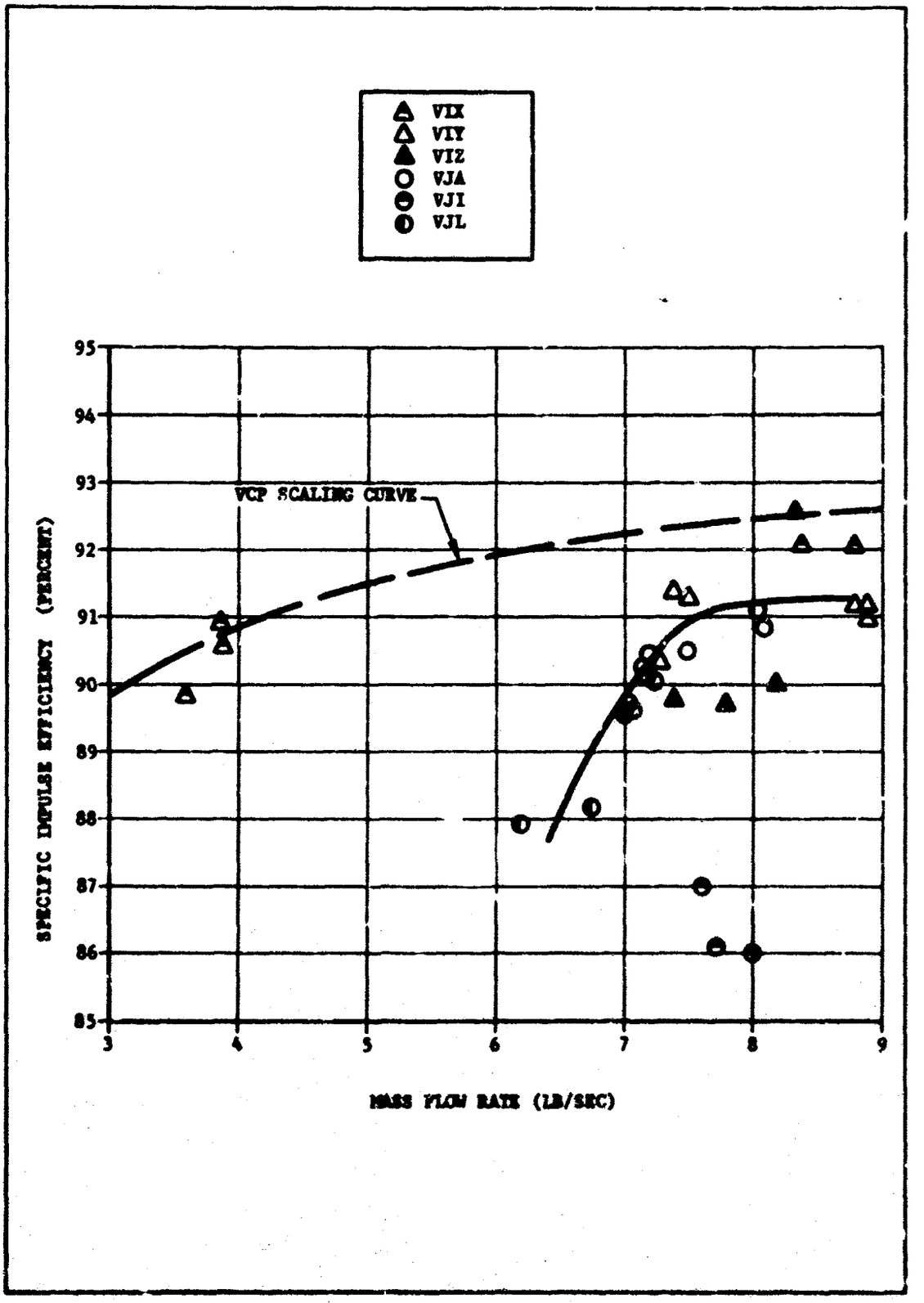

Figure 36. Impulse Efficiency as a Function of Mass-Flow Rate for LMR-2 Propellants

performance gains may be lost by using propellants which show higher performance at less favorable motor conditions in place of propellants with higher theoretical performance which give lower performance in small motors.

4. LMH-2 Performance Losses

The previous analysis and correlations have allowed optimization of propellant and motor parameters to a large extent and corresponding attainment of the program goal. However, the limitations of this semi-empirical approach in leading to a better understanding of losses observed with Be and LMH-2 propellants is acknowledged. The apparent rapid drop in efficiency at high LMH-2 loadings limits the attainment of the ultimate performance potential for LMH-2 propellants, and a clearer understanding of this phenomenon is particularly important. An attempt was thus made to further isolate the factors affecting impulse efficiency.

The basic behavior of LMH-2 in nitrasol propellants has been explored by other recent programs.

Under Contracts AF 04(611)-9097 and AF 04(611)-11219, Lockheed Propulsion Company[10] has used, with some success, the nonequilibrium flame temperature (T*), assuming fuel pyrolysis only, in predicting LMH-2 propellant efficiencies. Fundamental combustion studies have shown that metals such as Be that form protective oxide coatings require temperatures close to their oxide melting points for particle ignition. According to Lockheed, T* values should be in the neighborhood of 2500° to 2600° K, approximating the melting point of BeO (2820° K), for efficient LMH-2 combustion at LMH-2 loadings above 15 percent. Deviations at low LMH-2 loadings and low T* values, where high efficiencies were obtained, were explained in terms of the basic decomposition mechanism. For low LMH-2 loadings, it is suspected that the hydride was ejected into the gas stream; whereas for higher LMH-2 loadings, surface decomposition and metal agglomeration is a favored assumption. T* calculations were performed on six LMH-2 propellants tested and are shown correlated with impulse efficiency in Figure 37. A sharp drop in efficiency at low T* values is observed as predicted.

Under Contract AF 04(611)-10742, Hercules' Allegany Ballistics Laboratory[11] (ABL) has extensively explored the combustion behavior of LMH-2 using combustion-bomb and window-bomb techniques. Results of this work indicate agglomeration is the main cause of observed combustion-bomb inefficiencies. Limited data suggest flame temperature and oxidation ratio influence combustion efficiency by affecting agglomerate combustion rather than agglomerate formation.

A series of closed-bomb tests were also performed on selected Be and LMH-2 propellants tested in this program. Combustion-bomb tests for residue analysis and micro-window-bomb tests for agglomerate size data were performed at ABL using techniques previously employed under Contract AF 04(611)-10742. Heat-of-explosion tests were performed at Bacchus in a standard Parr bomb. Results of these tests are summarized in Table IX.

[10,11] Refer to List of References

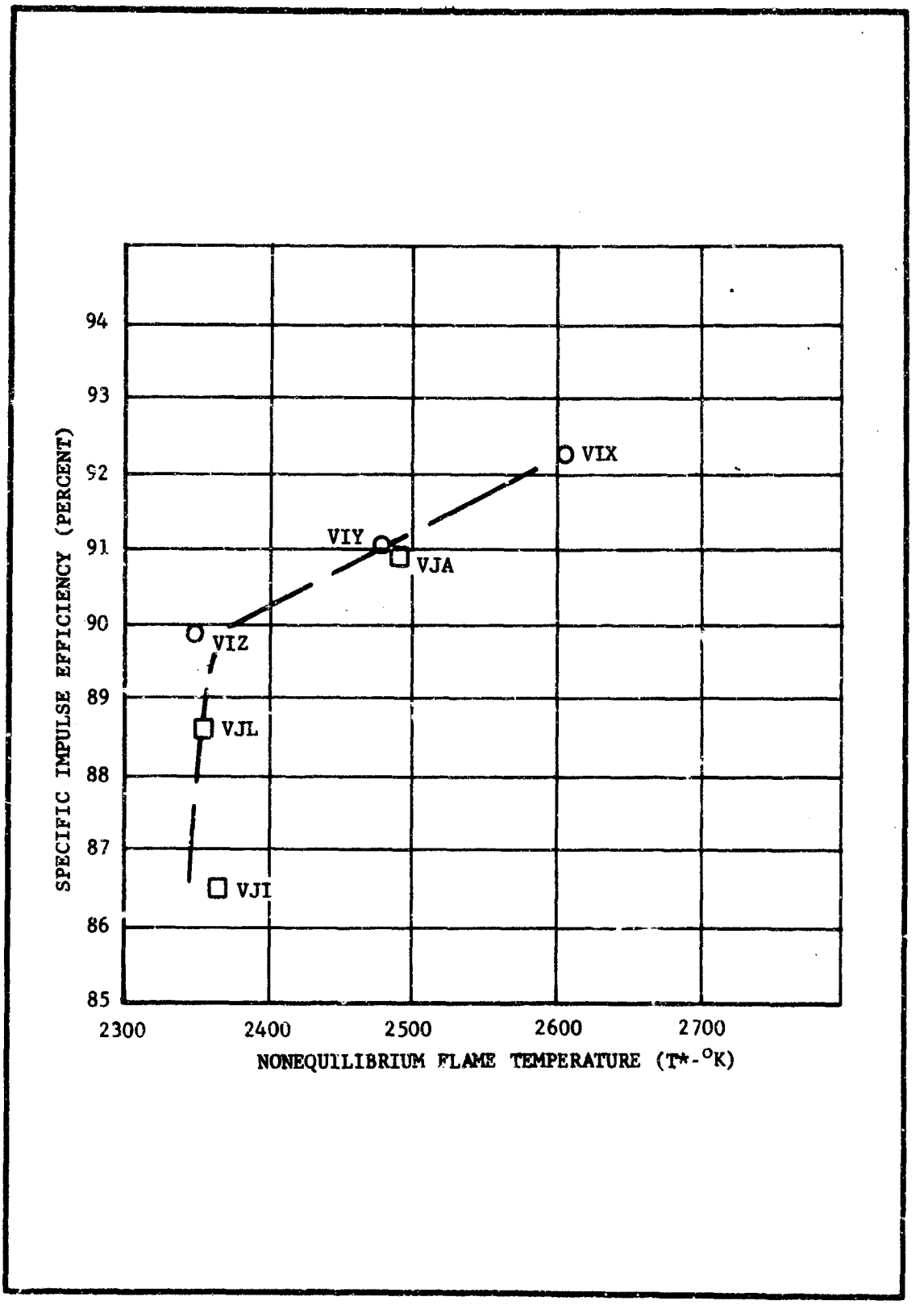

Figure 37. Effect of T* on Efficiency of LMH-2 Propellants

TABLE IX

CLOSED BOMB DATA

	Beryllium Propellants										LMH-2 Propellants								
	VIH (45μAP)	VII (90μAP)	VIJ (45μAP)	VIJ (90μAP)	VIJ (180μAP)	VIK (45μAP)	VIL (45μAP)	VIM	VIN	VIO (45μAP)	VIX	VIX[1]	VIY	VIY[2]	VIY[1]	VIZ[3]	VJA	VJI	VJL
Mix No.	37-40	69-41		37-95	83-100	27-96	37-99	70-73	70-87		37-97, 83-2	83-31	83-52	83-52	94-1	83-56			
Residue analysis[4]																			
Pressure (psia)																			
1000	100	97.5	99.7	100	98.5	99.8	100	77.0	83.3	99.8	100, 100	98.2		99.0	96.4		96.0	89.0	
400	99.7	90.8	99.6	100	82.6	99.4	100	43.8	50.9	99.5	96.4, 97.5	93.3		95.8	89.4		94.0	84.0	
Window bomb agglomerate																			
Size (mils)																			
Pressure (psia)																			
1000	<2	<2	<1	2.8	2.3	1.0	<2	8.0	6.5	<2	2.7, 3.4	3.6		4.1	4.[illegible]		3.5	4.1	
400	<2	2.5	<1	4.6	3.3	1.0	<2	15.8	14.1	<2	3.3, 4.7	4.3		4.5	5.2		4.1	4.8	
200	Small Flaking	--	--	Flaking	--		<2	--	12.8	--	4.5, 4.3	4.6		--	--		--	--	
Heat of explosion (cal/gm) experiment[5]				2628, 2606				2172	1992, 2024	1955	2311, 2280	2324, 2296	2320	2353, 2330	2303	1866, 2337	2001, 2142, 2158	2068	2235
Heat of explosion (cal/gm) theoretical[5]				2654				2331	2205	1867	2270	2270	2384	2384	2384	2500	2217	2305	2385
Percent of theoretical				98.3 to 99.2[6]				93.2	90.5 to 91.6	105	101 to 102	101 to 102	97.3	97.7 to 98.7	96.6	74.6 to 93.5	96.2 to 97.5	89.7	93.7

Notes:

(1) Contains AP treated LMH-2

(2) Contains 0.5 percent wax on LMH-2

(3) Contains 0.5 percent wax over-coat on AP treated LMH-2

(4) Percent beryllium converted to BeO

(5) Heat of explosion values refer to formulation but not necessarily mix numbers

(6) Values were obtained on VIJ (45μAP) and VIJ (180μAP) respectively

CONFIDENTIAL

Analysis of the data in Table IX indicates the following:

(a) Beryllium propellants--VIH, VII, VIJ, VIK, VIL and VIO --all showed good combustion efficiency at 1000 psia, with maximum impulse losses of 0.5 percent predicted for VII and VIJ (180μAP). VII and VIJ (180μAP) formulations showed combustion inefficiencies at 400 psia with an impulse loss of 1.5 percent predicted for VII and 3.0 percent for VIJ (180μAP). Based on agglomerate size, VIJ (90μAP) could also show efficiency losses at low pressures.

The VIM and VIN data show AN-oxidized systems to have a significantly lower efficiency than AP-oxidized systems. Based on these data, only a limited number of AN firings were made to confirm the combustion-bomb results.

(b) LMH-2 propellants, VIX and VIY formulations, gave good combustion-bomb efficiencies at high pressures with a trend toward lower efficiencies at lower pressures. The use of AP-treated LMH-2 also decreased efficiency. Of the remaining two formulations tested in the combustion bomb (VJA and VJI), both were HMX oxidized and were significantly less efficient than AP-oxidized propellants. As shown, heat-of-explosion data appeared to follow the same trend as the combustion-bomb data. Also of significance is the larger agglomerate size of LMH-2 propellants compared to efficient Be propellants.

Although decreasing combustion-bomb efficiencies imply lower impulse efficiencies, a direct relation remains to be established. Some insight may be gained, however, by calculating the impulse efficiency loss based on unburned Be and also by a direct comparison of closed-bomb data with observed impulse efficiencies. Table X contains calculated impulse losses assuming fixed percentages of unburned LMH-2 for VIY and VJI formulations. These data show a maximum calculated loss of 2 percent based on combustion-bomb efficiency for the VJI formulation. However, the impulse efficiency of VJI was 6 percent lower than that of the VIX formulation showing no unburned Be. This large discrepancy precludes the estimation of impulse losses from combustion-bomb data directly. However, Figures 38 and 39 show a definite trend toward lower impulse efficiences with lower combustion-bomb and heat-of-explosion efficiencies, although other effects are obvious. In addition, Figure 40 illustrates a trend toward lower motor efficiencies with increasing agglomerate size, as determined from window-bomb firings; although, again, a large variance is present. These trends support the agglomeration theory for the observed inefficiencies at high LMH-2 loading and low oxidation ratios. Data are too limited to determine the interaction of Tc, P*, or oxidation ratio on the

agglomerate formation. However, ABL has made the following observations relating to the effect of agglomerate formation on LMH-2 combustion efficiency:

(a) At constant flame temperature and oxidation ratio, combustion efficiency is inversely proportional to the agglomerate size.

(b) For constant agglomerate size, combustion efficiency increases with increasing flame temperature and oxidation ratio.

(c) Agglomerate size increases with increasing LMH-2 loadings and particle size.

(d) Agglomerate size increases with increasing AP particle size.

These observations, coupled with the developed flame-temperature and oxidation-ratio correlations, may be used as guides in optimizing LMH-2 performance. However, the determination of the interaction between agglomerate growth and the propellant environment appears necessary before the ultimate potential of LMH-2 propellants can be projected. The large differences between the observed efficiency losses and those predicted from combustion-bomb efficiency also warrants additional consideration. Because of the lower flame temperature of LMH-2 propellants, coupled with the high melting points of BeO, nozzle losses may be partially responsible for the discrepancy. Figure 13 shows that both Be and LMH-2 propellants show efficiency losses with increasing expansion ratio. If, as has been suggested, these losses are connected with supercooling phenomena, the lower flame temperature Be and LMH-2 propellants should exhibit these losses early in the expansion process. Calculations were performed on the VIY formulation to determine the magnitude of the losses to be expected from supercooling and are summarized in Table XI. As shown, a 1-percent loss is calculated for VIY at an expansion ratio of 10:1, whereas no loss is calculated for the high-temperature Be propellants at this expansion ratio. In addition, Table X shows that for 10-percent unburned Be in the VJI matrix, a flame temperature decrease of approximatley 200° K could reduce impulse efficiency by an additional 1 percent, assuming supercooling.

In summary, the performance losses associated with Be and LMH-2 propellants appear due to a combination of both combustion and expansion losses. The combustion losses appear due to agglomeration, which is improved mainly by higher flame temperatures and oxidation ratios. Nozzle losses also are probably a function of the combustion efficiency and flame temperature. Additional testing and analysis are needed to better define the interaction between the combustion process and the resultant impulse efficiency.

TABLE X

EFFECT OF UNBURNED Be ON THEORETICAL IMPULSE FOR LMH-2 PROPELLANTS

Wt % Unburned LMH-2*	Theoretical Isp(1000/14.7)	Calculated Efficiency	T_c (°K)	O.R.
VIY				
0	308.9	100	3679	1.22
5	306.6	99.3	3595	1.26
10	303.8	98.4	3503	1.30
20	297.3	96.2	3294	1.38
50	279.8	90.6	3020	1.73
VJI				
0	314.0	100	3623	1.06
5	311.2	99.1	3537	1.09
10	307.9	98.1	3440	1.12
20	301.2	95.9	3217	1.19
50	282.6	90.0	2959	1.45

*Calculations assume pyrolysis of LMH-2 to Be

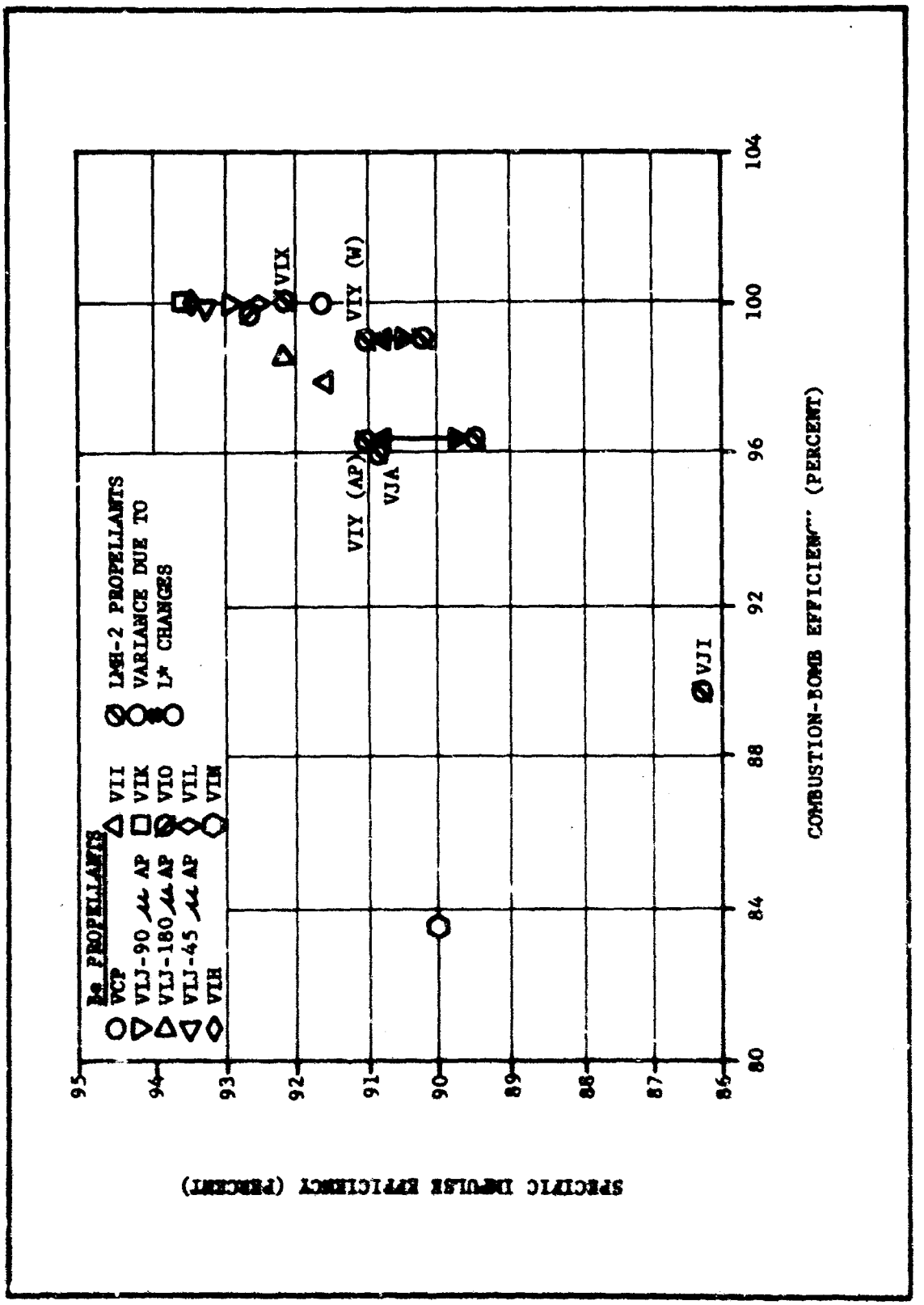

Figure 38. Impulse Efficiency as a Function of Combustion-Bomb Efficiency

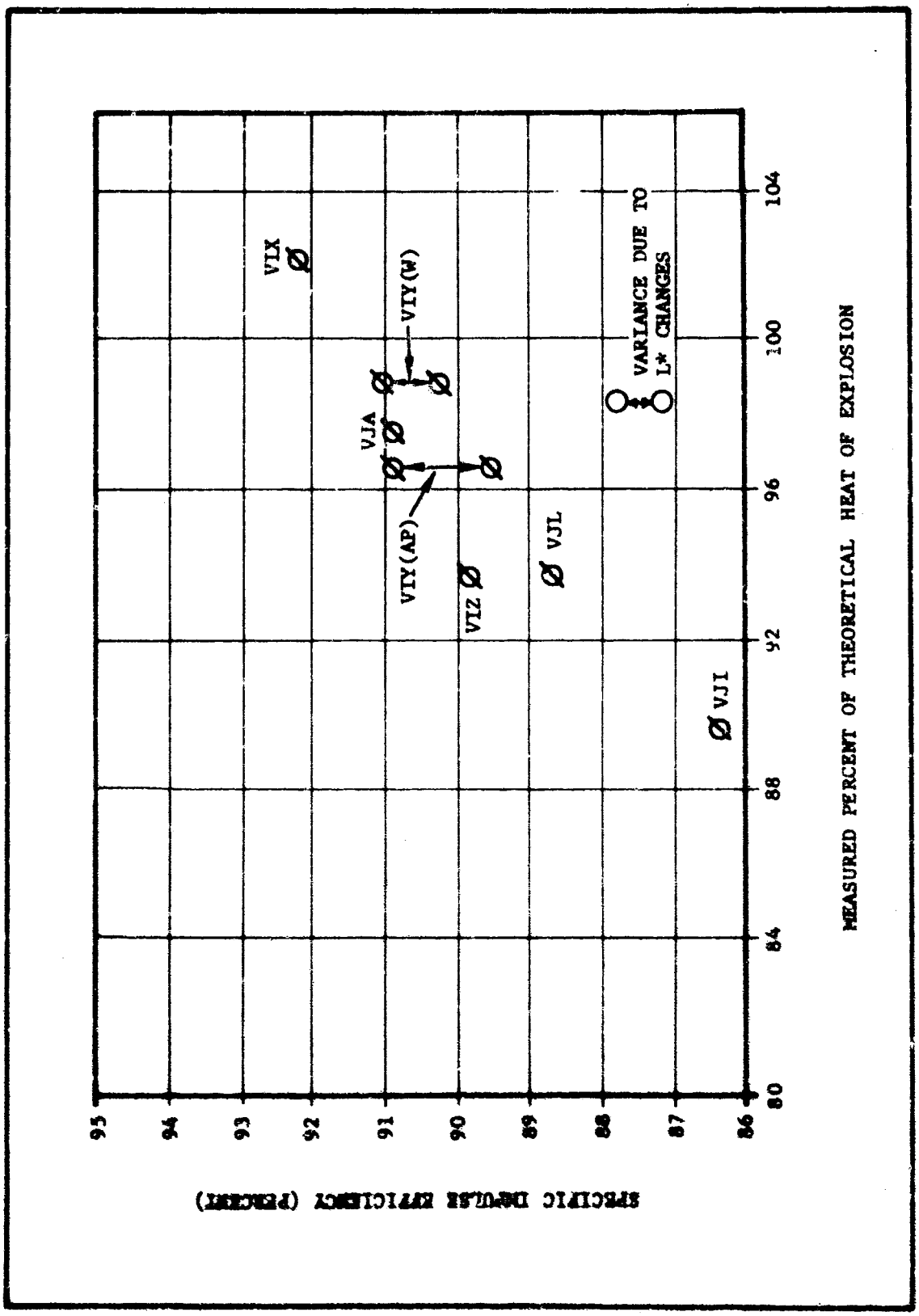

Figure 39. Impulse Efficiency as a Function of Heat-of-Explosion Efficiency for LMH-2 Propellants

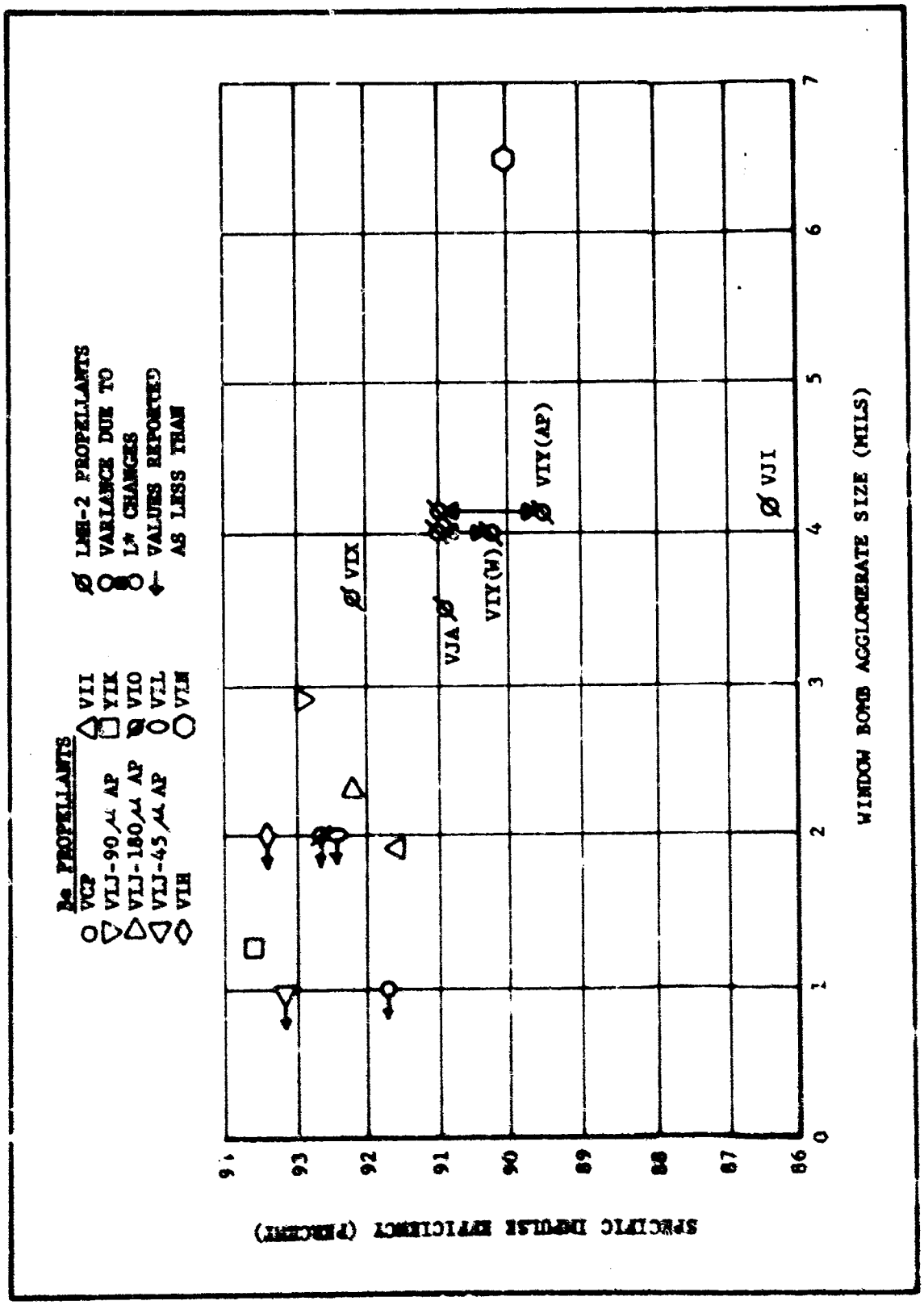

Figure 40. Impulse Efficiency as a Function of Agglomerate Size

TABLE XI

CALCULATED EFFECT OF SUPERCOOLING FOR THE VIY FORMULATION

Expansion Ratio	Equilibrium Exit Temp (^{o}K)	Equilibrium Vacuum Isp	Supercooled Exit Temp (^{o}K)	Supercooled Vacuum Isp	Efficiency (%)
3.5	2820	297.8	2764	297.8	100
5.0	2820	311.6	2623	310.8	99.7
7.5	2740	326.4	2471	324.0	99.3
10.0	2638	335.8	2367	332.4	99.0
30.0	2256	366.1	1994	359.3	98.1
50.0	2083	377.5	1836	369.5	97.9

F. ULTIMATE LMH-2 PERFORMANCE POTENTIAL

It should be emphasized that the high delivered impulses obtained for LMH-2 propellants in this program were achieved mainly by the use of a high-energy binder (16.4 NC/82.0 NG). The energy level of this binder is felt to be close to the maximum within the present state-of-the-art. As higher energy plasticizers and oxidizers become available, higher performance levels from LMH-2 propellants can be reasonably projected. Of particular interest are the advanced perchlorate oxidizers and difluoramino compounds.

Consideration must also be given to the effect of motor scaling on LMH-2 performance. Some estimate of the effect of motor scaling is available by considering data generated on L* and mass-flow rate effects for LMH-2 propellants tested to date. Figure 32 shows that additional improvements in efficiency can be expected by increasing L* levels above 300. Because of the increased heat loss to the high L* motor, improvements in addition to those shown can also be expected for a low-heat-loss motor. Data obtained from Task II firings indicate an increase of efficiency of 0.5 percent can be obtained by decreasing the nozzle approach angle from 30 to 15 degrees. Combining these effects, efficiencies as high as 99.5 percent can reasonably be projected for VIY, giving a delivered impulse of approximately 285 sec in PPC motors.

Although density was not a consideration in formulation of the initial LMH-2 propellants, it is now interesting to explore the optimum performance potential of LMH-2 propellants based on impulse-density considerations. To give some basis for comparison, a density exponent of 0.25 was arbitrarily selected as being representative of possible upper stage applications for LMH-2 propellants. Using this density exponent, a performance comparison of the four high performance propellants tested to date is presented in Table XII. The highest performance is obtained with VJA (HMX oxidized) formulation.

TABLE XII

Isp DENSITY POTENTIAL OF CANDIDATE LMH-2 PROPELLANTS

Propellant Type	VLX	VIY	VIZ	VJA
Theoretical Performance				
Isp (1000/14.7)	303.7	308.9	313.8	309.3
ρ (gm/cc)	1.356	1.319	1.284	1.355
Isp x $\rho^{0.25}$	328	331	334	334
Delivered Performance				
Isp^{15}_{1000}	280	281	282	281
Isp x $\rho^{0.25}$	302	301	300	303

Consideration was also given to the effect of solids loading and the use of mixed metal systems on theoretical impulse density using the same density exponent of 0.25. The effect of increasing solids loading from approximately 60 to 70 volume percent by increasing solid oxidizer loading for the formulations explored in this program is presented in Table XIII. Processing considerations would probably limit this increase to approximately 65 volume percent solids. Only a marginal increase in Isp x $\rho^{0.25}$ was obtained by increasing the solid oxidizer loading for either the AP or HMX systems. It should be pointed out that the VJI formulation (17-percent LMH-2/HMX) with an Isp x $\rho^{0.25}$ of 337 is nearly the maximum obtainable. There is little evidence to indicate increased solids oxidizer loading in place of NG would be beneficial for LMH-2 combustion, and this does not appear to be a desirable approach.

The effect of the addition of Be, Al, and Zr on impulse density is presented in Table XIV. The addition was made by replacing either solid oxidizer or liquid. The addition of any of these three metals is detrimental to the LMH-2/AP system performance over that presently available with the VIZ formulation. For the HMX system, calculations were performed on Be addition only. These calculations show that essentially equivalent performance is obtained by Be addition to that presently available.

TABLE XIII

EFFECT OF SOLIDS LOADING ON Isp ρ

Formulation*				Theo Isp	ρ (gm/cc)	T_c (^oK)	O.R.**	Ispx $\rho^{0.25}$
LMH-2	AP	HMX	NG					
12	26	0	50	295.7	1.415	3663	1.57	323
15	23	0	50	303.7	1.356	3678	1.34	328
17	21	0	50	308.9	1.319	3679	1.22	331
19	19	0	50	313.8	1.284	3672	1.11	334
21.45	16.55	0	50	319.0	1.244	3626	1.00	337
15	38	0	35	301.3	1.387	3680	1.43	328
17	36	0	35	307	1.341	3680	1.30	330
19	34	0	35	312	1.313	3680	1.17	334
22.30	30.7	0	35	319.3	1.258	3628	1.00	338
12	0	27	50	301.7	1.415	3602	1.29	329
15	0	24	50	309.3	1.355	3621	1.15	334
17	0	22	50	314.0	1.319	3623	1.06	337
18.7	0	20.3	50	317.3	1.290	3590	1.00	3[illegible]
15	0	39	35	310.3	1.384	3560	1.05	337
17	0	37	35	314.5	1.346	3530	1.00	339

*All calculations were made with 10 percent NC and 2 percent stabilizers for the AP system or 1 percent stabilizer for the HMX system

**Oxidation ratio

TABLE XIV

EFFECT OF ADDITIVES ON Isp ρ

Formulation*				Theoretical Isp	ρ (gm/cc)	Tc (°K)	O.R.**	Isp x $\rho^{0.25}$
LMH-2	AP	Be	NC					
12	26	0	50	295.7	1.415	3663	1.57	323
12	26	3	47	299.0	1.422	3779	1.32	327
12	26	6	44	300.9	1.427	3870	1.13	330
14	24	0	50	301.1	1.375	3675	1.41	326
14	24	3	47	304.0	1.382	3778	1.20	330
14	24	6	44	305.5	1.387	3837	1.04	332
16	22	0	50	306.3	1.337	3679	1.28	330
16	22	2	48	308.2	1.342	3741	1.15	332
16	22	4	46	309.3	1.345	3779	1.05	333
12	24	2	50	298.3	1.413	3742	1.39	326
12	22	4	50	300.3	1.412	3813	1.24	327
12	20	6	50	301.8	1.411	3869	1.11	329
14	22	2	50	303.5	1.374	3746	1.26	329
14	20	4	50	305.2	1.373	3804	1.13	331
14	18	6	50	306.2	1.372	3830	1.02	332
16	20	2	50	308.4	1.336	3740	1.15	332
16	18	4	50	309.8	1.335	3774	1.03	333
16	16	6	50	308.4	1.334	3706	0.94	331
	HMX							
12	27	0	50	301.7	1.415	3602	1.29	329
12	25	2	50	304.7	1.415	3689	1.17	332
12	23	4	50	306.7	1.414	3760	1.06	334
14	25	0	50	306.8	1.376	3616	1.19	332
14	23	2	50	309.4	1.375	3692	1.09	335
12	27	2	48	304.9	1.419	3682	1.16	333
12	27	4	46	307.3	1.422	3742	1.05	336
14	25	2	48	309.6	1.379	3684	1.08	336

*, ** Refer to end of table for legend

TABLE XIV (Cont)

EFFECT OF ADDITIVES ON Isp ρ

Formulation*				Theoretical Isp	ρ (gm/cc)	$\bar{T}c$ (°K)	O.R.**	Isp x $\rho^{0.25}$
IMH-2	AP	Al	NG					
12	26	0	50	295.7	1.415	3663	1.57	323
12	26	3	47	295.6	1.433	3719	1.42	323
12	26	6	44	295.3	1.449	3773	1.29	324
14	24	0	50	301.1	1.375	3675	1.41	326
14	24	3	47	300.8	1.392	3717	1.29	327
14	24	6	44	300.2	1.407	3756	1.17	327
16	22	0	50	306.3	1.337	3679	1.28	329
16	22	3	47	305.7	1.353	3701	1.17	330
16	22	6	44	304.7	1.367	3717	1.07	329
12	24	2	50	295.8	1.420	3698	1.46	323
12	22	4	50	296.0	1.426	3738	1.36	324
12	20	6	50	296.1	1.432	3772	1.27	324
14	22	2	50	301.1	1.380	3699	1.32	326
14	20	4	50	301.1	1.386	3730	1.23	327
14	18	6	50	300.1	1.391	3753	1.15	326
16	20	2	50	306.1	1.343	3689	1.20	330
16	18	4	50	305.9	1.347	3707	1.12	330
16	16	6	50	305.4	1.352	3710	1.05	329
		Zr						
12	26	0	50	295.7	1.415	3663	1.57	323
12	26	3	47	293.7	1.446	3697	1.49	322
12	26	6	44	291.6	1.476	3726	1.42	321
14	24	0	50	301.1	1.375	3675	1.41	326
14	24	3	47	297.0	1.433	3733	1.28	325
14	24	6	44					
16	22	0	50	306.3	1.337	3679	1.28	330
16	22	3	47	304.3	1.365	3711	1.22	329
16	22	6	44	302.2	1.392	3731	1.16	328

*, ** Refer to end of table for legend

TABLE XIV (Cont)

EFFECT OF ADDITIVES ON Isp ρ

Formulation*				Theoretical Isp	ρ (gm/cc)	Tc (°K)	O.R.**	Isp x $\rho^{0.25}$
LMH-2	AP	Zr	NG					
12	24	2	50	294.6	1.429	3687	1.50	322
12	22	4	50	293.5	1.444	3706	1.44	322
12	20	6	50	292.3	1.459	3724	1.38	321
14	22	2	50	300.0	1.388	3698	1.35	326
14	20	4	50	298.9	1.402	3714	1.30	325
14	18	6	50	297.7	1.416	3730	1.24	325
16	20	2	50	305.3	1.350	3702	1.23	329
16	18	4	50	304.1	1.363	3715	1.18	329
16	16	6	50	302.9	1.376	3727	1.13	328

*All calculations were made with 10-percent NC and 2-percent stabilizer for AP formulations or 1-percent stabilizer for the HMX formulations

**Oxidation ratio

It is concluded that any consideration of increased solids loading or the use of mixed-metal systems must be based on improved impulse efficiency.

In summary, four areas of investigation appear particularly attractive to obtain additional increases in performance of LMH-2 above those obtained to date on this program. They are as follows:

(1) Additional combustion studies to determine the interaction between closed-bomb data and motor performance

(2) Motor scaleup of selected high-energy LMH-2 propellants with close attention to motor design parameters

(3) Additional emphasis on those propellant ingredients which can appreciably improve the propellant combustion environment as represented by flame temperature and oxidation ratio

(4) Investigation of the potential of mixed metals to improve combustion efficiency in conjunction with higher solids loadings

SECTION III

TASK II, FORMULATION AND BALLISTIC EVALUATION

A. SCOPE

Task II comprised the majority of the program effort. The objective of this task was to formulate and test candidate high-performance propellant systems selected under Task I. This task utilized both Be control and analog formulations as well as LMH-2 formulations. Under this task, 35 LMH-2 and 70 Be motors were evaluated. The test motors contained a nominal 10- to 15-lb propellant charge and exhibited mass-flow rates of 5 lb/sec or greater. The task was divided into two phases. In phase A, formulation screening was conducted, with the bulk of the motors fired at approximately 1000 psia exhausted to Bacchus ambient pressure (~12.2 psia) with optimum expansion ratio. Phase B more extensively characterized selected high-performance LMH-2 formulations. Table XV contains a breakdown of various areas investigated under Task II.

TABLE XV

TASK II, FORMULATION SCREENING

Subtask	Purpose	No. Firings (Be)	No. Firings (LMH-2)
Phase A			
II-6	Efficiency correlations with Be propellants	43	--
II-7	Oxidizer particle size studies with Be propellants	8	--
II-8	Optimum nozzle geometry	11	--
II-9	Increased L* studies	4	9
II-10	LMH-2/AP propellants	--	6
II-11	LMH-2/AN or HMX propellants	--	9
Phase B			
II-12	Characterization of selected Be and LMH-2 propellants	4	11

B. LABORATORY FORMULATION AND PROCESSING STUDIES

1. Beryllium Propellants

Based on the results of Task I, laboratory formulation studies were performed on Be analog formulations of proposed LMH-2 propellants presented in Table II.

The VIH propellant was designed to have the same metal level, oxidation ratio as the proposed 19-percent LMH-2 formulation. The VII propellant was formulated to demonstrate the effect on efficiency due to decreasing oxidation ratio in a high-metal-level propellant. The VLJ propellant was designed to show the effect on efficiency of oxygen source (5 percent more AP for NG than the VIH formulation) at a constant metal level and oxidation ratio. VLJ was also formulated with 45, 90, and 180 μ AP to determine the effect of AP particle size on efficiency. The VIK, VIL, VIM, and VIN propellants represented the Be analogs of the 17-percent LMH-2/AP; 15-percent LMH-2/AP/HMX; 19-percent LMH-2/AN; and 17-percent LMH-2/AN, respectively, in both metal level and oxidation ratio. The VIO propellant was designed to determine the effect of oxidation ratio on efficiency at a low metal level, and VIG was formulated to evaluate $TAGNO_3$ as an oxidizer.

Processing studies were conducted to determine the tradeoff between liquid level and oxidizer particle size on processibility. In conjunction, a review was made of past processing experience with Be propellants. Consideration was given to weight and volume percent solids loading, solids particle size, particle size ratio, and overall composition. Figure 41 shows propellant viscosity as a function of the weight ratio of fine to coarse particles, based on the total solids content. Although the data are scattered due to ingredient and composition differences, the effect of increasing fines on viscosity was normally predictable.

For propellants containing 10 to 15 μ PNC and 12 μ Be, little effect on viscosity is noted by decreasing the oxidizer particle size down to 90μ, or a particle size ratio of approximately 6:1. However, for particle sizes less than 90μ, viscosity rapidly increased even at moderate solids loadings. This effect is further illustrated in Figure 42 for the VIH and VLJ formulations containing 57- and 61-percent-by-volume solids loading, respectively.

Using Figure 42 as a guide, formulation work was completed on the Be analog formulations with little processing difficulty. Table XVI shows the rheological criteria and Table XVII the pertinent propellant data for the analog formulations.

2. LMH-2 Propellants

Laboratory formulation screening and processing studies were conducted on six candidate LMH-2 propellants selected from the Task I correlations, which were predicted to meet the program objective of a delivered impulse in excess of 280 lbf-sec/lbm.

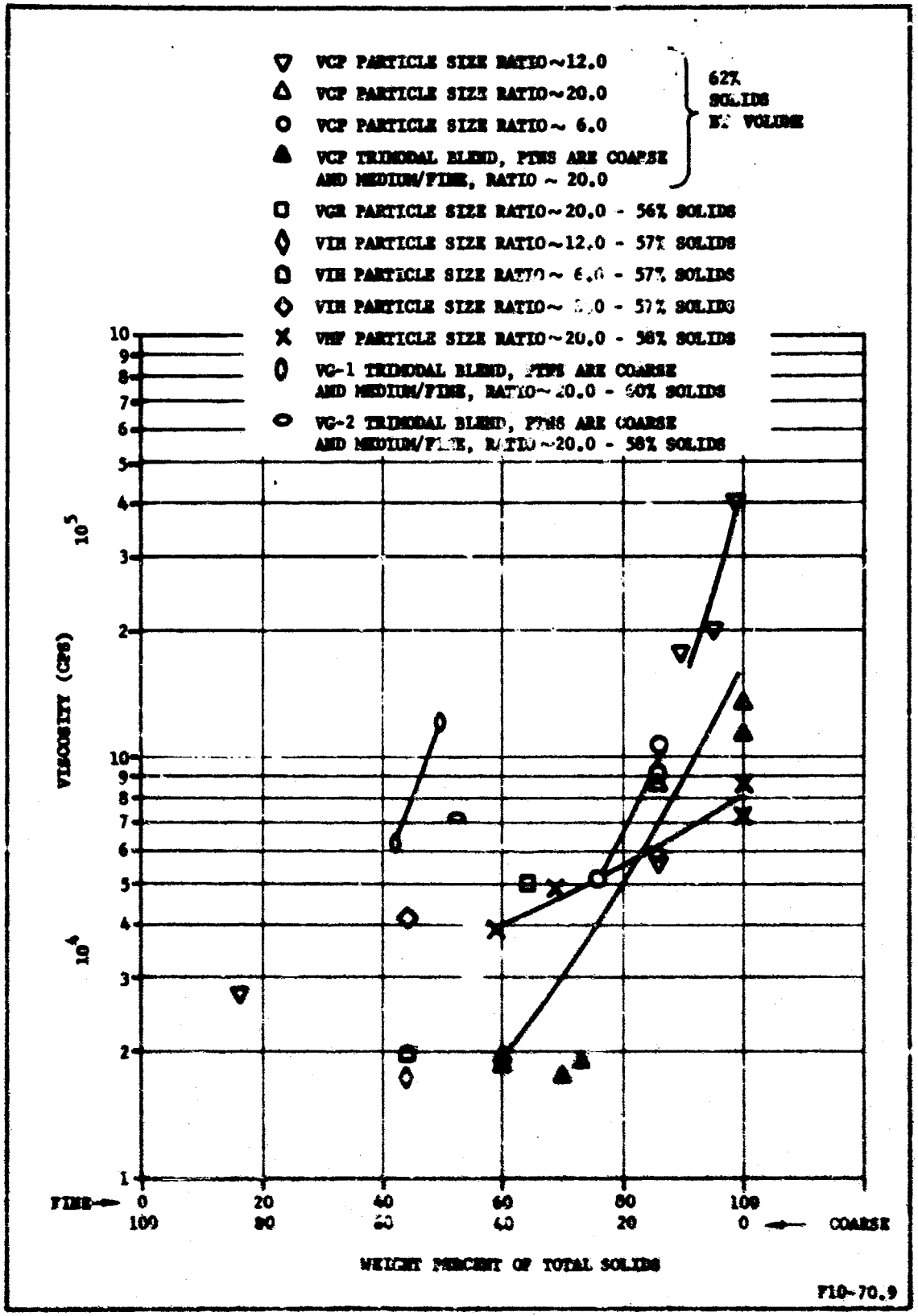

Figure 41. Viscosity as a Function of Percent Fine/Coarse Particles for Bu Double-Base Propellants

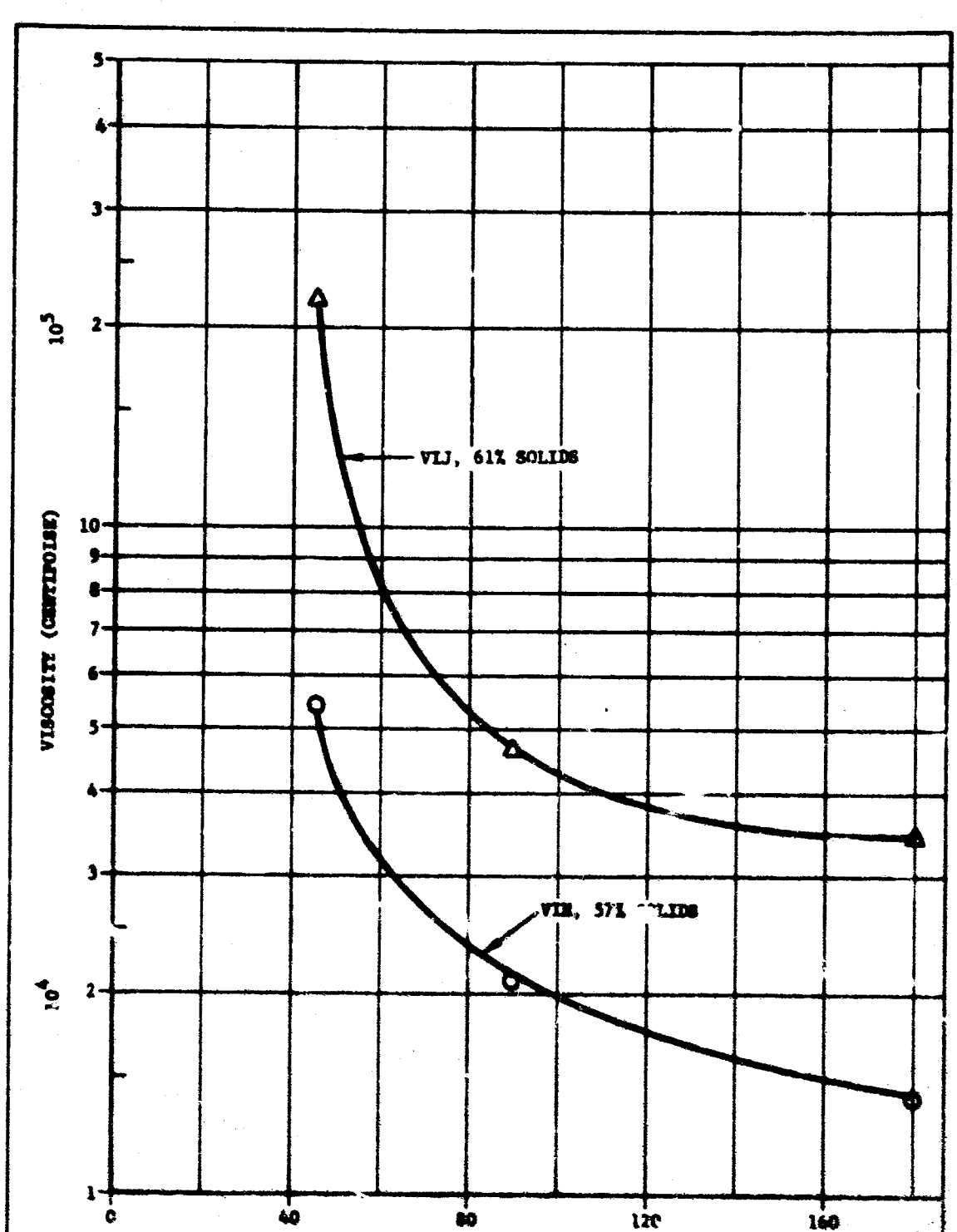

Figure 42. Viscosity as a Function of AP Particle Size

TABLE XVI

BERYLLIUM PROPELLANTS - RHEOLOGICAL CRITERIA

	Propellant Type									
	VIH	VII	VIJ	VIJ	VIJ	VIK	VIL	VIM	VIO	VIG
Volume percent solids	56.6	60.2	61.4	61.4	61.4	56.4	56.4	63.0	59.8	63.5
Weight percent solids	60.0	60.0	65.0	65.0	65.0	60.0	60.0	65.0	63.5	65.0
Percent coarse solids	54.1	57.7	57.7	57.7	57.7	56.7	60.0*	60.0	68.5*	60.8*
Particle size oxidizer (microns)	45	90	45	90	180	45	45/180	300	45/180	--
Particle size ratio	3	6	3	6	12	3	3-12	20	3-12	--
Viscosity (centipoise) at 3 rm and 80° F	54,000	45,000	220,000	46,000	35,000	66,000	22,000	46,400	22,000	--

*These formulations have a trimodal distribution of oxidizer and fuel

CONFIDENTIAL

CONFIDENTIAL

TABLE XVII

BERYLLIUM PROPELLANTS FOR IMPULSE EFFICIENCY STUDIES

	Propellant Type										
	VIH	VII	VIJ	VIJ	VIJ	VIK	VIL	VIM	VIN	VIO	VIP
Formulation (wt %)											
BE (PBB, 10μ)	10.0	15.0	10.0	10.0	10.0	10.0	10.0	10.0	10.0	10.0	10.0
BE	30.5	27.5	32.5	32.5	32.5	30.5	30.5	30.0	30.0	34.0	33.0
AP	32.5(45μ)	22.5(90μ)	37.5(45μ)	37.5(90μ)	37.5(180μ)	34.0(45μ)	18.0(45μ)	--	--	10.5(45μ)	8.0(90μ)
HMX (Class A)	--	--	--	--	--	--	18.0	--	--	33.0	--
AN (Hercules No. 3)	--	--	--	--	--	--	--	37.5	39.0	--	--
[illegible]	--	--	--	--	--	--	--	--	--	--	31.5
Bu (HP-17)	13.5	15.5	15.5	15.5	15.5	14.0	12.0	15.5	14.0	8.0	12.5
Neo	1.0	1.0	1.0	1.0	1.0	1.0	1.0	1.0	1.0	1.0	1.0
2-NDPA	1.0	1.0	1.0	1.0	1.0	1.0	1.0	1.0	1.0	1.0	1.0
TA	1.5	7.5	2.5	2.5	2.5	1.5	1.5	5.0	5.0	2.5	--
AlH3	--	--	--	--	--	--	--	--	--	--	2.0
Theoretical											
Imp-1000/lA.7 (sec)	278.0	278.7	277.4	277.4	277.4	276.5	281.1	281.2	280.1	281.1	280.7
Tc (°R)	4173	3971	4145	4145	4145	4109	4008	3820	3744	3758	3633
P (gm/cc)	1.718	1.679	1.717	1.727	1.727	1.728	1.715	1.639	1.638	1.718	1.688
Q.P.D	1.169	1.050	1.171	1.171	1.171	1.269	1.235	1.177	1.278	1.379	1.217
Sensitivity**											
Impact (cm/2kg)	11 (53)	11 (17)	3.5 (21)	3.5 (>1)	6.9 (11)	3.5 (64)	3.5 (26)	3.5 (51)	11 (64)	3.5 (3.5)	3.5 (33)
Friction (lb @ ft/sec)	32 @ 8 (37 @ 8)	32 @ 6 (156 @ 8)	23 @ 6 (86 @ 8)	23 @ 8 (52 @ 8)	40 @ 6 (48 @ 8)	40 @ 8 (54 @ 8)	40 @ 8 (48 @ 8)	29 @ 8 (230 @ 8)	48 @ 8 (280 @ 8)	30 @ 8 (156 @ 8)	17 @ 8 (300 @ 8)
Electrostatic discharge (Joules)	>6.25 (>6.25)	>5.0 (>5.0)	0.250 --	>5.0 (>6.25)	0.250 --	>6.25 (1.25)	>6.25 (>6.25)	>6.25 (>6.25)	>6.25 (>6.25)	0.25 (0.25)	0.25 (>5.0)
Autoignition (°C)	204 (309)	231 (199)	212 (201)	214 (193)	219 (201)	200 (190)	207 (189)	200 (223)	204 (223)	213 (213)	214 (218)
Differential thermal analysis, ignition (°C)	172 (179)	174 (174)	182 (180)	173 (171)	176 (163)	170 (173)	173 (172)	170 (173)	175 (175)	166 (172)	168 (169)
Physical properties											
Tensile (psi)	160	96	--	98	--	96	66	59	88	--	125
Elongation (%)	32	34	--	23	--	30	43	22	22	--	20
Modulus (psi)	304	377	--	526	--	398	280	340	425	--	1000
Burning rates***											
r @ 1000 psia	0.97	0.50	0.98	0.75	0.55	1.02	0.87	--	0.33	0.66	0.[illegible]
Exponent	0.49	0.39	--	0.47	--	0.39	0.38	--	--	0.76	0.57

*Oxidation ratio

**First number is for unaured propellant, number in parenthesis is for aured propellant

***Motor data

CONFIDENTIAL

a. Binder Selection

Because of the apparent dependency of the efficiency of LMH-2 propellants on flame temperature and oxidation ratio, it was necessary to formulate with a highly energetic binder. A 10-percent-NC level was selected as being the lower limit which would give adequate physical properties without crosslinking techniques. Based on predicted impulse values and projected processibility criteria, formulations containing up to 50-percent NG were considered. A series of 10-gm LMH-2 mixes were made with varying liquid compositions and AP, AP + HMX, and AN as primary oxidizers. At the 50-percent liquid level, the following liquid compositions were investigated for their effect on uncured sensitivity:

(1) 99-percent NG + 1-percent 2-NDPA

(2) 95-percent NG + 4-percent TA + 1-percent 2-NDPA

(3) 97-percent NG + 2-percent TDI + 1-percent 2-NDPA

Table XVIII contains the matrix compositions and the range of values obtained for the uncured sensitivities. The lower range of impact and friction sensitivity values obtained compared to conventional double-base propellants indicated an additional degree of hazard was involved in processing with these liquid compositions. There appeared to be no significant difference in the sensitivity levels of any of the three liquid compositions considered. Additional sensitivity tests were also run with a 90-percent NG, 9-percent-TA solvent, which showed only a marginal improvement in the sensitivity levels. These tests indicated the total amount of NG in the formulations was a major contributor to the lower uncured sensitivity values and that little advantage was gained by small coplasticizer dilutions.

Because of the increased sensitivity of the proposed LMH-2 propellants due to the high-energy solvent, additional sensitivity testing was performed to determine the hazards from thin propellant films. The test (thin film propagation) consisted of measuring the potential of thin propellant films to propagate in the uncured state from impact. The test apparatus utilized the standard impact apparatus modified for a thin propellant film ribboned out to 4 in. long and containing two intermediate breakwires. In a complete propagation, both breakwires fire. In a partial propagation, only one breakwire fires. Conventional double-base propellants show no tendency to propagate in this test. The LMH-2 candidate formulations containing both 90- and 99-percent-NG solvents were tested. The resulting data are the following:

VIY (99-percent NG)	VJA (99-percent NG)
7 complete propagations	10 complete propagations
3 partial propagations	

TABLE XVIII

LMH-2 PROPELLANTS FOR SENSITIVITY EVALUATION

	Propellant Designation*				
	BAP-15	BAP-17	BH-15	BHA-15	BAN-17
Formulation (wt %)					
NC	10.0	10.0	10.0	10.0	10.0
NG	48-50	48-50	48-50	48-50	48-50
AP	23.0	21.0	--	11.5	--
HMX	--	--	24.0	11.5	--
AN	--	--	--	--	21.0
LMH-2	15.0	17.0	15.0	15.0	17.0
Res	1.0	1.0	--	1.0	1.0
2-NDPA	1.0	1.0	1.0	1.0	1.0
TA + TDI	0-2	0-2	0-2	0-2	0-2
Theoretical					
I_{sp} (sec)	304	309	309	307	309
T_c (°K)	3620-3678	3620-3679	3564-3261	3578-3636	3469-3529
O.R.**	1.31-1.34	1.18-1.22	1.13-1.15	1.19-1.23	1.21-1.25
Sensitivity - Uncured					
Impact (cm/2Kg)	1.0-6.9	1.0-6.9	1.0-6.9	3.5	3.5-6.9
Friction (lb @ ft/sec)	40/3-18/8	17/4-50/8	13/4-72/8	100/6-50/8	72/8-100/8
ESD*** (Joules)	0.025- > 6.25	0.25- > 6.25	0.05- > 6.25	0.050-1.25	0.0125-0.025
Auto Ignition (°C)	200-226	205-231	210-230	196-210	194-204
Taliani (mm Hg)	19-43	38	12-26	17-73	117-141

*Legend: B - LMH-2 Fuel
AP - Ammonium Perchlorate Oxidizer
H - HMX Oxidizer
HA - HMX - Ammonium Perchlorate Oxidizer
AN - Ammonium Nitrate Oxidizer
15 - 15% LMH-2
17 - 17% LMH-2

**Oxidation Ratio

***Electrostatic discharge

VIY (90-percent NG)	VJA (90-percent NG)
10 partial propagations	7 partial propagations
	3 nonpropagations

Although a trend toward improved thin film propagations results when the lower NG solvents is evident, it is of such a magnitude as to be of questionable significance in indicating a reduced hazard.

Based on results of the propagation and standard sensitivity tests, modifications were made to the production facility to allow complete remote handling through castings of the 15PC motors. Of particular significance was the instigation of remote cleaning procedures to eliminate hazards from thin films during cleanup.

Using these added precautions, it was anticipated that the following binder could be processed safely:

Candidate LMH-2 propellant binder

Ingredient	Weight (percent)
NG (Plastisol NC 10 to 15μ)	16.4
NG	82.0
2-NDPA	1.6

Because of the anticipated problems with the incorporation of high percentages of LMH-2 (19 percent), the binder level was fixed at 61 percent by weight for all formulations representing between 57- and 60-percent-volume solids loading for those formulations under consideration.

b. Solid Oxidizer Considerations

The three primary oxidizers, AP, HMX, and AN, were originally considered for the LMH-2 propellants. Because of efficiency considerations, AN was subsequently eliminated. Of the final six formulations, three contained AP, two HMX, and one AP and HMX.

Oxidizer particle size selection for the candidate formulations was based on both processibility and impulse efficiency considerations. Since the ingredient types, particle size distributions, and volume solids loadings for the LMH-2 propellants were similar to the Be analog formulations, similar process considerations could be employed. Figure 42 shows viscosity is relatively insensitive to AP particle size down to 90μ but increases rapidly for decreasing particle sizes below this level. Figures 24 and 32 show the effect of AP particle size on the efficiency of

Al, Be, and LMH-2 double-base propellants. These data show an almost linear relation exists between AP particle size and impulse efficiency. Thus, some additional performance gains could be expected for formulations containing AP particle size less than 90μ. Because of the rapid viscosity increase with AP particle sizes less than 90μ, and the necessity to formulate up to 60-percent-solids loading at high LMH-2 loadings, 90μ AP was selected as the best compromise for the three all-AP oxidized LMH-2 propellants. For the HMX formulations, advantage was taken of the lack-of-efficiency loss with increasing HMX particle size, and Class A HMX (180μ) was used. This also allowed the incorporation of the fine AP (15μ) in the mixed AP/HMX propellant.

It should be pointed out that lower void volumes resulting in lower viscosities could have been obtained by the use of a bimodal or a trimodal oxidizer blend. A bimodal distribution is present with NC and LMH-2 considered in addition to the 90μ AP. However, little increase in packing is obtained by the addition of a third particle size until a particle size ratio of approximately 20 to 1 is exceeded. This would require a large percentage of the solid oxidizer to be in excess of 200μ and was felt to be prohibitive from efficiency considerations.

c. LMH-2 Incorporation

Work prior to the start of Contract AF 04(611)-10754 had shown that processibility of LMH-2 propellants became marginal at LMH-2 loadings above 15 percent (58-percent-volume-solids loading). Even at these low LMH-2 levels it was usually necessary to use ground LMH-2. This limitation was felt to be due to a combination of low bulk densities, a poor shape factor, and surface anomalies. Considerable effort was expended to improve the processibility and rheological properties to allow increased LMH-2 loadings. Primary emphasis was placed on the development of post-treatment methods to improve LMH-2 bulk density and shape factor and to mask surface effects. Of the various methods tried, the following were the most successful.

1) Grinding

All LMH-2 lots were ball-milled by the Ethyl Corporation for 30 min. This normally increased bulk density from 0.30 to 0.38 gm/cc, although variations in specific surface, particle size, and bulk density between lots was apparent.

2) Wax Coating

A 1-percent coating of CEC high vacuum wax was placed on the LMH-2 by stripping from a volatile solvent.

3) AP Treating

AP was recrystallized in the presence of LMH-2 from a saturated AP/LMH-2 water dispersion.

In addition, various LMH-2 lots exhibited a tendency to gas during cure, resulting in porous propellant. Two posttreatments were used to eliminate this gassing. These posttreatments consisted of an elevated temperature vacuum baking cycle or a room-temperature water-wash cycle.

Complete details of the characterization of LMH-2 and the developed posttreatments are contained in Section IV.

d. Propellant Selection

Based on the efficiency correlations, binder and oxidizer particle size studies, and the developed LMH-2 posttreatments, the six propellants listed in Table XIX were selected for ballistic screening. The VIX, VIY, and VIZ propellants were selected to explore the tradeoff between LMH-2 loadings and delivered impulse for an all-AP oxidized system. The VJA and VJI propellants were selected to explore an all-HMX oxidized system. It was also desirable to explore the use of fine AP in a mixed AP/HMX system from efficiency considerations. Several mixes were made to determine the effect on processibility due to substituting fine AP for HMX in the VJI matrix. These results are listed in the following tabulation:

Percent 15 μAP	0	5	8
Viscosity @ 3 rpm (cps)	77,000	160,000	393,000

Because of the marginal processibility with greater than 5-percent fine AP, VJL was chosen for ballistic evaluation.

Table XIX also contains a summary of pertinent data obtained on the six candidate LMH-2 formulations. As previously discussed, uncured sensitivity data was satisfactory for processing, although impact and friction values were lower than conventional double-base propellants. Cured sensitivity values were comparable to conventional double-base. Thermal stability was excellent, as evidenced by autoignition tests. Physical properties were more than adequate for subscale and some large motor applications. The lower tensile strength of 75 psi for VJA compared to 100 to 120 psi for VIX, VIY, and VIZ is due to the large Class A HMX particle used in VJA. Improvements in physical properties could be made in these formulations by cross-linking techniques. Experimental densities were greater than 98 percent of theoretical in all cases, confirming the adequacy of the posttreatments used.

TABLE XIX

PROPERTIES OF LMH-2 PROPELLANTS

Propellant Type	VIX	VIY	VIZ	VJA	VJI	VJL
Formulation (wt %)						
NC (FNC, 10 μ)	10.0	10.0	10.0	10.0	10.0	10.0
NG	50.0	50.0	50.0	50.0	50.0	50.0
AP	23.0 (90μ)	21.0 (90μ)	19.0 (90μ)	--	--	5.0 (15μ)
HMX (Class A)	--	--	--	24.0	22.0	16.0
LMH-2 (Ground)	15.0	17.0	19.0	15.0	17.0	17.0
Res	1.0	1.0	1.0	--	--	1.0
2-NDPA	1.0	1.0	1.0	1.0	1.0	1.0
Theoretical						
Isp (1000/14:7)	303.7	308.9	313.8	309.3	314.0	312.7
T_c (°K)	3678	3679	3672	3621	3623	3614
ρ (lb/in.^{3})	0.0490	0.0477	0.0464	0.0490	0.0477	0.0476
Oxidation ratio	1.342	1.219	1.113	1.146	1.062	1.082
Sensitivity*						
Impact (cm/2Kg)	3.5 (21)	3.5 (33)	3.5 (26)	3.5 (21)	3.5 (26)	3.5 (26)
Friction (lb_f at ft/sec)	23 @6 (90 @8)	17 @6 (90 @8)	23 @6 (90 @8)	50 @6 (154 @8)	46 @8 (63 @8)	30 @6 (156 @8)
Electrostatic discharge (joules)	1.25 (1.25)	1.25 (1.25)	>5.00 (>5.250)	0.625 (1.25)	>5.00 (>5.00)	>5.00 (1.25)
Autoignition (°C)	205 (230)	203 (208)	21[illegible] (223)	227 (235)	238 (212)	224 (215)
Differential thermal analysis, ignition (°C)	178 (178)	170 (178)	165 (172)	181 (178)	-- (182)	167 (167)

*First number is for uncured propellant, number in parenthesis is for cured propellant

TABLE XIX (Cont)

PROPERTIES OF LMH-2 PROPELLANTS

Propellant Type	VIX	VIY	VIZ	VJA	VJI	VJL
Physical Properties						
Tensile (psi)	110	100	120	75	--	--
Elongation (%)	22	20	20	22	--	--
Modulus (psi)	480	600	490	420	--	--
Density ($lb/in.^3$)	0.0485	0.0472	0.0457	0.0485	0.0473	0.0473
(% theoretical)	99.0	99.0	98.4	99.0	99.2	99.3
Burning Rate**						
γ @1000 psia	1.03	0.97	0.90	0.76	0.76	0.88
Exponent	--	0.332	--	0.485	--	--

**Motor data

e. Process Studies

Table XX shows the rheological criteria for the LMH-2 formulations. The VIZ formulation with 60-percent-volume solids and 19-percent LMH-2, and the VJL formulation with 59-percent-volume solids, 17-percent LMH-2, and 5-percent 15μ AP were the most difficult formulations to be processed in the program. The following techniques were used to facilitate mixing and casting of these formulations:

(1) Use of wax-treated or AP-treated LMH-2

(2) A heated mix cycle

(3) Agitation and vibration during casting

Figure 43 shows the effect of LMH-2 loadings (from 15 to 19 percent) on viscosity for two LMH-2 lots evaluated (99 and 97). Lot 99 gave significantly higher viscosities than lot 97 at both 15- and 19-percent LMH-2 loadings. The effect of wax treating and AP treating on lot 99 is also shown in Figure 43. Use of wax treatment for lot 99 decreased viscosity from 120,000 to 70,000 cps in VIX (15-percent LMH-2) formulation. The AP treatment further decreased viscosity from 300,000 to 240,000 cps in VIZ (19-percent LMH-2) formulation with lot 99. Viscosity reduction obtained with the wax-treated material was considered adequate and because of its simplicity was selected over AP treatment. For lot 97, significant improvements in solids loading over lot 99 could be made at loadings up to 19-percent LMH-2. This viscosity variance observed between LMH-2 lots becomes increasingly significant as higher density LMH-2 propellants are sought. Control of the LMH-2 lot variance is discussed in detail in Section IV.

The decrease of viscosity with increasing mix temperature is illustrated in Figure 44 for the VIX and VJA formulations. This same trend was apparent for all formulations and, as a result, elevated mixing cycles were employed. To determine the limit to which an elevated temperature cycle could be used, a pot-life study was run on the VJL formulation. Results obtained are listed in the following tabulation:

Mix Temperature (^{o}F)	Mixing Time (min)	Viscosity @ 3 rpm (cps)
110	13	160,000
108	45	293,000
111	68	>333,000

From the pot-life study it is apparent a definite tradeoff exists between viscosity, mixing temperature, and mixing time. For the 15PC castings, a progressive temperature mix cycle was used with the final 15 min of a 45-min cycle at 100^{o} to 110^{o} F.

TABLE XX

LMR-2 PROPELLANTS-RHEOLOGICAL CRITERIA

	Propellant Type					
	VIX	VIY	VIZ	VJA	VJI	VJL
Volume percent solids	57.6	58.8	59.9	57.6	58.8	58.8
Weight percent solids	50.0	50.0	50.0	50.0	50.0	50.0
Percent course solids	46.0	42.0	38.0	48.0	44.0	32.0
Particle size oxidiser (microns)	90	90	90	180	180	15-180
Particle size ratio	6	6	6	12	12	1-12
Viscosity (centipoise at 3 rpm and 100° F)	70,000	120,000	300,000	50,000	80,000	160,000

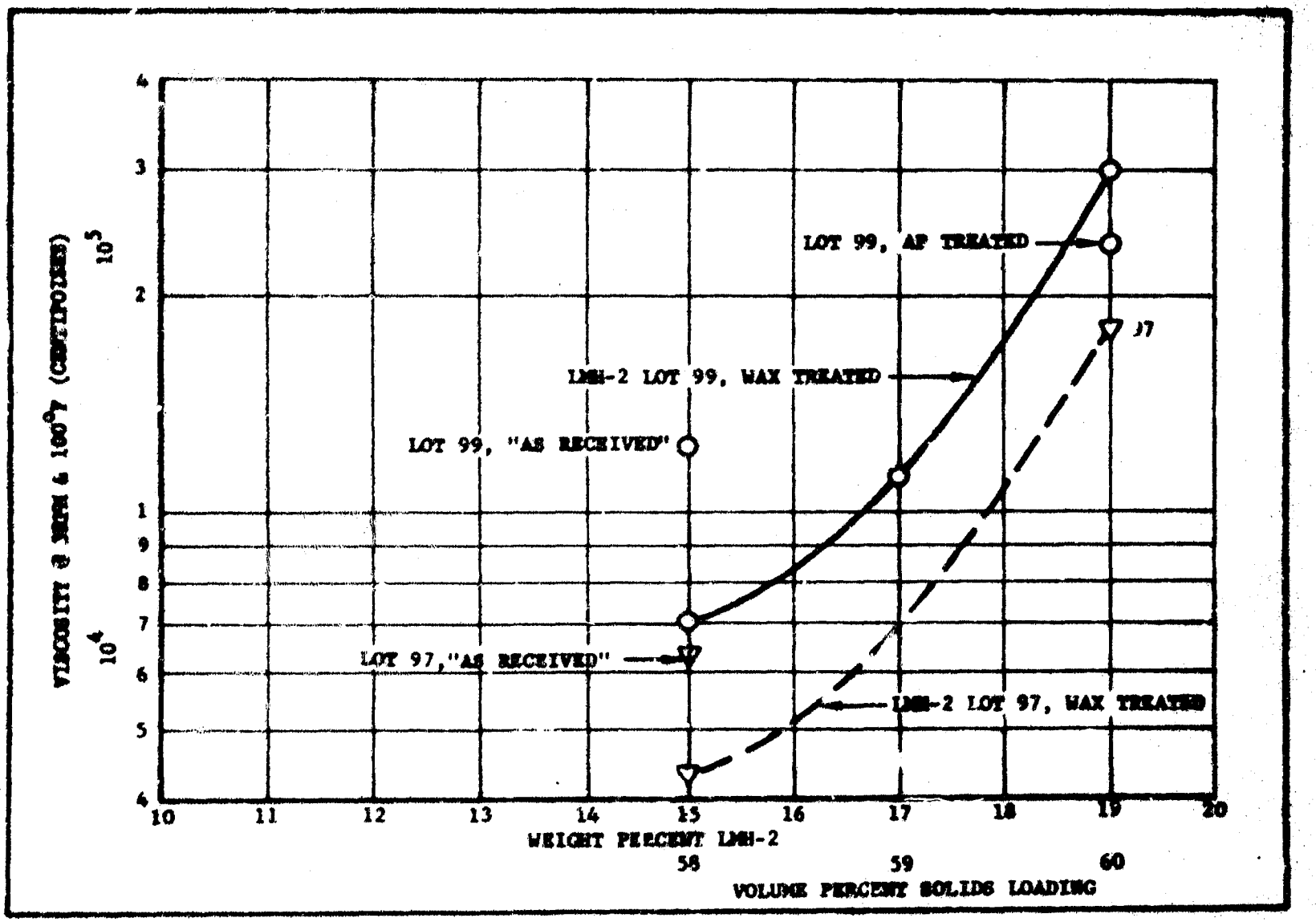

Figure 43. Viscosity as a Function of LMH-2 Loading

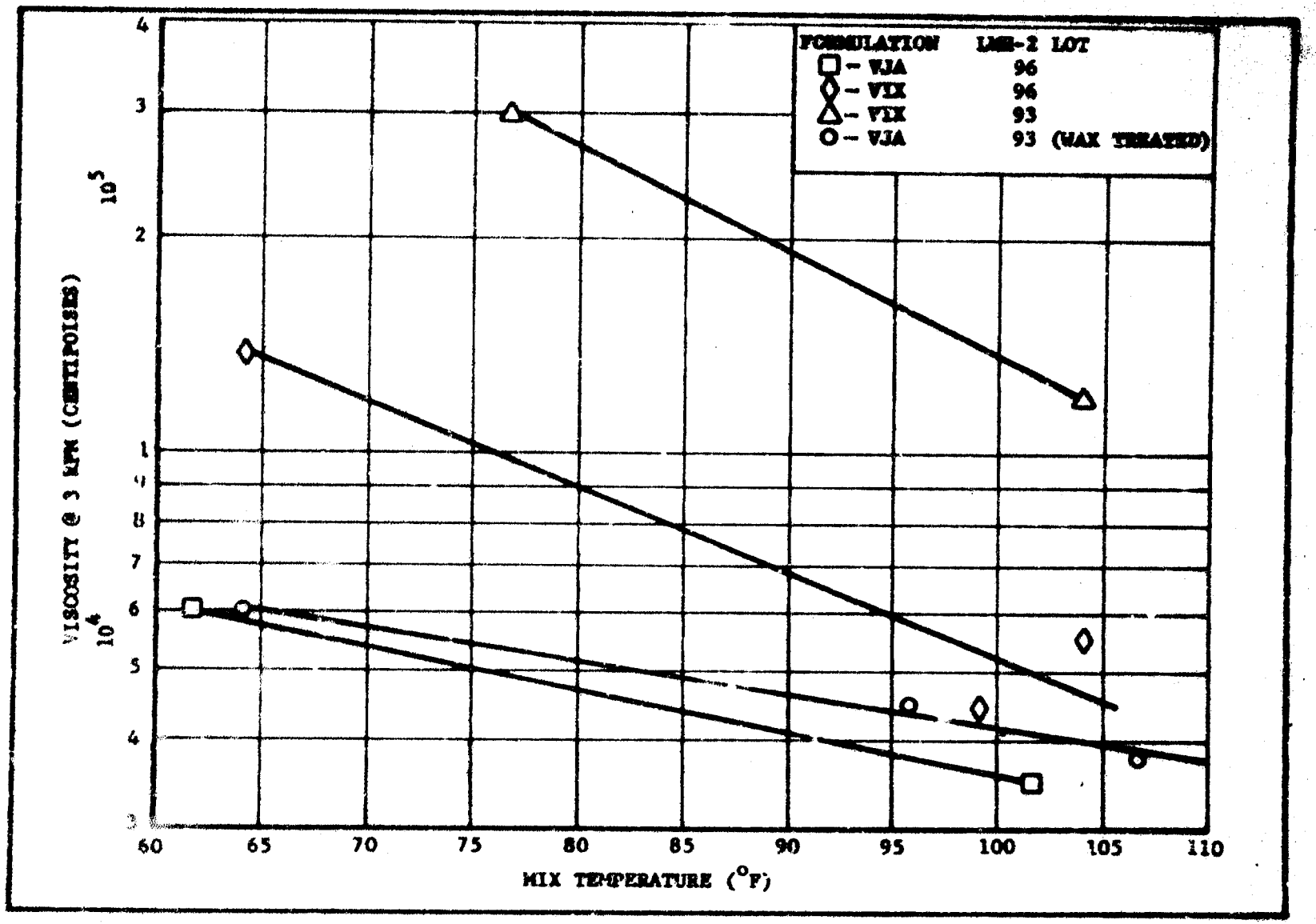

Figure 44. Viscosity as a Function of Temperature

Figure 45 shows viscosity as a function of shear rate for the VIZ and VJL formulations showing the typical thixotropic nature of LMH-2 formulations. To take advantage of this effect, all formulations were cast through the bottom dump valve of the mixer with the agitator rotating at 6 to 8 rpm. For the thicker mixes, some vibration was also applied to the mixing bowl.

C. BALLISTIC TESTING

1. Motor Design Studies

a. Grain Design

The basic motor configuration selected for motor firings on the Task II effort was the 15PC (nominal 15PC for a propellant density of 0.062 lb/in.^{3}). This motor was designed and developed under Contract AF 04(611)-9062 (Be/Taz).

The 15PC motor gave excellent results with VCP propellant; however, only a limited mass-flow range was covered (> 6 lb/sec). This range was extended under Contract AF 04(694)-127 to approximately 5 lb/sec. With this background, it was felt necessary to keep mass-flow rates on the current program above 5 lb/sec. Because of this requirement, coupled with anticipated low burning rates and low densities, it was necessary to modify the basic grain design. In reviewing new grain designs the following items were considered as desirable:

(1) No major alterations to existing hardware from implementation of the design

(2) A neutral pressure-time trace

(3) A minimum chance for propellant sliver at burnout

(4) A maximum propellant weight of 15 lb with VCP propellant

(5) Ease of propellant consolidation

It was decided to use a cylindrical, center-perforated grain with the standard 15PC inhibitor in order to maximize the use of existing hardware and minimize slivering.

In order for the initial burning surface (Si) to equal the final burning surface (Sf) for a center-perforated grain burning on both ends and the center core, the length (L) must equal 1.5 x OD + 0.5 x ID of the grain. The larger the web, the less neutral the burning surface is between Si and Sf. Conversely, a small web means a long grain and more difficult consolidation of high-viscosity mixes.

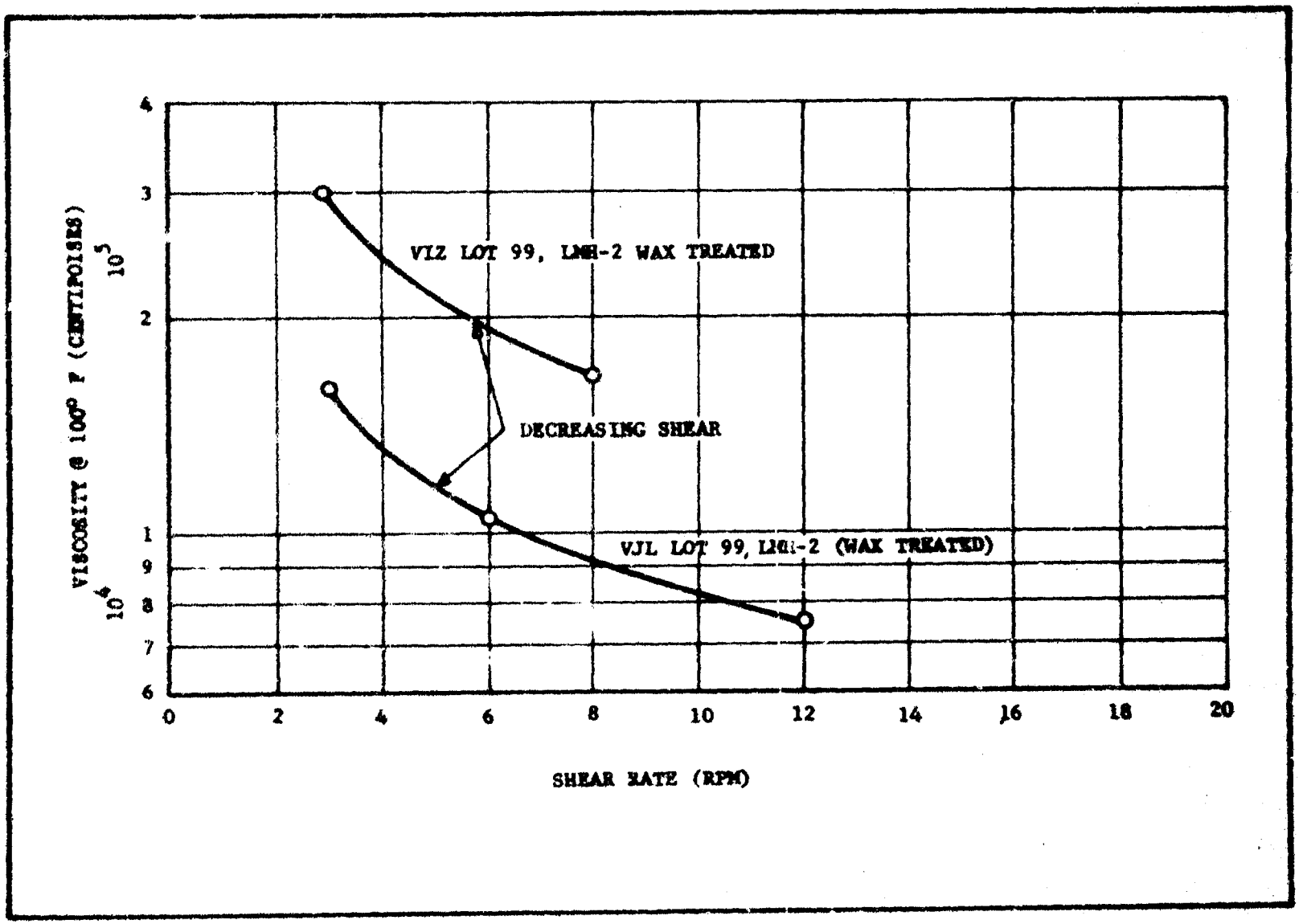

Figure 45. Viscosity as a Function of Shear Rate

Figure 46 shows a plot of grain design parameters for a single grain. The present 15PC design, which will be used for many of the firings, is almost on the intersection of the line where Si = Sf and the line where propellant weight is 15 lb for VCP propellant. In order to maintain the 5 lb/sec mass-flow rate with a reasonable web thickness, grain length must be increased at a considerable loss of neutrality. However, a single grain was selected from this grid which should provide a good compromise design. This grain (Mod-1 design) was 14 in. long with a web of 1.0 in. Although slightly progressive, it will maintain mass flows of 5 lb/sec down to burning rates of 0.45 in./sec and densities of 0.047 $lb/in.^3$.

It was expected that rates somewhat lower than 0.45 in./sec might be observed. For these tests, a single grain is not suitable, so a two-grain concept was reviewed. Figure 47 shows a plot of grain design parameters for a double grain. In order to avoid excessive case-bond area and yet accommodate rates as low as 0.3 in./sec, a combined length of 18 in. was chosen as a second alternate design. This design (Mod-2) is only slightly regressive. Figure 48 shows the predicted pressure-versus-time curves for the alternate designs.

The basic and two alternate grain designs gave a high degree of flexibility in matching burning rates and density-to-mass-flow rate. Figure 49 shows the standard 15PC compared with the Mod-2 configuration. Note the chamber extension added to accommodate the Mod-2 grain. By removal of the chamber extension, the chamber can be used for standard 15PC firings. Figure 50 shows the configuration for the Mod-1 grain design.

b. Residence Time Effects

Fourteen 15PC firings were scheduled to study the effect of L* on efficiency. The standard 15PC motor with VCP at K of 140 (1000 psi) has an L* of 160. In order to provide a larger free volume, the same chamber extension made with Mod-2 grain design was employed. By using this chamber extension and a standard grain design (Figure 50), an L* of 400 is achieved with VCP at a K of 140.

c. Optimum Nozzle Geometry Firings

Twelve 15PC firings were scheduled for evaluation of approach angle effect on efficiency. Both 15 and 5 degree approach cones were required for these tests. The 15 degree approach cones were fired in a standard 15PC altitude chamber, and the 5 degree approach cones were fired in the high L* chamber. (See Figure 51.) Table XXI compares the ballistic design criteria for the various test motors used on this program.

2. Control Propellant

Control firings of a well-characterized, efficient Be propellant were dispersed throughout the motor testing program to provide checks on data validity. Additional firings of the control propellant were also made

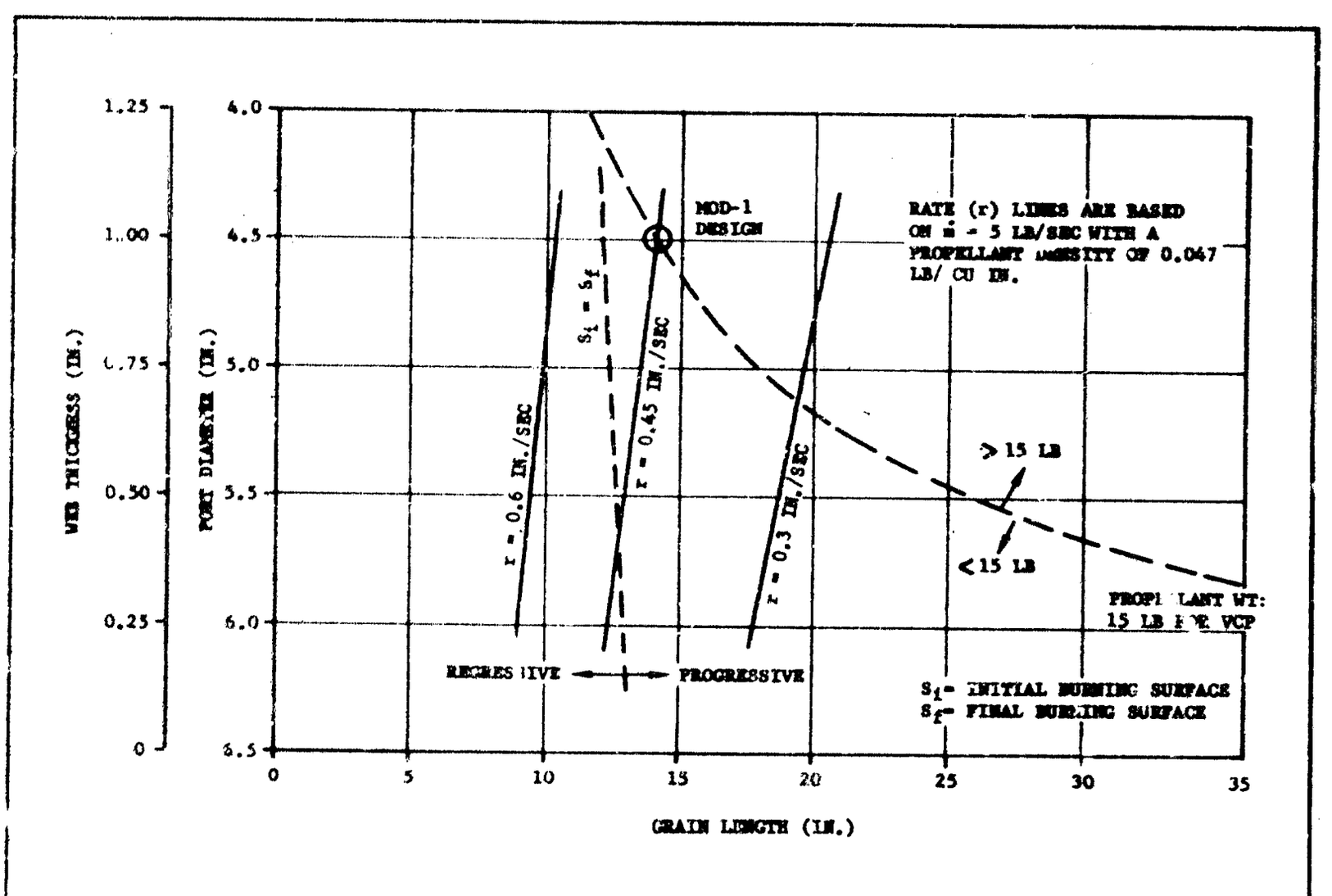

Figure 46. Grain Design Tradeoffs for Single-Length 15PC Motor at a Constant Mass Flow of 5 lb/sec

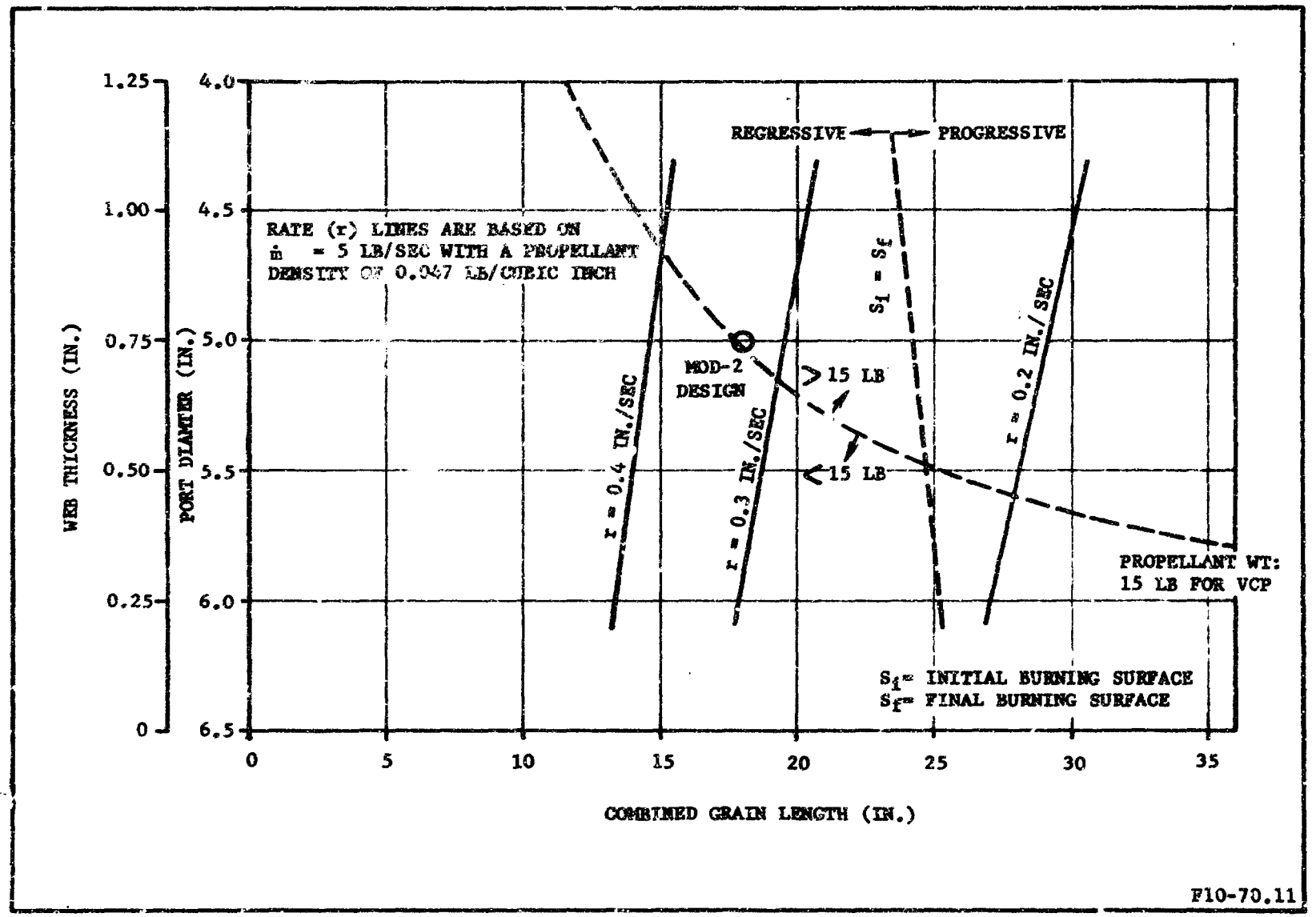

Figure 47. Grain Design Tradeoffs for Double-Length 15PC Motor as a Constant Mass Flow of 5 lb/sec

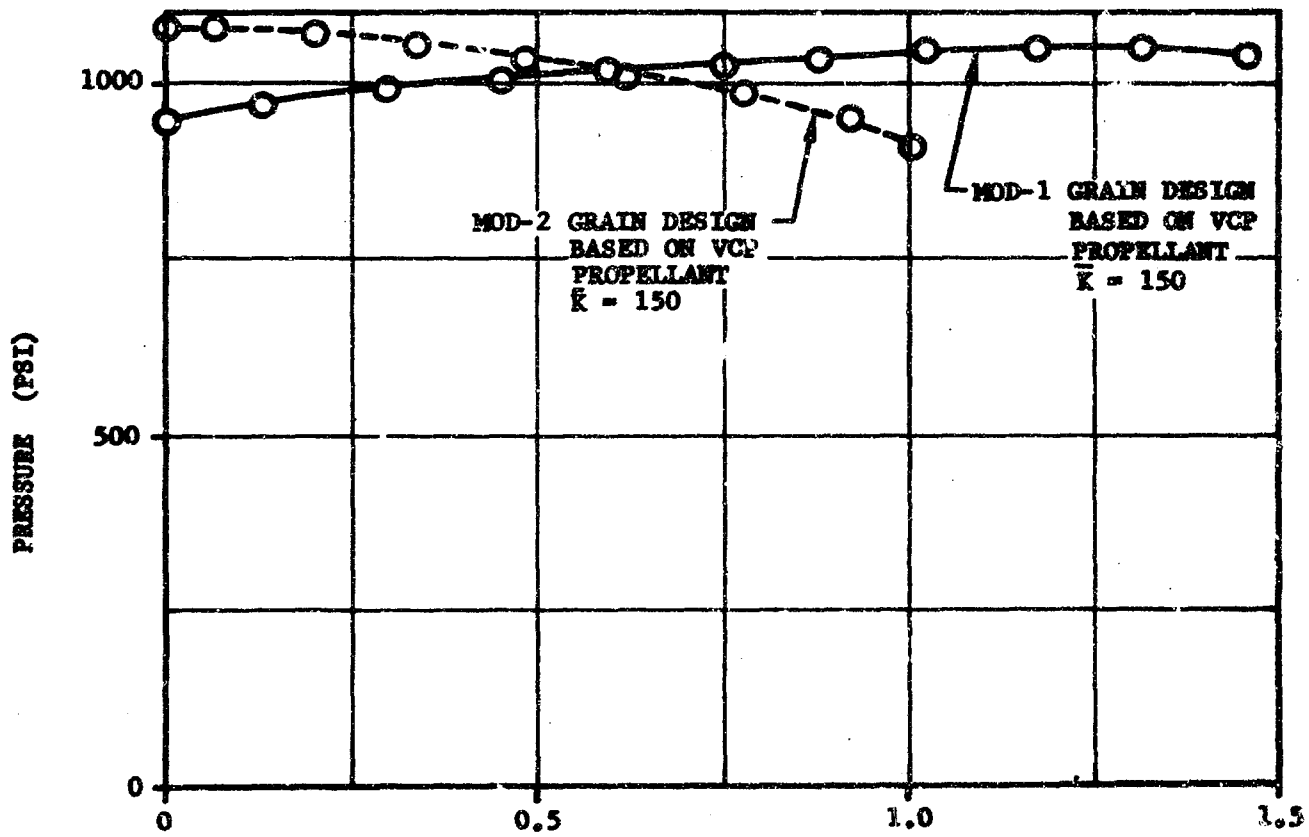
1000
500
0
0
0.5
1.0
1.5
PRESSURE (PSI)
TIME (SEC)
MOD-2 GRAIN DESIGN BASED ON VCP PROPELLANT $\bar{K}$ = 150
MOD-1 GRAIN DESIGN BASED ON VCP PROPELLANT $\bar{K}$ = 150

F10-70.13

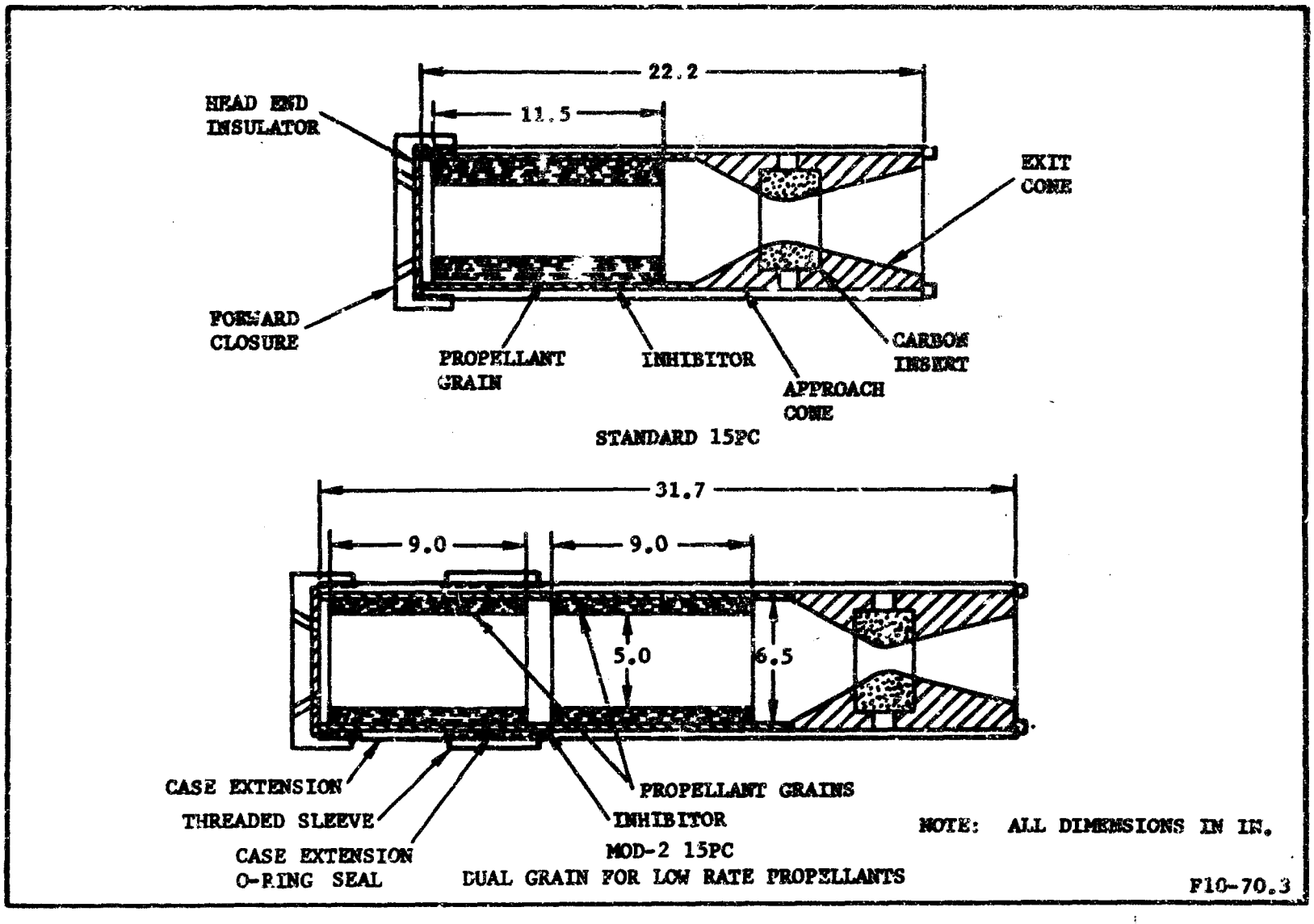

Figure 49. Motor Configurations for Standard 15PC Motor and Mod-2 Grain

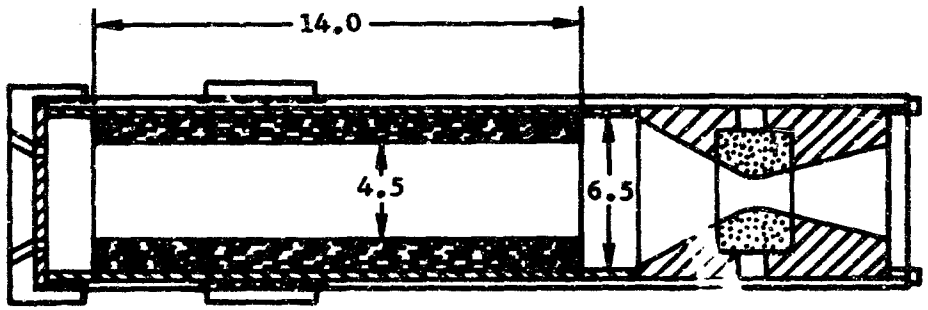

MOD-1 15PC
SINGLE GRAIN FOR INTERMEDIATE RATF PROPELLANT

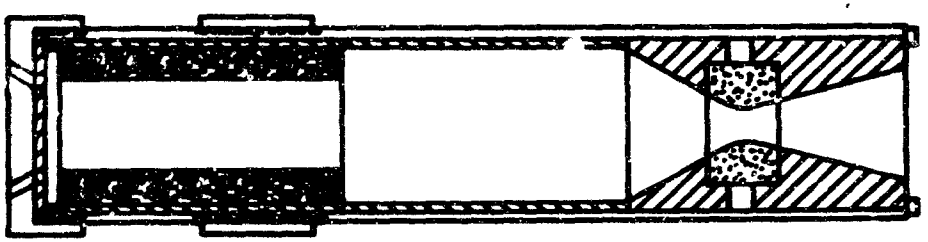

HIGH L* 15PC

NOTE: ALL DIMENSIONS IN IN.

F10-70.1

Figure 50. Motor Configurations for L* Firings

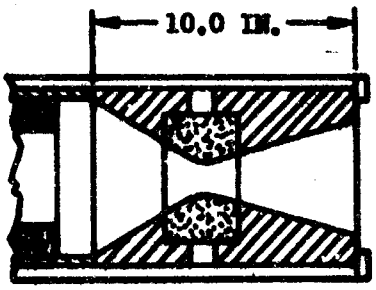

STANDARD 15PC WITH
30° APPROACH CONE

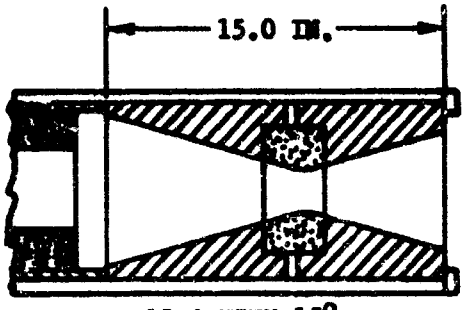

15PC WITH 15°
APPROACH CONE

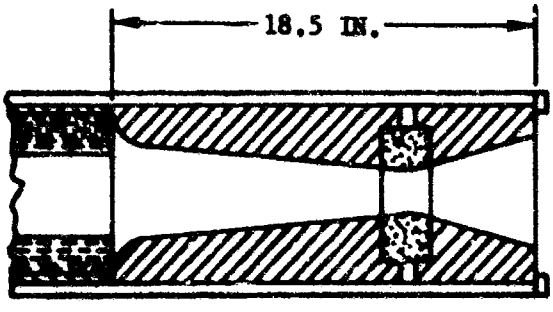

15PC WITH 5°
APPROACH CONE

NOZZLE LENGTH BASED ON
K = 140, ϵ = 9.5 TO 1

F10-70.2

Figure 51. Comparison of 15PC Motor Nozzle Configurations

TABLE XXI

COMPARISON OF BALLISTIC DESIGN CRITERIA FOR
AF 04(611)-10754 EVALUATION MOTORS

Motor Designation	5PC	Standard 15PC	Mod-1 15PC	Mod-2 15PC
Grain Dimensions				
OD (in.)	4.51	6.50	6.50	6.50
ID (in.)	2.6	3.9	4.5	5.0
No. grains per motor	1	1	1	2
Length (in.)	8.0	11.5	14.0	9.0
Web (in.)	0.95	1.3	1.0	0.75
S (in^2)	89.0	189	242	325
Volume of propellant (in^3)	84.5	246	242	244
Weight of propellant (lb @ 0.062 lb/in^3)	5.2	15.2	15.0	15.1
Free volume (VF-in^3)	77.0	242	297.3	510
Throat area[1] (A_t)	0.594	1.26	1.61	2.17
$L^* = V_p/A_t$	130	192	184	277
$\frac{Pmi}{P_p}/\frac{Pb}{Pb}/\frac{Pmax}{Pb}$	0.96/1.0/1.08	0.92/1.00/1.08	0.92/1.00/1.04	0.90/1.00/1.02
Divergence angle (°)	15	15	15	15
Expansion Ratio	4.8	3.7 to 30	3.7 to 30	3.7 to 30

[1] Based on VCP, K = 150 @ 1000 psi

CONFIDENTIAL

in the nozzle approach contouring and high L* studies to provide a firm basis for determining the effect of these motor parameters on motor efficiency. The control propellant selected was the VCP formulation which had previously been extensively characterized in 5PC, 15PC, and 400-lb motor firings over a wide pressure range and at high expansion ratios. A summary of properties for the VCP formulation is presented in Table XXII.

TABLE XXII

SUMMARY OF PROPERTIES FOR VCP

Propellant Type	VCP Control Propellant
Formulation (Wt %)	
NC	15.0
NG	32.4
AP	9.0
HMX	29.0
Be	10.0
Res	1.0
2-NDPA	1.0
TA	2.6
Theoretical Performance	
Isp(1000/14.7)(sec)	283.0
Tc (^{o}K)	3850.0
Oxidation ratio	1.22
ρ(lb/in.^{3})	0.062

3. Beryllium Castings and Firings

A total of 76 Be 15PC motors were cast and 70 were fired. A summary of the subtask castings and firings is presented in Table XXIII. All but six of the castings were completed successfully.

Processing problems were observed in manufacturing VIJ (45μ AP) and VIN compositions. Due to thick, highly viscous mixes the compositions were difficult to cast and consolidate. One grain of each composition was found to be discrepant because of poor propellant consolidation resulting from the marginal processibility. One mix of each formulation was also lost during attempts to reduce viscosity by use of an elevated temperature mixing cycle. Later mixes of the VIN formulation were successfully processed with 25 percent of the fines removed from the AN. Careful control of the heated mix cycle was successful for the completion of the VIJ (45μ AP) castings.

TABLE XXIII

SUMMARY OF Be CASTINGS AND FIRINGS

Purpose	Propellant Type	Grain Design	No. Castings	No. Firings
Be efficiency studies	VCP	Standard	3	3
		Mod-1	3	3
	VIG	Standard	4	3
	VIH	Standard	3	3
	VII	Mod-1	3	3
		Mod-2	3	3
	VIJ	Standard	4	3
		Mod-1	3	3
	VIK	Standard	3	3
		Mod-1	3	3
	VIL	Standard	3	3
		Mod-1	2	2
		Mod-2	1	1
	VIN	Mod-2	6	4
	VIO	Mod-1	3	3
Oxidizer particle size	VIJ (45μ AP)	Standard	4	2
	VIJ (90μ AP)	Standard	3	3
	VIJ (180μ AP)	Mod-1	3	3
Optimum nozzle geometry	VCP	Standard	4	4
	VIJ	Standard	7	7
Increased L*	VCP	Standard	2	2
	VII	Mod-1	2	2
Characterization of selected propellants	VCP	Standard	2	2
		Mod-2	2	2
Total			76	70

All firings except one were successful. One VIJ firing (LM 2-18) with a 15-degree nozzle approach cone suffered a burnthrough in the forward end of the motor. The burnthrough resulted from leakage in a pressure takeoff fitting, which allowed the chamber gasses to escape the forward end of the motor.

A problem with poor efficiency, resulting in apparent unstable burning, occurred with the VIN formulation containing AN. Figure 52 shows p-K-r data based on four VIN firings. As noted, an apparent slope change occurred in the p-r and p-K curves above 430 psia. This anomalous behavior is also apparent in a change in the discharge coefficients from 0.0078 sec^{-1} for the low pressure firings to 0.0064 sec^{-1} for the high pressure firings and is consistent with combustion-bomb data showing AN formulations to be significantly less efficient than AP or HMX formulations.

Firings made for optimum nozzle studies were observed to have greater nozzle erosion as the approach angle was reduced. Also VIJ firings were observed to have greater nozzle erosion than VCP. These results are shown in Figure 53.

A complete ballistic summary of the individual Be firings is given in Appendix B (Tables B-3 through B-7).

4. LHM-2 Castings and Firings

A total of twenty-six LMH-2 15PC mixes were made and twenty-four 15PC motors fired for ballistic screening of the six candidate LMH-2 propellants. A summary of the subtask castings and firings is presented in Table XXIV. As noted, all but two of the mixes resulted in acceptable grains with mixes containing up to 19-percent LMH-2 at 60-percent-volume solids loading successfully manufactured. Special procedures used for the LMH-2 castings have been described under laboratory formulation studies.

One VIY (containing AP-treated LMH-2) mix was not completed because of an abnormally high viscosity. When the LMH-2 was added to the solvent for this mix, the resulting material had the consistency of sand. A laboratory evaluation of the remaining AP-treated LMH-2 used for this mix was made and found to also give extremely high viscosities. A check of the process cycle showed the AP-treated material was allowed to stand for approximately 3 days in an alcohol slurry before stripping. It is believed that the LMH-2 and AP rearranged to give an abnormally low bulk density, resulting in the higher mix viscosity. Because of the higher delivered impulse obtained with initial firings of wax-treated LMH-2 in the VIY formulation, a wax-treated casting was substituted for the final AP-treated casting. The first VJL mix was also uncastable. The resultant mix was extremely tacky, indicating the pot life had been exceeded. Better mixing action of the larger mixer, coupled with the elevated temperature, appears to have resulted in a shorter pot life than was experienced in the laboratory. The remaining VJL grains were cast at a lower temperature and with a shorter elevated temperature mix cycle.

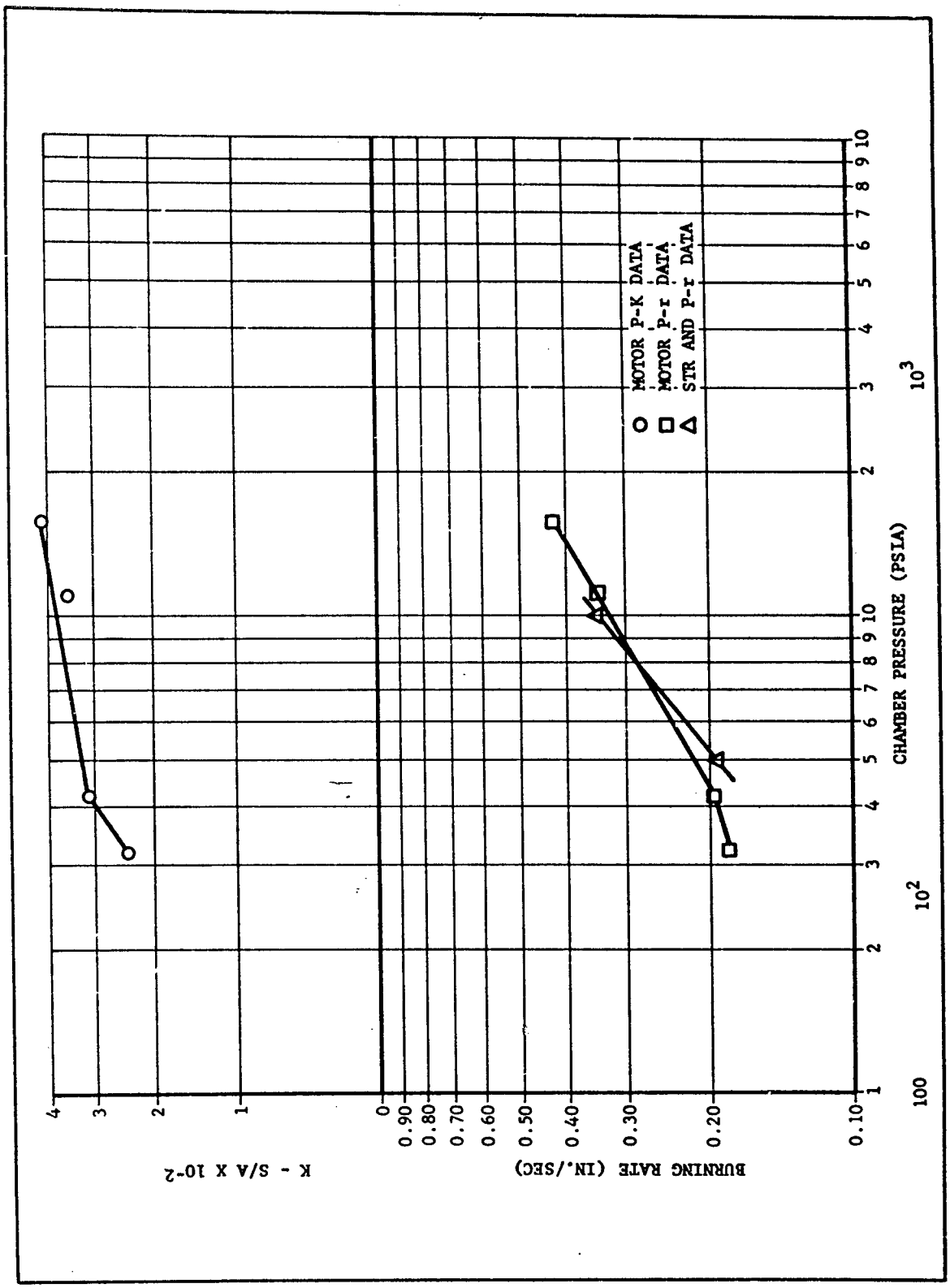

Figure 52. Burning Rate and K for VIN Propellant

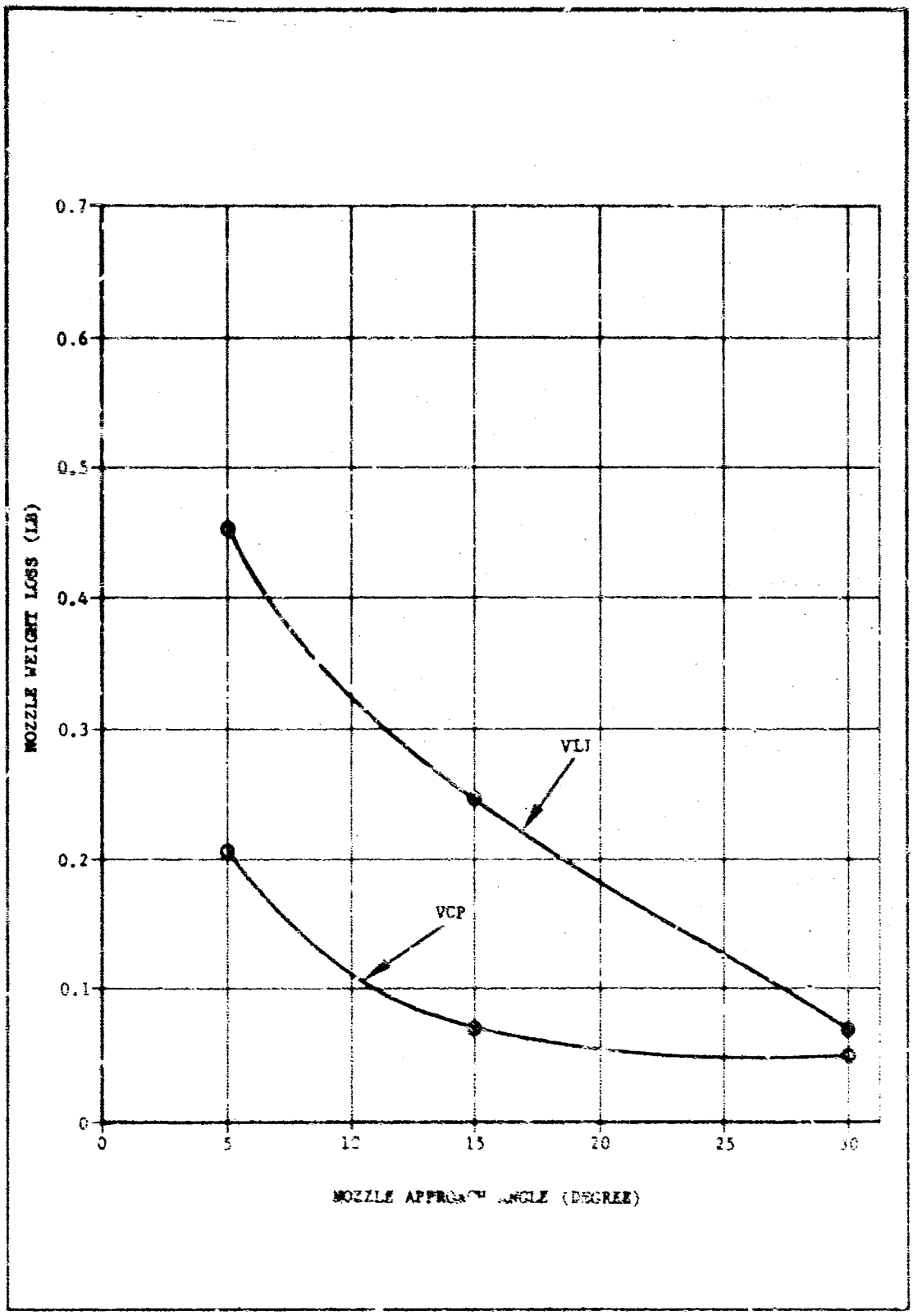

Figure 53. Nozzle Erosion Weight Loss vs Approach Angle

TABLE XXIV

SUMMARY OF LMH-2 CASTINGS AND FIRINGS

Purpose	Propellant Type	Grain Design	No. Castings	No. Firings
Increased L*	VIY (wax-treated LMH-2)	Standard	5	5
	VIY (AP-treated LMH-2)	Standard	5	4
LMH-2/AP Propellants	VIX	Standard	3	3
	VIZ	Standard	3	3
LMH-2/HMX Propellants	VJA	Mod-1	3	3
	VJI	Standard	3	3
	VJL	Standard	4	3
Final Characterization	VJA	Standard	3	3
		Mod-1	3	3
	VIY	Standard	5	5
Total			37	35

All LMH-2 firings were successful. Figure 54 shows a typical pressure-time curve for the VIY formulation. A complete ballistic summary of the individual firings is given in Appendix B (Tables B-8 through B-10), and a detailed analysis of the resulting data is given in Section II. A summary of performance data obtained from the ballistic screening firings made at high L* values with wax-treated LMH-2 is contained in the following tabulation:

Formulation	VIX	VIY	VIZ	VJA	VJI	VJL
Percent LMH-2	15	17	19	15	17	17
Oxidizer	AP	AP	AP	HMX	HMX	AP/HMX
Isp (1000/14.7)	303.7	308.9	313.8	309.3	314.0	312.7
Tc (^{o}K)	3678	3679	3672	3621	3623	3614
O.R.	1.34	1.22	1.11	1.15	1.06	1.08
ρ (gm/cc)	0.049	0.0477	0.0464	0.049	0.0477	0.0476
Efficiency	92.24	91.01	89.81	90.83	86.37	88.57
Isp_{1000}^{15}	280.1	281.1	281.8	280.9	271.2	277.0

As shown, the first four formulations all exceeded the target impulse goal. Based on these data the VJA and VIY formulations were chosen for the final characterization firings. VJA has the highest impulse-density and lowest burn rate. VIY offers almost equivalent performance with some advantage in mechanical properties.

5. Characterization of Selected Propellants

Five 15PC castings and firings of VIY and six 15PC castings and firings of VJA were ma to further characterize these formulations. Four 15PC VCP control firing were also made. Ballistic data from individual firings are summarized in Appendix B (Tables B-11 and B-12). Analysis of the data is given in Section II.

Figures 55 and 56 show the resulting p-K-r data for VIY and VJA, respectively. The VIY formulation gave a burning rate of 0.97 in./sec at 1000 psia with a pressure exponent of 0.332. VJA gave a burning rate of 0.77 in./sec at 1000 psia with a pressure exponent at 0.485.

6. Explosive Classification

Phase I testing of "Military Explosive Hazard Classification Procedure" was performed on VIY and VJA. The results are presented in Table XXV. These tests indicate VIY and VJA are TCC Class A explosives.

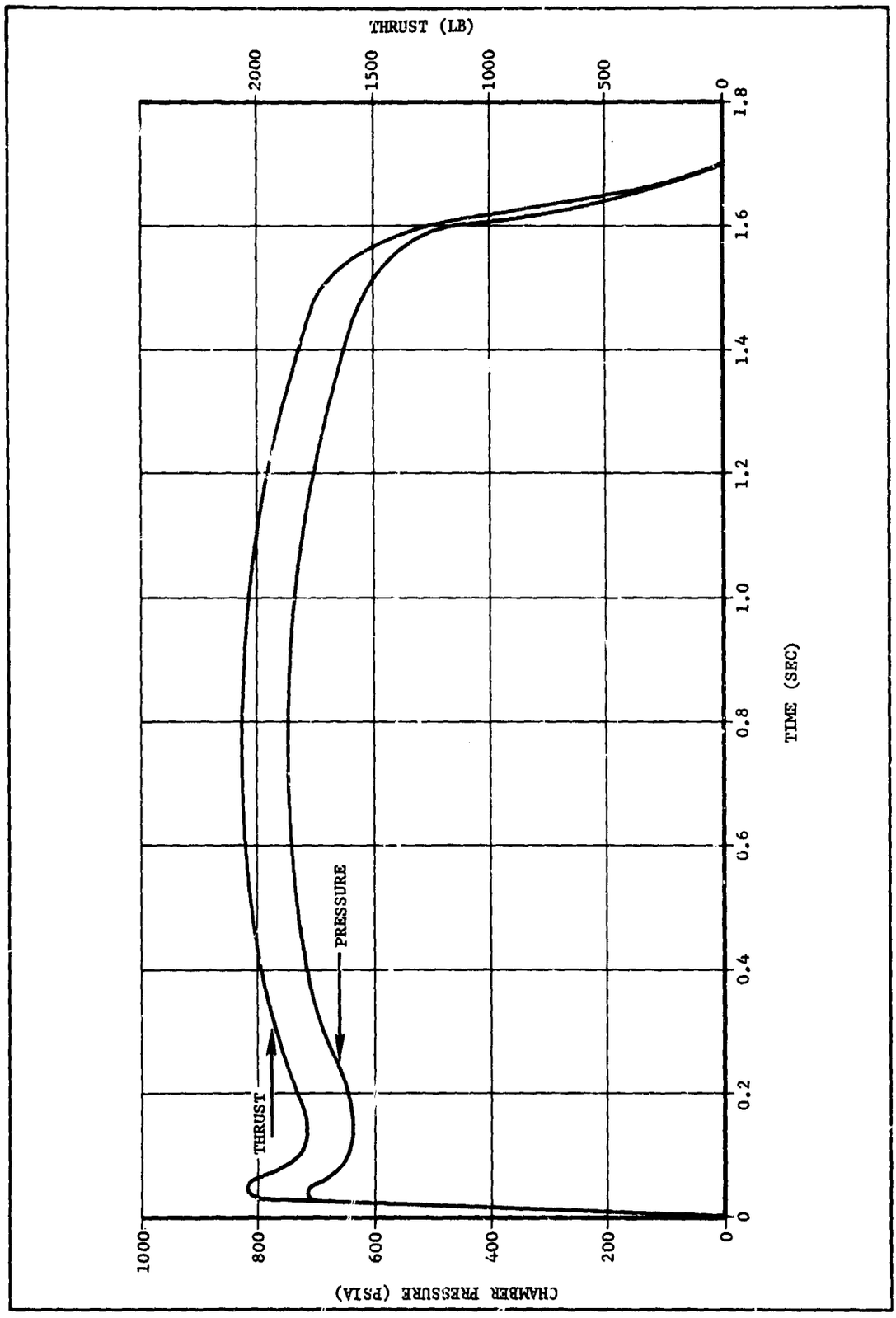

Figure 54. Pressure and Thrust-Time Curves for VIY Propellant Containing Waxed LMH-2

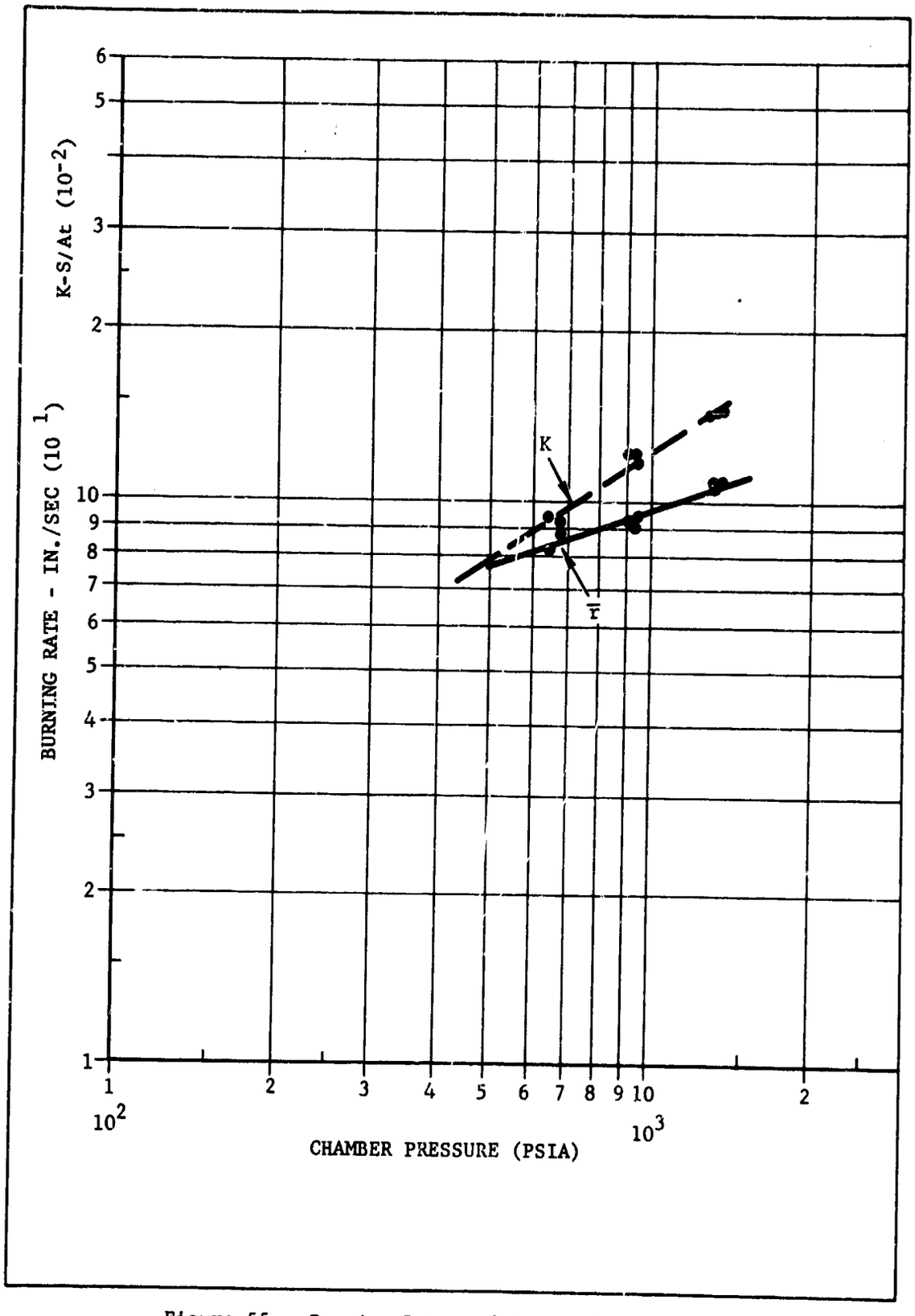

Figure 55. Burning Rate and K as a Function of Chamber Pressure for VIY

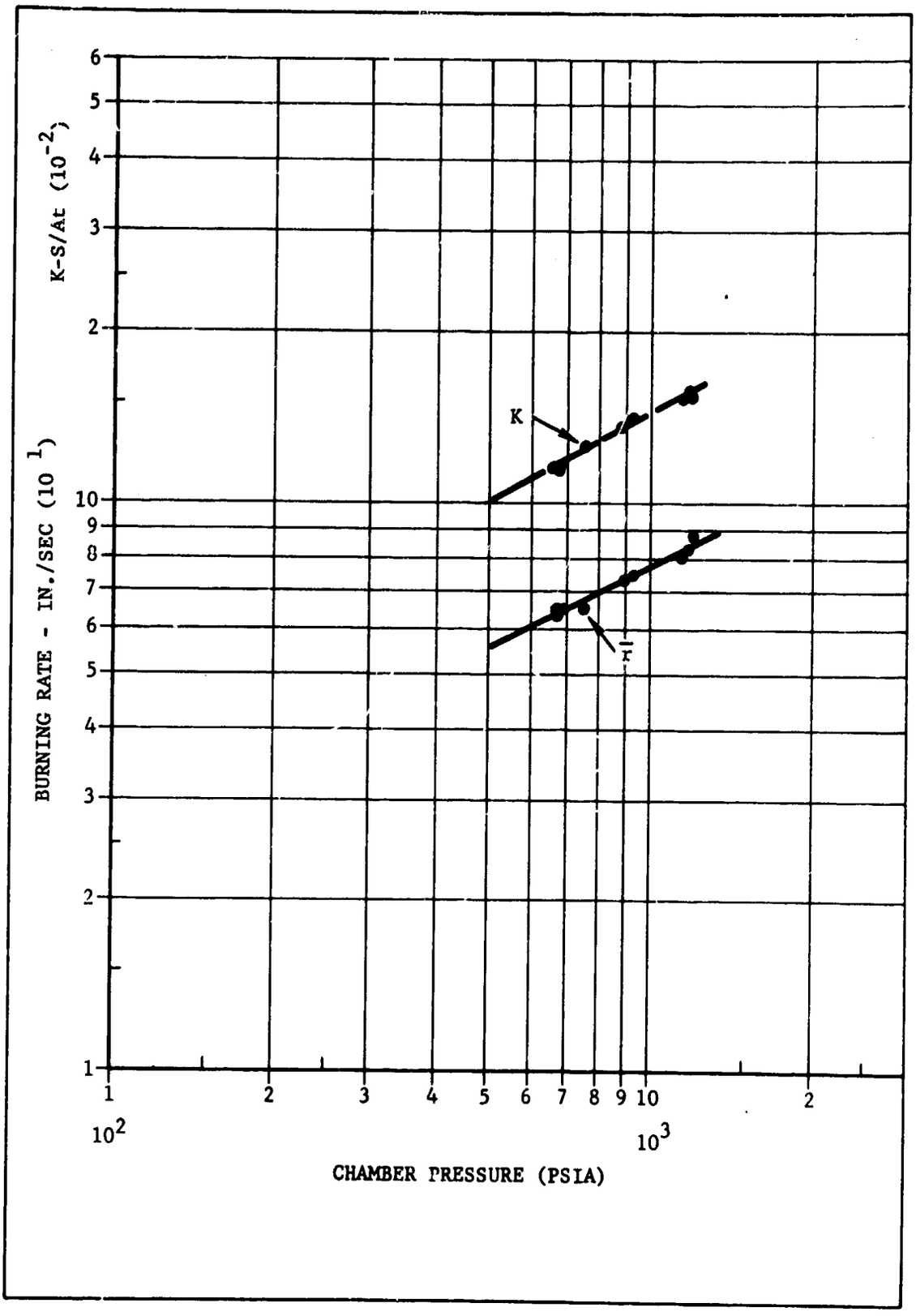

Figure 56. Burning Rate and K as a Function of Chamber Pressure for VJA

TABLE XXV

MILITARY EXPLOSIVE HAZARD CLASSIFICATION RESULTS

Test	VIY	VJA
Detonation Test		
(1) No. 8 blasting cap	Detonated	No. detonation
(2) No. 8 blasting cap		Detonated
Ignition and Unconfined Burning		
(1) One 1-in. cube	Burned without detonation	Burned without detonation
(2) One 2-in. cube	Burned without detonation	Burned without detonation
(3) One 2-in. cube	Burned without detonation	Burned without detonation
(4) Four 2-in. cubes	Burned without detonation	Burned without detonation
Thermal Stability		
(1) One 1-in. cube, 48 hr @ 75° C	No ignition	No ignition
Impact Sensitivity		
(1) 20 tests without ignition, 2 kg wt	21 cm	21 cm
Differential Thermal Analysis		
(1) 20 mg sample, temp at which exothermic reaction of sample occurs	175° C	182° C

SECTION IV

TASK III, ADVANCED CONCEPTS

A. SCOPE

The objective of Task III was to use advanced formulation or motor techniques to study and improve LMH-2 combustion. Six LMH-2, two Be, and one Al 5PC motors were fired. The experiments in this task were designed to evaluate the effect of the propellant combustion mode on performance. The task included the following three major areas of effort:

(1) Characterization of LMH-2

(2) Modification of LMH-2

(3) Fluorine addition

B. BACKGROUND

Based on the Task I correlations and theoretical calculations, two means of promoting higher efficiencies for LMH-2 propellants were originally selected for investigation under this task. The correlations showed that both decreasing the AP particle size and grinding LMH-2 would increase LMH-2 propellant efficiencies. This led to the belief that more intimate contact between the oxidizer and fuel might lead to additional performance gains. One means investigated was the pressing of LMH-2/AP binary mixtures. Work in the first quarter[12] showed pressing to be unattractive because of the poor physical properties of the pressed material and the corresponding high pressures required for consolidation. Another means of achieving intimate contact, developed under independent research and development funding, was the recrystallization of LMH-2/AP from an AP-saturated water dispersion. Initial attempts at incorporating the AP-treated material in propellant showed a marked improvement in processibility over "as received" LMH-2. As a result, emphasis was transferred from pressing LMH-2/AP mixtures to AP treatment of LMH-2. Other methods of surface treating LMH-2 were also investigated.

In addition to more intimate contact to improve LMH-2 performance, theoretical calculations showed that in LMH-2 fluorine systems, significant amounts of BeF_2 gas are formed, which may improve thrust efficiency by reducing particle lag effects. The possibility also exists that a fluorine environment may improve LMH-2 combustion efficiency. To study these possibilities, means of introducing fluorine into LMH-2 propellants were investigated.

---

[12] Refer to List of References

To provide support to Tasks II and III efforts, a limited amount of work was also scheduled to characterize the chemical and physical properties of LMH-2 being used on this and associated contracts. However, because of difficulties experienced with variable processing and apparent incompatibility problems with LMH-2, extensive laboratory work was required to develop adequate posttreatments to control processibility and eliminate porosity.

C. CHARACTERIZATION AND MODIFICATION OF LMH-2

1. Background

From previous work by Hercules and other propellant formulators, problems were anticipated with the processibility of formulations containing high LMH-2 loadings and with the tendency of certain "as received" LMH-2 lots to produce gassing and porous grains during cure.

The poor processing characteristics of LMH-2 propellants had generally been attributed to the low bulk density of the as-produced LMH-2 (approximately 44 percent of the true density), an unfavorable particle shape, and possibly surface anomalies. Grinding of LMH-2 generally improved processibility although exceptions for some lots were observed. The improved processibility of the ground material could be related to an improvement in bulk density and particle shape. Propellant gassing had been observed for certain LMH-2 lots in double-base propellant by both Hercules and the Atlantic Research Corporation (ARC). No explanation for the gassing was apparent, although various test methods for prior screening of LMH-2 lots had been developed by ARC. An elevated temperature and vacuum cycle had been used with some success at Hercules to eliminate gassing.

Since the present production of LMH-2 is confined to 5-lb batches, differences in the LMH-2 purity level, percentages of the various contaminants, and the rheological properties between lots were anticipated on this program. Prior to the shipment of major quantities of LMH-2, several small samples of LMH-2 lots having a wide range of impurities were requested from the Ethyl Corporation. It was hoped evaluation of these samples would provide a clue to the reasons for gassing and subsequently lead to the development of an adequate posttreatment. In addition, samples were requested both unground and ground. The samples were evaluated as follows:

(a) Unground

(b) Ground (ball milled by the Ethyl Corporation for 15 min)

(c) Unground and evacuated 4 hr at 100° C

(d) Ground and evacuated 4 to 8 hr at 100° C

An analysis of the LMH-2 lots tested is presented in Table XXVI. The samples were incorporated into an LMH-2 formulation containing 12-percent

TABLE XXVI

ANALYSIS OF LMH-2 LOTS FOR EVALUATION

Sample No.	Composition (Wt %)						True Density (g/cc)	Bulk Density (g/cc)
	LMH-2	Be Metal	Be Alkyls	Be Alkoxide	Total Chloride	Volatiles		
Lot 80	93.7	3.5	2.1	0.13	0.28	Nil	0.63	0.29
B-208	96.5	2.1	1.3	0.08	0.09	Nil	0.64	0.26
B222-3	94.2	1.0	1.2	0.11	0.05	0.16	0.63	0.26
B-249-50	92.2	2.4	2.4	0.27	0.08	Nil	0.56	0.25
B253-4	93.2	4.0	1.9	0.08	0.06	Nil	0.58	0.27
B270-2	94.1	2.0	1.2	0.31	1.02	Nil	0.65	0.26
B273-4	91.2	6.5	3.4	0.10	0.31	Nil	0.64	0.28
B297-8	94.7	1.9	1.8	0.30	1.18	0.07	0.65	0.31
B264-6	95.1	3.3	2.1	0.24	0.32	0.15	0.64	0.27
B267-9	94.5	2.5	3.0	0.22	0.37	Nil	0.65	0.27
B301-2	91.9	4.9	2.5	0.08	1.04	0.01	0.64	0.30
B275-7	94.2	2.7	5.7	0.33	0.17	0.06	0.63	0.28
B168-70	91.9	1.5	1.7	0.69	0.80	0.57	0.65	0.27
19	94.3	2.5	2.3	0.08	0.11	--	0.64	0.29

Analysis as reported by the Ethyl Corp

CONFIDENTIAL

LMH-2 with 57-percent-volume-solids loading. Ten-gram mixes were cast and cured. All of these samples showed varying degrees of porosity when cured at 140° F for 3 days or longer. However, four different lots cured at a lower temperature (120° F) showed no porosity with this formulation. Estimated viscosities for these mixes ranged from 40,000 to 300,000 centipoises with no apparent correlation between viscosity and porosity. This indicated high viscosities, and resulting poor deaeration was probably not the cause of the porosity. A comparison of viscosities from mixes containing ground versus unground lots showed improvement in processing for only certain lots; however, where no improvement was obtained, photomicrographs of the LMH-2 indicated incomplete grinding.

Based on the results of the above mixes, a second series of mixes was made with a formulation containing 8-percent LMH-2 which had a considerably lower viscosity to eliminate the possibility of poor deaeration as a cause of porosity. Using this formulation and curing at 120° F, void-free grains were consistently obtained with vacuum-baked lots.

Because of a limited supply of material, no additional tests were run with the above lots, and the results shed limited light on the nature of the gassing problem. However, cure temperatures in excess of 120° F were shown to be detrimental and all other LMH-2 propellants were cured at 120° F. Subsequent production lots were requested to be ground for an additional 15 min and vacuum baked for 4 hr at 100° C.

2. Modification of LMH-2

Preliminary studies conducted indicated that processing would become marginal at 15- to 17-percent LMH-2 loadings even at moderate total solids loading. A limited amount of work was conducted to determine if other posttreatments such as an acid or water bath or surfactants would improve processing. Neither of these surface treatments improved processing, and other more drastic methods were sought.

It was postulated that deposition of a surface coating might improve both the shape factor and surface character of LMH-2. As a result, preliminary work was conducted to determine if a surface coating could be applied. It was also suggested that a more intimate contact of oxidizer with LMH-2 might enhance combustion efficiency. Consequently, initial attempts for surface coating were made using the primary oxidizer, AP.

a. AP Treating

Attempts were made to place a surface coating of AP onto LMH-2 by both temperature recrystallization and crystallization by evaporation.

In the temperature recrystallization method, a saturated aqueous solution of AP containing dispersed LMH-2 was heated to 60° C. The mixture was shaken vigorously to ensure that all AP had dissolved. The

mixture was then cooled as rapidly as possible and suction filtered. The filter cake was washed twice with Freon-TA[1] solvent and dried for 16 hr under vacuum. A 1-percent addition of Triton X-100 surfactant was then applied to the AP-treated LMH-2, and the material was vacuum dried for 16 hr at 120° F. The ratio of AP to LMH-2 was controlled by the temperature-solubility difference of AP in the aqueous solution.

In the crystallization by evaporation method, a laboratory rotating evaporator (Rinco) was charged with an aqueous AP/LMH-2 dispersion. The water was stripped off by heating it at 60° C under 14 mm Hg.

Laboratory batches of the resulting materials were characterized by liquid separation techniques, chemical analysis, particle size analysis, and photomicroscopy. The AP-treated material was also evaluated for sensitivity, processing, and combustion characteristics.

1) Sensitivity

Representative runs made by temperature and vacuum recrystallization are presented in Table XXVII. Sensitivity data show AP-treated LMH-2 material to be satisfactory for safe handling with impact values between 40 and 115 cm/2Kg and friction between 10 lb at 6 ft/sec and 40 lb at 8 ft/sec. Sensitivity values show that wax-treated samples are comparable in sensitivity to AP-treated LMH-2, but isopropanol-wet material may be more sensitive to impact and electrostatic discharge. (Refer to paragraph b. for discussion on wax treatment.) No significant difference in sensitivity resulted from the two different methods of AP-treated LMH-2 preparation.

2) Microscopy

The AP-treated LMH-2 material was examined with a polarizing microscope under this contract and also under an independent research and development program. The photomicrographs are presented in Figure 57. Utilizing the birefringence phenomena of AP, the product was seen to be an agglomerate with the oxidizer forming the center. The LMH-2 particles appeared to be adhered to the surface of the AP crystal. The size of the agglomerates appeared to be approximately 75 to 150 microns.

3) Micromerographs

Micromerographs of AP-treated LMH-2 prepared by both the temperature recrystallization method and by crystallization through vacuum evaporation (Rinco method) were taken and are presented in Figure 58. The plots show that the particle size distribution was similar for the two methods, although dissimilar processing properties in propellants were observed, as discussed in subpara 6). The micromerograph data for the AP-treated LMH-2 gives a somewhat questionable picture of particle size distribution, since the material tested consists of free LMH-2, free AP, and LMH-2 adhered to AP crystals and, consequently, results in variable composition and density.

[1]Azeotrope of Freon TF and acetone

TABLE XXVII

AP-TREATED LMH-2 RUNS

	LMH-2 Lot	Material Balance			I	Sensitivity		Autoignition
		LMH-2 (gm)	AP (gm)	AP/LMH-2	(cm/2Kg)	F (lb/ft-sec)	ESD (Joules)	(°C)
Treated by Temp Recrystallization								
X-110-50	275-76	10	12.6	1.26/1	> 115	40/6	0.025	> 300
X-110-51	90A	10	7.4	0.74/1	> 115	10/6	0.025	> 300
X-110-52-1	90A	10	6.5	0.65/1	80	21/6	0.025	> 300
X-110-54	90A	125	127	1.03/1	41	48/8	0.025	> 300
Isopropanol wet					21	40/8	0.00125	> 300
X-110-56	90A	75	111	1.45/1	> 115	38/6	--	291
X-110-58	90A	100	81	0.81/1				
0.5% CEC wax					41	50/6	--	> 300
1.0% CEC wax					> 115	38/8	0.025	> 300
2.0% CEC wax					80	38/8	--	> 300
X-110-66	90A	250	330	1.32/1				
X-110-73	93-1	100	120	1.20/1				
X-110-74	93-1	100	122	1.22/1				
Treated by Vacuum Evaporation								
X-110-62 R	90A	10	12.4	1.24/1	> 115	38/6	--	292
X-110-68 R	90A	10	12.4	1.24/1	> 115	40/8	0.050	> 300

CONFIDENTIAL

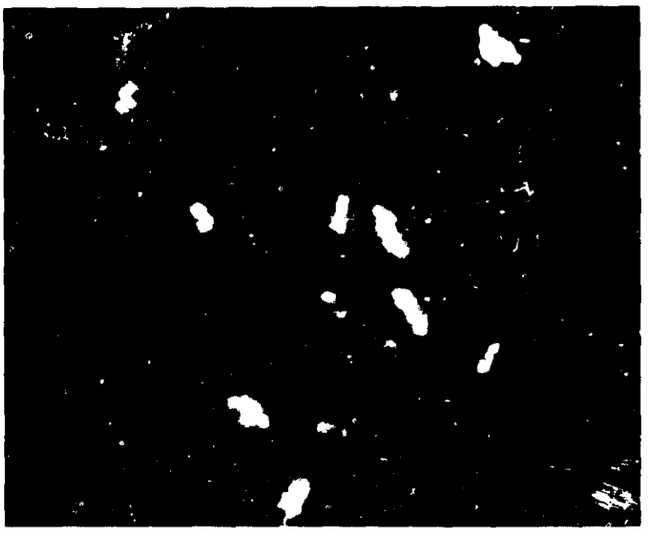

VIEW A. TEMPERATURE RECRYSTALLIZED AP/LMH-2 (100X)

VIEW B. VACUUM CRYSTALLIZED AP/LMH-2 (430X)

Figure 57. AP-Treated LMH-2 Under Polarized Light

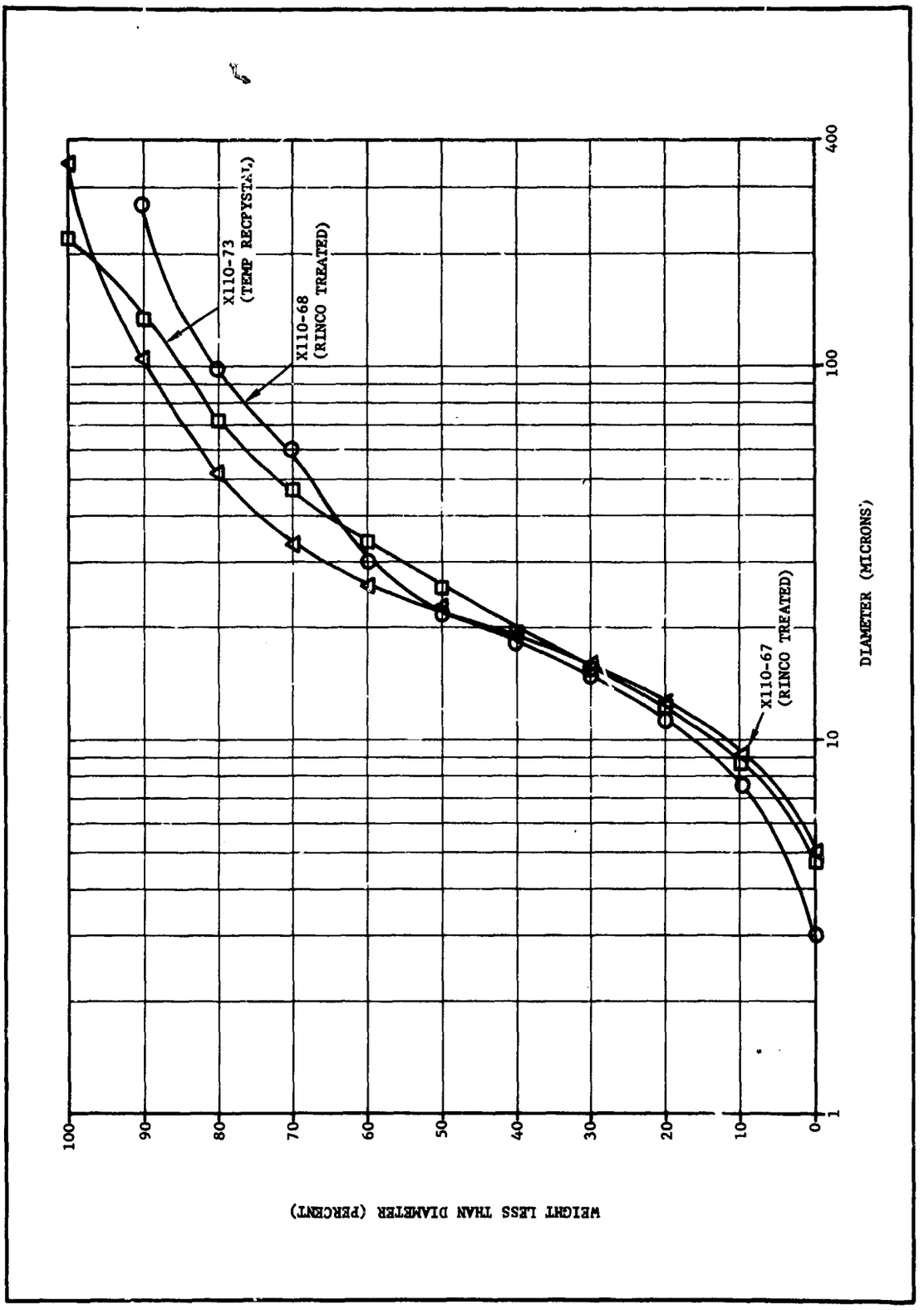

Figure 58. Particle Size Distribution Analysis by Micromerograph

4) Liquid Separation

Samples of AP-treated LMH-2 were separated with benzene into a light fraction (< 0.88 g/cc) and a heavy fraction (> 0.88 g/cc). With the temperature recrystallized material, the light fraction contained approximately 98-percent LMH-2, whereas the heavy fraction contained 5- to 8-percent LMH-2. Any LMH-2 in the heavy fraction would have to be adhered to the AP in some manner, since the density of LMH-2 is 0.65 g/cc. Based on the weight and analysis of each fraction, the separation indicated that the AP-treated LMH-2 is primarily free LMH-2 and free AP with only 5 to 10 percent of the total LMH-2 adhering to the surface of the AP. A run was also made in which the light fraction was recycled three times through the crystallization process, but the final combined product still showed only approximately 10-percent LHM-2 in the heavy fraction.

5) Chemical Analysis

The AP-treated LMH-2 was analyzed for active hydrogen to determine whether any LMH-2 decomposition had occurred during the crystallization process. The analysis showed the treated LMH-2 had the same active hydrogen content as the untreated LMH-2.

6) Processing Studies

Initial attempts at AP treating consisted of preparing a material for use in the VIX formulation by temperature recrystallization. For this formulation the AP-treated material should contain 60.5 percent AP and 39.5 percent LMH-2.

Table XXVIII contains a summary of mixes made with both untreated and treated LMH-2 at approximately 15-percent LMH-2 loadings. Also presented in Table XXVIII is the composition of the various AP-treated LMH-2 runs used. For mixes using the AP-treated material, it is necessary to either adjust them to the exact formulation by adding AP or LMH-2 or to have them suffer some compositional variance. Of particular interest in Table XXVIII is the comparison between the 300-gm mixes--83-2 using untreated LMH-2 and 83-31 using AP-treated LMH-2. As indicated, both viscosity and flow properties were markedly improved with the treated material. Figure 59 shows viscosity as a function of shear rate for these two mixes. This same marked improvement in processing was observed at higher LMH-2 loadings and with all LMH-2 lots investigated.

Only a limited amount of AP-treated material was prepared by vacuum crystallization. These samples failed to show the same process improvements as obtained by temperature recrystallization, and this method was eliminated from further consideration. The lack of improvement in processing was not sufficiently explored to allow a valid explanation to be made for this anomaly.

Based on the results of processing, liquid separation, and microscopy studies with the temperature recrystallized material, it

TABLE XXVIII

AP-TREATED LMH-2 PROCESS STUDIES, 15-PERCENT LOADINGS

Mix No.	Mix Size (gm)	Formulation (%)					Special Treatment	Viscosity** (Centipoise)	Flow	Heat of Explosion (cal/gm)	Specific Gravity (g/cc)
		Binder	Stabilizer	LMH-2	AP	AP Treated LMH-2*					
37-77	10	60	2	15	23	--	Ground	300,000	None	--	--
37-12	20	60	2	15	23	--	Ground	210,000	None	2286	--
37-97	300	60	2	15	23	--	Ground	250,000	None	--	1.334
83-2	300	60	2	15	23	--	Ground & baked	166,000	None	--	1.334
83-4	300	60	2	15	23	--	None	Could not mix	--	--	--
80-28	20	60	2	15	23	--	Ground & benzene washed	--	None	--	--
80-29	20	60	2	15	23	--	Ground, benzene washed, & surfactant applied	--	None	--	--
83-11	20	60	2	7.4(15.0)***	--	30.6(1)	--	200,000	Slight	2297	--
83-13	20	60	2	(15.0)	12.9	25.1(2)	--	150,000	Slight	2272	--
83-14	20	60	2	(15.0)	--	38.0(3)	--	200,000	Slight	2324	--
83-19	20	60	2	(15.9)	--	38.0(4)	Triton added AP treated LMH-2	100,000	None	--	1.378
83-20	20	60	2	(16.1)	--	38.0(5)	--	120,000	None	--	1.361
83-31	276	60	2	9.9(15.0)	1.5	26.6(6)	Triton	66,000	Good	2306	1.334
83-34	20	60	2	(14.4)	--	28.0(7)	Ungrounc & Triton	Could not mix	--	--	--
83-35	20	60	2	(14.3)	--	38.0(8)	Unground	Could not mix	--	--	--

* AP treated LMH-2 compositions (%)

	(1)	(2)	(3)	(4)	(5)	(6)	(7)	(8)
LMH-2	24.6	58.9	Blend of	41.9	42.3	20.0	38.0	37.6
AP	75.4	41.1	56.1(1)	57.1	57.7	79.0	62.0	61.3
Triton X-100	--	--	43.1(2)	1.0		1.0		1.1

** Viscosities for 10 and 20 gm mixes are estimated

*** Actual LMH-2 loadings are in parentheses, (15.0)

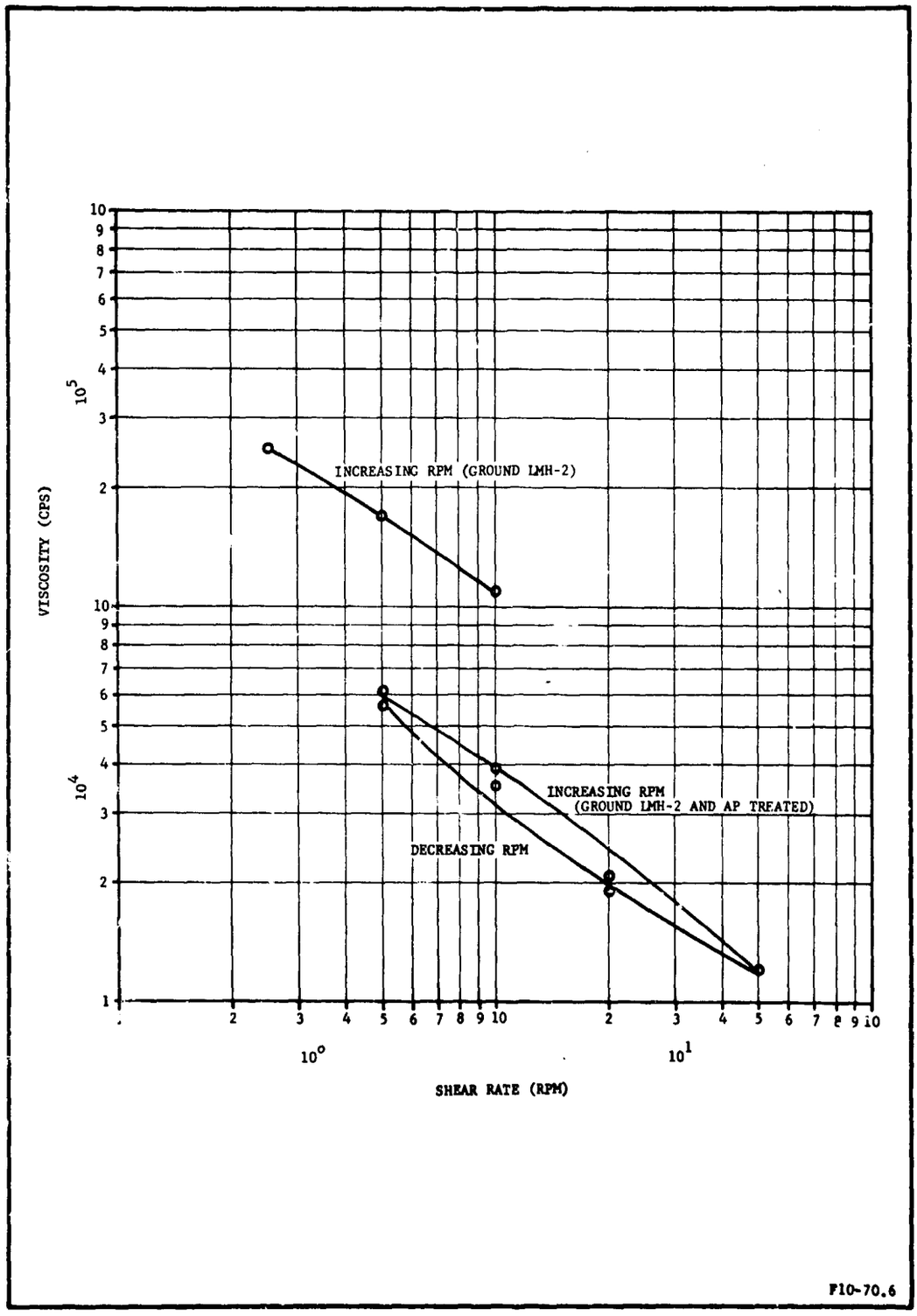

Figure 59. Viscosity as a Function of Shear Rate for the VLX Formulation Containing Nontreated and AP-Treated LMH-2

appears the improvements in processing are due to a general improvement in packing and particle shape.

7) Closed Bomb Studies

Combustion bomb, window bomb, and heat of explosion tests were conducted on VIX and VIY formulations containing AP-treated LMH-2 and compared to those with untreated LMH-2. These results have been previously given in Table IX and show propellants made with the AP-treated material to be slightly less efficient, contrary to expectations. This lower efficiency was later confirmed in motor firings at low L* values, but at high L* values there was no significant difference in efficiency between AP-treated and non-treated LMH-2. The reasons for the lower efficiency are not readily apparent.

b. Wax Coating Studies

Coating LMH-2 with a wax obtained from Consolidated Electrodynamics Corporation was also found to improve propellant processing of LMH-2 propellants. Wax coatings were applied to LMH-2 in which the weight percent of wax on LMH-2 was varied from 0.01 to 10.0 percent. Optimum wax content for best processing with "as received" LMH-2 was found to be 1 percent at the 17-percent LMH-2 level.

As-received LMH-2 and vacuum-baked LMH-2 were wax coated by the addition of an acetone-isopropanol solution of the wax, calculated to give the desired percent of wax after the solvent was stripped off. Extended heated vacuum drying times were required to completely remove all traces of solvent which, when present, caused premature gelation of the nitrocellulose and excessively high mix viscosities. As the wax became coated on the LMH-2 surface, a hard outer shell formed that trapped some process solvent, causing solvent removal to be difficult. Heated vacuum drying removed the last traces of acetone-isopropanol solvent.

Figures 60 and 61 show a comparison of the effects of wax treating and AP treating for two LMH-2 lots in the VIY formulation. As shown, the wax treatment reduced the viscosity by approximately a factor of two, whereas the AP treatment reduced viscosity by a factor of three. The viscosity reduction achieved with the waxed material was sufficient to allow incorporation with up to 19-percent LMH-2.

3. Final Characterization

Five different LMH-2 lots were received for formulation and motor evaluation on this program. Lot designations and quantities were as follows:

LMH-2 Lot	Quantity (lb)
90A	5
93	20

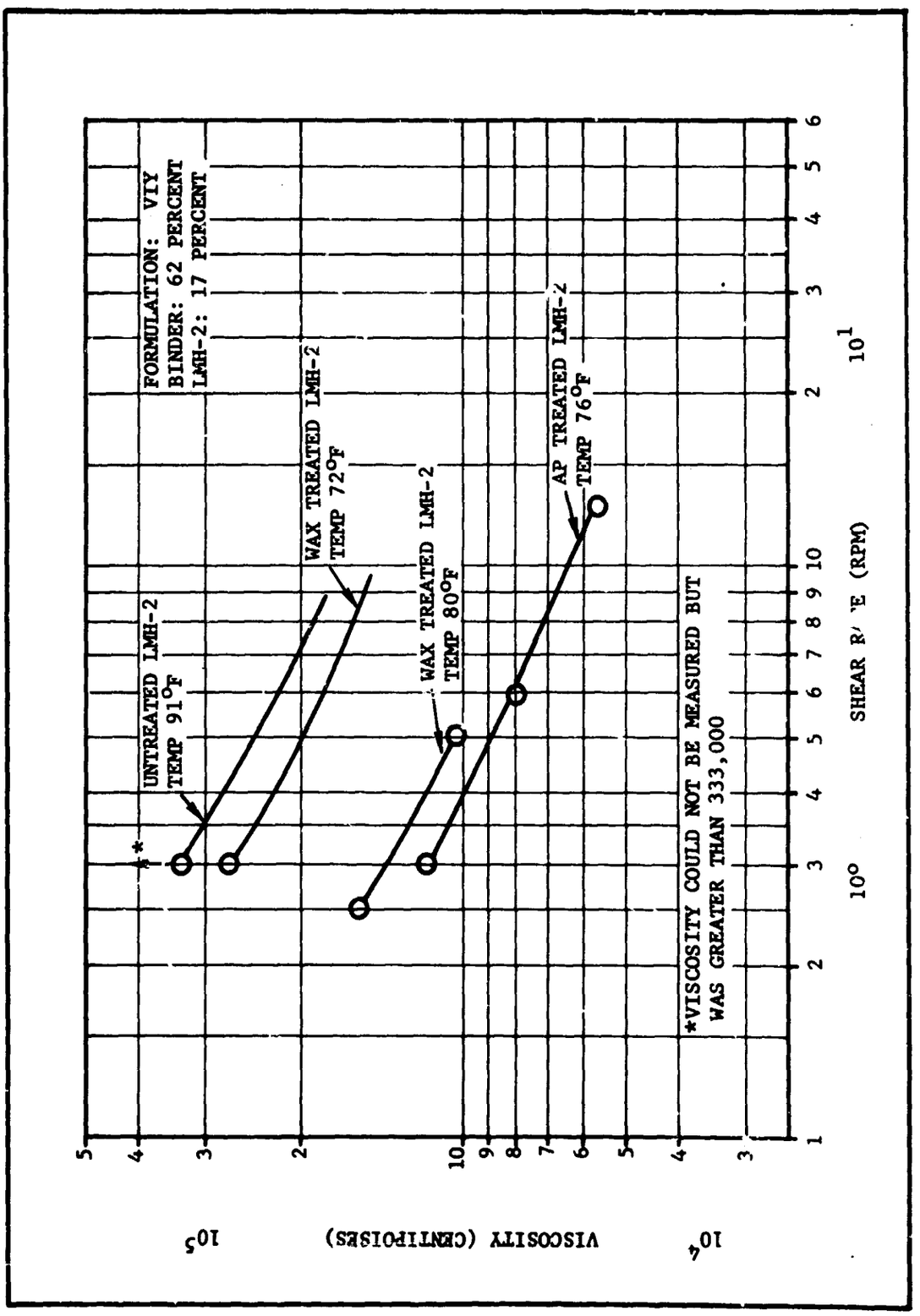

Figure 60. Viscosity as a Function of Shear Rate For Posttreated LMH-2, Lot 90A

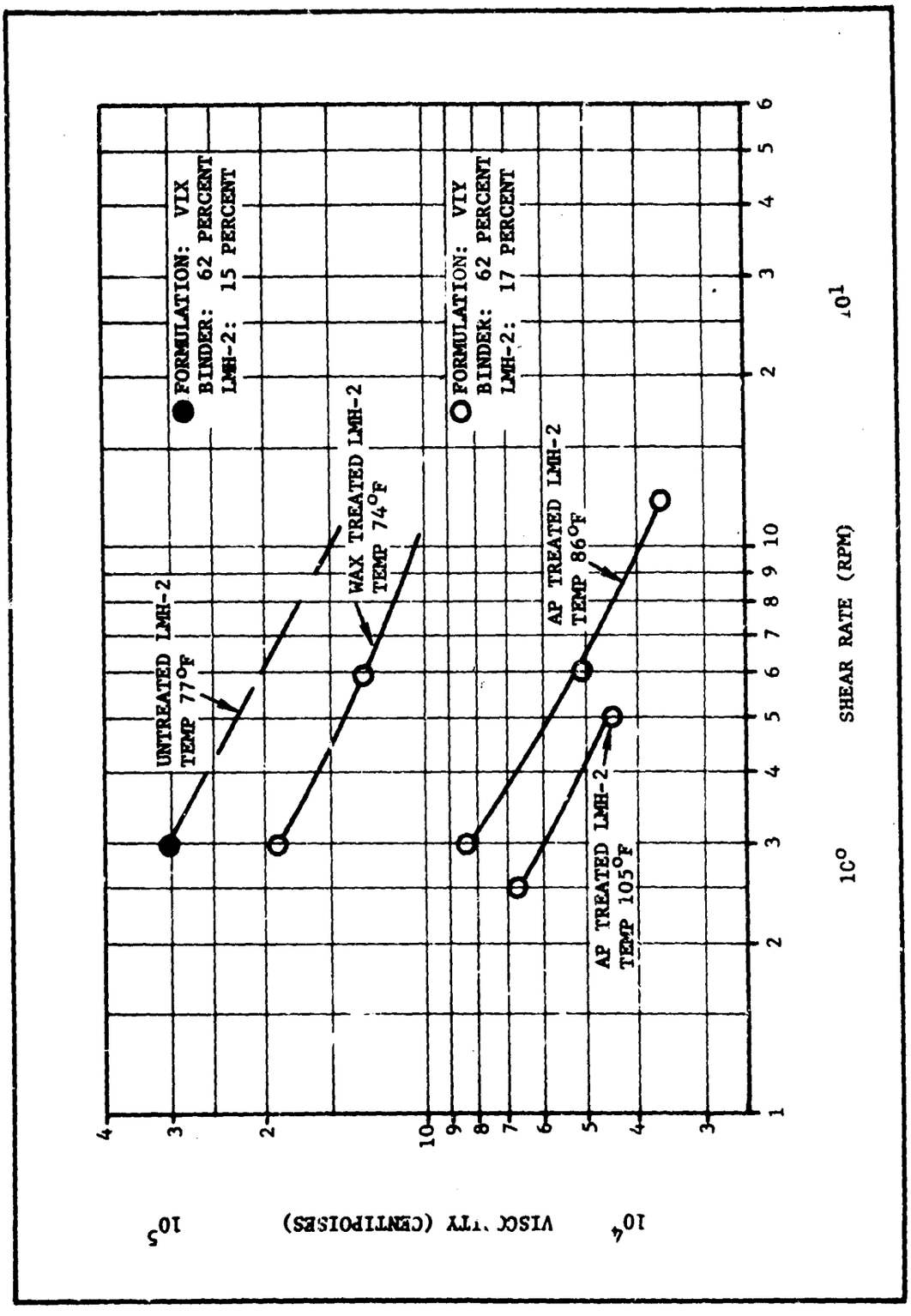

Figure 61. Viscosity as a Function of Shear Rate For Posttreated LMH-2, Lot 93-1

LMH-2 Lot (Cont)	Quantity (lb) (Cont)
96	24
97	20
99	40

In addition, data was available on lots 95 and 95A from motor evaluation work on Contract AF 04(611)-10742 and on lot 275-7 from a previous IR & D program. Data obtained from testing of these lots is included to provide added information on LMH-2 characterization. Table XXIX summarizes analyses of these lots, and Figure 62 shows the particle size analysis by micromerograph. The analyses provided by the Ethyl Corporation were run prior to grinding and the 4-hr vacuum bake cycle. All of the lots except lot 95 were ball milled for 30 min. Table XXX contains results of evaluation of these lots with the various candidate LMH-2 formulations. This comparison shows gross differences between lots as to processibility and the extent of the posttreatment required to eliminate porosity. The posttreatments shown are in addition to the 4-hr initial vacuum-bake cycle given all lots by the Ethyl Corporation. In addition, there was a significant difference in the posttreatment required for formulations containing HMX (VJA, VJI) with porosity in these formulations being more severe. As shown for lot 275-7, no additional posttreatment was required. For lots 90A and 93, a 4-hr bake cycle coupled with the wax or AP treatments was sufficient to eliminate porosity in the AP systems but not for the HMX propellants. For lots 95, 95A, 96, and 97, a 16-hr bake cycle was sufficient to eliminate porosity in both the AP and HMX propellants. However, lot 99 required an extended 32-hr vacuum-bake cycle for AP propellants and a water-wash cycle for the HMX systems. In general, the auxilliary wax and AP treatments reduced the amount of time required for the bake cycle, possibly because of the solvent action or the vacuum stripping operation.

Laboratory mixes of VIX, VIZ (AP systems), and VJI (HMX systems) made to evaluate lot 99 are summarized in Table XXXI. The initial evaluation was made with lot 99 vacuum baked for 16 hr at 100° C and wax treated. However, mixes 38 through 44 showed that porous grains were obtained in all three formulations with this posttreatment. A series of mixes was then made in which lot 99 was given an elevated temperature and extended baking cycle or a water-wash cycle. The results obtained (Table XXXI) show that nonporous grains in the LMH-2/AP system were produced with a 32-hr, 120° C bake cycle with both a 3-mm-Hg and 40-mm-Hg propellant evacuation cycle. Although nonporous at 3 mm Hg, the LMH-2 propellant (VJI) was porous at 40 mm Hg. (The 40-mm Hg evacuation cycle is necessary to prevent foaming during the pilot plant mix cycle.) To eliminate the VJI porosity at 40 mm Hg, lot 99 was given a water-wash cycle. Results obtained using the water-washed material show a 1/2-hr contact time at room temperature was adequate to eliminate porosity for VIX with a 3-mm-Hg evacuation cycle, whereas a 16-hr contact time was necessary for VJI at 3 and 40 mm Hg. Using the extended and elevated temperature vacuum-bake cycle for VIZ and the water-wash cycle for VJI, nonporous 15PC castings were consistently produced.

TABLE XXIX

ANALYSIS OF LMH-2 LOTS

	Lot No.												
	275-7	90A	93		95		95A	96		97		99	
	(a)	(a)	(a)	(b)	(a)	(b)	(b)	(a)	(b)	(a)	(b)	(a)	(b)
Analysis (wt %)													
LHM-2	94.2	92.9	92.6	--	96.4	--	--	95.5	--	94.0	--	94.4	--
Active hydrogen	17.73	17.52	17.44	16.3	17.87	17.20	18.0	17.66	17.40	17.55	18.7	17.58	17.0
Be metal	2.7	2.2	2.3	--	1.0	--	--	1.1	--	2.0	--	1.5	--
Be alkyls	2.6	2.5	3.1	4.7	3.2	--	3.8	2.3	2.4	3.3	4.8	2.5	3.7
Be alkoxides	0.33	0.14	0.15	0.28	0.14	--	0.13	0.15	0.26	0.16	0.20	0.13	0.8
Total chlorides	0.17	0.38	0.42	0.63	0.11	--	0.10	0.16	0.14	0.22	0.35	0.26	0.21
Volatiles	0.06	0.23	0.09	0.4	0.01	--	0.20	Nil	0.22	--	1.7	Nil	0.6
Particle size (μ)	--	--	--	11	--	37.5	28	--	25	--	25	--	--
Surface area (m^2/gm)	--	--	--	--	--	0.918	1.56	--	1.39	--	2.20	--	1.84
Bulk density (gm/cc) (c)	0.28	--	--	--	--	0.33	--	--	--	--	--	--	--
Bulk density (gm/cc) (d)	--	--	--	0.40	--	--	0.41	--	--	--	--	--	0.39
True density (gm/cc)	0.63	0.62	0.63	--	0.64	--	--	0.64	--	0.64	--	0.64	--

(a) Analyzed by Ethyl

(b) Analyzed by Bacchus

(c) Unground

(d) Ground

CONFIDENTIAL

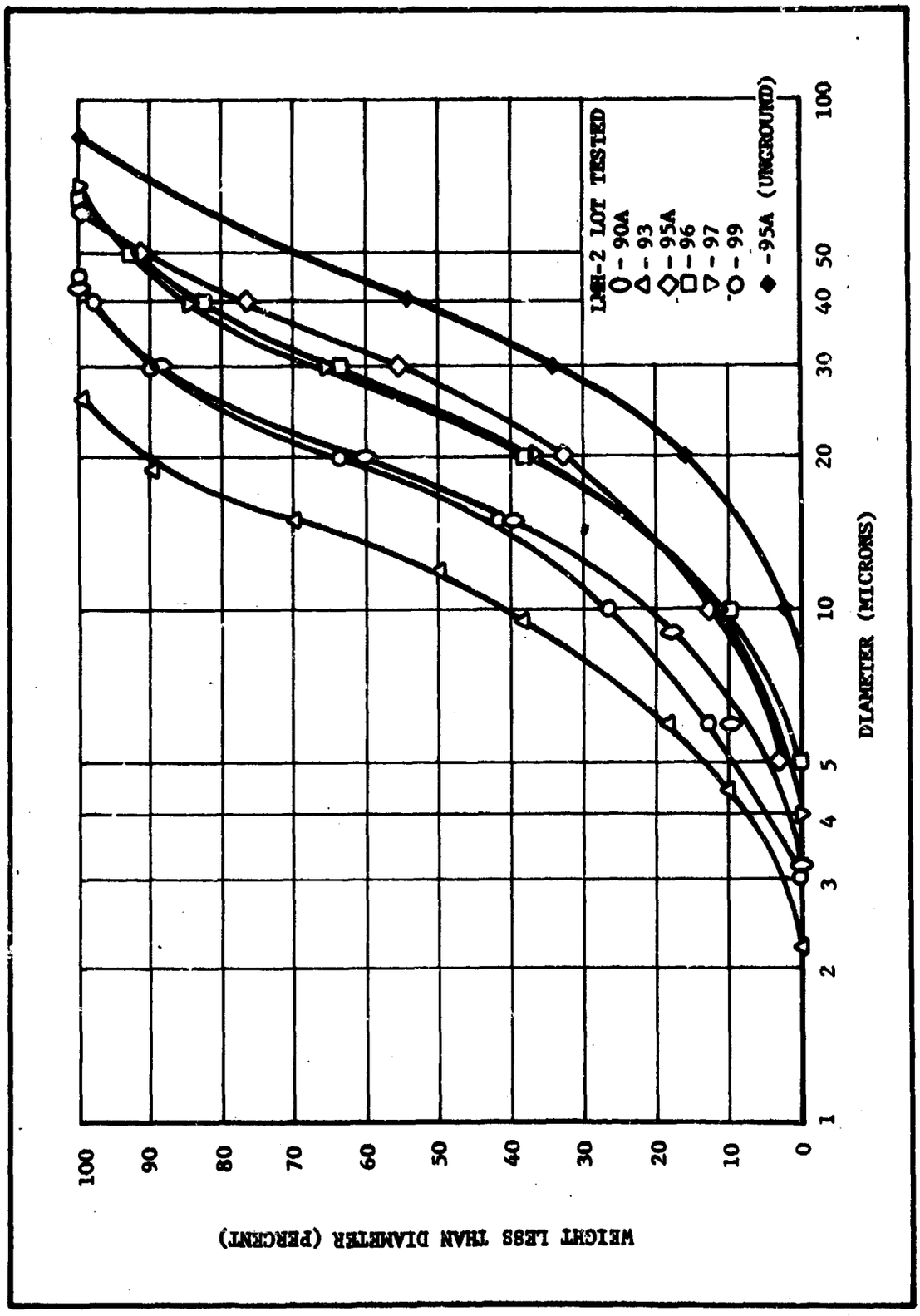

Figure 62. Particle Size Distribution Analysis for LMR-2 Lots by Micromerograph

TABLE XXX

EFFECT OF VARIOUS POSTTREATMENTS ON APPARENT COMPATIBILITY AND PROCESSIBILITY WITH SEVERAL LMH-2 LOTS

LMH-2 Lot No.	Treatment	Formulation*		Specific Surface	Particle Size	Viscosity
		AP	HMX			
275-7	None	(1)		--	--	Too thick for mixing
275-7	Ground	Nonporous(1)				225,000/76
275-7	Ground, ApT	Nonporous(1)				100,000/78
90A	Ground	Porous(2)		--	18	333,000/91
90A	Ground, ApT	Nonporous(2)				116,000/76
90A	G, 4 hr bake, waxed	Nonporous(2)				266,000/72
90A	G, 4 hr bake, waxed		Porous(4)			51,200/78
93	Ground	Porous(1)		--	12	303,000/77
						120,000/104
93	Ground, ApT	Slight Porosity(2)				83,000/86
93	Ground, 4 hr bake, ApT	Nonporous(2)				117,000/72
						60,000/105
93	Ground, 4 hr bake, waxed	Nonporous(2)				190,000/74
93	Ground, 16 hr bake		Porous(4)			250,000/102
93	Ground, 4 hr bake, waxed		Porous(4)			61,000/64
93	Ground, 16 hr bake, waxed		Porous(4)			45,000/96
93	Ground, 16 hr bake, waxed and rebaked 8 hr		Porous(4)			38,000/107
93	Ground, 10 hr bake, waxed	Nonporous(1)				58,000/105
95	4 hr bake	Slight porosity(5)		0.92	38	
95	18 hr bake	Nonporous(5)				

*Formulation Key: (1) VIX, (2) VIY, (3) VIZ, (4) VJA, (5) FIQ, (6) VJI

CONFIDENTIAL

TABLE XXX (Cont)

EFFECT OF VARIOUS POSTTREATMENTS ON APPARENT COMPATIBILITY AND PROCESSIBILITY WITH SEVERAL LMH-2 LOTS

LMH-2 Lot No.	Treatment	Formulation*		Specific Surface	Particle Size	Viscosity
		AP	HMX			
95A	Ground, 4 hr bake	Porous(5)		1.59	28	
95A	Ground, 8 hr bake	Slight porosity(5)				
95A	Ground, 16 hr bake	Nonporous(5)				
95A	Ground, water washed	Nonporous(5)				
95A	Ground	Porous(1)				50,000/81
95A	Ground		Porous(4)			32,000/83
96	Ground, 4 hr bake	Porous(1)		1.4	25	140,000/64
96	Ground, 8 hr bake	Porous(1)				45,000/98
96	Ground, 16 hr bake	Nonporous(1)				56,000/104
96	Ground, 8 hr bake, waxed	Nonporous(2)				93,000/98
96	Ground, 8 hr bake, waxed	Nonporous(2)				32,000/105
96	Ground, 4 hr bake		Porous(4)			61,000/62
96	Ground, 16 hr bake		Nonporous(4)			35,000/102
97	Ground, 16 hr bake	Nonporous(1)		2.2	25	65,000/102
97	Ground, 16 hr bake, waxed	Nonporous(1)				43,000/104
97	Ground, 16 hr bake		Nonporous(4)			68,000/100
99	Ground, 16 hr bake	Porous(1)		1.84	17	123,000/100
99	Ground, 16 hr bake, waxed	Porous(3)				300,000
99	Ground, 16 hr bake, waxed		Porous(6)			70,000

*Formulation Key: (1) VIX, (2) VIY, (3) VIZ, (4) VJA, (5) FIQ, (6) VJA/ 17% LMH-2

CONFIDENTIAL

TABLE XXXI

POSTTREATMENT EVALUATION FOR LMH-2, LOT 99

Propellant Type	VIX	VIZ	VIJ	VIX	VIX	VIX	VIX
Mix No.	95-38	95-41	95-42	95-44	95-52	95-50	95-71
Mix size (gm)	500	500	500	300	300	300	300
LMH-2 lot	99	99	99	99	99	99	99
Special treatment	Vac baked 16 hr @ 100° C	Vac baked 16 hr @ 100° C, waxed	Vac baked 16 hr @ 100° C, waxed	Vac baked 16 hr @ 100° C, waxed	Vac baked 16 hr @ 120° C, waxed	Vac baked 32 hr @ 120° C, waxed	Vac baked 32 hr @ 120° C, waxed
Mixing temperature (°F)	100	109	100	106	106	103	110
Mix viscosity @ 3 RPM	123,000	300,000	70,000	40,000	83,000	70,000	73,000
Comments	Quite porous	Porous	Porous	Porous at 3 and 40 mm Hg evacuation	Slight porosity at 3 mm Hg	Nonporous at 3 mm Hg	Nonporous at 3 and 40 mm Hg
Propellant Type	VIX	VJI	VIX	VIX	VJI	VJI	
Mix No.	95-47	95-54	95-48	95-49	95-51	95-56	
Mix size (gm)	300	300	300	300	500	300	
Special treatment	Vac baked 32 hr @ 120° C, 2% waxed	Vac baked 32 hr @ 120° C, waxed	Water washed 1/2 hr	Water washed 1/2 hr, waxed	Water washed 1/2 hr, waxed	Water washed 16 hr, waxed	
Mix temperature (°F)	100	104	101	102	101	106	
Mix viscosity @ 3 RPM	85,000	77,000	111,000	97,000	133,000	107,000	
Comments	Nonporous at 3 mm Hg	Porous at 40 Nonporous at 3 mm Hg	Nonporous at 3 mm Hg	Nonporous at 3 mm Hg	Porous at 3 mm Hg	Nonporous at 3 and 40 mm Hg	

A study was also conducted on the desorption of gas by LMH-2 under vacuum. This study was initiated because of the large volume increase experienced with propellants during the pot deaeration vacuum cycle. Volume increases of as much as 400 percent were observed.

This large volume increase presented a problem with the pilot-plant mixer which had a free-board limited to approximately 150 percent. It was also felt that the precure gassing might be related to the porous grain problem. As a consequence, a series of tests was run in which various LMH-2 lots were exposed to solvent under vacuum conditions. Results of these tests are summarized in Table XXXII. The test method consisted of placing 50 gm of preevacuated solvent and 12 gm of LMH-2 in a slurry in a vacuum bell jar. Vacuum was then applied and the volume increase observed visually.

In Run No. 1 (Table XXXII) a full vacuum of 4 mm Hg was applied for a period of 40 min to lots 95A and 96 with various posttreatments. A significant volume increase occurred with all samples tested which were exposed to NG solvent. The water-washed lot 95A showed a volume increase of 400 percent, whereas the wax- and AP-treated material both showed approximately 100-percent increases. Lots 95A and 96, with extended baking cycles, showed volume increases intermediate to these extremes. Visual observation of these tests indicated the volume change was the result of gas liberation coupled with a thick (high surface tension) layer of LMH-2 tapping the gas during expansion. Estimates of the volume of gas liberated were made from the volume increases, but this volume could be considerably lower than the actual amount because of gas loss through the film. It was also noted in Run No. 1 that LMH-2 exposed to TA showed no gas evolution.

Because of the apparent solvent differences, a compatibility problem between LMH-2 and NG was indicated. Micro tests were conducted to collect and analyze the off gases by gas chromatography. The resulting analysis showed only air was liberated.

Two additional runs were made (Table XXXII) in which the vacuum was incrementally decreased beginning at 40 mm Hg to see if the amount of air liberated was pressure dependent. None of the materials tested, with the exception of the two "as received" lots, showed any desorption above 20 mm Hg. Possibly, because of the nature of the test, the amount of gas desorbed with a given material was only partially pressure dependent.

Only limited conclusions can be made from the above tests; however, it has been shown that significant amounts of adsorbed air were liberated from LMH-2 under certain conditions. The data in Table XXXII show that between 1 and 8 cc of gas per 100 gm LMH-2 at standard conditions were liberated, depending on the various LMH-2 lot or posttreatment. To obtain more quantitative results, the Ethyl Corporation was contacted, which reported approximately 11 cc of air were desorbed from lot 95A under vacuum at room temperature. To determine the effect of not removing the adsorbed air on cured propellant, FIQ mixes were made at both Bacchus and ABL with

TABLE XXXII

FOAMING STUDIES

Run No.	Material	LMH-2 Lot	Special Treatment	Vacuum (mm Hg)	Time (min)	Volume Change (%)	Volume Liberated (STP/100 gm)
1	NG + LMH-2	96	AP treated	4	40	100	2.1
	NG + LMH-2	96	Waxed	4	40	100	2.1
	NG + LMH-2	96	16 hr vacuum bake	4	40	200	4.2
	NG + LMH-2	95A	Water washed	4	40	400	8.4
	TA + LMH-2	95A	Water washed	4	40	None	0
	NG + LMH-2	95A	12 hr vacuum bake	4	40	125	2.5
	NG + LMH-2	95A	16 hr vacuum bake	4	40	175	3.5
2	NG + LMH-2	96	AP treated	40	40	None	0
	NG + LMH-2	96	Waxed	40	40	None	0
	NG + LMH-2	96	16 hr vacuum bake	40	40	None	0
	NG + LMH-2	96	AP treated	20	20	25	2.1
	NG + LMH-2	96	Waxed	20	20	None	0
	NG + LMH-2	96	16 hr vacuum bake	20	20	None	0
	NG + LMH-2	96	AP treated	10	20	40	2.1
	NG + LMH-2	96	Waxed	10	20	None	0
	NG + LMH-2	96	16 hr vacuum bake	10	20	40	2.1
	NG + LMH-2	96	AP treated	4	20	50	1.1
	NG + LMH-2	96	Waxed	4	20	50	1.1
	NG + LMH-2	96	16 hr vacuum bake	4	20	150	3.3
3	NG + LMH-2	95A	None	40	40	25	0.8
	NG + LMH-2	96	None	40	40	25	0.8
	NG + LMH-2	95A	None	4	20	75	1.5
	NG + LMH-2	96	None	4	20	100	2.0

CONFIDENTIAL

evacuation cycles at 40 mm Hg. The ABL mix was made entirely under vacuum. The Bacchus mix was pot deaerated only prior to casting. The ABL mix was nonporous, and the Bacchus mix showed slight porosity (mix 95-1), which could have resulted from a larger amount of air entrapped during mixing. Both mixes used lot 95A baked for 16 hr. Based on these results, it is questionable whether the porous grain problem is related directly to desorbed air. Additional quantitative work is recommended to determine the amount of adsorbed air present between lots and with various posttreatments.

In an attempt to further define the apparent incompatibility problem, an analysis was made of the gases evolved during cure from propellants containing LMH-2 (lot 99). Analysis of these gases above propellants containing HMX or AP and unbaked LMH-2 showed 500 percent more nitrous oxide and nitric oxide than was found in the same propellant with baked LMH-2. Hydrogen was present in all of the gas samples; however, there did not appear to be a correlation between the concentration of hydrogen and porosity.

Analysis of lot 99 LMH-2 before and after vacuum baking showed that in addition to the adsorbed air of the material being lowered the water content was also decreased 50 percent. The analysis also showed that this particular sample contained above average concentrations of Be chlorides and alkoxides.

Previous experience with various chlorides had shown that they were incompatible with double-base propellants and that water catalyzed the incompatibility. Therefore, a study was initiated to determine if Be chloride and also Be alkoxides were incompatible with double-base propellants or some particular ingredient and if water catalyzed the incompatibility. The test utilized was a microcompatibility test, which consisted of heating the test material with some propellant ingredient and/or double-base propellant at 135° C for 30 min. The gases generated were then analyzed for the presence of decomposition gases. HMX was chosen as the propellant ingredient to test the various compounds against for two reasons: (a) HMX formulations were generally more porous than AP formulations, and (b) HMX alone does not thermally decompose at 135° C in 30 min. The results of this investigation are summarized in the following tabulation:

	CCS/gm				
Test Compound	CO_2	N_2O	N_2	NO	NO_2
Be Ethoxide	1.0	3.3	Trace	0.0	0.0
$BeCl_2$	1.0	2.3	0.3	15.9	2.3
Be Methoxide	1.0	26.5	14.2	0.0	3.0
LMH-2 unbaked	Trace	0.2	1.6	0.0	0.0
LMH-2 vacuum baked with water added	Trace	0.2	1.6	0.0	0.0

As was shown by this data, Be chloride and Be alkoxides were to a degree incompatible with HMX. This data also showed that the vacuum-baked LMH-2 with water added to its original concentration generated as much gas as the unbaked LMH-2. It was, therefore, very likely that porosity in LMH-2 propellants was in part due to Be chloride and Be alkoxides.

Of the various lots evaluated there was no apparent trend in contaminants with the observed porosity. However, since the majority of the lots evaluated were composite blends of several pyrolysis runs of varying chemical content, it is likely any trend would be obscured. To overcome this difficulty, several samples of individual pyrolysis runs were obtained from the Ethyl Corporation for evaluation. In Table XXXIII an analysis of these samples is presented. All samples were ground 30 min and given a 4-hr vacuum-bake cycle by the Ethyl Corporation. The samples were subsequently vacuum baked 16 hr at 100° C, wax treated at Bacchus, and incorporated in the VIX formulation. All mixes were split into two samples; one was evacuated at 40 mm Hg and one at 3 mm Hg to determine if adsorbed air was a factor. Results of these analyses are presented in Table XXXIV.

Only one sample (357-8) gave serious gassing at 3 mm Hg. This sample had both a high chloride and alkoxide content. (Refer to Table XXXIV.) Several of the other samples showed some porosity with the 40-mm Hg evacuation. This problem is suspected to be due to adsorbed air. There is a definite trend in porosity with the 40-mm Hg evacuation cycle for those samples showing the largest specific surface area and smallest particle size distribution as would be suspected if adsorbed air were a problem. Additional tests are needed to isolate the apparent incompatibility from adsorbed air and to confirm the source of the incompatibility.

Insight into the lot-to-lot variation in processibility can also be obtained from individual LMH-2 pyrolysis runs. A comparison of viscosity with bulk density, specific surface area, and particle size is presented in Table XXXV. Also presented for comparison purposes are lots 93, 95A, and 99, which show extremes in processibility. There was no clear trend apparent of viscosity with either specific surface or particle size. However, Figure 63 shows bulk density of wax-treated material appears to significantly influence processibility. Limited data on as-received LMH-2 indicates factors other than bulk density can drastically alter processibility. These results indicate wax treating may alter the surface character of LMH-2, possibly by filling surface defects, and render the particle more rheologically predictable. Additional studies are needed to further define the process behavior of LMH-2 in plastisol propellants.

D. FLUORINE ADDITION

1. Formulation Screening

There is some basis for believing introduction of fluorine into LMH-2 propellants could improve impulse efficiency. The fluorine environment in itself may improve combustion efficiency, and the formation of

TABLE XXXIII

ANALYSIS OF INDIVIDUAL LMH-2 PYROLYSIS RUNS

Sample Number	B357-8	B362-3	B383-5	B386-7	B388-91	B403-7	B414-6
Analysis (wt %)							
LMH-2	92.0	92.5	96.5	95.6	94.2	96.6	94.0
Active hydrogen	17.14	17.14	17.87	17.63	17.41	17.75	17.50
Be metal	2.6	2.8	<1.0	<1.0	2.2	<1.0	3.3
Be alkyls	2.6	5.5	1.9	2.1	2.2	2.4	2.1
Be alkoxides	1.26	0.05	0.13	0.10	0.05	0.13	--
Total chlorides	0.54	0.15	0.09	0.03	0.03	0.03	--
Volatiles	Nil	Nil	0.01	Nil	Nil	Nil	--
True density	0.64	0.63	0.65	0.65	0.65	0.64	--
Bulk density	0.36	0.34	0.32	0.29	0.30	0.30	--
Particle size(μ)(2)	19.0	23.0	20.0	18.0	21.0	22.0	21.0
Specific surface(2) (M^2/gm)	2.25	1.32	1.51	2.94	1.81	1.60	1.61

Notes: (1) Analysis reported by the Ethyl Corporation before posttreating, except as noted

(2) Analyzed at Bacchus

CONFIDENTIAL

TABLE XXXIV

EVALUATION OF INDIVIDUAL LMH-2 PYROLYSIS RUNS
IN THE VIX FORMULATION

Mix No.	95-73	95-74	95-64	95-66	95-75	95-65	95-67
Mix size (gm)	300	300	300	300	300	300	300
LMH-2 sample	B357-8	B362-3	B383-5	B386-7	B388-91	B403-7	B414-6
Mix temperature (°F)	111	110	105	106	107	107	107
Mix viscosity at 3 RPM	95,000	78,000	110,000	100,000	77,000	133,000	143,000
Comments							
40 mm Hg evacuation	Gassed, doming	Nonporous	Nonporous	Slight porosity	Porous	Porous	Porous
3 mm Hg evacuation	Gassed, doming	Nonporous	Nonporous	Nonporous	Nonporous	Nonporous	Nonporous

CONFIDENTIAL

TABLE XXXV

COMPARISON OF VISCOSITY WITH PHYSICAL DATA FOR LMH-2 SAMPLES

LMH-2 Lot	Viscosity (cps)	Bulk Density* (as received) (gm/cc)	Bulk Density* (waxed) (gm/cc)	Specific Surface Area* (M^2/gm)	Particle Size* (μ)
B357-8	--	0.35	--	2.25	19
Waxed	95,000		0.36		
B362-3	--	--	--	1.32	23
Waxed	78,000		0.36		
B383-5	--	--	--	1.51	20
Waxed	110,000		--		
B386-7	--	--		2.94	18
Waxed	100,000		--		
B388-91	--	--		1.81	21
Waxed	77,000		0.36		
B403-7	--	--		1.60	22
Waxed	133,000		0.33		
B414-6	--	--		1.61	21
Waxed	143,000		0.35		
Lot 93	120,000	0.40		--	12
Waxed	58,000		0.39		
Lot 95A	38,000	0.41		1.59	28
Waxed	--		--		
Lot 99	123,000	0.39		1.84	17
Waxed	70,000	--	0.37	--	--

*Analysis performed at Bacchus

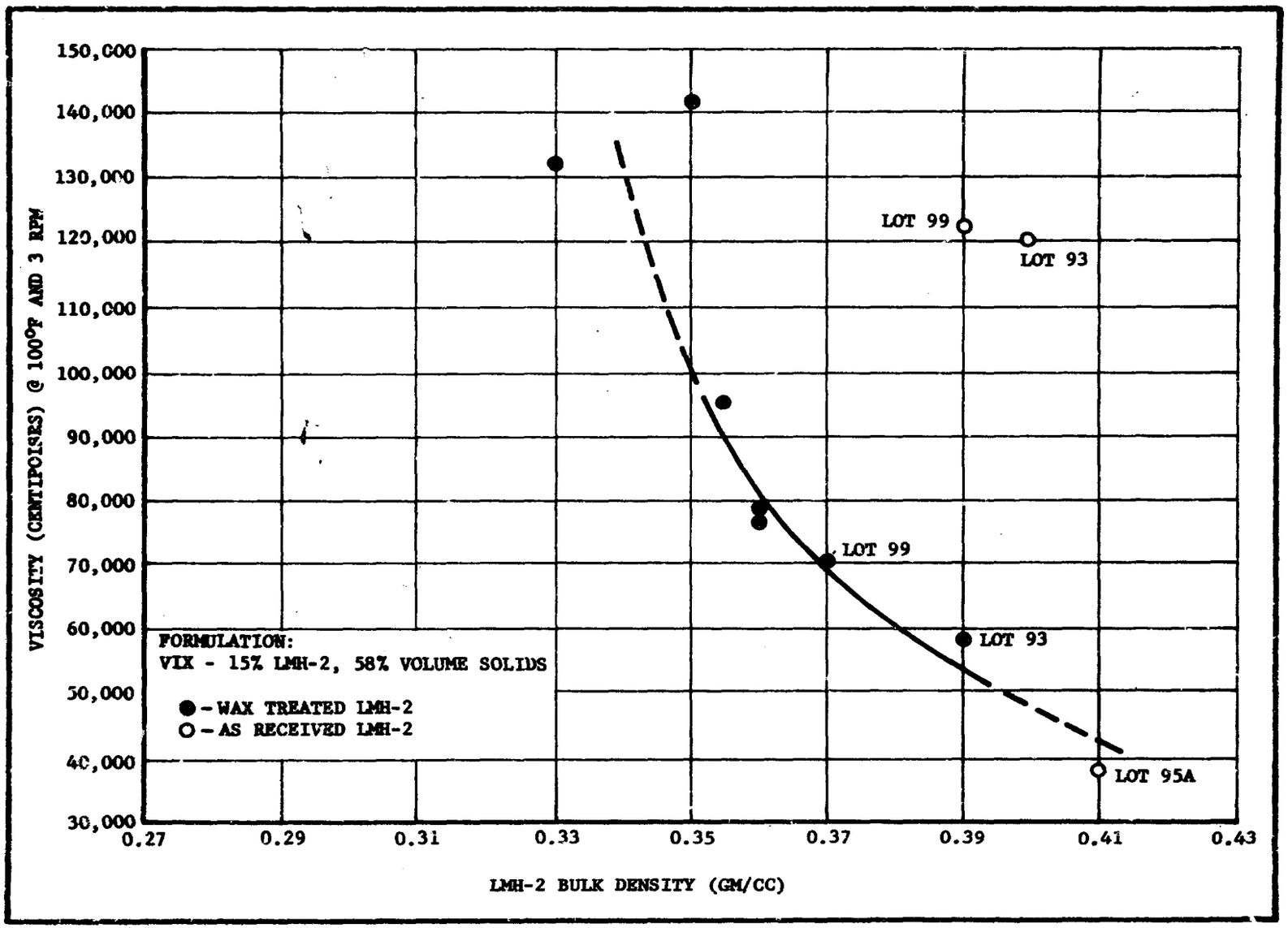

Figure 63. Viscosity as a Function of LMH-2 Bulk Density

significant amounts of the gaseous metal fluoride should reduce particle lag effects. Several means were investigated to incorporate fluorine into an LMH-2 system. The use of the high energy "Douino" compounds was not within the scope of this program, although this would be the most desirable approach. Pressed propellants containing LMH-2/AP and Teflon were investigated experimentally. Because of high compaction pressures required for consolidation, this approach also appeared undesirable at this time. Direct addition of Teflon was not possible because of the low contact angle of Teflon and corresponding propellant segregation. The most promising method investigated was the direct addition of low-molecular-weight Viton-LM. Initial formulation work indicated it was possible to incorporate up to 20-percent-by-weight Viton-LM in double-base propellants while maintaining adequate physical properties. Table XXXVI summarizes theoretical calculations performed on Al, Be, and LMH-2 propellants containing Viton-LM. As shown, at 16- to 20-percent Viton levels, significant amounts of metal fluorides are formed with all three metal fuels.

Because the Viton-LM is a highly viscous thermoplastic, a temperature of approximately 140° F was required to achieve initial dispersion of the Viton-LM in NG. After dispersion of the Viton-LM the temperature could be lowered to approximately 115° F and the mix completed while maintaining a good dispersion. At temperatures much below 115° F, separation occurred. However, at 115° F a serious pot-life problem existed and mix cycles had to be carefully controlled.

Formulation studies showed the following propellants could be processed adequately:

Propellant Type	VJE	VJF	VJG
Formulation (wt %)			
NC	10.0	10.0	10.0
NG	32.5	40.0	45.0
LMH-2	--	--	15.0
Be	--	12.0	--
Al	18.0	--	--
Viton-LM	20.0	20.0	18.0
AP	17.5(90 μ)	16.0(90 μ)	10.5(90 μ)
Res	1.0	1.0	0.5
2-NDPA	1.0	1.0	1.0

TABLE XXXVI

FLUORINE ADDITION

Formulation (%)	LMH-2							Be	Al	
NC	10.0	10.0	10.0	10.0	10.0	10.0	10.0	10.0	10.0	10.0
NG	45.0	45.0	45.0	45.0	45.0	45.0	42.5	40.0	40.0	40.0
BeH_2	14.0	14.0	16.0	15.0	15.0	12.0	15.0	--	--	--
Be	--	--	--	--	--	--	--	12.0	--	--
Al	--	--	--	--	--	--	--	--	18.0	21.6
Viton LM	20.0	16.0	16.0	20.0	18.0	20.0	20.0	20.0	--	--
AP	4.0	8.0	6.0	8.5	10.5	11.5	8.5	16.0	10.0	6.4
TA	5.0	5.0	5.0	--	--	--	2.5	--	--	--
Res	1.0	1.0	1.0	0.5	0.5	0.5	0.5	1.0	1.0	1.0
2NDPA	1.0	1.0	1.0	1.0	1.0	1.0	1.0	1.0	1.0	1.0
Theoretical Performance										
I_{sp} (1000/14.7)	283.4	289.6	291.4	292.9	296.5	286.7	288.9	276.2	254.7	249.6
T_c (°K)	2820	3036	2909	3117	3218	2194	2950	3633	3439	3377
Oxidation ratio	0.935	0.997	0.915	0.984	1.017	1.129	0.950	1.032	1.089	0.960
MeO* (moles/100 gm)	0.907	0.969	1.124	0.975	1.058	0.893	0.977	1.034	0.282	0.253
MeFx*	0.319	0.254	0.255	0.322	0.257	0.161	0.322	0.265	0.092	0.267

* Concentration of primary metal oxide and metal fluoride at exit conditions

Propellant Type (Cont)	VJE (Cont)	VJF (Cont)	VJG (Cont)
Theoretical			
Isp (1000/14.7)	254.7	276.2	296.5
ρ (gm/cc)	1.811	1.696	1.294
Tc (^{o}K)	3465	3633	3218
Oxidation ratio	1.12	1.032	1.017
MeO* moles/100 gm	0.292	1.034	1.058
MeF*	0.068	0.265	0.257

*Concentration of primary metal oxides and metal fluorides at exit conditions.

Pertinent propellant data for these formulations is presented in Table XXXVII.

2. Firings - Task III

The six 5PC grains containing Viton-LM were successfully cast and fired. Table XXXVIII summarizes ballistic data obtained from these firings. Table XXXIX summarizes ballistic data obtained from three 5PC firings of VIX used as the control formulation. A summary of pertinent data from these firings is presented in the following tabulation:

Formulation	VIX	VJE	VJF	VJG
Al	--	18.0	--	--
Be	--	--	12.0	--
LMH-2	15.0	--	--	15.0
Viton LM	--	20.0	20.0	18.0
Tc (^{o}K)	3678	3463	3633	3218
Oxidation Ratio (with Fluorine)	--	1.12	1.03	1.02
Oxidation Ratio (Oxygen only)	1.34	0.98	0.91	0.91
MeO*	1.25	0.292	1.034	1.058
MeF*	--	0.068	0.265	0.257

*Concentration of primary metal oxide and metal fluorides at exit conditions

TABLE XXXVII

VITON-LM FORMULATION DATA

Propellant Type	VJE	VJF	VJG
Process Data			
Viscosity (cps @ °F)	10,600 @ 106	24,642 @ 114	76,360 @ 113
Castability time (max)	35 - 45 min	35 - 45 min	30 - 40 min
Sensitivity Data*			
Impact (cm/2kg)	3.5 (26)	6.9 (33)	3.5 (33)
Sliding friction (lb_f @ ft/sec)	88 @ 8 (700 @ 8)	23 @ 8 (200 @ 8)	156 @ 8 (500 @ 8)
Electrostatic discharge (joules)	1.25 (0.625)	0.075 (0.625)	0.625 (0.625)
Autoignition (°C)	226 (245)	210 (212)	219 (223)
Differential thermal analysis, ignition (°C)	173 (169)	171 (166)	171 (170)
Taliani (ΔP mm @ 93.3°C/ 23 hr)	10 (4)	6 (16)	12 (5)
Ballistic Data			
Strand Rates			
500 psi	0.334	0.332 - 0.338	0.541
750 psi	0.434	0.474 - 0.477	0.568 - 0.576
1000 psi	0.541	0.560 - 0.566	0.614 - 0.616
1500 psi	--	--	--
Physical Properties (Instron Uniaxial Properties)			
Tensile strength (psi)	36	27	--
Elongation (%)	34.1	30.5	--
Modulus of elasticity (psi)	186	112	--

*First No. is for uncured propellant; No. in parenthesis is for cured propellant

Formulation (Cont)	VIX (Cont)	VJE (Cont)	VJF (Cont)	VJG (Cont)
$\dot{m}$ (lb/sec)	3.8	1.5	1.9	1.7
Efficiency	90.47	89.10	85.43	84.78
Efficiency Adjusted**	86.9	89.4	85.3	84.8

**Adjusted to a mass flow rate of 1.7 lb/sec

As shown, the efficiencies of the Be and LMH-2 fluorine systems were approximately 85 percent. A direct comparison between the fluorine propellants and VIX is not possible because of widely varying mass-flow rates. However, by use of the VCP scaling curve a comparison is possible. Figure 64 shows efficiency as a function of mass-flow rate for VCP in 5PC, 15PC, and FPC motors. Superimposed on this scaling curve are the VIX 5PC and 15PC firings. As shown, VIX appears to fit the curve, and an estimate of the efficiency of VIX at mass-flow rates comparable to the Viton firings can be made. This comparison shows that VIX is approximately 2 percent more efficient than the VJF or VJG formulations. However, the 15PC firings of the low-oxidation-ratio VJI propellant were 6 percent below VIX. (Refer to Section II.) It should be noted that both VJF and VJG had oxidation ratios (including fluorine) well below VJI, and thus some improvement in efficiency could be attributed to the use of fluorine in Be or LMH-2 systems.

Figure 64 also shows the VCP scaling curve correlates 5PC data for the efficient aluminum propellant, DDP. Using the scaling curve as a basis for comparison for the Al/fluorine system indicates an increase in efficiency was also obtained over DDP.

It is also interesting to note at this time that recent data reported by ARC (1966 ICPRG Bulletin) in which a formulation containing LMH-2/TVOPA/NFPA with an oxidation ratio (including fluorine) of 0.98 gave an efficiency of 91 percent in 5PC firings. This data supports the findings of this program.

Only limited conclusions can be made from the data generated on this and other programs as to the effect of fluorine substitution. However, there is a strong indication that fluorine may improve combustion efficiency at low oxidation ratios, and additional testing appears warranted.

TABLE XXXVIII

VITON-LM 5PC FIRINGS

Propellant Type	VJE	VJF	VJF	VJG	VJG	VJG
Motor Design	N5PC	N5PC	N5PC	N5PC	N5PC	N5PC
Grain No.	S731	S732B	S733B	S739BH	S738BH	S739BH
Firing No.	2-501	2-505	2-506	2-509	2-507	2-508
Propellant wt (lb)	5.32	4.86	3.46	3.97	3.90	3.92
Powder wt (lb)	0.03	0.03	0.03	0.03	0.02	0.02
K (S/A_t)	143.3	140.6	171.0	151.0	180.0	181.4
t_a (sec)	3.460	2.603	5.152	2.514	2.122	2.164
t_b (sec)	3.047	2.243	4.483	2.387	2.008	2.023
$\bar{P}_a$ (psia)	380	487	351	558	800	800
$\bar{P}_b$ (psia)	410	518	382	572	823	807
$\bar{P}$max (psia)	474	630	450	656	938	904
$\bar{P}$amb (psia)	12.32	12.41	12.29	12.26	12.24	12.26
$\bar{r}$ (in./sec)	0.302	0.406	0.205	0.387	0.453	0.450
$\dot{m}$ (lb/sec)	1.54	1.87	0.67	1.58	1.84	1.81
C_d (sec^{-1})	0.00637	0.00603	0.00517	0.00479	0.00465	0.00474
ϵ (A_e/A_t)	9.269	9.275	5.834	8.321	8.129	8.388
$\bar{F}_a$ (lb_f)	313	412	145	378	463	456
Isp del $\left(\frac{lb_f\text{-sec}}{lbm}\right)$	203.9	221.3	215.3	239.8	252.4	252.2
Theoretical Isp at firing conditions	227.9	258.2	249.0	284.6	294.7	294.2
Efficiency	89.46	85.70	86.47	84.26	85.65	85.72
Isp^{15}_{1000}	228.0	236.7	238.8	249.8	254.0	254.1
Isp del (c)*	203.0	219.8	213.5	238.3	251.3	251.1
Efficiency (c)*	89.1	85.12	85.74	83.73	85.27	85.35
Isp^{15}_{1000} (c)*	226.9	235.1	236.8	248.3	252.8	253.1

*Values corrected for powder embedment

Notes: All efficiency values were calculated at the actual firing conditions.

Isp^{15}_{1000} and Isp^{15}_{1000} (c) values were calculated by multiplying efficiency times the theoretical Isp at standard conditions.

TABLE XXXIX

VIX 5PC FIRINGS

Propellant Type	VIX	VIX	VIX
Motor Design	N5PC	N5PC	N5PC
Grain No.	S728BH	S730BH	S729BH
Firing No.	2-502	2-503	2-504
Propellant wt (lb)	3.93	3.88	3.69
Powder wt (lb)	0.02	0.03	0.03
K (S/A_t)	111.5	108.9	106.4
t_a (sec)	1.003	1.001	1.020
t_b (sec)	0.931	0.928	0.946
$\bar{P}_a$ (psia)	928	909	861
$\bar{P}_b$ (psia)	964	941	895
$\bar{P}$max (psia)	1022	1010	958
$\bar{P}$amb (psia)	12.17	12.30	12.28
$\bar{r}$ (in./sec)	0.994	0.997	0.973
$\dot{m}$ (lb/sec)	3.92	3.88	3.62
C_d (sec^{-1})	0.00527	0.00523	0.00524
ϵ (A_e/A_t)	9.758	9.537	9.957
$\bar{F}_a$ (lb_f)	1087	1045	989
Isp del $\left(\frac{lb_f\text{-sec}}{lbm}\right)$	278.4	279.0	275.1
Theoretical Isp at firing conditions	306.0	305.0	304.0
Efficiency	90.98	91.48	90.49
Isp^{15}_{1000}	276.3	277.8	274.8
Isp del (c)*	277.3	277.3	273.2
Efficiency (c)*	90.62	90.92	89.87
Isp^{15}_{1000} (c)*	275.2	276.1	272.9

*Values corrected for powder embedment.

Notes: All efficiency values were calculated at the actual firing conditions.

Isp^{15}_{1000} and Isp^{15}_{1000} (c) values were calculated by multiplying efficiency times the theoretical Isp at standard conditions.

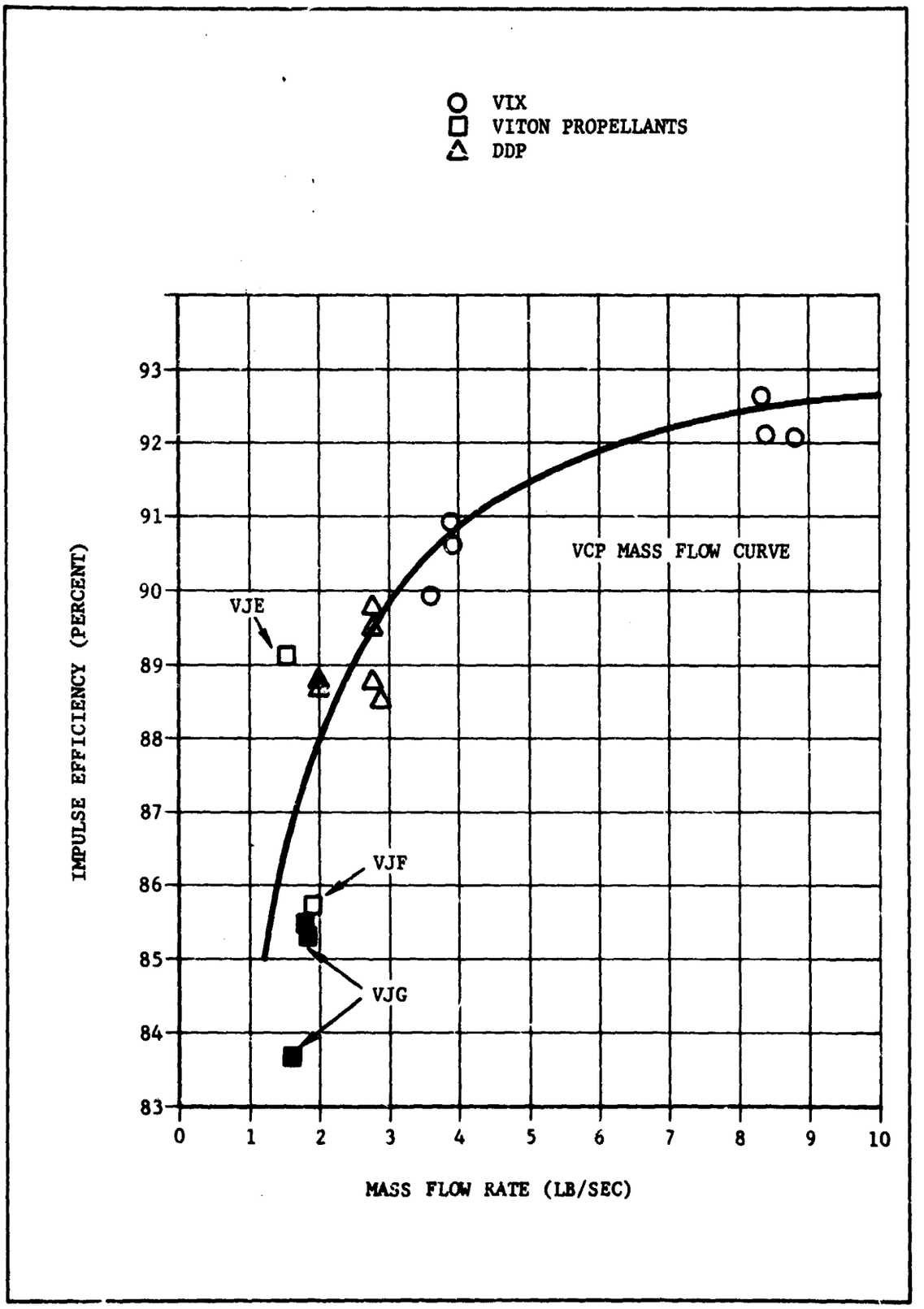

Figure 64. Impulse Efficiency as a Function of Mass-Flow Rate for Viton Propellants

SECTION V

INDUSTRIAL HYGIENE

All personnel associated with this contract who worked with Be or Be compounds were examined by the medical department physicians prior to this assignment and reexamined every 3 months thereafter. There were no suspected exposures, and all personnel were found to be free of symptoms associated with Be exposure.

An air-monitoring program was conducted throughout the contract period. Air samples were obtained at the worker breather zone in all areas where Be materials were used on an 8-hr shift basis and analyzed as soon thereafter as possible. The recommended maximum acceptable concentration for Be was never exceeded.

A total of 10 air samplers are strategically located at the plant periphery and operate continually. The samples are not routinely analyzed, but are stored for future reference. Periodic spot-check analyses have indicated no change in the background level of Be.

A total of 10 air samplers are located off the plant property in populated areas and are controlled through a telephone network. These samplers do not operate on a shift or continual basis, but can be activated through the plant telephone switchboard. The system will be activated in the event of a fire or explosion in the plant area. The system is activated at least 1 day per month and checked by the Instrument Calibration Group personnel.

The 16-meter meteorological tower and the continuous recording equipment (W/D, W/S, Δ T) are routinely checked and calibrated by the Instrument Calibration Group personnel. All subscale motor static testing operations are scheduled with and monitored by the Utah State Health Department. All test firings are accomplished in the scrubber facility.

All propellant mixing and testing operations involving Be were performed during periods of favorable meteorological conditions. There were no unusual incidents during the period of this contract relating to industrial hygiene problems.

Air sampling analysis data will be forwarded to AFRPL under separate cover.

SECTION VI

CONCLUSIONS AND RECOMMENDATIONS

Conclusions reached as a result of work on this contract are:

(1) Delivered Isp values in excess of the 280 lbf-sec/lbm, ARPA Project PRINCIPIA goal, have been achieved at density levels of 0.046 to 0.049 lb/in.^{3} in 15PC motors. Allowing for motor scaling, delivered impulses of 285 lbf-sec/lbm now appear state-of-the-art. These high values were obtained by using an energetic binder consisting of 16.4 NC/82.0 NG/ 1.6 2-NDPA.

(2) The Isp efficiency of both Be and LMH-2 propellants was found to depend on flame temperature, oxidation level (and/or metal level), and motor residence time. Highest efficiencies are obtained by keeping all three of these parameters as high as possible.

(3) The Isp efficiency of propellants having LMH-2 concentrations in excess of 15 percent is particularly sensitive to oxidation ratio. Agglomerate growth appears to control the combustion efficiency at these high fuel concentrations. The temperature before metal combustion (T*) may be a significant parameter in determining combustion efficiency.

(4) Limited testing indicates that a fluorine environment improves the combustion efficiency of LMH-2 propellants at low-oxidation ratios.

(5) Analyses of "off gases" obtained from propellants during cure indicate an incompatibility problem exists between one or more LMH-2 contaminants and plastisol binder ingredients. This incompatibility, coupled with desorption of air from the LMH-2 during cure, is believed responsible for the low-density grains obtained with some LMH-2 lots.

The demonstrated high-performance gains of LMH-2 propellants have not been achieved without some sacrifice in other important propellant properties. Some of these are:

(1) The high energy binder results in increased sensitivity and increased processing hazards as evidenced by the low impact and friction values obtained for the uncured propellants. Cured propellants exhibit sensitivity values comparable to conventional double base propellants.

(2) The high energy binder results in higher burning rates (0.77 to 0.97 in./sec @ 1000 psi) than are desirable for upper stage applications.

(3) The volumetric solids loading is currently limited to 60 percent, with a corresponding density penalty.

Based on these results, the following recommendations are made to further extend the performance level of LMH-2 propellants and improve the properties of the high performance propellants developed in this program:

(1) The influence of the propellant environment, as represented by flame temperature, oxidation ratio, and nonequilibrium flame temperatures, on combustion and impulse efficiency is not entirely clear and warrants further investigation. Investigation of the effect of mixed metals in high performance systems, therefore, appears worthwhile. A demonstration of motor scaling effects, with close attention to motor design parameters, for high performance propellants of the VIY type also appears worthwhile at this time.

(2) Further investigation of the effect of fluorine addition to improve LMH-2 performance efficiency appears worthwhile. To minimize theoretical performance losses, the direct addition of small percentages of TVOPA to double-base propellants having high theoretical impulses (VJI, VIZ type) seems a best first approach.

(3) Prior to the scale-up of LMH-2 propellants to larger demonstration motors, additional studies should be performed which include development of a wider range of available burning rates, density improvements, optimization of mechanical properties, and further development of methods to ensure uniformity of LMH-2 lots. These studies should be combined with (1) above.

LIST OF REFERENCES

1. Combustion of High Energy Solid Propellants, First Quarterly Report, Volume II, Report No. RPL-TDI-65-142, Contract AF 04(611)-10742, Hercules Powder Company (ABL), July 1965

2. Proceedings of the Second Beryllium Propellant Symposium, Technical Documentary Report No. RTD-TDR-63-1091, Air Force Rocket Propulsion Laboratory, October 1963

3. High Energy Solid Propellant Efficiency Investigation, Second Quarterly Progress Report, Report No. RPL-TDR-64-126, Contract AF 04(611)-9709, Atlantic Research, September 1964

4. Rocket Motor Performance - Nozzle Configuration Effects, Preprint 2E, 53rd Meeting AIChE, Pittsburg, Pa, E. Brown, May 17-20, 1964

   Proceedings of First Meeting ICPRG Working Group on Thermo Chemistry, B. Brown, June 1964

5. ABL-AGC Motor Interchange, Reference Report, 10 March 1961

6. JPL Space Programs Summary No. 37-30, Volume V

7. Preliminary Data for Aerojet General Corporation obtained from AFRPL

8. Performance of Propellants Containing Beane, Bulletin of the 21st ISP Meeting, CPIA Pub. No. 71, Volume 1, June 1965

9. Third Stage Minuteman Production Support Program Final Report, HPC-MTD-22-IV, January 1966, Hercules Incorporated, Magna, Utah

10. Characterization and Evaluation of Light Metal Hydrides, AFRPL-TR-66-48, March 1966, Lockheed Propulsion Co., Redlands, California

11. Combustion of High Energy Solid Propellants, Preliminary Final Report, AF 04(611)-10742, Hercules Incorporated, Cumberland, Md

12. Development and Test of High Energy Solid Propellants, HPC-230-12-5-1, 28 October 1965, Hercules Incorporated, Magna, Utah

APPENDIX A

THEORETICAL SPECIFIC IMPULSE CALCULATIONS

Theoretical Isp calculations for LMH-2 and Be containing propellant systems were made with a variety of binders and oxidizers. Nitrate, hydrocarbon, and fluorocarbon binders were investigated. Oxidizers included ammonium perchlorate (AP), ammonium nitrate (AN), cyclotetramethylene tetranitramine (HMX), mixtures of AP/HMX, triaminoguanidine nitrate (TAGN), and, to a lesser extent, hydrazinium diperchlorate (HDP) and nitronium perchlorate (NP). In addition, additives to improve theoretical LMH-2 combustion included the metals Al, Be, Li, Mg, Si, and Zr and lithium perchlorate (LIP) and triaminoguanidine azide (TAZ).

A. PRESENTATION OF RESULTS

Since calculations for the most part involve systematic treatment of three and four variable systems, the results are best presented in tabular form in Tables A-1 through A-5. Three dimensional grid network graphs (ternary systems within specified limits of the variables) are also presented, as are the usual binary systems on a common graph. The tables, however, show general characteristics of Isp, chamber temperature (T_c) and oxidation ratio (O.R.) and may be used to form many more grid networks and binary lines for comparison.

B. RESULTS OF THEORETICAL CALCULATIONS

1. Double-Base Systems - LMH-2

Tables A-1 through A-5 represent the LMH-2 calculations performed with various oxidizers. These oxidizers are AN, AP, HMX, AP/HMX mixtures, and TAGN. LMH-2, double-base propellants optimize at high Isp values (315 to 325 sec) but at relatively low temperatures ($3600^{\circ} \pm 100^{\circ}$ K). Table A-6 illustrates the comparitive results of all oxidizers in the 10 NC, 50 NG, 1 NDPA, 1 RES, LMH-2 system. The data is presented in tabular form for more accurate comparisons. Graphical presentation of these results shows considerable overlapping. The oxidizers are arranged in the order of their oxidizing potential. For these calculations, oxidation ratio is defined as $O.R. = \frac{O}{C + Be}$ when oxygen is the only oxidizing element present. If fluorine is also present, $O.R. = \frac{O + 1/2F}{C + Be}$.

Nitronium perchlorate, with the highest oxidizing potential and a positive heat of formation (+8.0 kcal/mole), produces the high temperatures desirable with LMH-2; however, its incompatibility with double base and poor combustion characteristics make it an unlikely candidate. The similarity of HDP and AP with molecular weights in almost exact 2:1 ratios accounts for the fact that the impulse results are similar for those two oxidizers regardless of the binder system.

Figures A-1, A-2, and A-3 show the basic grid networks in graphical form for the oxidizers AN, AP, and HMX. The basic networks contain no triacetin (TA). Peak impulse values are usually found at OMOX (OMOX condition implies an oxidation ratio = 1.0) or slightly in the fuel rich area, whereas peak T_c values occur on the oxygen rich side of OMOX, with very rapid decrease in T_c occurring on the negative (fuel rich) side of OMOX. The rate of climb of Isp is also very steep for LMH-2 systems, often rising 3 to 4 Isp units per 1-percent hydride addition.

The magnitude of peak impulse has been found to generally follow the oxygen level of the oxidizer. The order is AN, AP, HMX, TAGN, with a fairly large gap between AP and HMX. AP/HMX mixtures fill this gap. Temperatures do not follow the same order, however. From a temperature standpoint, the AP system gives fairly constant T_c values at all NG levels. HMX exceeds 3600° K only at the higher NG levels. The TAGN system does not appear promising in LMH-2 systems because of its very low T_c values (3400° K max).

2. Double-Base Systems - Be

All LMH-2 systems have been repeated with Be metal replacing the hydride. The calculations are represented in Tables A-7 through A-11. With Be systems, the maximum Isp values are 280 to 290, whereas T_c values are usually very high (3900° to 4200° K). In general, the effect of oxidizers on Isp is reversed for Be systems as compared to LMH-2 systems. For example, HMX and TAGN (the lower oxygen level ingredients) give higher Isp values than AP and AN. Highest temperatures, however, are shown by the latter ingredients. TAGN gives the highest Isp values within the range studied (~ 293 sec), but again TAGN does not produce the high temperature values with Be as do the other oxidizers.

3. Effect of Additives on LMH-2/AP, Double-Base Systems

The effect of addition of up to 6 percent of certain additives on impulse of the propellant system 10 NC, 50 NG, 1 NDPA, 1 RES, LMH-2/AP is summarized in Table A-12. The additives considered are the metals Al, Be, Li, Mg, Si, and Zr; the oxidizer lithium perchlorate (LIP); and the fuel triaminoguanidine azide (TAZ). Selected data from this table is plotted in Figure A-4 to show the comparison when LMH-2 is 16 percent. In general, only Be, Li, and TAZ show an Isp potential of greater than 308 sec, and Be is the only additive showing an increasing T_c value with increasing Isp. TAZ, being a nonmetal fuel, has the advantage of maintaining low metal content.

4. Hydrocarbon and Fluorocarbon Binders

The basic ternary LMH-2, AP, binder systems are presented in Figures A-5 through A-7. The binders included a hydrocarbon binder (HC) and two fluorocarbons. The fluorocarbon binders were FAAV (a mixture of 20-percent C7A, 60-percent C7M, and 20-percent Viton) and pure Teflon (TFLN). The ingredients in FAAV are fluorinated acrylates and methacrylates.

In general, low fluorocarbon binder levels, viz, 10 to 15 percent, are required for peak performance at any constant hydride level. Chamber temperatures drop rapidly with increasing binder level. It should be noted that a binder level of zero represents the basic LMH-2/AP binary system, which would necessarily be a pressed charge propellant. This binary system is basic to all three graphs. The performance of the hydrocarbon binder HC (polybutadiene type) is shown to peak sharply at about 10 percent binder level. Chamber temperature and Isp drop very rapidly within this system from peak levels. This system is also representative of the type whose peak performance is not at, or near, OMOX.

5. Thermochemical Ingredient Data

The thermochemical ingredient data used in the theoretical impulse calculations are presented in Table A-13.

TABLE A-1

THEORETICAL I_{sp} OF LMH-2, AN, DOUBLE-BASE SYSTEMS

NG (Wt %)	AN (Wt %)	LMH-2 (Wt %)	I_{sp} (Sec)	T_c (°K)	O.R.*	NG	AN	LMH-2	I_{sp}	T_c	O.R.*	NG	AN	LMH-2	I_{sp}	T_c	O.R.*
TA = 0 Wt %																	
30	44	14	298.5	3341	1.62	40	34	14	299.8	3417	1.53	50	24	14	301.1	3492	1.45
30	42	16	304.3	3373	1.45	40	32	16	305.5	3446	1.38	50	22	16	306.6	3518	1.31
30	40	18	310.0	3402	1.31	40	30	18	311.0	3471	1.25	50	20	18	312.0	3540	1.19
30	38	20	315.4	3427	1.18	40	28	20	316.3	3492	1.13	50	18	20	317.1	3555	1.09
30	34.38	23.62	324.2	3428	1.00	40	25.25	22.75	322.7	3472	1.00	50	16.11	21.89	321.2	3530	1.00
TA = 2 Wt %																	
30	42	14	297.9	3290	1.54	40	32	14	299.3	3367	1.46	50	22	14	300.7	3444	1.39
30	40	16	303.9	3324	1.38	40	30	16	305.2	3398	1.32	50	20	16	306.4	3471	1.26
30	38	18	309.7	3354	1.25	40	28	18	310.8	3424	1.20	50	18	18	311.8	3494	1.15
30	36	20	315.2	3381	1.14	40	26	20	316.2	3446	1.09	50	16	20	317.0	3506	1.05
30	33.18	22.82	322.2	3380	1.00	40	24.04	21.96	320.7	3430	1.00	50	14.91	21.09	319.2	3484	1.00
TA = 4 Wt %																	
30	40	14	297.2	3237	1.48	40	30	14	298.7	3315	1.40	50	20	14	300.2	3393	1.33
30	38	16	303.4	3273	1.33	40	28	16	304.7	3348	1.27	50	18	16	306.1	3222	1.21
30	36	18	309.3	3305	1.20	40	26	18	310.5	3376	1.15	50	16	18	311.6	3446	1.11
30	34	20	314.9	3333	1.10	40	24	20	315.9	3397	1.05	50	14	20	316.8	3447	1.01
30	31.98	22.02	320.0	3330	1.00	40	22.84	21.16	318.6	3382	1.00	50	13.71	20.29	317.3	3435	1.00

*Oxidation Ratio

Percentage Limits of Variables:

LMH-2 14-20% & OMOX
NG 30-50%
TA 0-4%
AN Difference

Sum = 88%

Percentage of Constants:

NC 10%
NDPA 1%
RES 1%

CONFIDENTIAL

TABLE A-2

THEORETICAL I_{sp} OF LMH-2, AP, DOUBLE-BASE SYSTEMS

NG (Wt %)	AP (Wt %)	LMH-2 (Wt %)	I_{sp} (Sec)	T_c (°K)	O.R.*	NG	AP	LMH-2	I_{sp}	T_c	O.R.*	NG	AP	LMH-2	I_{sp}	T_c	O.R.*
TA = 0 Wt %																	
30	[illegible]	14	298.6	3679	1.54	40	34	14	299.9	3677	1.47	50	24	14	301.1	3675	1.41
30	42	16	303.9	3685	1.38	40	32	16	305.1	3682	1.33	50	22	16	306.3	3679	1.28
30	40	18	309.0	3685	1.25	40	30	18	310.2	3680	1.20	50	20	18	311.4	3677	1.16
30	38	20	313.8	3675	1.13	40	28	20	315.0	3668	1.10	50	18	20	316.1	3661	1.06
30	35.33	22.67	319.4	3628	1.00	40	25.94	22.06	319.2	3627	1.00	50	16.55	21.45	319.0	3626	1.00
TA = 2 Wt %																	
30	42	14	298.9	3626	1.47	40	32	14	300.0	3622	1.41	50	22	14	301.1	3618	1.36
30	40	16	304.2	3631	1.33	40	30	16	305.3	3626	1.28	50	20	16	306.4	3622	1.23
30	38	18	309.6	3629	1.20	40	28	18	310.4	3623	1.16	50	18	18	311.5	3618	1.12
30	36	20	314.1	3616	1.09	40	26	20	315.2	3607	1.06	50	16	20	316.3	3596	1.03
30	34.10	21.90	318.0	3579	1.00	40	24.71	21.29	317.8	3577	1.00	50	15.32	20.68	317.5	3575	1.00
TA = 4 Wt %																	
30	40	14	298.9	3568	1.41	40	30	14	299.9	3563	1.36	50	20	14	301.0	3558	1.30
30	38	16	304.3	3573	1.27	40	28	16	305.3	3569	1.23	50	18	16	306.4	3561	1.19
30	36	18	309.4	3570	1.16	40	26	18	310.5	3563	1.12	50	16	18	311.6	3557	1.09
30	34	20	314.3	3553	1.05	40	24	20	315.2	3539	1.02	50	14	20	315.9	3518	0.996
30	32.87	21.13	316.5	3528	1.00	40	23.48	20.52	316.2	3524	1.00	50	14.09	19.91	315.8	3522	1.00

*Oxidation Ratio

Percentage Limits of Variables:

LMH-2 12-18% & OMOX
NG 30-50%
TA 0-4%
AP/HMX Difference
50/50

Sum = 88%

Percentage of Constants:

NC 10%
NDPA 1%
RES 1%

TABLE A-3

THEORETICAL I_{sp} OF LMH-2, AP AND HMX, DOUBLE-BASE SYSTEMS

NG (Wt %)	50/50 AP/HMX (Wt %)	LMH-2 (Wt %)	I_{sp} (Sec)	T_c (°K)	O.R.*	NG	50/50 AP/HMX	LMH-2	I_{sp}	T_c	O.R.*	NG	50/50 AP/HMX	LMH-2	I_{sp}	T_c	O.R.*
TA = 0 Wt %																	
30	46	12	298.8	3591	1.40	40	36	12	298.8	3606	1.40	50	26	12	298.7	3621	1.40
30	44	14	304.1	3601	1.27	40	34	14	304.0	3617	1.28	50	24	14	304.0	3632	1.28
30	42	16	309.1	3604	1.16	40	32	16	309.1	3621	1.17	50	22	16	309.0	3638	1.18
30	40	18	313.9	3596	1.07	40	30	18	313.9	3615	1.07	50	20	18	313.8	3634	1.08
30	38.50	19.50	316.9	3567	1.00	40	28.27	19.73	317.3	3582	1.00	50	18.00	20.00	317.9	3596	1.00
TA = 2 Wt %																	
30	44	12	298.1	3532	1.36	40	34	12	298.1	3548	1.36	50	24	12	298.1	3564	1.36
30	42	14	303.5	3542	1.24	40	32	14	303.5	3559	1.24	50	22	14	303.5	3575	1.24
30	40	16	308.7	3546	1.13	40	30	16	308.7	3564	1.14	50	20	16	308.7	3581	1.14
30	38	18	313.5	3534	1.04	40	28	18	313.6	3555	1.05	50	18	18	313.6	3575	1.05
30	37.15	18.85	315.1	3514	1.00	40	26.92	19.08	315.7	3530	1.00	50	16.65	19.35	316.2	3545	1.00
TA = 4 Wt %																	
30	42	12	297.3	3470	1.31	40	32	12	297.3	3486	1.32	50	22	12	297.4	3502	1.32
30	40	14	302.9	3481	1.20	40	30	14	302.9	3498	1.20	50	26	14	302.9	3514	1.21
30	38	16	308.2	3485	1.10	40	28	16	308.2	3503	1.10	50	18	16	308.2	3521	1.11
30	36	18	312.9	3464	1.01	40	26	18	313.0	3488	1.02	50	16	18	313.1	3511	1.03
30	35.81	18.19	313.2	3458	1.00	40	25.58	18.42	313.8	3475	1.00	50	15.31	18.69	314.4	3491	1.00

*Oxidation Ratio

Percentage Limits of Variables:

LMH-2 12-18% & CMOX
NG 30-50%
TA 0-4%
AP/HMX Difference
50/50

Sum = 88%

Percentage of Constants:

NC 10%
NDPA 1%
RES 1%

TABLE A-4

THEORETICAL I_{sp} OF LMH-2, HMX, DOUBLE-BASE SYSTEMS

NG (Wt %)	HMX (Wt %)	LMH-2 (Wt %)	I_{sp} (Sec)	T_c (°K)	O.R.*	NG	HMX	LMH-2	I_{sp}	T_c	O.R.*	NG	HMX	LMH-2	I_{sp}	T_c	O.R.*
TA = 0 Wt %																	
30	47	12	303.2	3526	1.18	40	37	12	302.5	3565	1.24	50	27	12	301.7	3602	1.29
30	45	14	308.6	3538	1.09	40	35	14	307.8	3578	1.14	50	25	14	306.8	3616	1.19
30	43	16	313.4	3520	1.01	40	33	16	312.7	3581	1.06	50	23	16	311.7	3624	1.10
30	41	18	312.0	3368	0.934	40	31	18	315.2	3517	0.979	50	21	18	316.2	3612	1.02
30	42.81	16.19	313.7	3512	1.00	40	31.58	17.42	315.6	3552	1.00	50	20.34	18.66	317.3	3590	1.00
TA = 2 Wt %																	
30	45	12	302.0	3465	1.16	40	35	12	301.4	3506	1.21	50	25	12	300.7	3545	1.26
30	43	14	307.5	3478	1.07	40	33	14	306.8	3521	1.12	50	23	14	306.0	3560	1.17
30	41	16	311.3	3437	0.987	40	31	16	311.9	3522	1.03	50	21	16	311.0	3569	1.08
30	39	18	310.0	3279	0.916	40	29	18	312.7	3420	0.961	50	19	18	315.5	3546	1.01
30	41.34	15.66	311.5	3457	1.00	40	30.10	16.90	313.7	3500	1.00	50	18.86	18.14	315.6	3540	1.00
TA = 4 Wt %																	
30	43	12	300.6	3401	1.13	40	33	12	300.2	3444	1.18	50	23	12	299.6	3485	1.23
30	41	14	306.3	3416	1.05	40	31	14	305.8	3461	1.09	50	21	14	305.1	3502	1.14
30	39	16	308.6	3338	0.968	40	29	16	311.0	3458	1.01	50	19	16	310.2	3512	1.06
30	37	18	307.9	3229	0.900	40	27	18	310.3	3322	0.943	50	17	18	313.6	3466	0.987
30	39.87	15.13	309.1	3399	1.00	40	28.62	16.38	311.6	3445	1.00	50	17.38	17.62	313.8	3488	1.00

*Oxidation Ratio

Percentage Limits of Variables:

LMH-2 12-18% & OMOX
NG 30-50%
TA 0-4 %
HMX Difference

Sum = 89%

Percentage of Constants:

NC 10%
NDPA 1%

CONFIDENTIAL

TABLE A-5

THEORETICAL I_{sp} OF LMH-2, TAGN, DOUBLE-BASE SYSTEMS

NG (Wt %)	TAGN (Wt %)	LMH-2 (Wt %)	I_{sp} (Sec)	T_c (°K)	O.R.*	NG	TAGN	LMH-2	I_{sp}	T_c	O.R.*	NG	TAGN	LMH-2	I_{sp}	T_c	O.R.*
TA = 0 Wt %																	
30	50	8	283.5	2948	1.41	40	40	8	285.8	3102	1.48	50	30	8	287.5	3250	1.54
30	48	10	291.4	3015	1.27	40	38	10	293.1	3160	1.33	50	28	10	294.2	3300	1.39
30	46	12	298.8	3076	1.15	40	36	12	300.0	3213	1.21	50	26	12	300.5	3346	1.27
30	44	14	305.7	3129	1.05	40	34	14	306.3	3259	1.11	50	24	14	306.4	3386	1.17
30	42.93	15.07	309.0	3140	1.00	40	31.52	16.48	313.4	3285	1.00	50	20.11	17.89	316.4	3417	1.00
TA = 2 Wt %																	
30	48	8	281.3	2890	1.37	40	38	8	283.8	3046	1.43	50	28	8	285.7	3198	1.49
30	46	10	289.4	2961	1.24	40	36	10	291.4	3108	1.30	50	26	10	292.7	3251	1.36
30	44	12	297.0	3024	1.12	40	34	12	298.4	3164	1.18	50	24	12	299.2	3299	1.24
30	42	14	304.1	3079	1.03	40	32	14	305.0	3213	1.08	50	22	14	305.2	3342	1.14
30	41.43	14.57	305.9	3084	1.00	40	30.02	15.98	310.8	3236	1.00	50	18.61	17.39	314.2	3373	1.00
TA = 4 Wt %																	
30	46	8	279.0	2830	1.33	40	36	8	381.7	2989	1.39	50	26	8	283.9	3144	1.45
30	44	10	287.4	2904	1.20	40	34	10	289.5	3054	1.26	50	24	10	291.0	3201	1.32
30	42	12	295.2	2972	1.10	40	32	12	296.8	3113	1.16	50	22	12	297.7	3252	1.21
30	40	14	302.4	3024	1.003	40	30	14	303.5	3165	1.06	50	20	14	304.0	3297	1.12
30	39.93	14.07	302.6	3024	1.00	40	28.52	15.48	308.0	3113	1.00	50	17.11	16.89	311.9	3326	1.00

*Oxidation Ratio

Percentage Limits of Variables:

LMH-2 8-14% & CMOX
NG 30-50%
TA 0-4%
TAGN Difference

Sum = 88%

Percentage of Constants:

NC 10%
NDPA 1%
RES 1%

CONFIDENTIAL

TABLE A-6

COMPARATIVE PERFORMANCE OF VARIOUS LMH-2, OXIDIZER SYSTEMS

BeH_2 (w. %)	NP			AN			HDP			AP			HMX			TAGN		
	T_c (°K)	I_{sp} (sec)	O.R.*	T_c (°K)	I_{sp} (sec)	O.R.	T_c (°K)	I_{sp} (sec)	O.R.	T_c (°K)	I_{sp} (sec)	O.R.	T_c (°K)	I_{sp} (sec)	O.R.	T_c (°K)	I_{sp} (sec)	O.R.
10	3896	288.5	1.858	--	--	--	3712	290.3	1.756	3641	290.1	1.752	--	--	--	3300	294.2	1.392
12	3938	294.7	1.657	3461	295.3	1.610	3735	295.8	1.570	3663	295.7	1.567	3602	301.7	1.290	3346	300.5	1.270
14	3951	300.3	1.487	3492	301.1	1.447	3743	301.2	1.414	3675	301.1	1.411	3616	306.8	1.191	3386	306.4	1.156
16	3943	305.5	1.343	3518	306.6	1.309	3741	306.3	1.281	3679	306.3	1.278	3624	311.7	1.103	3420	311.3	1.075
18	3920	310.5	1.219	3540	312.0	1.190	3732	311.3	1.166	3677	311.4	1.164	3612	316.2	1.024	3349	315.5	0.960
20	3883	315.3	1.111	3555	317.1	1.086	3709	316.0	1.066	3661	316.1	1.064	3493	316.2	0.954	--	--	--
22	3818	319.6	1.016	3524	321.3	0.995	3641	319.5	0.979	3598	319.5	0.997	--	--	--	--	--	--
CHOX	3800	320.2	1.000	3530	321.2	1.000	3667	319.0	1.000	3626	319.0	1.000	3590	317.3	1.000	3417	316.4	1.000
BeH_2 at CHOX		22.35			21.89			21.49			21.45			18.66			17.89	

Percentage of Constants

NC 10%
NG 50%
HDPA 1%
RES 1% (HMX contains no RES)

*Oxidation Ratio

TABLE A-7

THEORETICAL I_{sp} OF Be, AN, DOUBLE-BASE SYSTEMS

NG (Wt %)	AN (Wt %)	Be (Wt %)	I_{sp} (Sec)	T_c (°K)	O.R.*	NC	AN	Be	I_{sp}	T_c	O.R.*	NG	AN	Be	I_{sp}	T_c	O.R.*
TA = 0 Wt %																	
30	46	12	276.7		1.61	40	36	12	277.2	3799	1.52	50	26	12	277.8	3879	1.44
30	44	14	278.3	3835	1.42	40	34	14	279.0	3914	1.35	50	24	14	279.9	3996	1.29
30	42	16	280.1	3940	1.26	40	32	16	281.0	4020	1.21	50	22	16	281.9	4100	1.16
30	40	18	282.0	4032	1.13	40	30	18	282.8	4103	1.09	50	20	18	283.4	4167	1.05
30	37.61	20.39	282.9	4066	1.00	40	28.35	19.65	283.1	4112	1.00	50	19.10	18.90	283.3	4160	1.00
TA = 2 Wt %																	
30	44	12	277.5	3691	1.53	40	34	12	278.0	3771	1.45	50	24	12	278.5	3853	1.38
30	42	14	279.0	3802	1.36	40	32	14	279.6	3883	1.30	50	22	14	280.4	3966	1.24
30	40	16	280.6	3905	1.21	40	30	16	281.4	3984	1.16	50	20	16	282.4	4063	1.12
30	38	18	282.4	3990	1.09	40	28	18	283.1	4054	1.05	50	18	18	283.5	4100	1.01
30	36.30	19.70	283.0	4002	1.00	40	27.04	18.96	283.2	4047	1.00	50	17.79	18.21	283.4	4095	1.00
TA = 4 Wt %																	
30	42	12	278.1	3655	1.47	40	32	12	278.6	3737	1.40	50	22	12	279.2	3820	1.33
30	40	14	279.8	3764	1.30	40	30	14	280.2	3846	1.25	50	20	14	280.9	3930	1.19
30	38	16	281.2	3865	1.17	40	28	16	281.9	3943	1.12	50	18	16	282.7	4019	1.08
30	36	18	282.7	3939	1.05	40	26	18	T. N. Result			50	16	18	282.4	4004	0.977
30	34.99	19.01	282.9	3936	1.00	40	25.73	18.27	283.0	3981	1.00	50	16.48	17.52	283.3	4028	1.00

*Oxidation Ratio

Percentage Limits of Variables:

Be 12-18% & OMOX
NG 30-50%
TA 0-4%
AP Difference

Sum = 88%

Percentage of Constants:

NC 10%
NLPA 1%
RES 1%

CONFIDENTIAL

CONFIDENTIAL

TABLE A-8

THEORETICAL I_{sp} OF Be, AP, DOUBLE-BASE SYSTEMS

NG (Wt %)	AP (Wt %)	Be (Wt %)	I_{sp} (Sec)	T_c (°K)	O.R.*	NG	AP	Be	I_{sp}	T_c	O.R.*	NG	AP	Be	I_{sp}	T_c	O.R.*
TA = 0 Wt %																	
30	46	12	271.8	4003	1.53	40	36	12	273.7	4024	1.46	50	26	12	275.6	4045	1.40
30	44	14	274.1	4116	1.35	40	34	14	276.0	4135	1.30	50	24	14	277.9	4154	1.25
30	42	16	276.0	4210	1.20	40	32	16	277.9	4225	1.16	50	22	16	279.7	4240	1.13
30	40	18	277.3	4274	1.08	40	30	18	279.0	4281	1.05	50	20	18	280.7	4282	1.02
30	38.50	19.50	277.6	4291	1.00	40	29.03	18.97	279.1	4286	1.00	50	19.55	18.45	280.7	4280	1.00
TA = 2 Wt %																	
30	44	12	273.0	3982	1.46	40	34	12	274.8	3999	1.40	50	24	12	276.5	4017	1.35
30	42	14	275.2	4086	1.30	40	32	14	277.0	4101	1.25	50	22	14	278.8	4117	1.21
30	40	16	277.1	4170	1.16	40	30	16	278.8	4181	1.12	50	20	16	280.6	4192	1.09
30	38	18	278.2	4219	1.04	40	28	18	280.0	4217	1.02	50	18	18	281.1	4206	0.990
30	37.17	18.84	278.2	4223	1.00	40	27.69	18.31	279.7	4217	1.00	50	18.21	17.79	281.2	4210	1.00
TA = 4 Wt %																	
30	42	12	273.9	3953	1.40	40	32	12	275.6	3966	1.35	50	22	12	277.3	3981	1.30
30	40	14	276.2	4049	1.25	40	30	14	277.8	4061	1.21	50	20	14	279.5	4073	1.17
30	38	16	277.9	4123	1.12	40	28	16	279.6	4129	1.09	50	18	16	281.2	4134	1.06
30	35	18	278.7	4154	1.01	40	26	18	280.0	4139	0.980	50	16	18	280.6	4106	0.960
30	35.82	18.18	278.7	4153	1.00	40	26.35	17.65	280.1	4145	1.00	50	16.87	17.13	281.4	4136	1.00

*Oxidation Ratio

Percentage Limits of Variables:

Be 12-18% & OMOX
NG 30-50%
TA 0-4%
AP Difference

Sum = 88%

Percentage of Constants:

NC 10%
NDPA 1%
RES 1%

TABLE A-9

THEORETICAL I_{sp} OF Be, AP AND HMX, DOUBLE-BASE SYSTEMS

NG (Wt %)	AP/HMX (Wt %)	Be (Wt %)	I_{sp} (Sec)	T_c (°K)	O.R.*	NG	AP/HMX	Be	I_{sp}	T_c	O.R.*	NG	AP/HMX	Be	I_{sp}	T_c	O.R.*
TA = 0 Wt %																	
30	50	8	277.2	3806	1.59	40	40	8	277.0	3817	1.59	50	30	8	276.8	3829	1.58
30	48	10	279.14	3922	1.41	40	38	10	278.9	3935	1.41	50	28	10	278.7	3948	1.41
30	46	12	281.1	4026	1.26	40	36	12	280.9	4026	1.26	50	26	12	280.8	4058	1.27
30	44	14	282.9	4111	1.13	40	34	14	282.8	4132	1.14	50	24	14	282.7	4153	1.15
30	41.43	16.57	283.8	4157	1.00	40	31.24	16.76	283.8	4184	1.00	50	21.04	16.96	283.8	4211	1.00
TA = 2 Wt %																	
30	48	8	277.6	3773	1.53	40	38	8	277.4	3785	1.53	50	28	8	277.2	3798	1.53
30	46	10	279.6	3883	1.36	40	36	10	279.4	3899	1.36	50	26	10	279.1	3912	1.37
30	44	12	281.3	3982	1.22	40	34	12	281.2	3999	1.23	50	24	12	281.0	4017	1.23
30	42	14	283.0	4059	1.10	40	32	14	282.9	4082	1.11	50	22	14	282.9	4104	1.12
30	39.99	16.01	283.7	4087	1.00	40	29.79	16.21	283.7	4114	1.00	50	19.60	16.40	283.8	4121	1.00
TA = 4 Wt %																	
30	46	8	277.8	3732	1.48	40	36	8	277.6	2746	1.48	50	26	8	277.5	3760	1.48
30	44	10	280.0	3838	1.32	40	34	10	279.8	3854	1.32	50	24	10	279.6	3870	1.32
30	42	12	281.6	3932	1.19	40	32	12	281.4	3951	1.19	50	22	12	281.2	3980	1.20
30	40	14	283.0	4002	1.08	40	30	14	283.0	4026	1.08	50	[illegible]	14	282.9	4050	1.09
30	38.55	15.45	283.4	4015	1.00	40	28.35	15.65	283.5	4042	1.00	50	18.16	15.84	283.6	4070	1.00

*Oxidation Ratio

Percentage Limits of Variables:

Be 8-14% & OMOX
NG 30-50%
TA 0-4%
AP/HMX Difference
50/50

Sum = 88%

Percentage of Constants:

NC 10%
NDPA 1%
RES 1%

CONFIDENTIAL

TABLE A-10

THEORETICAL I_{sp} OF Be, HMX, DOUBLE-BASE SYSTEMS

NC (Wt %)	HMX (Wt %)	Be (Wt %)	I_{sp} (Sec)	T_c (°K)	O.R.*	NG	HMX	Be	I_{sp}	T_c	O.R.*	NG	HMX	Be	I_{sp}	T_c	O.R.*
TA = 0 Wt %																	
30	51	8	285.4	3819	1.31	40	41	8	28.39	3842	1.37	50	31	8	282.1	3858	1.42
30	49	10	287.6	3926	1.18	40	39	10	285.7	3952	1.23	50	29	10	283.7	3973	1.29
30	47	12	288.9	4010	1.07	40	37	12	287.2	4049	1.12	50	27	12	285.4	4077	1.17
30	45	14	288.0	4002	0.980	40	35	14	288.4	4101	1.03	50	25	14	286.9	4157	1.07
30	45.45	13.55	289.1	4020	1.00	40	34.41	14.59	288.2	4093	1.00	50	23.38	15.62	287.0	4165	1.00
TA = 2 Wt %																	
30	49	8	284.8	3765	1.28	40	39	8	283.5	3794	1.33	50	29	8	281.9	3816	1.39
30	47	10	287.3	3871	1.15	40	37	10	285.6	3902	1.21	50	27	10	283.7	3928	1.26
30	45	12	288.7	3949	1.05	40	35	12	286.9	3995	1.10	50	25	12	285.1	4029	1.15
30	43	14	287.1	3899	0.961	40	33	14	287.7	4029	1.01	50	23	14	286.5	4100	1.05
30	43.89	13.11	288.7	3949	1.00	40	32.85	14.15	287.5	4025	1.00	50	21.82	15.18	286.5	4099	1.00
TA = 4 Wt %																	
30	47	8	284.0	3707	1.25	40	37	8	282.8	3740	1.30	50	27	8	281.5	3768	1.36
30	45	10	286.8	3811	1.13	40	35	10	285.3	3848	1.18	50	25	10	283.6	3878	1.23
30	43	12	288.5	3882	1.03	40	33	12	286.8	3938	1.08	50	23	12	285.0	3977	1.12
30	41	14	285.5	3779	0.944	40	31	14	286.7	3944	0.988	50	21	14	286.1	4037	1.03
30	42.33	12.67	288.4	3876	1.00	40	31.29	13.71	287.1	3955	1.00	50	20.25	14.75	285.9	4030	1.00

*Oxidation Ratio

Percentage Limits of Variables:

Be 8-14% & OMOX
NG 30-50%
TA 0-4%
HMX Difference

Sum = 89%

Percentage of Constants:

NC 10%
NDPA 1%

CONFIDENTIAL

TABLE A-11

THEORETICAL I_{sp} OF Be, TAGN, DOUBLE-BASE SYSTEMS

NG (Wt %)	TAGN (Wt %)	Be (Wt %)	I_{sp} (Sec)	T_c (°K)	O.R.*	NG	TAGN	Be	I_{sp}	T_c	O.R.*	NG	TAGN	Be	I_{sp}	T_c	O.R.*
TA = 0 Wt %																	
30	52	6	277.2	3159	1.48	40	42	6	278.7	3315	1.54	50	32	6	279.4	3455	1.59
30	50	8	284.2	3309	1.29	40	40	8	284.5	3455	1.36	50	30	8	283.9	3588	1.41
30	48	10	289.5	3444	1.15	40	38	10	288.7	3583	1.21	50	28	10	287.0	3713	1.27
30	46	12	293.2	3553	1.03	40	36	12	291.4	3696	1.09	50	26	12	288.0	3826	1.15
30	45.41	12.59	293.7	3558	1.00	40	34.24	13.76	292.3	3740	1.00	50	23.06	14.94	289.3	3916	1.00
TA = 2 Wt %																	
30	50	6	275.2	3100	1.43	40	40	6	277.0	3261	1.49	50	30	6	277.9	3410	1.55
30	48	8	282.6	3255	1.26	40	38	8	283.2	3406	1.32	50	28	8	282.9	3546	1.38
30	46	10	288.3	3395	1.12	40	36	10	287.7	3538	1.18	50	26	10	286.2	3672	1.24
30	44	12	292.3	3494	1.01	40	34	12	290.7	3651	1.07	50	24	12	288.3	3787	1.12
30	43.83	12.17	292.3	3493	1.00	40	32.66	13.34	291.6	3681	1.00	50	21.48	14.52	288.9	3860	1.00
TA = 4 Wt %																	
30	48	6	273.1	3039	1.38	40	38	6	275.1	3205	1.44	50	28	6	276.4	3360	1.50
30	46	8	281.0	3200	1.22	40	36	8	281.7	3354	1.28	50	26	8	281.7	3500	1.34
30	44	10	287.0	3343	1.10	40	34	10	286.7	3490	1.15	50	24	10	285.5	3629	1.21
30	42	12	290.2	3417	0.987	40	32	12	290.0	3603	1.05	50	22	12	287.8	3745	1.10
30	42.24	11.75	290.7	3425	1.00	40	31.08	12.92	290.6	3620	1.00	50	19.90	14.10	288.5	3803	1.00

*Oxidation Ratio

Percentage Limits of Variables:

Be 6-12%
NG 30-50%
TA 0-4%
TAGN Difference

Sum = 88%

Percentage of Constants:

NC 10%
NDPA 1%
RES 1%

CONFIDENTIAL

CONFIDENTIAL

TABLE A-12

EFFECT OF VARIOUS ADDITIVES ON
THEORETICAL I_{sp} OF LMH-2, AP, DOUBLE-BASE SYSTEMS

LMH-2 (Wt %)	AP (Wt %)	"X" (Wt %)	I_{sp} (Sec)	T_c (°K)	O.R.*	LMH-2	AP	"X"	I_{sp}	T_c	O.R.*	LMH-2	AP	"X"	I_{sp}	T_c	O.R.*
Additive "X" = AL																	
12	26	-	295.7	3663	1.57	14	24	-	301.1	3675	1.41	16	22	-	306.3	3679	1.28
12	24	2	295.8	3698	1.46	14	22	2	301.1	3699	1.32	16	20	2	306.1	3689	1.20
12	22	4	296.0	3738	1.36	14	20	4	301.1	3730	1.23	16	18	4	305.9	3707	1.12
12	20	6	296.1	3772	1.27	14	18	6	301.0	3753	1.15	16	16	6	305.4	3710	1.05
Additive "X" = Be																	
12	26	-	295.7	3663	1.57	14	24	-	301.1	3675	1.41	16	22	-	306.3	3679	1.28
12	24	2	298.3	3742	1.39	14	22	2	303.5	3746	1.26	16	20	2	308.4	3740	1.15
12	22	4	300.3	3813	1.24	14	20	4	305.2	3804	1.13	16	18	4	309.8	3774	1.03
12	20	6	301.8	3869	1.11	14	18	6	305.2	3830	1.02	16	16	6	308.4	3706	0.94
Additive "X" = LI																	
12	26	-	295.7	3663	1.57	14	24	-	301.1	3675	1.41	16	22	-	306.3	3679	1.28
12	24	2	298.4	3656	1.43	14	22	2	303.6	3658	1.30	16	20	2	308.6	3652	1.18
12	22	4	298.6	3591	1.32	14	20	4	303.6	3577	1.20	16	18	4	308.5	3554	1.09
12	20	6	297.8	3491	1.22	14	18	6	302.6	3459	1.11	16	16	6	307.1	3415	1.02

*Oxidation Ratio

Percentage Limits of Variables:

LMH-2 12-16%

Additive "X" 0-6%

AP Difference

Sum = 38%

Percentage of Constants:

NC 10%

NG 50%

NDPA 1%

RES 1%

CONFIDENTIAL

TABLE A-12 (Cont)

EFFECT OF VARIOUS ADDITIVES ON
THEORETICAL I_{sp} OF LMH-2, AP, DOUBLE-BASE SYSTEMS

LMH-2 (Wt %)	AP (Wt %)	"X" (Wt %)	I_{sp} (Sec)	T_c (°K)	O.R.*	LMH-2	AP	"X"	I_{sp}	T_c	O.R.*	LMH-2	AP	"X"	I_{sp}	T_c	O.R.*
Additive "X" = MG																	
12	26	-	295.7	3663	1.57	14	24	-	301.1	3675	1.41	16	22	-	306.3	3679	1.28
12	24	2	294.4	3626	1.48	14	22	2	299.7	3636	1.33	16	20	2	304.9	3640	1.21
12	22	4	293.6	3584	1.39	14	20	4	298.6	3593	1.26	16	18	4	303.6	3597	1.15
12	20	6	293.0	3554	1.31	14	18	6	297.7	3547	1.19	16	16	6	302.4	3551	1.09
Additive "X" = SI																	
12	26	-	295.7	3663	1.57	14	24	-	301.1	3675	1.41	16	22	-	306.3	3679	1.28
12	24	2	294.1	3633	1.44	14	22	2	299.6	3642	1.30	16	20	2	304.9	3645	1.18
12	22	4	292.5	3598	1.32	14	20	4	298.9	3606	1.20	16	18	4	303.4	3606	1.10
12	20	6	290.9	3559	1.22	14	18	6	296.4	3565	1.11	16	16	6	301.8	3563	1.02
Addtive "X" = ZR																	
12	26	-	295.7	3663	1.57	14	24	-	301.1	3675	1.41	16	22	-	306.3	3679	1.28
12	24	2	294.6	3687	1.50	14	22	2	300.0	3698	1.35	16	20	2	305.3	3702	1.23
12	22	4	293.5	3706	1.44	14	20	4	298.9	3714	1.30	16	18	4	304.1	3715	1.18
12	20	6	292.3	3724	1.38	14	18	6	297.7	3730	1.25	16	16	6	302.9	3727	1.13

*Oxidation Ratio

Percentage Limits of Variables:

LMH-2 12-16%
Additive "X" 0-6%
AP Difference
Sum = 36%

Percentage of Constants:

NC 10%
NG 50%
NDPA 1%
RES 1%

CONFIDENTIAL

CONFIDENTIAL

TABLE A-12 (Cont)

EFFECT OF VARIOUS ADDITIVES ON
THEORETICAL I_{sp} OF LMH-2, AP, DOUBLE-BASE SYSTEMS

LMH-2 (Wt %)	AP (Wt %)	"X" (Wt %)	I_{sp} (Sec)	T_c (°K)	O.R.*	LMH-2	AP	"X"	I_{sp}	T_c	O.R.*	LMH-2	AP	"X"	I_{sp}	T_c	O.R.*
Additive "X" = LIP																	
12	26	--	295.7	3663	1.57	14	24	--	301.1	3675	1.41	16	22	--	306.3	3679	1.28
12	24	2	295.4	3678	1.56	14	22	2	300.8	3690	1.41	16	20	2	305.9	3694	1.28
12	22	4	294.8	3688	1.56	14	20	4	300.2	3700	1.41	16	18	4	305.3	3705	1.27
12	20	6	294.2	3697	1.56	14	18	6	299.6	3710	1.40	16	16	6	304.7	3714	1.27
Additive "X" = TAZ																	
12	26	--	295.7	3663	1.57	14	24	--	301.1	3675	1.41	16	22	--	306.3	3679	1.28
12	24	2	296.8	3637	1.52	14	22	2	302.2	3646	1.37	16	20	2	307.5	3650	1.24
12	22	4	297.8	3608	1.48	14	20	4	303.3	3616	1.33	16	18	4	308.6	3619	1.21
12	20	6	298.8	3577	1.44	14	18	6	304.3	3585	1.30	16	16	6	309.6	3587	1.18

*Oxidation Ratio

Percentage Limits of Variables:

LMH-2 12-16%
Additive "X" 0-6%
AP Difference

Sum = 38%

Percentage of Constants:

NC 10%
NG 50%
NDPA 1%
RES 1%

CONFIDENTIAL

CONFIDENTIAL

TABLE A-13
THERMOCHEMICAL INGREDIENT DATA

Ingred Symbol	Chemical Name	Chemical Formula	ΔH_{f298} (kcal/mole)	Density (g/cc)
Al	Aluminum	Al	0	2.7
AN	Ammonium Nitrate	NH_4NO_3	-87.27	1.725
AP	Ammonium Perchlorate	NH_4ClO_4	-69.42	1.950
BE	Beryllium	Be	0	1.816
LMH-2	Beryllium Hydride	$Be_{8.86}H_{17.38}C_{.293}C_{.002}$	-5.5	0.650
C5A	Pentyl Fluoroalkyl Acrylate	$C_8F_8H_6O_2$	-492.0	1.481
C7A	Fluorinated Acrylate Adhesive	$C_{2.59}F_{3.108}H_{1.55}O_{.518}$	-177.6	1.5
C7M	Fluorinated Acrylate Adhesive	$C_{2.75}F_3H_2O_{.5}$	-179.4	1.5
C9M	Nonylfluoroalkyl Methacrylate	$C_{13}F_{16}H_8O_2$	-911.1	1.606
FAAV	20 C7A/60C7M/20 Viton	$C_{2.63}H_{1.70}F_{3.17}O_{.403}$	-143.1	1.364
FAV	23 C5A/67C9M/10 Viton	$C_{2.62}H_{1.65}F_{3.16}O_{.429}$	-161.6	1.487
HC	Polybutadiene Type Rubber (Thiokol)	$C_{7.19}H_{10.982}N_{.042}O_{.124}$	-2.1	0.908
HDP	Hydrazine Diperchlorate	$N_2H_4 \cdot 2HClO_4$	-92.554	1.86
HMX	Cyclotetramethylenetetranitramine	$C_4H_8N_8O_8$	+25.03	1.903
LI	Lithium	Li	0	0.53
LIP	Lithium Perchlorate	$LiClO_4$	-92.00	2.492
MG	Magnesium	Mg	0	1.74
NC	Nitrocellulose	$C_6H_{7.55}N_{2.45}O_{9.9}$	-159.8	1.660
NDPA	2-Nitrodiphenylamine	$C_{12}H_{10}N_2O_2$	+30.0	1.200
NFPA	1,2-bis (Difluoramino) Propyl Acetate	$C_5F_4H_6N_2$	-124.0	1.57
NG	Nitroglycerine	$C_3H_5N_3O_9$	-88.40	1.600
NP	Nitronium Perchlorate	NO_2ClO_4	+8.0	2.25
RES	Resorcinol	$C_6H_6O_2$	-85.26	1.272
SI	Silicon	Si	0	2.4
TA	Triacetin	$C_9H_{14}O_6$	-291.0	1.150
TAZ	Triaminoguanidine Azide	CH_9N_9	+105.65	1.44
TAGN	Triaminoguanidine Nitrate	$CH_9N_7O_3$	-11.8	1.574
TFLN	Teflon	C_2F_4	-196.0	2.2
TVOPA	Hexakis (Difluoramino) Vinoxy Propane	$C_9F_{12}H_{14}N_6O_3$	-202.0	1.5
VITON	Viton Rubber	$C_5F_8H_2$	0	1.0
ZR	Zirconium	ZR	0	6.4

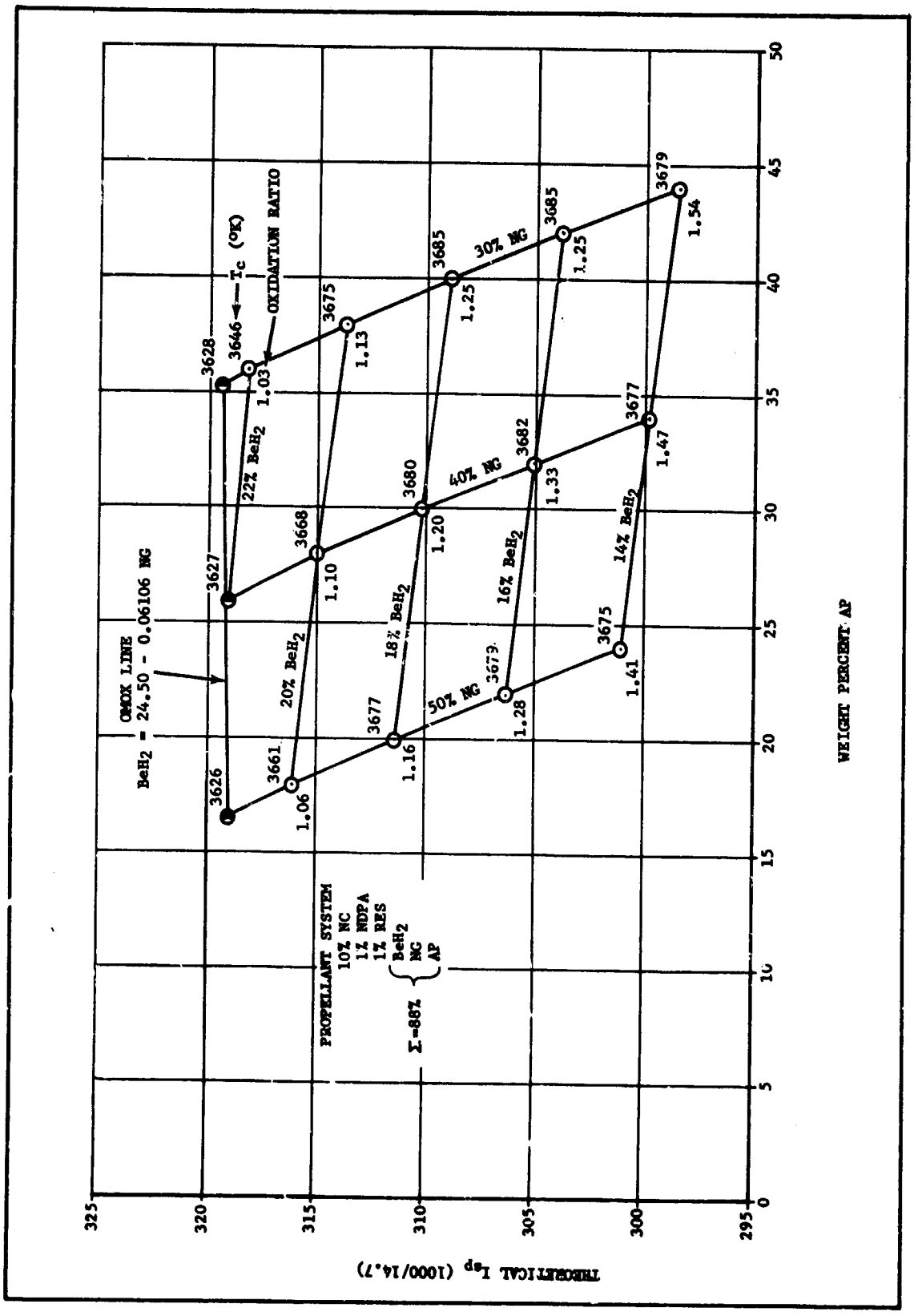

Figure A-1. Theoretical I_{sp} Potential of a Double-Base, LMH-2, AP System

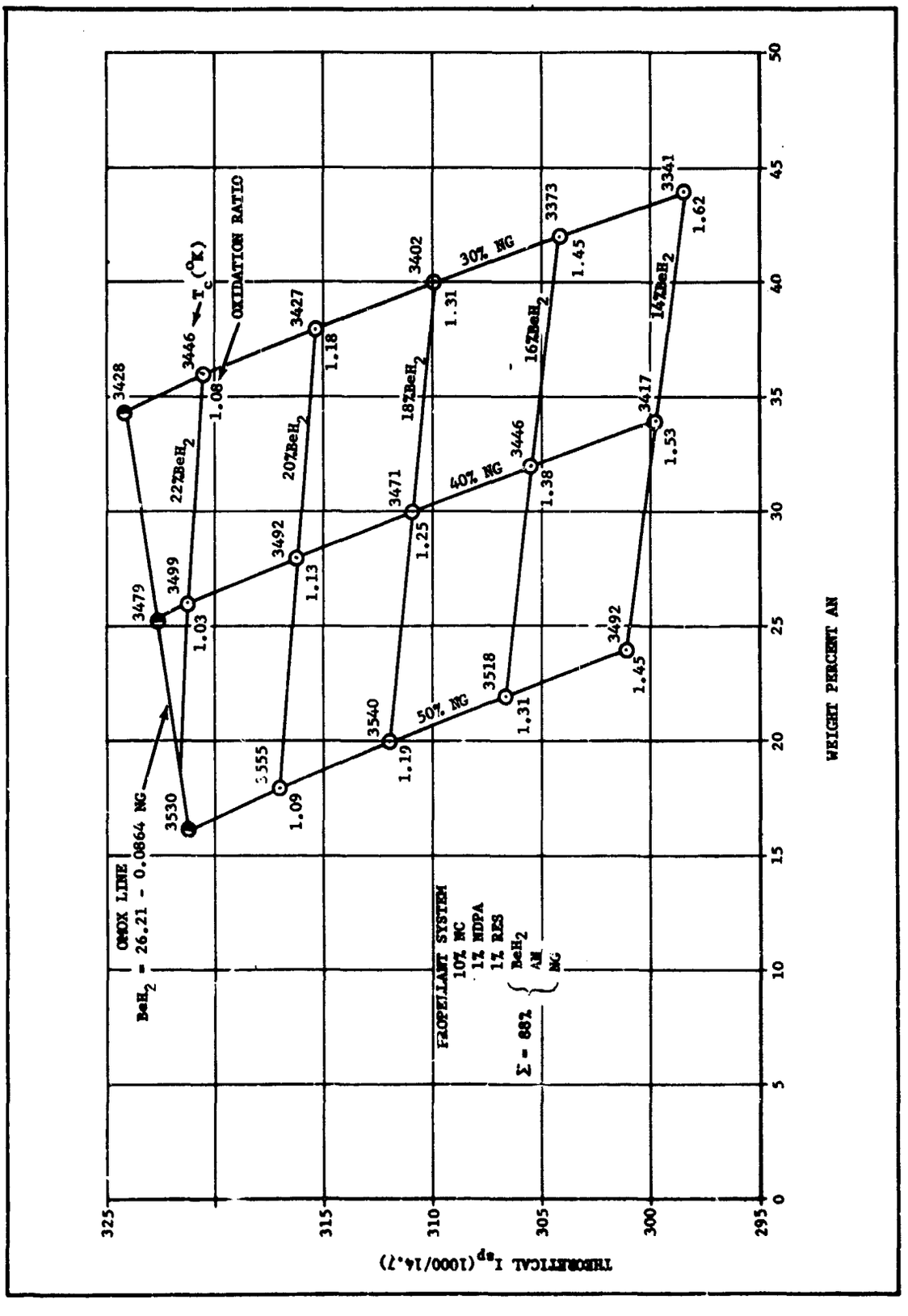

Figure A-2. Theoretical I_{sp} Potential of a Double-Base, LMH-2 AN System

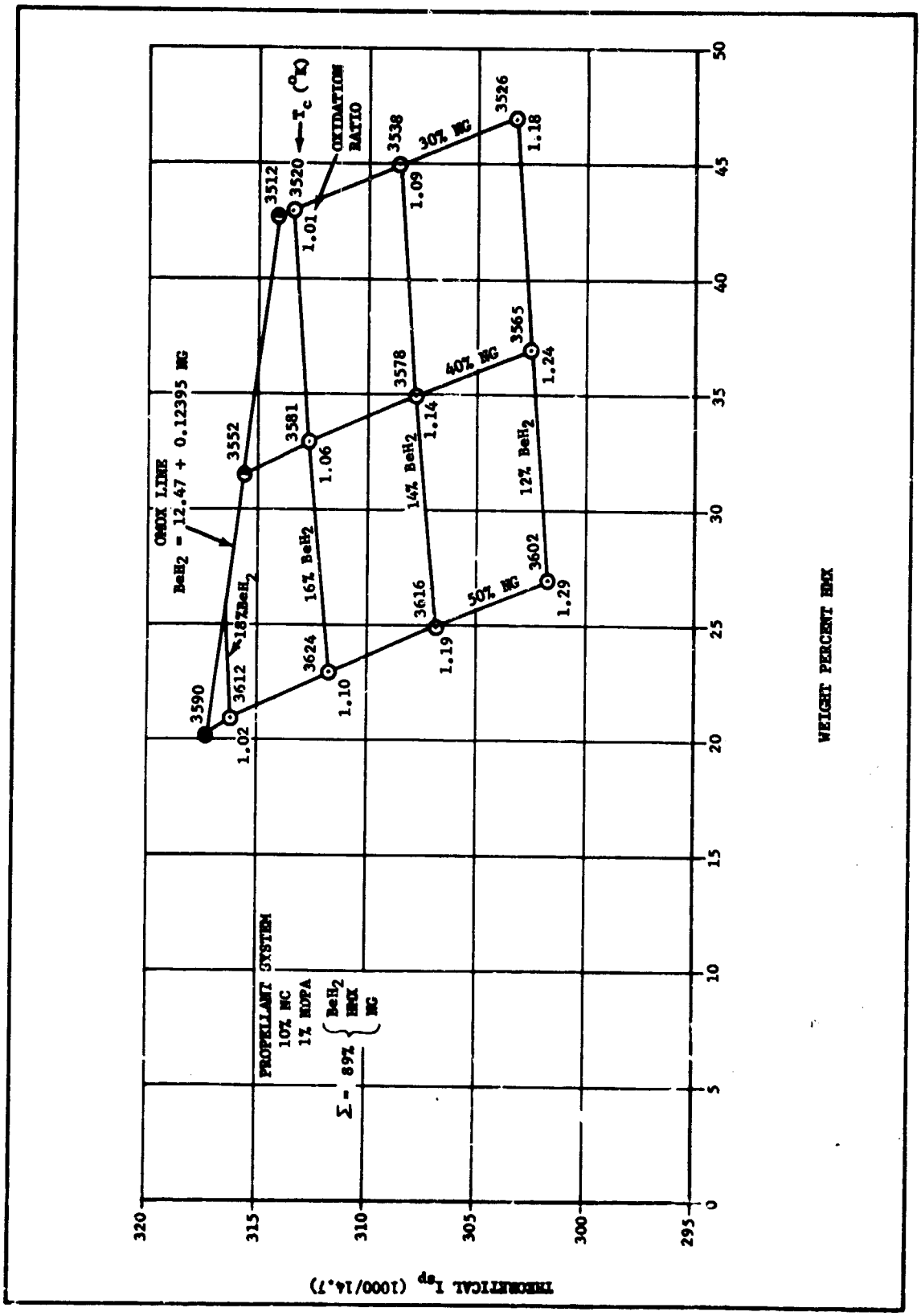

Figure A-3. Theoretical I_{sp} Potential of a Double-Base, LMH-2, HMX System

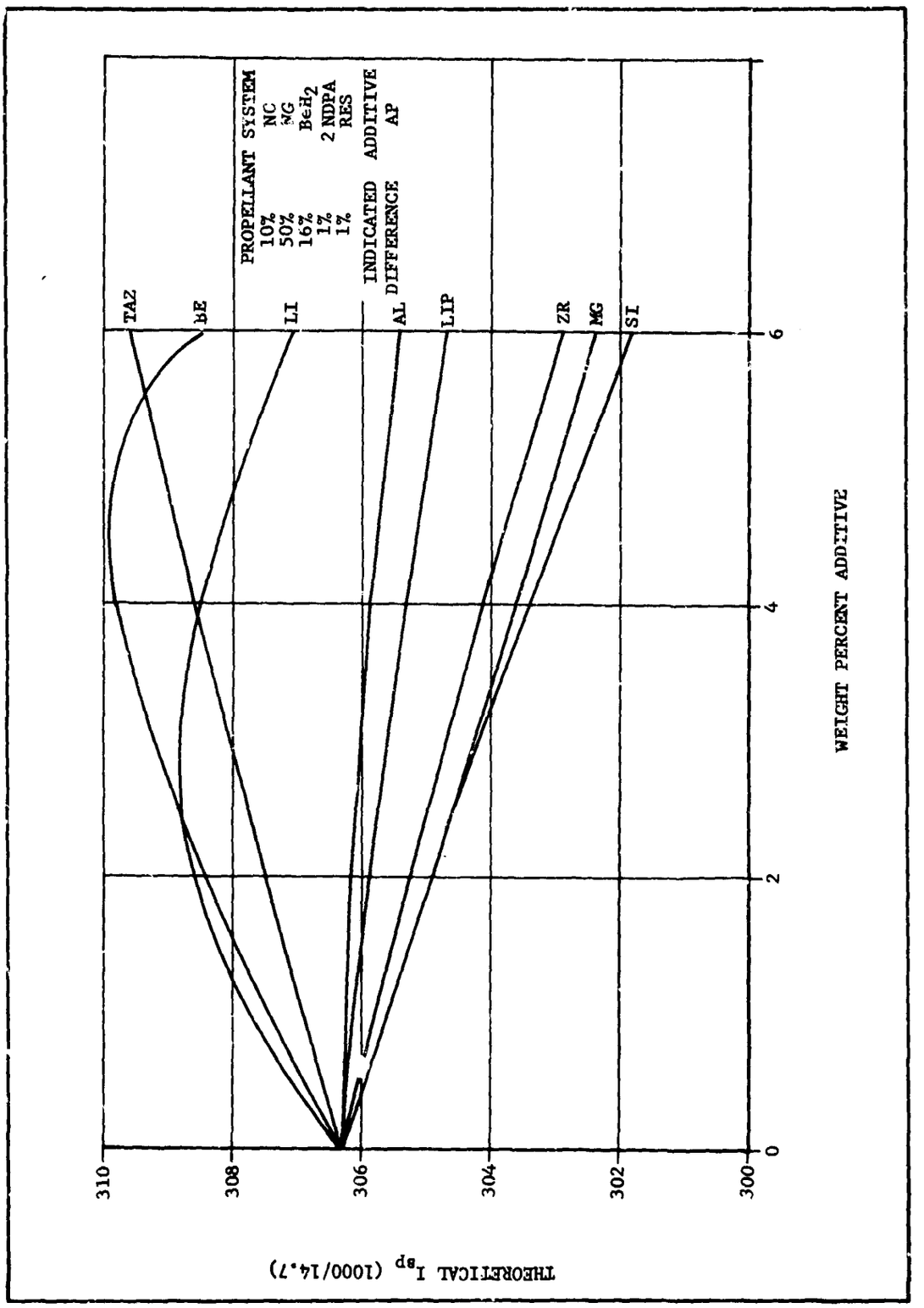

Figure A-4. Effect of Various Additives on a Double-Base, LMH-2, AP System

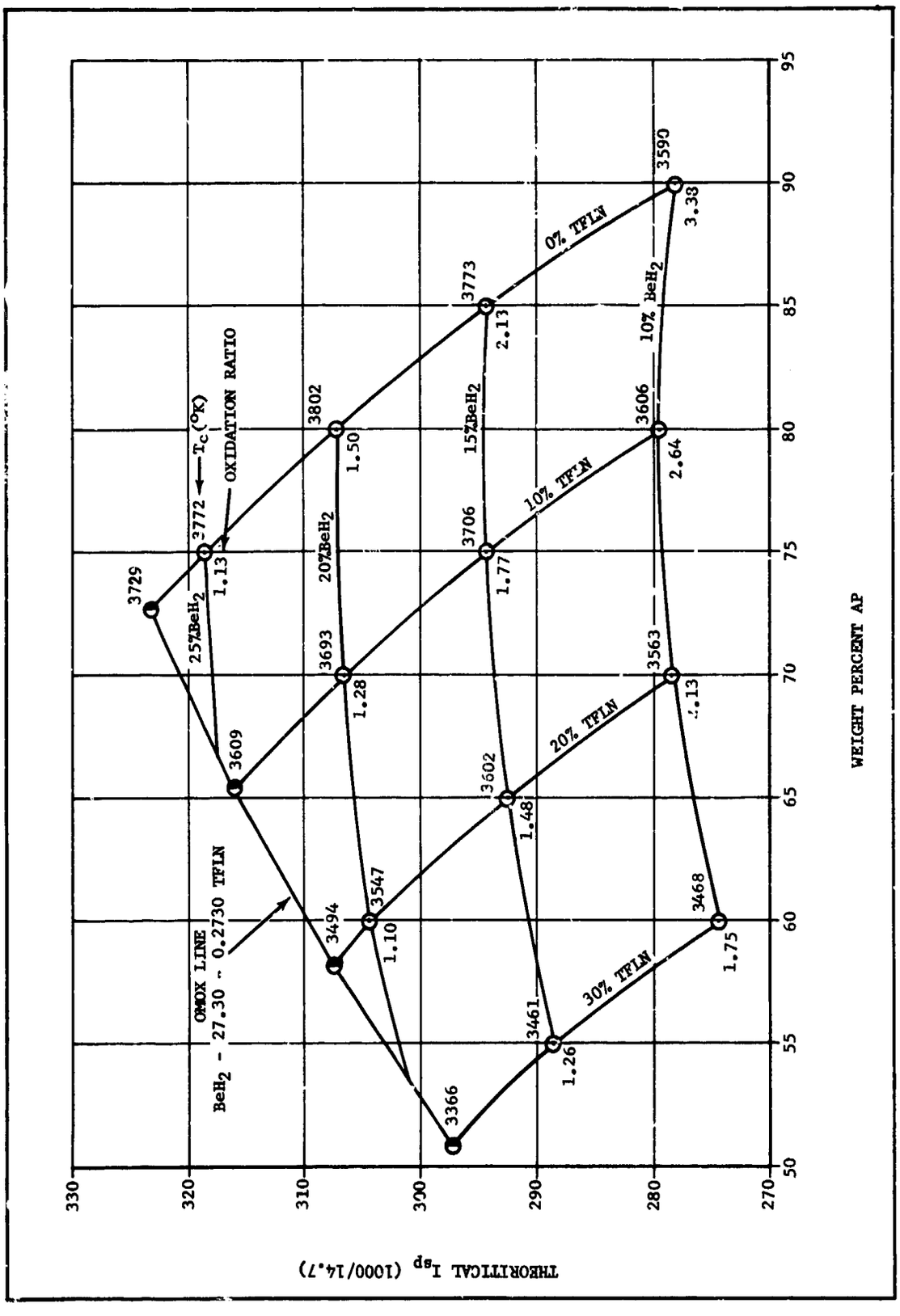

Figure A-5. Theoretical I_{sp} Potential of a LMH-2, AP, TFLN System

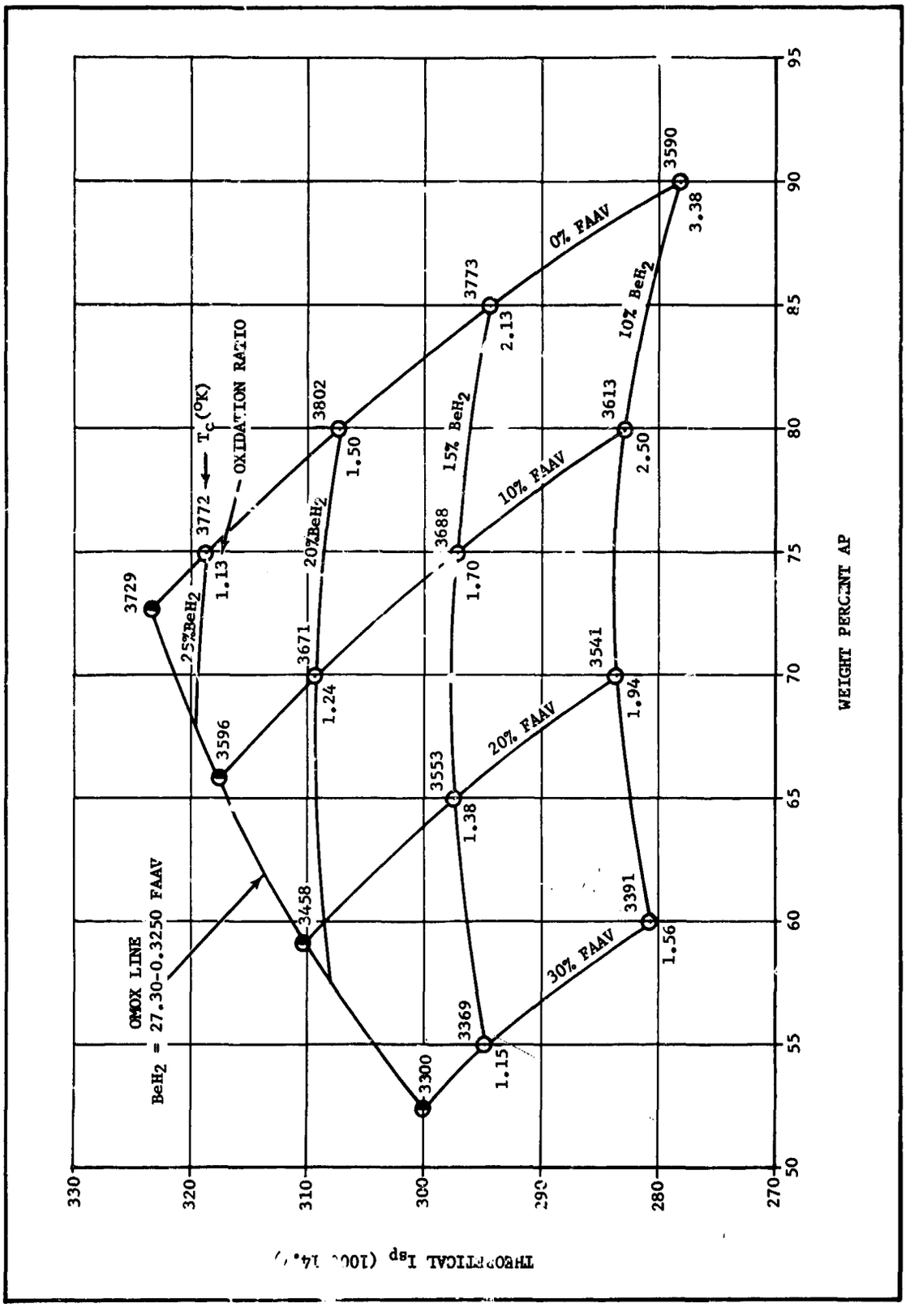

Figure A-6. Theoretical I_{sp} Potential of a LMH-2, AP, FAAV System

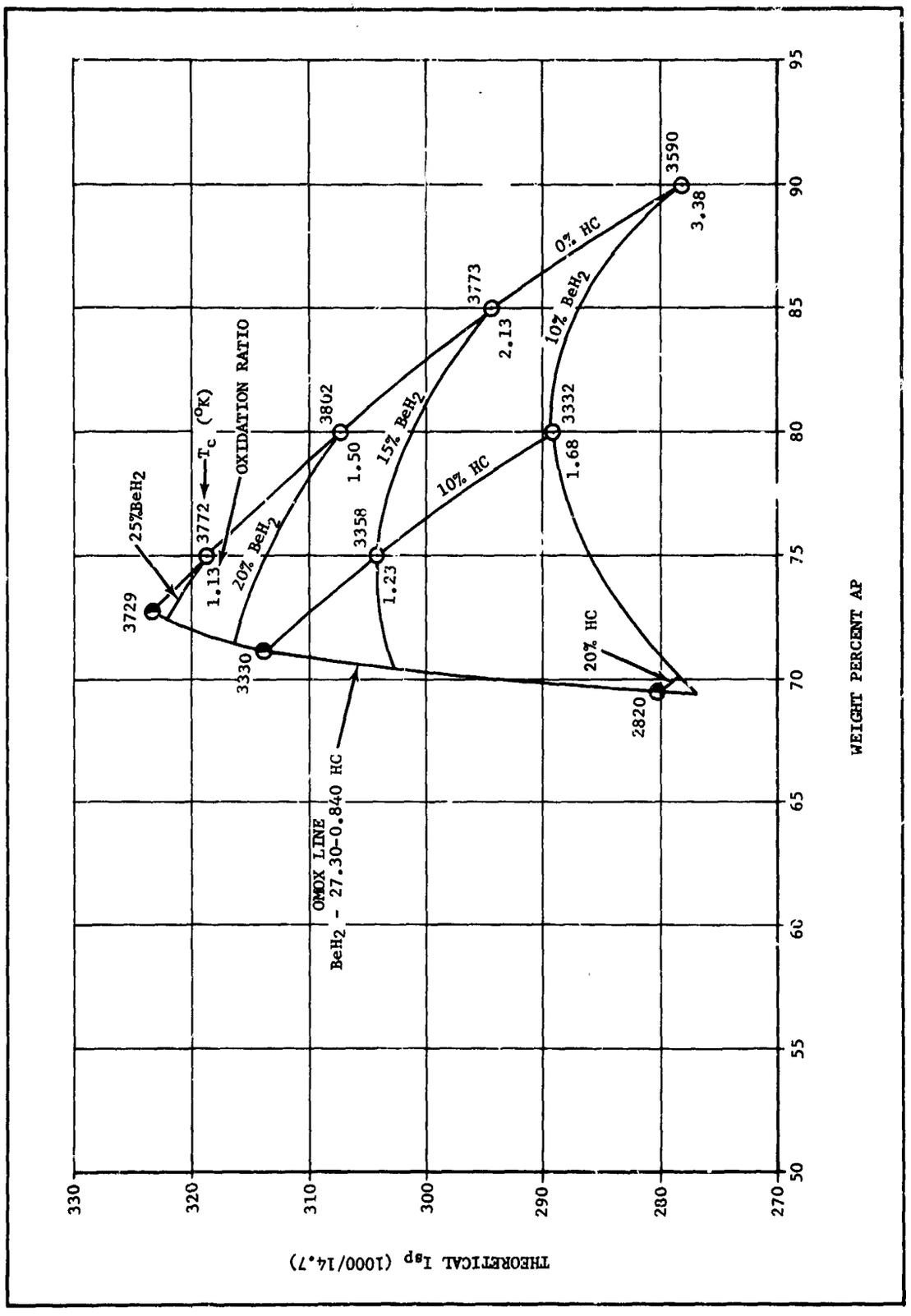

Figure A-7. Theoretical I_{sp} Potential of a LMH-2, AP, HC System

APPENDIX B

THEORETICAL PERFORMANCE CALCULATIONS AND BALLISTIC DATA SUMMARY

Theoretical performance calculations on Be analog formulations and LMH-2 candidate propellants are summarized in Tables B-1 and B-2. Also included are ballistic summary tables (Tables B-3 through B-12) of individual Be and LMH-2 firings made under the Task II effort.

TABLE B-1

THEORETICAL PERFORMANCE CALCULATIONS FOR
CANDIDATE LMH-2 PROPELLANTS

Equilibrium Flow	Propellant Type					
	VIX	VIY	VIZ	VJA	VJI	VJL
Chamber						
P_c (psia)	1000	1000	1000	1000	1000	1000
T_c (^oK)	3678	3679	3672	3620	3623	3614
γ (Heat capacity ratio)	1.075	1.075	1.074	1.088	1.083	1.083
Molecular wt gas	16.35	14.82	13.83	15.40	13.87	14.01
Total moles*	5.469	5.778	6.085	5.729	5.953	6.112
Composition**						
BeO	22.5	24.4	24.8	21.9	23.8	23.8
HCl	3.0	2.5	2.0	--	--	0.5
N_2	8.7	8.1	7.6	12.2	11.2	10.2
CO	17.9	17.4	16.8	22.1	21.0	20.6
CO_2	1.0	0.6	0.3	0.5	0.2	0.2
H_2	27.0	31.3	35.3	31.8	35.4	35.1
H_2O	12.0	8.1	4.7	5.5	2.6	3.4
H	4.8	5.1	5.3	4.6	4.9	4.7
Other	3.1	2.5	3.2	1.4	0.9	1.5
Throat						
C* (ft/sec)	5896	5994	6078	6000	6063	6063
C_d ($sec^{-1} \times 10^3$)	5.46	5.37	5.30	5.37	5.31	5.31
Exit						
P_e (psia)	14.7	14.7	14.7	14.7	14.7	14.7
Teq (^oK)	2570	2596	2619	2421	2472	2474
I_{sp} (1000/14.7)	303.7	308.9	313.8	309.3	314.0	312.7
γ (Heat capacity ratio)	1.104	1.100	1.096	1.135	1.126	1.124

*,**Refer to end of table for footnotes

TABLE B-1 (Cont)

THEORETICAL PERFORMANCE CALCULATIONS FOR
CANDIDATE LMH-2 PROPELLANTS

Equilibrium Flow	VIX	VIY	VIZ	VJA	VJI	VJL
Molecular wt gas	16.47	14.91	13.43	15.39	14.04	14.14
Total moles*	5.392	5.704	6.019	5.677	5.960	5.927
Composition**						
BeO	24.2	26.0	27.6	23.1	25.0	25.1
HCl	3.5	3.0	2.5	--	--	0.7
N_2	8.9	8.2	7.7	12.4	11.4	10.4
CO	17.9	17.5	17.1	22.3	21.3	20.9
CO_2	1.3	0.7	0.3	0.7	0.2	0.3
H_2	28.9	33.5	37.7	34.5	38.2	37.8
H_2O	13.3	8.8	4.7	6.0	2.6	3.4
H	1.6	1.9	2.2	0.9	1.2	1.2
Other	0.4	0.4	0.2	0.1	0.1	0.2
Wt % condensibles						
Frozen Flow						
I_{sp} (1000/14.7)	299.4	305.1	310.3	305.1	310.1	308.8
T_e (^oK)	2257	2302	2336	2157	2207	2210
γ (Heat capacity ratio)	1.176	1.173	1.170	1.187	1.183	1.182

*Total moles (gas plus solids) per 100 gm propellant

**Mole percent of combustion products

TABLE B-2

THEORETICAL PERFORMANCE CALCULATIONS FOR BERYLLIUM PROPELLANTS

Equilibrium Flow	Propellant Type								
	VCP	VIG	VIH	VII	VIJ	VIK	VIL	VIN	VIO
Chamber									
P_c (psia)	1000	1000	1000	1000	1000	1000	1000	1000	1000
T_c (^oK)	3835	3633	4173	3971	4145	4109	4008	3744	3758
γ(Heat capacity ratio)	1.072	1.082	1.083	1.054	1.043	1.044	1.055	1.069	1.073
Molecular wt gas	20.78	17.10	19.86	18.60	19.82	20.78	20.74	17.94	22.10
Total moles*	4.602	5.238	4.633	4.839	4.639	4.524	4.569	4.986	4.418
Composition**									
BeO	22.1	25.1	33.6	32.2	33.5	31.4	26.9	29.9	18.7
HCl	1.2	0.8	3.4	3.2	4.0	4.0	2.2	--	1.6
N_2	15.4	18.8	9.3	8.1	9.0	9.6	13.4	14.6	17.1
CO	27.9	21.2	18.4	22.5	17.6	18.3	23.4	17.6	26.8
CO_2	1.7	0.1	11.0	0.5	1.0	1.6	1.7	1.2	3.2
H_2	14.8	26.8	12.7	18.8	13.3	11.3	12.7	19.1	12.0
H_2O	7.7	1.3	5.9	3.3	6.2	8.3	7.7	10.4	12.0
H	4.8	4.3	7.4	6.5	7.3	6.4	6.0	4.4	3.8
Other	3.8	1.6	8.3	4.9	8.1	9.1	6.0	2.8	4.8
Throat									
C* (ft/sec)	5512	5680	5391	5409	5374	5358	5479	5426	5464
Cd ($sec^{-1} \times 10^3$)	5.84	5.67	5.97	5.95	5.99	6.00	5.88	5.93	5.89
Exit									
P_e (psia)	14.7	14.7	14.7	14.7	14.7	14.7	14.7	14.7	14.7
Teq (^oK)	2690	2531	3015	2820	2992	2959	2820	2780	2569
I_{sp} (1000/14.7)	283.0	290.7	278.0	278.7	277.4	276.5	281.1	280.1	281.1
γ (Heat capacity ratio)	1.046	1.115	1.046	1.045	1.047	1.049	1.072	1.074	1.115
Molecular wt gas	21.20	17.21	20.18	20.28	20.12	21.43	23.86	18.07	22.67
Total moles*	4.520	5.185	4.555	4.587	4.585	4.413	4.143	4.946	4.319
Composition**									
BeO	24.3	26.7	36.8	32.3	36.7	34.4	24.0	31.1	20.3
HCl	1.5	1.2	4.6	4.9	5.4	5.1	3.2	--	1.9
N_2	15.8	19.0	9.7	8.5	9.3	10.1	15.0	14.8	17.7
CO	27.9	21.5	18.4	23.8	17.6	18.1	25.0	17.4	26.2
CO_2	2.4	1.0	1.3	0.5	1.3	2.3	2.6	1.5	13.1
H_2	16.3	29.3	13.9	22.3	14.5	11.8	15.0	19.9	4.6
H_2O	9.1	0.8	7.3	2.9	7.5	10.8	10.5	11.7	14.4
H	1.9	1.3	4.9	3.4	4.7	3.9	3.0	2.8	1.1
Other	0.8	0.1	3.1	1.4	3.0	3.5	1.7	0.8	0.7
Wt % Condensibles									
Frozen Flow									
I_{sp} (1000/14.7)	275.0	287.3	273.5	276.1	273.0	272.3	277.7	278.6	275.6
T_e (^oK)	2347	2261	2820	2791	2820	2820	2723	2577	2186
γ(Heat capacity ratio)	--	1.177	1.135	1.143	1.202	1.238	1.158	1.145	1.188

* Total moles (gas plus solids) per 100 gm propellant

** Mole percent of combustion products

TABLE B-3

BERYLLIUM EFFICIENCY STUDIES

Propellant type	VCP	VCP	VCP	VCP	VCP	VCP	VIH	VIH	VII	VII	VII	VII	VII	VII
Motor design	15PC-1	15PC-1	15PC-1	15PC	15PC	15PC	15PC	15PC	15PC	15PC-2	15PC-2	15PC-2	15PC-1	15PC-1
Grain No.	S82B	S87B	S139B	S86B	S76B	S75B	S89B	S81B	S78B	S129B	S130B	S131B	S132B	S133B
Firing No.	LM2-1	LM2-6	LM2-55	LM2-16	LM2-25	LM2-7	LM2-3	LM2-8	LM2-9	LM2-36	LM2-47	LM2-48	LM2-39	LM2-49
Propellant wt (lb)	14.88	14.92	14.91	15.21	15.17	15.12	15.11	15.24	15.04	14.84	14.82	14.66	14.71	14.73
Powder wt (lb)	0.04	0.05	0.04	0.06	0.05	0.05	0.05	0.05	0.06	0.06	0.07	0.06	0.05	0.06
K (S/A_t)	104.0	103.3	104.0	142.5	142.5	143.2	139.8	110.5	109.2	111.1	138.1	139.0	204.9	182.2
t_a (sec)	1.884	1.874	2.237	1.900	1.804	1.817	1.148	1.322	1.350	2.49	2.218	2.228	2.205	2.409
t_b (sec)	1.794	1.770	2.117	1.756	1.708	1.715	1.043	1.274	1.280	2.36	2.021	2.080	2.061	2.264
$\bar{P}_a$ (psia)	578	586	489	1043	1069	1074	1604	1121	1085	337	460	454	903	751
$\bar{P}_b$ (psia)	592	600	502	1085	1098	1103	1695	1144	1118	348	484	472	935	775
$\bar{P}_{max}$ (psia)	657	650	545	1159	1160	1175	1885	1223	1202	399	544	527	1066	881
$\bar{P}_{amb}$ (psia)	12.41	12.12	12.29	11.94	11.85	12.10	12.41	10.20	12.19	12.17	12.22	12.307	8.141	12.15
$\bar{r}$ (in./sec)	0.557	0.565	0.477	0.751	0.773	0.764	1.246	1.028	1.023	0.317	0.371	0.373	0.490	0.446
$\dot{m}$ (lb/sec)	7.90	7.96	6.67	8.01	8.41	8.32	13.16	11.53	11.14	5.96	6.68	6.58	6.67	8.12
C_d (sec^{-1})	0.00580	0.00578	0.00583	0.00576	0.00587	0.00581	0.00613	0.00604	0.00603	0.00600	0.00614	0.00614	0.00623	0.00611
ϵ (A_e/A_t)	5.615	5.616	5.717	9.640	9.590	9.607	9.576	9.624	9.607	5.627	5.623	5.604	9.477	.625
$\bar{F}_a$ (lb_f)	1939	1995	1629	2112	2227	2209	3570	3088	2949	1350	1586	1554	1757	1530
Isp del $\left(\frac{lb_f\text{-sec}}{lbm}\right)$	245.6	250.7	244.5	263.9	265.1	265.5	272.1	267.4	264.0	226.7	237.6	236.2	263.7	250.3
Theoretical Isp at firing conditions	268.7	269.5	265.0	287.9	288.5	288.2	289.6	286.8	283.4	250.4	259.9	259.1	287.3	275.5
Efficiency	91.40	93.02	92.26	91.66	91.89	92.1	93.96	93.48	93.44	90.54	91.42	91.16	91.79	90.86
Isp $^{15}_{1000}$	258.7	263.2	261.1	259.4	260.1	260.6	261.2	259.9	259.8	252.3	254.8	254.1	255.8	253.2
Isp del (c)*	245.0	250.0	243.9	263.1	264.4	264.9	271.4	267.4	264.0	225.9	236.6	235.4	262.7	249.5
Efficiency (c)*	91.18	92.76	92.04	91.39	91.65	91.92	93.71	93.24	93.16	90.22	91.04	90.85	91.44	90.56
Isp $^{15}_{1000}$(c)*	258.0	262.5	260.5	258.6	259.4	260.1	260.5	259.2	259.0	251.4	253.7	253.2	254.6	252.4

Note: Refer to end of table for footnotes

TABLE B-3 (Cont)

BERYLLIUM EFFICIENCY STUDIES

Propellant type	VII	VLJ	VLJ	VLJ	VLJ	VLJ	VLJ	VIK	VIK	VIK	VIK	VIK	VIK	VIL
Motor design	15PC-1	15PC-1	15PC-1	15PC-1	15PC	15PC	15PC	15PC-1	15PC-1	15PC-1	15PC	15PC	15PC	15PC-1
Grain No.	S134B	S84B	S94B	S85B	S91B	S92B	S97B	S88B	S89B	S90B	S72B	S105B	S114B	S116B
Firing No.	LM2-50	LM2-2**	LM2-12	LM2-13	LM2-4	LM2-5	LM2-11***	LM2-14	LM2-27	LM2-28	LM2-10	LM2-15	LM2-29	LM2-26
Propellant wt (lb)	14.38	14.95	15.12	15.01	15.20	15.24	15.00	15.03	14.95	14.94	14.92	14.74	15.30	15.03
Powder wt (lb)	0.04	0.06	0.04	0.05	0.04	0.03	0.05	0.05	0.05	0.04	0.05	0.04	0.05	0.06
K (S/A_t)	209.3	101.8	102.9	102.5	140.5	141.3	128.	77.00	70.2	70.8	109.6	96.5	98.1	95.8
t_a (sec)	1.809	1.824	1.820	1.831	1.694	1.830	1.947	1.238	1.332	1.436	1.227	1.459	1.425	1.460
t_b-sec	1.713	1.686	1.697	1.720	1.593	1.72	1.875	1.164	1.246	1.368	1.165	1.413	1.357	1.363
$\bar{P}_a$ (psia)	1135	566	576	568	1103	1019	892	621	534	491	1182	879	925	680
$\bar{P}_b$ (psia)	1167	595	597	587	1141	1054	907	640	552	503	1216	895	950	703
$\bar{P}_{max}$ (psia)	1291	671	647	639	1245	1145	999	696	595	537	1303	959	1022	762
$\bar{P}_{amb}$ (psia)	12.303	12.41	11.97	11.92	12.11	12.10	12.00	12.09	12.18	12.14	12.08	11.44	10.33	11.54
$\bar{r}$ (in./sec)	0.590	0.593	0.589	0.581	0.822	0.761	0.693	0.859	0.797	0.731	1.116	0.927	0.965	0.737
$\dot{m}$ (lb/sec)	7.95	8.20	8.31	8.20	8.97	8.33	7.78	12.14	11.22	10.40	12.81	10.10	10.74	10.29
C_d (sec^{-1})	0.00603	0.00611	0.00611	0.00614	0.00608	0.00612	0.00610	0.00619	0.00606	0.00614	0.00606	0.00606	0.00606	0.00597
ϵ (A_e/A_t)	9.742	5.591	5.616	5.644	9.595	9.609	9.022	5.555	5.489	5.631	9.653	9.478	9.425	5.528
$\bar{F}_a$ (lb_f)	2082	1979	2031	1996	2367	2180	1991	3000	2725	2495	3221	2638	2839	2605
Isp del $\left(\frac{lb_f\text{-sec}}{lbm}\right)$	262.1	244.2	244.6	243.7	263.9	261.9	255.8	247.3	243.1	240.0	265.1	261.5	264.8	253.3
Theoretical Isp at firing conditions	284.6	262.9	264.1	263.9	283.1	281.6	280.6	264.6	261.1	259.4	283.7	278.5	279.8	271.9
Efficiency	92.09	92.89	92.62	92.35	93.22	93.00	91.17	93.46	93.11	92.52	93.44	93.90	94.64	93.16
Isp $\frac{15}{1000}$	256.7	257.7	256.9	256.2	258.6	258.0	252.9	258.4	257.5	255.8	258.4	259.6	261.7	261.9
Isp del (c)*	261.5	243.4	244.1	243.0	263.4	261.5	255.1	246.6	242.4	239.5	264.4	260.9	263.8	252.5
Efficiency (c)*	91.88	92.58	92.43	92.08	93.04	92.86	90.91	93.20	92.84	92.33	93.20	93.68	94.28	92.87
Isp $\frac{15}{1000}$ (c)*	256.1	256.8	256.4	255.4	258.1	257.6	252.2	257.7	256.7	255.3	257.7	259.0	260.7	261.1

Note: Refer to end of table for footnotes

TABLE B-3 (Cont)

BERYLLIUM EFFICIENCY STUDIES

Propellant type	VIL	VIL	VIL	VIL	VIL	VIN****	VIN	VIN	VIN	VIO	VIO	VIO	VIG	VIG	VIG
Motor design	15PC-2	15PC-1	15PC	15PC	15PC	15PC-2	15PC-2	15PC-2	15PC-2	15PC-1	15PC-1	15PC-1	15PC-1	15PC-1	15PC-1
Grain No.	S109B	S117B	S110B	S111B	S115B	S112B	S144B	S142B	S143B	S120B	S121B	S122	S135B	S136B	S137B
Firing No.	LM2-40	LM2-41	LM2-42	LM2-43	LM2-44	LM2-30	LM2-58	LM2-56	LM2-73	LM2-31	LM2-51	LM2-52	LM2-38	LM2-45	LM2-46
Propellant wt (lb)	15.14	14.96	15.13	15.15	15.24	14.66	14.00	14.12	14.12	15.07	14.93	15.00	14.09	14.11	14.12
Powder wt (lb)	0.06	0.04	0.06	0.04	0.03	0.06	0.06	0.06	0.06	0.06	0.05	0.05	0.04	0.04	0.04
K (S/A_t)	86.6	81.4	114.8	115.0	115.5	245.0	308.3	414.0	359.0	162.4	119.6	119.8	179.7	207.1	206.0
t_a (sec)	1.261	1.548	1.578	1.565	1.582	4.931	4.203	1.900	2.282	1.163	1.725	1.866	2.310	2.032	2.097
t_b-sec	1.109	1.536	1.509	1.507	1.522	4.184	3.885	1.734	2.084	1.071	1.636	1.767	2.192	1.953	1.966
$\bar{P}_a$ (psia)	538	526	983	998	992	296	398	1482	1085	1472	749	698	772	969	936
$\bar{P}_b$ (psia)	569	545	1008	1020	1013	324	421	1567	1142	1532	778	717	794	990	1010
$\bar{P}_{max}$ (psia)	611	585	1077	1124	1097	406	576	1817	1381	1639	873	801	848	1096	1052
$\bar{P}_{amb}$ (psia)	12.16	12.18	12.16	12.34	12.13	12.27	12.35	12.28	12.22	12.14	12.21	12.17	12.26	12.21	12.21
$\bar{r}$ (in./sec)	0.680	0.657	0.875	0.876	0.861	0.192	0.193	0.421	0.350	0.943	0.618	0.574	0.456	0.512	0.509
$\dot{m}$ (lb/sec)	12.01	9.08	9.59	9.68	9.63	2.97	3.33	7.43	6.19	12.96	8.66	8.04	6.10	7.22	7.18
C_d (sec^{-1})	0.00591	0.00596	0.00598	0.00594	0.00593	0.00752	0.00786	0.00638	0.00629	0.00586	0.00569	0.00572	0.00582	0.00609	0.00609
ϵ (A_e/A_t)	5.609	5.568	9.546	9.565	9.493	9.648	9.633	6.631	7.029	9.621	9.476	9.463	9.507	9.552	9.400
$\bar{F}_a$ (lb_f)	3008	2237	2523	2549	2548	597	710	1903	1570	3516	2223	2038	1562	1810	1740
Isp del $\left(\frac{lb_f\text{-sec}}{lbm}\right)$	250.8	246.7	263.6	263.5	264.7	200.0	213.1	256.6	254.2	271.9	258.3	254.7	256.3	260.9	258.5
Theoretical Isp at firing conditions	268.1	265.7	284.5	284.6	284.7	235.3	252.4	282.4	280.0	291.9	277.8	275.9	288.0	293.5	292.8
Efficiency	93.55	92.85	92.65	92.59	92.98	85.3	84.43	90.80	90.79	93.15	92.98	92.32	88.99	88.89	88.29
$Isp\ {}^{15}_{1000}$	263.0	261.0	260.4	260.3	261.4	238.9	236.5	254.4	254.3	261.9	261.4	259.5	258.7	258.4	256.7
Isp del (c)*	250.0	246.2	262.8	263.0	264.3	200.0	212.2	255.7	253.4	271.1	257.4	254.1	255.8	260.3	257.9
Efficiency (c)*	93.25	92.66	92.37	92.41	92.83	85.00	84.07	90.55	90.50	92.87	92.73	92.10	88.82	88.69	88.08
$Isp\ {}^{15}_{1000}$ (c)*	262.1	260.5	259.7	259.8	261.0	238.1	235.5	253.6	253.5	261.1	260.7	258.9	258.2	257.8	256.0

Notes: All efficiency values were calculated at the actual firing conditions.
$Isp\ {}^{15}_{1000}$ and $Isp\ {}^{15}_{1000}$ (c) values were calculated by multiplying efficiency times the theoretical Isp at standard conditions

* Values corrected for powder embedment
** 4 second hangfire
*** Poor thrust-time trace data is questionable
**** All impulse data questionable because of possible flow separation

TABLE B-4

NOZZLE APPROACH STUDY

Propellant type	VCP	VCP	VCP	VCP	VIJ	VIJ	VIJ	VIJ	VIJ	VIJ
Motor Design	15PC	15PC	15PC	15PC	15PC	15PC	15PC	15PC	15PC	15PC
Grain No.	S96B	S100B	S101B	S119B	S93B	S98B	S99B	S108B	S140B	S141B
Firing No.	LM2-19*	LM2-2[illegible]*	LM2-22**	LM2-37**	LM2-17*	LM2-21*	LM2-23*	LM2-20**	LM2-53**	LM2-54
Propellant wt (lb)	15.15	15.09	15.25	15.25	15.14	15.22	15.10	15.36	15.23	15.33
Powder wt (lb)	0.05	0.03	0.05	0.05	0.04	0.05	0.04	0.04	0.05	0.03
K (S/A_t)	141.3	140.0	140.2	139.9	139.3	137.7	136.2	141.3	142.4	142.8
t_a (sec)	1.953	1.975	1.837	1.890	1.815	1.903	1.961	1.833	1.760	1.784
t_b (sec)	1.850	1.881	1.745	1.817	1.646	1.822	1.859	1.737	1.690	1.695
$\bar{P}_a$ (psia)	974	957	1057	1046	1022	962	939	1044	1050	1055
$\bar{P}_b$ (psia)	1001	979	1089	1068	1053	984	968	1074	1074	1088
$\bar{P}$max (psia)	1054	1019	1153	1146	1138	1080	1060	1173	1198	1388
$\bar{P}_{amb}$ (psia)	11.69	11.64	11.43	12.26	11.93	7.29	11.59	7.61	12.26	12.32
$\bar{r}$ (in./sec)	0.708	0.702	0.756	0.721	0.796	0.719	0.705	0.754	0.775	0.779
$\dot{m}$ (lb/sec)	7.76	7.64	8.30	8.07	8.34	8.00	7.70	8.38	8.65	8.59
α_d (sec^{-1})	0.00595	0.00592	0.00583	0.00568	0.00611	0.00612	0.00604	0.00600	0.00611	0.00613
ϵ (A_e/A_t)	9.626	9.599	9.555	9.507	9.633	9.411	9.551	9.544	9.451	9.414
F_a (lb_f)	2056	2022	2204	2162	2200	2168	2029	2278	2261	2268
Isp del $\left(\frac{lb_f\text{-sec}}{lbm}\right)$	265.2	265.0	265.7	267.8	264.0	271.5	263.7	272.2	261.6	264.2
Theoretical Isp at firing conditions	286.9	286.6	288.9	287.3	281.9	288.0	280.6	288.8	281.7	281.8
Efficiency	92.44	92.46	91.97	93.21	93.65	94.27	93.98	94.25	92.87	93.75
Isp $^{15}_{1000}$	261.6	261.7	260.3	263.8	259.8	261.5	260.7	261.5	257.6	260.1
Isp del (c)*	264.6	264.6	265.0	267.2	263.5	270.8	263.2	271.7	260.9	263.8
Efficiency (C)*	92.23	92.32	91.72	93.00	93.47	94.03	93.80	94.08	92.62	93.61
Isp $^{15}_{1000}$ (c)*	261.0	261.3	259.6	263.2	259.3	260.8	260.2	261.0	256.9	259.7

Notes: *5° Approach
**15° Approach
Firing LM2-18 suffered a case burnthrough and all data was lost.
All efficiency values were calculated at the actual firing conditions.
Isp $^{15}_{1000}$ and Isp $^{15}_{1000}$ (c) values were calculated by multiplying efficiency times the theoretical Isp at standard conditions.

TABLE B-5

AP PARTICLE SIZE STUDY

Propellant type	VIJ-5021	VIJ-5021	VIJ-5021	VIJ-5061	VIJ-5061
Motor Design	15PC-1	15PC-1	15PC-1	15PC	15PC
Grain No.	S123B	S124B	S125B	S126B	S128B
Firing No.	LM2-32	LM2-33	LM2-34	LM2-35	LM2-59
Propellant wt (lb)	15.10	15.07	15.16	15.36	14.27
Powder wt (lb)	0.05	0.05	0.05	0.04	0.05
K (S/A_t)	167.2	179.7	181.5	97.3	109.4
t_a (sec)	2.343	2.053	2.305	1.717	1.427
t_b (sec)	2.224	1.902	2.305	1.649	1.314
$\bar{P}_a$ (psia)	736	896	785	756	968
$\bar{P}_b$ (psia)	757	932	811	774	1014
$\bar{P}$max (psia)	846	1065	911	838	1117
$\bar{P}$amb (psia)	12.22	12.27	12.27	12.16	12.32
$\bar{r}$ (in./sec)	0.450	0.531	0.465	0.800	0.997
$\dot{m}$ (lb/sec)	6.45	7.34	6.58	8.95	10.0
C_d (sec^{-1})	0.00602	0.00607	0.00620	0.00609	0.00605
ϵ (A_e/A_t)	9.573	9.527	9.555	9.243	9.520
$\bar{F}_a$ (lb_f)	1637	1892	1659	2279	2637
Isp del $\left(\frac{lb_f\text{-sec}}{lbm}\right)$	254.2	257.9	252.1	255.0	264.0
Theoretical Isp at firing conditions	273.2	278.3	275.0	274.2	281.0
Efficiency	92.98	92.67	91.67	93.00	93.95
Isp $^{15}_{1000}$	257.9	257.1	254.3	258.0	260.6
Isp del (c)*	253.5	257.2	251.4	254.4	263.3
Efficiency (c)*	92.72	92.42	91.42	92.78	93.70
Isp $^{15}_{1000}$ (c)*	257.2	256.4	253.6	257.4	259.9

Notes: VIJ-5021 contains 180μ AP, VIJ-5061 contains 45μ AP
All efficiency values were calculated at the actual firing conditions.
Isp^{15}_{1000} and Isp $^{15}_{1000}$ (c) values were calculated by multiplying efficiency times the theoretical Isp at standard conditions.
*Values corrected for powder embedment

TABLE B-6

HIGH L* BERYLLIUM FIRINGS

Propellant Type	VCP	VCP	VII	VII
Motor Design	15PC	15PC	15PC-1	15PC-1
Grain No.	S118B	S113B	S160B	S161B
Firing No.	LM2-57	LM2-66	LM2-67	LM2-68
Propellant wt (lb)	15.17	15.38	14.63	14.62
Powder wt (lb)	0.04	0.04	0.03	0.03
K (S/A)	142.2	143.9	203.2	206.5
L* (V_F/A_t)	440	450	390	390
t_a (sec)	1.885	1.955	2.190	2.173
t_b (sec)	1.787	1.834	2.071	1.970
$\bar{P}_a$ (psia)	1063	1013	895	945
$\bar{P}_b$ (psia)	1094	1049	922	992
$\bar{P}$max (psia)	1165	1154	1043	1142
$\bar{P}$amb (psia)	12.29	12.24	12.04	12.23
$\bar{r}$ (in./sec)	0.738	0.714	0.488	0.513
$\dot{m}$ (lb/sec)	8.05	7.87	6.68	6.73
C_d (sec^{-1})	0.00057	0.00585	0.00624	0.00605
ϵ (A_e/A_t)	9.631	9.586	9.274	9.386
$\bar{F}_a$ (lb_f)	2136	2065	1719	1733
Isp del $\left(\frac{lb_f\text{-sec}}{lbm}\right)$	265.6	262.8	258.0	257.8
Theoretical Isp at firing conditions	287.7	286.8	280.0	280.9
Efficiency, Eff	92.32	91.63	92.14	91.78
Isp^{15}_{1000}	261.3	259.3	256.8	255.8
Isp del (c)*	265.1	262.3	257.6	257.4
Efficiency (c)*	92.14	91.46	92.00	91.63
Isp^{15}_{1000} (c)*	260.8	258.8	256.4	255.4

*Values corrected for powder embedment

Notes: All efficiency values were calculated at the actual firing conditions.

Isp^{15}_{1000} and $Isp\ ^{15}_{1000}$ (c) values were calculated by multiplying efficiency times the theoretical Isp at firing conditions.

TABLE B-7

VCP FINAL CHARACTERIZATION FIRINGS

Propellant Type	VCP	VCP	VCP	VCP
Motor Design	15PC-1	15PC-1	15PC	15PC
Grain No.	S83B	S145B	S138B	S77B
Firing No.	LM2-90	LM2-91	LM2-88	LM2-89
Propellant wt (lb)	14.79	14.99	15.27	15.09
Powder wt (lb)	0.04	0.04	0.04	0.05
K (S/A_t)	103.6	103.8	141.6	141.7
t_a (sec)	1.886	2.172	1.972	1.794
t_b (sec)	1.793	2.076	1.878	1.709
$\bar{P}_a$ (psia)	571	509	989	1064
$\bar{P}_b$ (psia)	583.5	515	1013	1090
$\bar{P}$max (psia)	650	570	1090	1165
$\bar{P}$amb (psia)	12.51	12.10	12.19	12.25
$\bar{r}$ (in./sec)	0.558	0.486	0.697	0.767
$\dot{m}$ (lb/sec)	7.84	6.90	7.74	8.41
C_d (sec^{-1})	0.00582	0.00576	0.00584	0.00586
$\epsilon(A_e/A_t)$	5.658	5.694	9.521	9.520
$\bar{F}_a$ (lb_f)	1961	1698	2041	2220
Isp del $\left(\frac{lb_f\text{-sec}}{lbm}\right)$	250.2	246.1	263.8	264.2
Theoretical Isp at firing conditions	268.3	266.4	286.2	287.6
Efficiency, Eff	93.25	92.38	92.17	91.86
Isp^{15}_{1000}	263.9	261.4	260.8	260.0
Isp del (c)*	249.6	245.6	263.3	263.5
Efficiency (c)*	93.03	92.19	92.00	91.62
Isp^{15}_{1000} (c)*	263.3	260.9	260.4	259.3

*Values corrected for powder embedment

Notes: All efficiency values are calculated at the actual firing conditions.

Isp^{15}_{1000} and Isp^{15}_{1000} (c) values were calculated by multiplying efficiency times the theoretical Isp at firing conditions.

TABLE B-8

L* STUDY FOR LMH-2 PROPELLANTS

Propellant Type	VIY*	VIY*	VIY*	VIY*	VIY**	VIY**	VIY**	VIY**	VIY**
Motor	15PC	15PC	15PC	15PC	15PC	15PC	15PC	15PC	15PC
Grain No.	S152BH	S156BH	S151BH	S157BH	S150BH	S154BH	S153BH	S155BH	S156BH
Firing No.	LM2-61	LM2-64	LM2-63	LM2-70	LM2-60	LM2-65	LM2-62	LM2-69	LM2-78
Propellant Wt (lb)	11.79	11.44	11.48	11.39	11.34	11.32	11.56	11.40	11.45
Powder Wt (lb)	0.05	0.05	0.04	0.05	0.05	0.05	0.04	0.05	0.04
K (S/A_t)	127.3	110.8	112.4	110.6	100.2	122.1	122.1	121.9	116.9
L* (V_F/A_t)	133	158	330	294	112	178	325	328	315
t_a (sec)	1.199	1.163	1.052	1.229	1.690	1.595	1.561	1.567	1.521
t_b (sec)	1.106	1.044	0.943	1.090	1.592	1.399	1.437	1.436	1.370
$\bar{P}_a$ (psia)	1192	1042	1294	1033	671	835	873	881	897
$\bar{P}_b$ (psia)	1245	1100	1376	1100	695	884	920	924	946
$\bar{P}$max (psia)	1355	1246	1571	1241	749	953	1054	995	1024
$\bar{P}$amb (psia)	12.29	12.08	12.24	12.25	12.27	12.07	12.01	12.25	12.22
$\bar{r}$ (in./sec)	1.166	1.254	1.389	1.183	0.823	0.936	0.912	0.905	0.949
$\dot{m}$ (lb/sec)	9.83	9.84	10.91	9.27	6.71	8.09	7.41	7.28	7.53
C_d (sec^{-1})	0.00556	0.00553	0.00546	0.00525	0.00530	0.00552	0.00542	0.00533	0.00519
$\epsilon(A_e/A_t)$	9.663	9.462	9.644	9.466	7.446	9.626	9.629	9.595	9.189
$\bar{F}_a$ (lb_f)	2778	2778	3149	2647	1822	1993	2097	2039	2128
Isp del $\frac{lb_f\text{-sec}}{lbm}$	283.2	282.8	289.4	286.2	271.5	279.7	283.7	280.5	283.4
Theoretical Isp at firing conditions	316.6	313.7	317.8	313.1	300.0	308.5	309.6	309.5	309.7
Efficiency, Eff	89.45	90.15	91.06	91.41	90.50	90.67	91.63	90.63	91.51
Isp^{15}_{1000}	276.3	278.5	281.3	282.4	279.6	280.1	283.0	280.0	282.7
Isp del (c)***	282.3	281.9	288.7	285.3	270.6	278.8	283.0	279.6	282.7
Efficiency (c)***	89.16	89.86	90.84	91.12	90.20	90.37	91.41	90.34	91.28
Isp^{15}_{1000} (c)***	275.4	277.6	280.6	281.5	278.6	279.2	282.4	279.1	282.0

*Contains AP-treated LMH-2

**Contains Wax-treated LMH-2

***Values corrected for powder embedment

Notes: All efficiency values were calculated at the actual firing conditions.

Isp^{15}_{1000} and Isp^{15}_{1000} (c) values were calculated by multiplying efficiency times the theoretical Isp at firing conditions

TABLE B-9

LMH-2/AP FIRINGS

Propellant Type	VIX	VIX	VIX	VIZ	VIZ	VIZ
Motor Design	15PC	15PC	15PC	15PC	15PC	15PC
Grain No.	S162BH	S163BH	S164BH	S171BH	S172BH	S173BH
Firing No.	LM2-71	2-72	2-75	LM2-79	LM2-80	LM2-81
Propellant Wt (lb)	11.55	11.74	11.69	10.97	11.08	11.29
Powder Wt (lb)	0.05	0.05	0.05	0.05	0.05	0.05
K (S/A_t)	117.8	120.1	121.7	144.6	140.0	135.7
t_a (sec)	1.309	1.404	1.401	1.480	1.430	1.384
t_b (sec)	1.160	1.307	1.286	1.381	1.332	1.283
$\bar{P}_a$ (psia)	1055	1006	1007	1016	1076	1110
$\bar{P}_b$ (psia)	1121	1046	1052	1060	1124	1156
$\bar{P}$max (psia)	1268	1141	1138	1188	1215	1250
$\bar{P}$amb (psia)	12.23	12.29	12.16	12.22	12.26	12.22
$\bar{r}$ (in./sec)	1.112	0.995	1.011	0.941	0.976	1.021
$\dot{m}$ (lb/sec)	8.82	8.36	8.34	7.41	7.75	8.16
C_d (sec^{-1})	0.00524	0.00529	0.00531	0.00558	0.00533	0.00528
$\epsilon(A_e/A_t)$	9.426	9.486	9.553	9.740	9.473	9.199
$\bar{F}_a$ (lb_f)	2509	2370	2379	2122	2220	2345
Isp del $\frac{lb_f\text{-sec}}{lbm}$	284.9	283.9	285.7	286.6	287.1	288.2
Theoretical Isp at firing conditions	308.5	307.4	307.7	318.2	319.1	319.4
Efficiency, Eff	92.35	92.38	92.85	90.07	89.97	90.23
Isp^{15}_{1000}	280.5	280.5	282.0	282.6	282.3	283.1
Isp del (c)*	284.0	283.0	284.9	285.7	286.2	287.3
Efficiency (c)*	92.06	92.06	92.59	89.79	89.69	89.95
Isp^{15}_{1000} (c)*	279.6	279.6	281.2	281.8	281.5	282.3

*Values corrected for powder embedment

Notes: All efficiency values were calculated at the actual firing conditions.

Isp^{15}_{1000} and Isp^{15}_{1000} values were calculated by multiplying efficiency times the theoretical Isp at firing conditions.

TABLE B-10

LMH-2/HMX FIRINGS

Propellant Type	VJA	VJA	VJA	VJI	VJI	VJI	VJL	VJL	VJL
Motor Design	15PC-1	15PC-1	15PC-1	15PC	15PC	15PC	15PC	15PC	15PC
Grain No.	S165BH	S166BH	S167BH	S176BH	S177BH	S178BH	S180BH	S181BH	S179BH
Firing No.	LM2-74	LM2-76	LM2-77	LM2-82	LM2-83	LM2-84	LM2-86	LM2-87	LM2-85
Propellant wt (lb)	11.46	11.39	11.50	11.45	11.56	11.63	11.32	11.32	11.41
Powder wt (lb)	0.05	0.04	0.04	0.28	0.27	0.20	0.06	0.05	0.06
K (S/A_t)	126.8	142.2	136.2	149.0	150.4	156.3	109.3	130.0	132.1
t_a (sec)	1.530	1.409	1.428	1.501	1.499	1.455	1.832	1.674	1.630
t_b (sec)	1.515	1.328	1.342	1.391	1.416	1.355	1.549	1.552	1.500
$\bar{P}_a$ (psia)	752.4	898	886	842	857	922	683	889	948
$\bar{P}_b$ (psia)	759	928	915	879	886	962	724	931	993
$\bar{P}_{max}$ (psia)	866	1032	1015	934	954	1038	797	1013	1090
$\bar{P}_{amb}$ (psia)	12.23	12.17	12.32	12.19	12.23	12.18	12.26	12.22	12.18
$\bar{r}$ (in./sec)	0.647	0.745	0.738	0.719	0.706	0.738	0.794	0.844	0.867
$\dot{m}$ (lb/sec)	7.49	8.08	8.05	7.63	7.71	7.99	6.18	6.76	7.00
C_d (sec^{-1})	0.00517	0.00527	0.00507	0.00553	0.00555	0.00555	0.00527	0.00529	0.00519
ϵ (A_e/A_t)	9.309	9.558	0.944	9.53	9.62	9.57	9.451	9.951	8.469
$\bar{F}_a$ (lb_f)	2074	2281	2273	2080	2080	2164	1667	1876	1976

CONFIDENTIAL

TABLE B-10 (Cont)

LMH-2/HMX FIRINGS

Propellant Type	VJA	VJA	VJA	VJI	VJI	VJI	VJL	VJL	VJL
Isp del $\left(\frac{lb_f\text{-sec}}{lbm}\right)$	277.5	282.9	282.8	272.9	270.5	271.5	270.2	277.8	282.6
Theoretical Isp at firing conditions	305.7	310.6	309.6	312.40	312.9	314.8	306.0	314.1	314.2
Efficiency, Eff	90.78	91.08	91.34	87.36	86.46	86.24	88.30	88.44	89.97
Isp^{15}_{1000}	280.8	281.7	282.5	274.3	271.5	270.8	276.1	276.6	281.4
Isp del (c)*	276.7	282.2	282.1	271.9	269.4	270.6	269.1	276.9	281.6
Efficiency (c)*	90.51	90.86	91.12	87.04	86.10	85.96	87.94	88.16	89.62
Isp^{15}_{1000} (c)*	280.0	281.0	281.8	273.3	270.4	269.9	275.0	275.7	280.2

*Values corrected for powder embedment

Notes: All efficiency values were calculated at the actual firing conditions.

Isp^{15}_{100} and Isp^{15}_{1000} values were calculated by multiplying efficiency times the theoretical Isp at firing conditions.

TABLE B-11

VIY FINAL CHARACTERIZATION FIRINGS

Propellant Type	VIY	VIY	VIY	VIY	VIY
Motor Design	15PC	15PC	15PC	15PC	15PC
Grain No.	S183BH	S185BH	S184BH	S186BH	S187BH
Firing No.	LM2-92	LM2-94	LM2-93	LM2-95	LM2-96
Propellant wt (lb)	11.76	11.68	11.65	11.62	11.65
Powder wt (lb)	0.04	0.03	0.04	0.03	0.03
K (S/A_t)	91.0	93.6	145.7	144.6	143.5
t_a (sec)	1.619	1.676	1.305	1.319	1.303
t_b (sec)	1.495	1.593	1.208	1.230	1.212
$\bar{P}_a$ (psia)	655	627	1305	1285	1280
$\bar{P}_b$ (psia)	681	645	1356	1333	1328
$\bar{P}$max (psia)	743	704	1474	1440	1430
$\bar{P}$amb (psia)	12.26	12.19	12.27	12.17	12.09
$\bar{r}$ (in./sec)	0.883	0.822	1.093	1.065	1.089
$\dot{m}$ (lb/sec)	7.208	6.968	8.927	8.809	8.979
C_d (sec^{-1})	0.00528	0.00533	0.00527	0.00524	0.00530
$\epsilon(A_e/A_t)$	5.622	5.622	9.507	9.52	9.422
$\bar{F}_e$ (lb_f)	1929	1847	2589	2555	2584
Isp del $\left(\frac{lb_f\text{-sec}}{lbm}\right)$	267.9	265.3	290.7	290.3	289.4
Theoretical Isp at firing conditions	296.0	295.2	317.9	317.8	317.6
Efficiency, Eff	90.51	89.87	91.44	91.35	91.12
Isp^{15}_{1000}	279.6	277.6	282.5	282.2	282.3
Isp del (c)*	267.2	264.8	290.0	289.8	289.0
Efficiency (c)*	90.27	89.70	91.22	91.19	90.99
Isp^{15}_{1000} (c)*	278.8	277.1	281.8	281.7	281.1
L*	334	3	318	315	313

*Values corrected for powder embedment.

Notes: All efficiency values were calculated at the actual firing conditions.

Isp^{15}_{1000} and Isp^{15}_{1000} (c) values were calculated by multiplying efficiency times the theoretical Isp at firing conditions.

TABLE B-12

VJA FINAL CHARACTERIZATION FIRINGS

Propellant Type	VJA	VJA	VJA	VJA	VJA	VJA
Motor Design	15PC-1	15PC-1	15PC-1	15PC	15PC	15PC
Grain No.	S188BH	S189BH	S190BH	S191BH	S192BH	S193BH
Firing No.	LM2-97	LM2-98	LM2-99	LM2-100	LM2-101	LM2-102
Propellant wt (lb)	11.87	11.85	11.86	12.07	12.07	12.05
Powder wt (lb)	0.04	0.04	0.03	0.04	0.04	0.03
K (S/A_t)	117.3	116.9	116.4	156.5	154.2	155.2
t_a (sec)	1.641	1.652	1.645	1.701	1.714	1.667
t_b (sec)	1.523	1.540	1.577	1.587	1.643	1.572
$\bar{P}_a$ (psia)	658	655	658	1137	1127	1156
$\bar{P}_b$ (psia)	682	678	672	1176	1154	1191
$\bar{P}$max (psia)	75	763	743	1285	1270	1304
$\bar{P}$amb (psia)	12.15	11.85	12.32	12.28	12.22	12.22
$\bar{r}$ (in./sec)	0.656	0.656	0.634	0.832	0.803	0.883
$\dot{m}$ (lb/sec)	7.233	7.173	7.209	7.09	7.042	7.228
C_d (sec^{-1})	0.00530	0.00527	0.00525	0.00517	0.00509	0.00513
$\epsilon(A_e/A_t)$	5.72	5.664	5.637	9.520	9.364	9.588
$\bar{F}_a$ (lb_f)	1947	1922	1933	2010	1997	2055
Isp del $\left(\frac{lb_f\text{-sec}}{lbm}\right)$	269.5	268.2	268.3	283.6	284.1	285.0
Theoretical Isp at firing conditions	297.9	297.0	297.4	315.9	315.7	316.4
Efficiency, Eff	90.47	90.30	90.22	89.78	89.99	90.08
Isp^{15}_{1000}	279.8	279.3	279.0	277.6	278.3	278.4
Isp del (c)*	268.9	267.5	267.8	282.9	283.4	284.5
Efficiency (c)*	90.27	90.07	90.05	89.55	89.77	89.92
Isp^{15}_{1000} (c)*	279.2	278.6	278.5	277.0	277.7	278.1
I*	337	336	334	347	342	344

*Values corrected for powder embedment

Notes: All efficiency values were calculated at the actual firing conditions.

Isp^{15}_{1000} and Isp^{15}_{1000} (c) values were calculated by multiplying efficiency times the theoretical Isp at firing conditions.